DISSERTATION

submitted to the

Combined Faculty of Natural Sciences and Mathematics

of the Ruperto-Carola University of Heidelberg, Germany

for the degree of

Doctor of Natural Sciences

presented by

Lucie Magdalena Wolf, M.Sc.

born in Nuremberg, Germany

Date of oral examination: 2nd February 2021

Ubiquitin-dependent regulation of the WNT cargo protein EVI/WLS

Referees:

Prof. Dr. Michael Boutros

apl. Prof. Dr. Viktor Umansky

If you don’t think you might, you won’t.

Terry Pratchett

This work was accomplished from August 2015 to November 2020 under the supervision of Prof. Dr. Michael Boutros in the Division of Signalling and Functional Genomics at the German Cancer Research Center (DKFZ), Heidelberg, Germany.

Contents

1 Abstract

Cellular communication by WNT signalling is crucial for growth, patterning, and tissue homeostasis of metazoan animals and has been associated with various human diseases, such as cancer. The different branches of this signalling cascade are induced after the secretion of WNT ligands by the WNT cargo protein evenness interrupted/Wntless (EVI/WLS). The availability and stability of many proteins involved in the WNT signalling pathways is regulated by post-translational mechanisms. In the absence of WNTs, EVI/WLS is modified with ubiquitin and subjected to endoplasmic reticulum (ER)-associated degradation (ERAD) by the proteasome. ERAD is well known to remove misfolded proteins from the ER but can also affect cellular signalling by degrading mature proteins associated with secretory routes. However, the latter type of regulation is not well studied in mammals. In addition, the mechanisms leading to the recognition, ubiquitination, and proteasomal targeting of EVI/WLS remain largely elusive.

To gain insights into how ERAD and ubiquitination components regulate EVI/WLS, I performed a RNAi-based screen on EVI/WLS protein stability and used biochemical and cell biological methods in human cells with diverse genetic backgrounds. I discovered that the ER-membrane associated proteins ERLIN2, FAF2, and UBXN4 are novel components of the EVI/WLS 'destruction complex'. Mechanistically, ERLIN2 links EVI/WLS to the ubiquitination machinery, while FAF2 and UBXN4 interact with EVI/WLS and VCP, potentially to mediate its extraction from the ER membrane. Surprisingly, I also found that EVI/WLS is ubiquitinated and degraded in cells irrespective of their WNT activity. This K11-, K48-, and K63-linked ubiquitination is mediated by the E2 ubiquitin conjugating enzymes UBE2J2, UBE2K, and UBE2N and leads not only to the regulation of EVI/WLS protein levels, but also influences WNT secretion. Analysing the functional impact of EVI/WLS abundance revealed that EVI/WLS protein levels and the secretion of WNT11 influence the invasive capacity of malignant melanoma cells. This suggests that the adaptive regulation of EVI/WLS can be important for the phenotypic manifestation and presumably progression of human malignancies.

In summary, my data shows an unanticipated complex ubiquitination pattern of EVI/WLS and three novel interaction partners, thus providing important details on the post-translational modification and fate of an endogenous ERAD substrate in mammalian cells. The abundance of EVI/WLS is essential for context-dependent WNT ligand secretion and thus governs the malignancy of several tumours, among them melanoma. Targeting EVI/WLS protein levels *via* its post-translational regulations could be used to treat WNT-dependent diseases.

1 Zusammenfassung

Die Zellkommunikation mittels WNT Signalwegen ist notwendig für das Wachstum, die Musterbildung und die Gewebehomöostase aller vielzelligen Tiere. Störungen oder Veränderungen in WNT Signalwegen tragen zu der Entstehung zahlreicher Krankheiten bei, wie beispielsweise Krebs. Die Initiation der WNT Signalkaskaden geschieht durch die Sekretion von WNT Liganden mit Hilfe des Transportproteins *evenness interrupted/Wntless* (EVI/WLS), wobei viele der beteiligten Proteine posttranslational reguliert werden können. Sind keine WNT Liganden vorhanden, wird EVI/WLS ubiquitiniert und durch den endoplasmatischen Retikulum (ER)-assoziierten Abbau (engl. *ER-associated degradation*, ERAD) dem Proteasom zugeführt. ERAD dient normalerweise dazu, fehlgefaltete Proteine aus dem ER zu entfernen, kann aber durch den Abbau funktionaler Proteine auch Signaltransduktionswege beeinflussen. Diese Art der Regulation wurde allerdings in Säugetierzellen bisher nur wenig untersucht und auch bezüglich der Erkennung, der Ubiquitinierung und der Überführung von EVI/WLS an das Proteasom bleiben viele Fragen offen.

Um die Regulation von EVI/WLS durch Ubiquitinierung und ERAD besser verstehen zu können, habe ich einen RNAi-basierten Screen von zahlreichen ERAD-assoziierten Faktoren durchgeführt und die Ergebnisse durch biochemische und zellbiologische Experimente in verschiedenen genetischen Hintergründen validiert. Ich habe herausgefunden, dass ERLIN2, FAF2 und UBXN4 am Abbau von EVI/WLS beteiligt sind. ERLIN2 verbindet EVI/WLS mit dem Ubiquitinsystem, wohingegen FAF2 und UBXN4 mit EVI/WLS und der ATPase VCP interagieren, vermutlich um EVI/WLS aus der ER Membran zu entfernen. Überraschenderweise wurde EVI/WLS in Zellen unabhängig von deren WNT Aktivität ubiquitiniert und abgebaut. Diese K11-, K48-, und K63-verbundene Ubiquitinierung wurde durch die E2 Ubiquitin-konjugierenden Enzyme UBE2J2, UBE2K und UBE2N gewährleistet und beeinflusste nicht nur die Verfügbarkeit von EVI/WLS, sondern auch die Sekretion von WNT Liganden. Weitere Untersuchungen zur Funktionalität von EVI/WLS ergaben, dass die Verfügbarkeit von EVI/WLS und die Sekretion von WNT11 einen Einfluss auf die Invasivität von Melanomzellen hatten. Dies lässt vermuten, dass die Feinregulation von EVI/WLS möglicherweise wichtig für den Verlauf von menschlichen Krankheiten sein kann.

Zusammengefasst zeigen meine Daten ein unerwartet komplexes Muster der EVI/WLS-Ubiquitinierung sowie drei neue EVI/WLS Interaktionspartner, wodurch neue Erkenntnisse hinsichtlich der posttranslationalen Modifizierung und Verarbeitung von endogenen ERAD Substraten in Säugetierzellen geliefert werden. Dabei ist die Menge an EVI/WLS Protein nicht nur entscheidend für die kontextabhängige Sekretion von WNT Liganden, sondern letztlich für die Malignität verschiedener Tumoren, wie dem Melanom. Die posttranslationale Regulation von EVI/WLS könnte deshalb neue Ansatzpunkte zur Behandlung von WNT-abhängigen Krankheiten bieten.

2 Introduction

To maintain protein homeostasis is a major challenge for all organisms and changes in protein abundance can alter cellular physiology and lead to diseases. Both the adequate synthesis and the organised removal of proteins are essential to avert cellular stress. Importantly, quality control mechanisms can also impact on a cell's signalling by regulating protein quantity. A better understanding of these processes, their components, and their interplay will advance basic research and can potentially help to find novel treatment possibilities for diseases dependent on these signalling pathways.

The WNT pathways are well-known signalling cascades which can be regulated by protein abundance. For example, β-catenin, which is one of their major effectors, is degraded by the proteasome in the absence of WNT ligands, thus blocking downstream effects. In this PhD thesis, I present novel insights into ubiquitination and endoplasmic reticulum (ER)-associated degradation of the WNT cargo protein evenness interrupted/Wntless (EVI/WLS) and discuss possible implications for cancer progression and treatment.

2.1 The WNT signalling pathways and cancer

Cellular communication and intercellular signalling are the cornerstones of metazoan life. Growth and patterning during development and tissue homeostasis in adults require well regulated, coordinated action of proteins over short and long ranges and on organismal level. Delineating signalling cascades, their interaction and regulation, allows us to better understand the logic behind cellular activity and to draw informed conclusions about their deregulation in diseases, such as cancer. Many developmental signalling programmes are reactivated during malignant transformation and offer potential targets for tumour therapy.

2.1.1 Intercellular communication

The exchange of information between cells is complex and relies on various different mechanisms (Alberts et al., 2008). Information units can be transmitted between cells directly through a continuous, porous link (e.g. electrical signals passing through gap junctions between heart muscle cells) or by the exchange of molecules between cells, which are released from one cell and detected by receptors on the receiving cell (also referred to as 'chemical synapse'). The three major modes of action of secreted signalling molecules are distinguished by their range: (i) autocrine messages are produced and received by the same cell, e.g. during clonal T cell

expansion after antigen recognition, (ii) paracrine signals instruct cells within immediate vicinity to the source signal, for instance during Wingless (Wg)-mediated patterning of the Drosophila wing imaginal disc, and (iii) endocrine signalling affects tissues far away from the molecule's origin, as do for example hormones after release in the blood stream. The three most common types of cell surface receptors are ligand-gated ion channels (for example the acetylcholine receptors at the neuromuscular junction), guanine nucleotide-binding (G) protein-coupled receptors (which can be activated upstream of the phosphatidylinositol signal pathway) and enzyme-linked receptors, such as the epidermal growth factor receptor (EGFR), which dimerises upon ligand binding, causing the intracellular domains to phosphorylate each other. After reception, the message of these signals is transduced inside the cell *via* a coordinated interaction of downstream proteins to evoke a cellular response. In many cases, signal transduction is propagated by reciprocal phosphorylation of proteins and eventually results in the activation of specific transcription factors that activate or repress the transcription of target genes. An example is the mitogen-activated protein kinase (MAPK) pathway downstream of *exempli gratia* (e.g.) EGFR activation. This results in the subsequent phosphorylation and activation of rat sarcoma (RAS), rapidly accelerated fibrosarcoma (RAF), MAPK/extracellular signal-regulated kinase (ERK) kinase (MEK), and finally ERK/MAPK, which in turn regulates several transcription factors and other downstream effects (Schadendorf et al., 2015).

2.1.2 WNT ligands are conserved morphogens

Tight spatiotemporal regulation of gene expression is imperative to ensure proper growth and patterning during development. A common mechanism among metazoans to achieve this are morphogens, conserved secreted signalling cues that build opposing gradients in the early embryo and govern target gene transcription through availability and activity in combination with underlying transcription networks (Briscoe & Small, 2015). An important family of morphogens are Wnt ligands, which are involved in the pattering of the vertebrate neural tube or the drosophila wing, for example (Briscoe & Small, 2015; Wiese et al., 2018). Though it is still under debate whether Wnt ligand gradient formation or spreading in the drosophila wing imaginal disc is necessary for wing development, the importance of Wnt signalling itself is undisputed (Alexandre et al., 2014; Ewen-Campen et al., 2020; J. J. S. Yu et al., 2020). In adults, Wnt ligands play an important role in tissue homeostasis, turnover, and repair by regulating the adult stem cell populations of various tissues (Nusse & Clevers, 2017; T. Sato et al., 2009). Wnt ligands are secreted glycoproteins which often carry a lipid-modification. They can be grouped in 13 subfamilies with high vertical conservation and are encoded in the genomes of most

animals, but are absent from unicellular organisms, as well as from plants and fungi (Holstein, 2012).

Binding to a distinct subset of receptors and co-receptors on the Wnt receiving cell sets several intracellular signal transduction cascades in motion, which can be grouped functionally in β-catenin dependent ('canonical') or independent ('non-canonical') pathways (see 2.1.4 and 2.1.5). In this regard, the human WNT ligands WNT1, WNT3/3A, and WNT10A/B are classified as 'canonical' and have very well-defined physiological roles and receptor binding partners, whereas WNT5A and WNT11 induce the less well studied 'non-canonical' WNT- Frizzled (FZD)/planar cell polarity (PCP) and the WNT/Ca^{2+} pathways (Niehrs, 2012; Nusse & Clevers, 2017; Voloshanenko et al., 2017; Zhan et al., 2017). The cellular response depends on the specific pair of WNT ligand and receptor, the cell-type and the tight interplay with other pathways, such as MAPK or hedgehog signalling (Ishitani et al., 2003; Ouspenskaia et al., 2016; Zhan et al., 2019). Mutations in components of the WNT signalling pathways can lead to hereditary diseases, such as Robinow syndrome, delays in development (Mancini et al., 2020), or lead to cancer (Afzal et al., 2000; Nusse & Clevers, 2017; van Bokhoven et al., 2000).

2.1.3 WNT ligand maturation and secretion

The expression of each of the 19 human WNT ligands is tightly regulated and induced in a context and tissue-dependent manner in the WNT secreting cell. WNTs are about 40 kDa large, cysteine rich proteins, which are co-translationally imported into the ER, where they are glycosylated and lipid-modified by the protein-serine O-palmitoleoyltransferase porcupine (PORCN) on a conserved serine (Siegfried et al., 1994; Takada et al., 2006; Willert et al., 2003). This modification allows their interaction with the WNT cargo protein EVI/WLS, which helps in the anterograde transport of WNTs to the extracellular space (Bänziger et al., 2006; Bartscherer et al., 2006; Goodman et al., 2006). Furthermore, the lipid modification is important for the binding of WNTs to the cysteine-rich domain (CRD) of FZD receptors on their target cell (Janda et al., 2012). It was also recently reported that several non-acylated WNTs could induce downstream signalling (Speer et al., 2019), however, this study awaits further independent confirmation. Surprisingly for a pathway this intricate, the secretion and activity of most WNT ligands was hitherto reported to depend on the lipid-modification and the interaction with EVI/WLS, the only exception being the distantly related Drosophila WntD (Ching et al., 2008). This in turn allows researchers to block all WNT signalling pathways by inhibiting either EVI/WLS or PORCN, for example with the small-molecule PORCN inhibitor LGK974 (J. Liu et al., 2013). LGK974 and several other WNT signalling inhibitory agents are the focus of multiple ongoing clinical trials in liquid and solid cancers, but systemic inhibition of WNT signalling results in side effects such

as decreased bone mass and strength or loss of taste sensation (Jung & Park, 2020; L.-S. Zhang & Lum, 2018).

2.1.3.1 WNT ligand secretion

Mature WNT ligands associate with EVI/WLS in the ER and are recruited into coat protein complex (COP) II vesicles by association with secretion associated RAS related GTPase 1 (SAR1) and the help of transmembrane p24 trafficking proteins (Buechling et al., 2011; Port et al., 2011; Jiaxin Sun et al., 2017; J. Yu et al., 2014). They are then transported to the Golgi and to the plasma membrane in an RAS-associated binding (RAB) 8A dependent mechanism (Das et al., 2015). Subsequent free diffusion of WNTs in the extracellular space without any binding partner is unlikely due to their lipid modification. Therefore, several distinct routes have been proposed to explain how WNT ligands are delivered to the target cell over short and long distances (Figure 1). It is conceivable that these routes are used in parallel and in an organism and context dependent manner. One proposed mechanism to stabilise lipidated WNTs in the extracellular space are glypicans, plasma membrane associated heparan sulphate proteoglycans

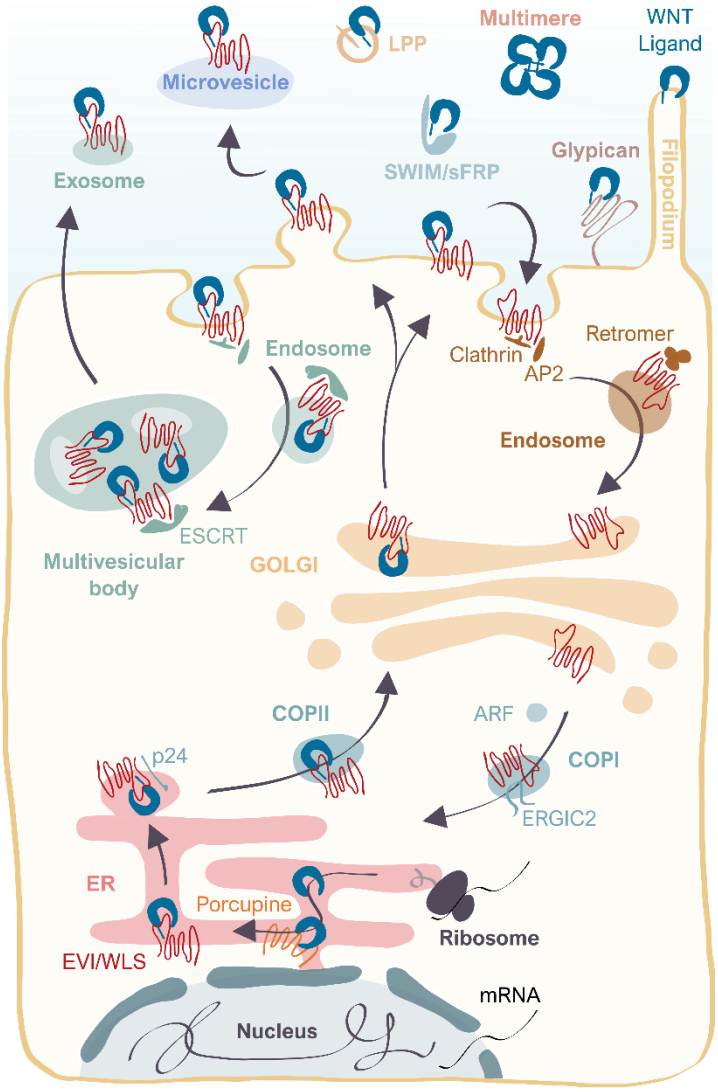

Figure 1. WNT ligand secretion is coupled to EVI/WLS and its recycling

WNT ligands are co-translationally imported into the endoplasmic reticulum (ER), where they are lipid-modified by the acyl-transferase Porcupine and associate with the cargo protein EVI/WLS. From the ER, WNTs and EVI/WLS travel to the Golgi apparatus with coat protein complex (COP) II vesicles and then to the plasma membrane. Several mechanisms for WNT ligand secretion or presentation on the cell surface with or without EVI/WLS have been proposed and it is conceivable that they operate in a context dependent manner. EVI/WLS is re-internalised from the plasma membrane with the help of clathrin and AP2 and shuttled back to the Golgi in a retromer-dependent process. From there, it is recycled back to the ER by ADP-ribosylation factor (ARF), endoplasmic reticulum-Golgi intermediate compartment protein 2 (ERGIC2) and COP I vesicles. In the ER, EVI/WLS can engage again with WNT ligands and assist in their secretion. See main text for further details and abbreviations.

(Routledge & Scholpp, 2019). Other observed ways for short-range signalling rely on the transport of WNTs in a cell membrane-bound manner by cell division (Farin et al., 2016) and through signalling filopodia, so-called cytonemes (Mattes et al., 2018).

It was also shown that active WNTs bound to EVI/WLS (or WNT or EVI/WLS alone) are secreted on exosomes after sorting to multivesicular bodies with the help of the endosomal sorting complexes required for transport (ESCRT) complex and the synaptobrevin homolog YKT6 (Gross et al., 2012; Korkut et al., 2009). This process was dependent on retromer and depletion of retromer led to the sorting of EVI/WLS to lysosomes (Gross et al., 2012). In general, several mechanism have been proposed that explain WNT long range transport by association of WNTs with other proteins or particles, ranging from transport on microvesicles and lipoprotein particles (LPP) to multimere formation and association with lipid-binding proteins, e.g. secreted wingless-interacting molecule (SWIM) or soluble FZD related proteins (sFRP, Routledge & Scholpp, 2019). Nevertheless, it remains unclear how WNTs are 'handed-over' to their receptor after they arrive at their target cell. This process probably involves several conformational changes (Routledge & Scholpp, 2019).

2.1.3.2 The WNT cargo protein EVI/WLS

It is commonly accepted that the transport of lipid-modified WNT ligands in the secreting cell depends on EVI/WLS, the only known dedicated WNT cargo protein (Najdi et al., 2012). Indeed, several examples demonstrate that WNT protein secretion is regulated by the availability of EVI/WLS protein (Galli et al., 2014, 2016; Glaeser et al., 2018). Despite this important function, only little is known about the structure and regulation of EVI/WLS. The human *EVI/WLS* gene (Genecode transcript: ENST00000262348.9) is located on the minus strand of chromosome 1. It encodes 12 exons and three different transcript variants with presumably overlapping but not identical functions (Petko et al., 2019). The canonical sequence (Uniprot ID: Q5T9L3-1) encodes a protein that is 541 amino acids in length and has a predicted mass of 63 kDa. However, the detected size of EVI/WLS in Western blots ranges rather from 35 kDa to 45 kDa and the difference remains unexplained.

EVI/WLS gene expression is regulated by SOX2 in human embryonic stem cells (Zhou et al., 2016), and while one early study also described *EVI/WLS* as being transcriptionally regulated by canonical WNT signalling in mice (Fu et al., 2009), this could not be confirmed in flies or humans (Glaeser et al., 2018; Herr & Basler, 2012). By contrast, Glaeser et al., 2018, showed that EVI/WLS protein levels increase after overexpression of WNT ligands due to posttranslational stabilisation through inhibition of ERAD. EVI/WLS is ubiquitinated by UBE2J2 and cell growth regulator with really interesting new gene (RING) finger domain protein 1 (CGRRF1), but the knock-down of both enzymes did not completely abolish EVI/WLS ubiquitination,

indicating the involvement of further proteins or residual enzyme activity (Glaeser et al., 2018). The degradation of EVI/WLS was mediated by a complex containing EVI/WLS, PORCN, and Valosin-containing protein (VCP/p97, Cdc48 in yeast), but it is still unclear how VCP is recruited to the complex or if additional interaction partners are involved (Glaeser et al., 2018). A recent study in *Caenorhabditis elegans (C. elegans)* found that K63-linked Ubiquitin was important for the transport and function of EVI/WLS, however without directly showing its ubiquitination or the presence of other linkage types (J. Zhang et al., 2018). Beside ubiquitination, EVI/WLS is also posttranslationally modified with N-linked oligosaccharides, but the exact amino acid position(s) of either modification have not been fully elucidated (Jin, Morse, et al., 2010).

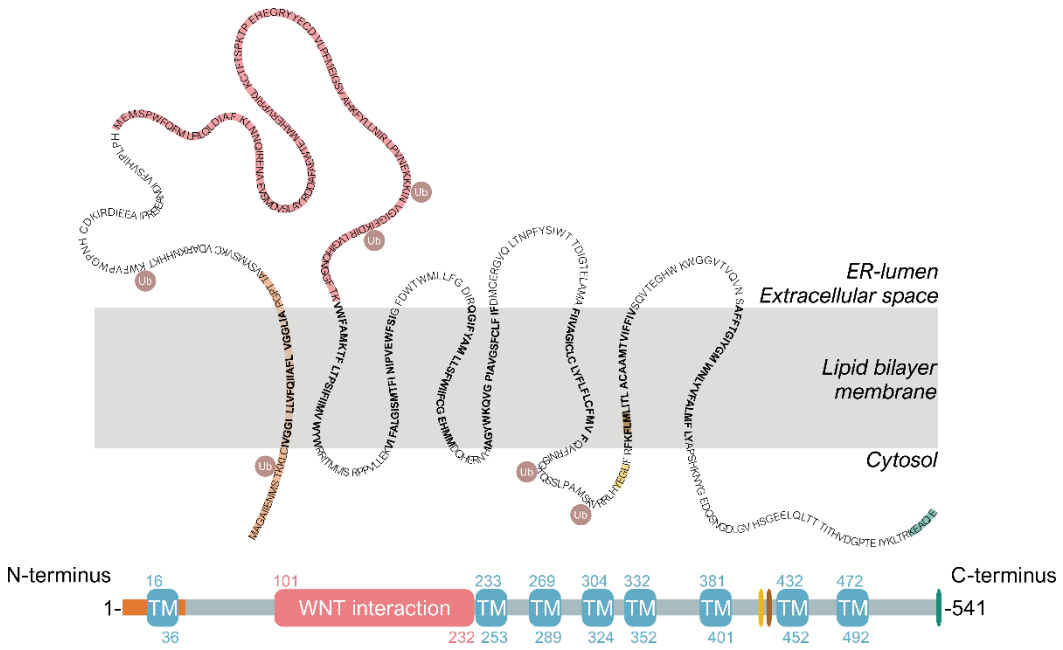

Figure 2. Protein structure of EVI/WLS with reported ubiquitination sites

EVI/WLS is an 8-pass transmembrane protein with a large, unstructured luminal loop close to its N-terminus. This loop is important for its binding to lipid modified WNTs (salmon colour). The first 42 amino acids (orange colour) were predicted to be the signal peptide (Das et al., 2012), but studies showed that it is not cleaved off (Jin, Morse, et al., 2010). The third cytosolic loop contains the internalisation motif YEGL (yellow colour) and the FLM motif (brown colour), which is important for the interaction with the retromer complex. The KEAQE sequence (teal colour) at the C-terminus is the signal for retrograde transport to the ER. Numbers indicate amino acid positions, TM = transmembrane domain, Ub = ubiquitin, topology according to UniProt ID: Q5T9L3, entry version 133

The N-terminus of EVI/WLS contains a putative signalling peptide which presumably regulates its co-translational insertion into the ER membrane (Figure 2). This sequence does not contain a cleavage site and experiments with N-terminal protein tags suggest that the 'signal peptide' is indeed not cleaved and still present in the mature protein, forming the first of eight transmembrane domains (Bartscherer et al., 2006; Jin, Morse, et al., 2010). This notion is supported by analyses that show that both the N- and the C-terminus face the cytoplasm, suggesting an even number of transmembrane domains (Jin, Morse, et al., 2010; Korkut et al., 2009). The first ER-luminal or extracellular loop at the N-terminus contains an unstructured

region required for the interaction of EVI/WLS with lipidated WNTs (Coombs et al., 2010; Fu et al., 2009; Herr & Basler, 2012). Modelling of this region by Coombs et al., 2010, suggested it had a structure similar to the lipocalin-family fold, however analysis in our lab could not recapitulate this (Michaela Holzem, personal communication). Additional important structural features are the YEGL and the FLM tripeptide motif in the third intracellular loop (Figure 2).

The former is recognised by adaptor protein 2 (AP-2) to initiate clathrin- and casein kinase (CK) 2-mediated internalisation of EVI/WLS from the plasma membrane (de Groot et al., 2014; Gasnereau et al., 2011; Pan et al., 2008). These carriers are destined to fuse with early endosomes, which play a major role in cargo sorting to either lysosomal degradation or recycling. The latter motif, FLM, is thought to be important for the interaction of EVI/WLS with the conserved heterotrimeric peripheral membrane protein complex retromer (Belenkaya et al., 2008; Franch-Marro et al., 2008; Port et al., 2008; P.-T. Yang et al., 2008). Under physiological conditions, EVI/WLS is recruited into recycling vesicles already at early endosomes by its interaction with the sorting nexin 3 (SNX3) retromer complex in a phosphatidylinositol-3-phosphate dependent manner (Harterink et al., 2011; Lorenowicz et al., 2014; P. Zhang et al., 2011). This special retromer variant requires a membrane remodelling complex composed of MON2, DOPEY2, and probable phospholipid-transporting ATPase IIA (ATP9A) to form transport carriers (McGough et al., 2018; Zhao et al., 2020). After retromer-dependent retrieval of EVI/WLS to the trans-Golgi network, it is recycled back to the ER by endoplasmic reticulum-Golgi intermediate compartment protein 2 (ERGIC2) and the COP I vesicle regulator ADP-ribosylation factor (ARF) in a process dependent on the KEAQE sequence at its C-terminus (see Figures 1 and 2, J. Yu et al., 2014).

The requirement of WNT signalling for development and homeostasis of multiple embryonic and adult tissue types explains the broad expression pattern of mammalian EVI/WLS (Jin, Morse, et al., 2010) and why its homozygous knock-out is embryonic lethal in mouse models (Carpenter et al., 2010; Fu et al., 2009). Conditional, tissue specific mouse models were developed and confirmed the importance of EIV/WLS for liver growth (Leibing et al., 2018), development of the pulmonary vasculature (Cornett et al., 2013; Jiang et al., 2013), or mammary development (Maruyama et al., 2013), among others. EVI/WLS was even implicated in drug addiction through its interaction with the mu-opioid receptor (Jin, Kittanakom, et al., 2010). Importantly, it is frequently overexpressed in various types of cancer (Augustin et al., 2012; Glaeser et al., 2018; Seo et al., 2018; Voloshanenko et al., 2013; H. Xu et al., 2016), and also regulates immune cell recruitment (Augustin et al., 2016). Conversely, EVI/WLS was found to be decreased in melanoma cell lines and patient samples compared to non-malignant controls

and its downregulation induced metastasis formation in a xenograft melanoma mouse model (P.-T. Yang et al., 2012).

2.1.4 β-catenin-dependent/canonical WNT signalling

β-catenin has two distinct cellular functions: on the one hand, it is part of the cadherin cell adhesion system at the plasma membrane (Peifer et al., 1992), on the other hand it is an important signalling molecule in the cytoplasm that can translocate into the nucleus (Behrens et al., 1996; Molenaar et al., 1996). β-catenin can be exchanged between these two pools (Grossmann et al., 2013) and is additionally constantly replenished by newly translated protein. The best-studied WNT-dependent signalling pathway, the 'canonical' pathway (Figure 3), relies on the accumulation of β-catenin in the cytoplasm and the subsequent activation of target gene expression in a tissue and context dependent manner. It mainly activates proliferation or differentiation, for example *via* the proto-oncogene *MYC* (He et al., 1998). A universal target gene is *axis inhibition protein (AXIN) 2*, which is also commonly used as a read-out for β-catenin-dependent WNT signalling activation (Lustig et al., 2002; Nusse & Clevers, 2017). In the absence of WNT ligands, cytoplasmic β-catenin is constantly targeted for degradation by the 'destruction complex' grouped around the scaffold protein AXIN (Ikeda et al., 1998; L. Zeng et al., 1997). AXIN and its interaction partners, most notably AXIN2, adenomatous polyposis coli (APC), and the two serine/threonine kinases glycogen synthase kinase-3 (GSK-3α/β) and CK 1α/δ, bind β-catenin and mediate its N-terminal phosphorylation (Behrens et al., 1998; Ikeda et al., 1998; Chunming Liu et al., 2002; Munemitsu et al., 1996). Phosphorylated β-catenin is recognised and ubiquitinated by β-transducin repeat-containing protein (β-TrCP), and subsequently degraded by the proteasome (Aberle et al., 1997; Kitagawa et al., 1999; Winston et al., 1999). Additionally, β-catenin can be ubiquitinated by other proteins and cause context-dependent effects (Chenxi Gao et al., 2014). In the absence of β-catenin in the nucleus, the transcription factors T cell factor (TCF) and lymphoid enhancer factor (LEF) repress transcription of their target sites by interaction with transducin-like enhancer protein (TLE, Groucho in Drosophila), among others (Cavallo et al., 1998; Roose et al., 1998).

Binding of canonical WNT ligands to FZD receptors and low-density lipoprotein-receptor-related proteins 5/6 (LRP5/6) induces the phosphorylation of LRP5/6 by GSK3 and CK1γ (Davidson et al., 2005; X. Zeng et al., 2005) and the recruitment of Dishevelled (DVL) to FZD (Tauriello et al., 2012). Thus, AXIN and other components of the destruction complex are recruited to the cell membrane and inhibited (Fiedler et al., 2011; Zhan et al., 2017). The hereby stabilised cytosolic β-catenin can then translocate into the nucleus, where it interacts with TCF/LEF and converts their repressive function transiently into transcriptional activation,

together with additional binding partners, e.g. B-cell lymphoma 9 (BCL9, J. Behrens et al., 1996; Kramps et al., 2002; Molenaar et al., 1996).

The abundance of FZD receptors at the plasma membrane determines WNT signalling and they are important targets of posttranslational regulation. The two homologous transmembrane Ub ligases RING finger protein (RNF) 43 and zinc and RING finger 3 (ZNRF3) ubiquitinate FZD receptors and LRP6 and thus initiate their lysosomal degradation. Secreted R-Spondin (RSPO) inhibits these two ligases by recruiting them to complexes with leucine-rich repeat containing G protein-coupled receptor 4/5 (LGR4/5), resulting in increased responsiveness of the cell towards WNT ligands (H.-X. Hao et al., 2012; Koo et al., 2012; Nusse & Clevers, 2017). WNT signalling can also be inhibited by secreted antagonists. Dickkopf (DKK) and Sclerostin (SOST) bind to LRP5/6, possibly interrupting the interaction with FZD receptors, and sFRP and WNT inhibitory protein (WIF) can interfere with WNTs directly (Glinka et al., 1998; Nusse & Clevers, 2017).

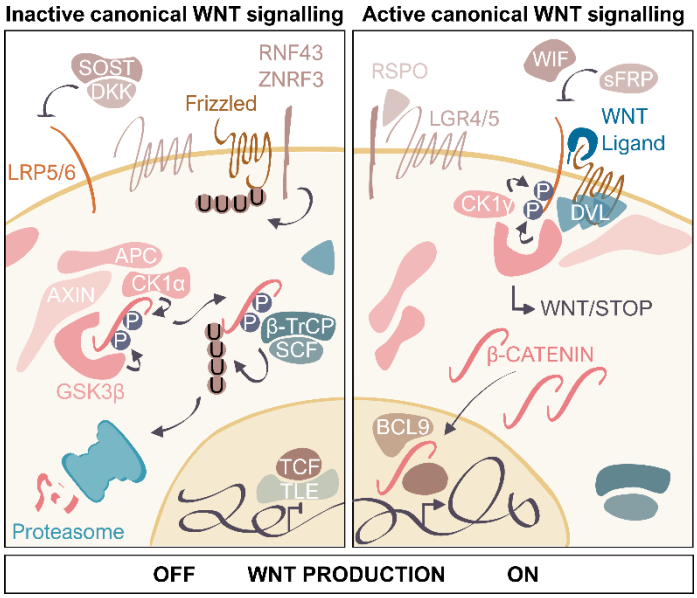

Figure 3. The canonical/β-catenin dependent WNT signalling pathway

The binding of WNT ligands to Frizzled and LRP5/6 receptors on the cellular surface of a WNT responsive cell leads to several downstream events and the inhibition of the β-catenin destruction complex, consisting of AXIN, APC, GSK3, and CK1. Subsequently, β-catenin accumulates in the cytoplasm and translocates into the nucleus to interact with TCF/LEF, thus activating transcription of cell type specific and context-dependent target genes. In the absence of WNT ligands, the destruction complex phosphorylates β-catenin, thus allowing its binding to the E3 ligase complex β-TrCP/SRC and its polyubiquitination and proteasomal degradation. Other inhibitors of canonical WNT signalling include the secreted factors DKK, SOST, WIF, and sFRP, which have various distinct modes of action. An important enhancer of the displayed signalling cascade is RSPO, which can bind to LGR4/5 and the E3 ligases RNF43 and ZNRF3, thus inhibiting the ubiquitination and degradation of Frizzled receptors and leading to increased abundance of the receptors. See main text or 6.4.1 for protein name abbreviations.

Importantly, the inhibition of GSK3 after the engagement of FZD and LRP5/6 with WNTs does not only activate β-catenin dependent signalling. In addition, it also prevents the phosphorylation, ubiquitination, and degradation of other GSK3 substrates and thus has an important role in various cellular processes, such as cell-cycle progression. This effect is called

WNT-dependent stabilisation of proteins (WNT/STOP) and is one of several alternative branches of this intricate pathway (Acebron & Niehrs, 2016).

2.1.5 Non-canonical WNT signalling by WNT5A and WNT11

In contrast to canonical WNT signalling, several so-called 'non-canonical' signalling pathways exist, which act downstream of FZD and DVL but do not primarily result in the stabilisation of β-catenin (Chan Gao & Chen, 2010). They have important instructive or permissive roles during embryonal pattern formation or cell migration, among others (Y. Yang & Mlodzik, 2015). In general, these pathways have no well-defined molecular endpoint and are therefore more difficult to analyse and less well studied (Voloshanenko et al., 2018). The best characterised non-canonical WNT ligands in vertebrates are WNT5A and WNT11. Notably, WNT5A can also regulate β-catenin, demonstrating the high degree of overlap and complexity of the WNT pathways (van Amerongen et al., 2012). To exemplify the function of non-canonical WNT signalling, the two most investigated branches, WNT-FZD/PCP and WNT/Ca^{2+}, are described in more detail below (Figure 4).

PCP is essential to break symmetry during embryonal development and to pattern functional complex organ structures. To achieve this, the core PCP components establish an asymmetric network of protein complexes across the membranes of neighbouring cells by simultaneously inhibiting each other within the same cell and stabilising each other in bordering cells. These core PCP components are FZD, Vang-like protein (VANGL), Cadherin EGF LAG seven-pass G-type receptor (CELSR), Prickle-like protein (PK), and DVL (Y. Yang & Mlodzik, 2015). In addition to this short-range signalling, the PCP components FZD and VANGL can also transduce long-range cues. To do so, WNT5A or WNT11 bind FZD and its co-receptors receptor tyrosine kinase like orphan receptor (ROR) 1/2, receptor like tyrosine kinase (RYK), or protein tyrosine kinase (PTK) 7 to recruit and activate DVL, which in turn relieves repression of the cytoplasmic protein DVL associated activator of morphogenesis 1 (DAAM1) and associates with small GTPases of the RAS homolog family (Rho, especially with RHOA and RAC1). They then trigger Rho-associated protein kinase (ROCK) and rearrangements of the cytoskeleton as well as JUN N-terminal kinase (JNK) and transcriptional regulation, for example by cyclic AMP-dependent transcription factor 2 (ATF2) and JUN phosphorylation (Boutros et al., 1998; Y. Yang & Mlodzik, 2015; Zhan et al., 2017).

WNT5A binding to ROR2 also activates VANGL by phosphorylation (Y. Yang & Mlodzik, 2015). Previously, it was suggested that the formation of a WNT ligand gradient was required for PCP during Drosophila wing development and that several WNTs had redundant functions in this process (J. Wu et al., 2013). However, recent studies described the formation of PCP in

the wing in the absence of WNT ligands, indicating that many of the underlying processes are still only rudimentary understood and suggesting that it might be important to reconsider the general role of WNT in PCP (Ewen-Campen et al., 2020; J. J. S. Yu et al., 2020).

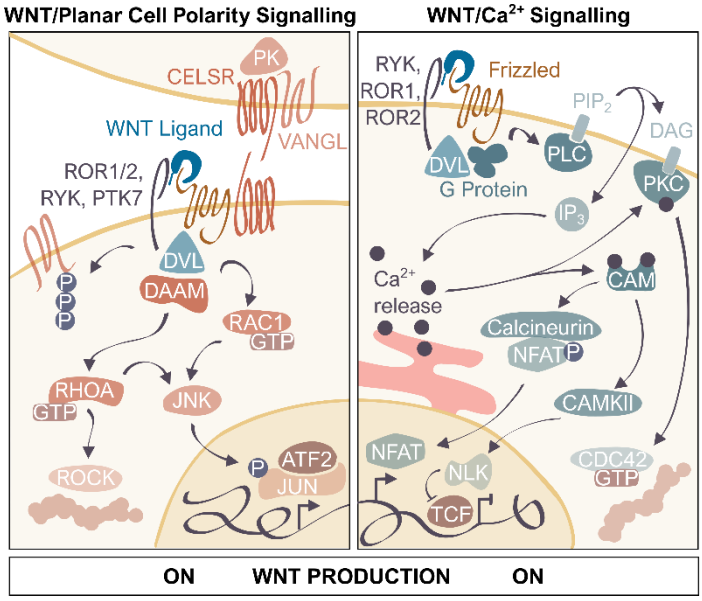

Figure 4. The 'non-canonical' WNT signalling pathways

The so-called 'non-canonical' WNT signalling pathways act downstream of Frizzled and Dishevelled (DVL) and do not primarily result in the stabilisation of β-catenin but have important roles during embryonal pattern formation or cell migration, amongst others. The core WNT/Planar Cell Polarity (PCP) components Frizzled, VANGL, CELSR, PK, DVL and the Diego orthologs Inversin and Diversin establish an asymmetric network of protein complexes by inhibiting each other in the same cell and stabilising each other in neighbouring cells. They can also transduce long-range signalling by WNT5A or WNT11 and ROR1/2, RYK, or PTK7. The subsequent recruitment and activation of DVL, DAAM1, Diego and several members of the Ras homolog family (especially RHOA and RAC1) leads to ROCK-dependent rearrangements of the cytoskeleton or JNK mediated transcriptional regulation.
WNT/Ca^{2+} signalling is initiated by WNT interaction with Frizzled and RYK, ROR1, or ROR2, which results in the intracellular activation of G protein and cleavage of PIP_2 by PLC into IP_3 and DAG. Binding of IP_3 with its receptor at the ER membrane triggers the release of Ca^{2+} and activation of PKC and CAM. This leads to actin rearrangements by CDC42 and the activation of transcriptional programmes via NFAT and NLK, which can inhibit the transcription factor TCF/LEF and canonical/β-catenin dependent signalling. See main text or 6.4.1 for protein name abbreviations and further details.

FZD proteins belong to the group of G protein-coupled receptors, and its attached heterotrimeric G protein is implicated in the recruitment of DVL and in various branches of WNT/FZD signalling, among them the WNT/Ca^{2+} pathway (Chan Gao & Chen, 2010; Xianjun Zhang et al., 2018). Engagement of WNT5A with FZD and non-canonical co-receptors (e.g. ROR2) results in the intracellular activation of G protein and subsequent cleavage of phosphatidylinositol-4,5-bisphosphate (PIP_2) by phospholipase C (PLC) into inositol 1,4,5-trisphosphate (IP_3) and diacylglycerol (DAG). Binding of IP_3 with its receptor at the ER membrane triggers the release of Ca^{2+} and thus initiates further downstream events, such as conformational changes of protein kinase C (PKC) and calmodulin (CAM, Sheldahl et al., 2003; Slusarski et al., 1997). The activation of PKC by Ca^{2+} together with its binding to DAG at the plasma membrane leads to the polymerisation of actin through the GTPase cell division control protein 42 (CDC42) and also has major effects on mechanocoupling between endothelial cells (Carvalho et al., 2019; Schlessinger et al., 2007). CAM can in turn activate calcineurin, a Ca^{2+}-dependent

phosphatase, and the Ca^{2+}/CAM-dependent kinase II (CAMKII). Calcineurin dephosphorylates nuclear factor of activated T cells (NFAT), thus stimulating its translocation into the nucleus, where it controls various signalling programmes. The interaction of NFAT with deoxyribonucleic acid (DNA) is inhibited by GSK3β-mediated phosphorylation (J. W. Neal & Clipstone, 2001). It plays an important role in cancer, for example by mediating resistance to apoptosis or dedifferentiation (Griesmann et al., 2013; Perotti et al., 2016). CAMKII activates nemo-like kinase (NLK), which can inhibit the transcription factor TCF/LEF by phosphorylation in the nucleus and thus impacts on canonical/β-catenin dependent signalling (Ishitani et al., 2003).

2.1.6 Deregulated WNT signalling and melanoma

Multi-layered misappropriation of autocrine, paracrine, or even endocrine cellular communication is cause or consequence of many 'hallmarks of cancer', for example when the tumour sustains its own proliferative signalling, activates invasion and metastasis, or escapes immune surveillance (Hanahan & Weinberg, 2011). WNT1 itself was first discovered as a proto-oncogene in mouse mammary tumours (Nusse & Varmus, 1982) and WNT signalling was later implicated in the pathogenesis of various tumours, most prominently in colorectal cancer, where nearly all cases harbour alterations in WNT signalling components (Schatoff et al., 2017; Zhan et al., 2017). In contrast, the role of WNT signalling in melanoma seems to be less causative and more modulatory but is still only incompletely understood and requires further investigation (Webster et al., 2015).

2.1.6.1 Cutaneous melanoma

Cutaneous melanoma is a type of non-epithelial skin cancer that originates from melanocytes, neural crest derived cells that reside (among other locations) in the skin's epidermis with close connection to the basement membrane and are responsible for skin colour (Schadendorf et al., 2015; J. X. Wang et al., 2016). Cutaneous melanoma is a common disease with an incidence of 10.2 and 13.8 per 100 000 person-years in 2012 in the European Union and North America, respectively, and responsible for the majority of skin cancer-related deaths (ca. 60 % in the United States of America, USA, in 2020, excluding basal-cell and squamous cell carcinoma, Schadendorf et al., 2018; Siegel et al., 2020). This is surprising, considering that clinical diagnosis and surgical management of patients with non-metastatic melanoma are at a very high level in central Europe and the USA, which results in a favourable outcome with a 5-year survival rate after primary diagnosis of over 90 % (Schadendorf et al., 2015; Siegel et al., 2020). However, patients with metastatic melanoma faced very poor prognosis and a median survival of only 6 months to 12 months until the early 2010s (Schadendorf et al., 2015). In the USA, the overall mortality rate of cutaneous melanoma dropped by 6.4 % in the years 2013 to 2017

(Siegel et al., 2020) and the 5-year overall survival rates for melanoma with distant metastasis increased from below 10 % to up to 40 % or higher by 2018 (Schadendorf et al., 2018). This unprecedented improvement in melanoma patient care is mainly attributed to better understanding of the molecular mechanisms of melanoma carcinogenesis and the according development and approval of targeted therapies.

The development of melanocytic neoplasms is driven by the sequential accumulation of point mutations and copy-number alterations. In many cases, the activating BRAF p.V600E mutation can already be found in benign precursor lesions and is accompanied in later intermediate stages by mutations in the *telomerase reverse-transcriptase (TERT)* promotor and by the biallelic inactivation of *cyclin-dependent kinase-inhibitor 2A (CDKN2A)* in invasive melanoma. Metastatic melanoma is additionally characterised by mutations in *phosphatase-and-tensin homologue (PTEN)* and *tumour-protein p53* (Hodis et al., 2012; Schadendorf et al., 2018; Shain et al., 2015). In general, the point mutation burden and the number of mutations with ultraviolet (UV) radiation signature (e.g. C → T nucleobase exchange) is particularly high in many cutaneous melanomas compared to other cancers and reflect sun-induced damage (Alexandrov et al., 2013; Shain et al., 2015). The hyperactivation of the MAPK pathway is the main driver of melanomas and only 10 % of cases do not harbour mutations in either *BRAF* (ca. 50 % of melanoma cases), the *RAS* genes (*NRAS*, *KRAS*, *HRAS*, ca. 25 % of melanoma cases), or *Neurofibromin-1* (ca. 15 % of melanoma cases), which is a negative regulator of RAS (Schadendorf et al., 2018). Another important characteristic of melanoma cells is immune evasion by inhibiting the antitumour immune response, for example by activating the programmed cell death protein 1 (PD-1) immune checkpoint through the expression of PD-1 ligands (Hassel et al., 2017). Accordingly, a combination therapy of BRAF and MEK inhibitors are now routinely used in the clinics to target the MAPK pathway and several immune checkpoint inhibitors are being implemented with great success (Schadendorf et al., 2018). However, not all patients benefit from these exciting developments and there are only few treatment options available for patients without overactivation of the MAPK pathway. Moreover, many patients develop resistance against BRAF- and MEK-inhibitors, leading to rapid relapse. Recent studies indicate that a large subset of patients do not respond to checkpoint inhibition and/or develop severe adverse events (Schadendorf et al., 2018; Wagle et al., 2011). This shows that the treatment of metastatic melanoma remains a major challenge and that further investigations of underlying pathomechanisms are required.

2.1.6.2 WNT signalling and phenotype switching in melanoma cells

Melanocytes are neural crest derived cells that require WNT/β-catenin signalling for their embryonic induction and depend on WNT/PCP signalling *via* WNT5A and WNT11 for their migration to the target tissue (Baker et al., 1997; De Calisto et al., 2005; Ikeya et al., 1997; Ji et al., 2019; Ossipova & Sokol, 2011). Later during development, WNT/β-catenin signalling is important for melanocyte lineage specification by regulation of the transcription of *microphthalmia-associated transcription factor* (*MITF*) and its downstream targets, such as *premelanosome protein* (*PMEL*), *melan-A* (*MLANA*), and *tyrosinase* (*TYR*, Gajos-Michniewicz & Czyz, 2020; Hari et al., 2002; Kawakami & Fisher, 2017; Steingrímsson et al., 2004; Widlund et al., 2002). Additionally, adult epidermal keratinocytes can secrete the canonical WNT7A ligand upon UV-light irradiation to induce the differentiation of melanocytes from multipotent, dermal precursor cells (J. X. Wang et al., 2016).

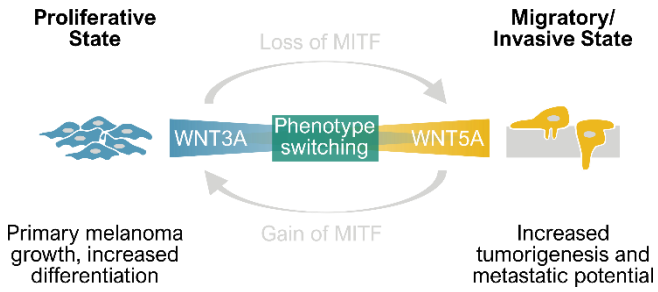

Figure 5. The phenotype switching model of melanoma pathogenesis
Melanoma cells can rewire their signalling programmes according to external cues and thus adopt a more 'proliferative' or 'migratory/invasive' state. This so called 'phenotype switching' is associated with the expression of canonical WNT3A or non-canonical WNT5A and respective gain or loss of microphthalmia-associated transcription factor (MITF) expression.

Considering that WNT signalling is required for melanocyte differentiation and migration, it is not surprising that its role in melanoma tumorigenesis has also become more and more apparent, albeit it is far from being understood. In general, the occurrence of mutations in the β-catenin gene (*CTNNB1*) or other WNT signalling pathway components are low and thus, they are not considered to be main drivers of melanoma progression (Gajos-Michniewicz & Czyz, 2020). Nevertheless, researchers have unravelled a highly sophisticated dependency of melanoma on canonical and non-canonical WNT signalling in different stages of the disease. Canonical WNT3A signalling is assumed to be necessary for melanoma initiation but it inhibits disease progression in later stages. Furthermore, switching from canonical to non-canonical signalling (e.g. *via* WNT5A expression) has been demonstrated to allow metastasising of the tumour (Grossmann et al., 2013; M. P. O'Connell et al., 2010; O'Connell & Weeraratna, 2009; Weeraratna et al., 2002). This so-called 'phenotype switching' hypothesis (Figure 5) affects not only WNT signalling, but general transcriptional networks in melanoma cells (Hoek et al., 2008). It has replaced the idea of cancer stem cells in melanoma after it was shown that a large proportion (25 % to 28 %) of melanoma cells have tumourigenic potential and no hierarchical organisation (Quintana et al., 2010, 2008; Restivo et al., 2017). In contrast to these findings

concerning WNT ligand expression, studies on the role of WNT secretion demonstrated that cell proliferation and metastasis formation is enhanced upon *EVI/WLS* knock-down (and reduced secretion of WNT5A) in a mouse xenograft model using the A375 cell line (P.-T. Yang et al., 2012). The authors further show decreased EVI/WLS levels in patient tumours and melanoma cell lines compared to healthy controls (P.-T. Yang et al., 2012). This apparent discrepancy remains mostly unexplained.

The role of β-catenin in melanoma is controversial: several studies indicated a positive correlation of nuclear β-catenin, dependent on WNT3A, with patient survival (Chien et al., 2009) and a reduction of β-catenin-dependent activity of MITF with a more invasive phenotype and poor prognosis (Carreira et al., 2006; Hartman & Czyz, 2015). By contrast, other studies argue that β-catenin dependent signalling is associated with the formation of metastases and a more aggressive disease (Damsky et al., 2011). Grossman et al., 2013, used a gelatin degradation assay to show that stabilisation of β-catenin increased melanoma cell invasiveness. This assay relies on the formation of actin-based, proteolytic protrusions that are called podosomes in healthy cells or invadopodia in cancer (Paterson & Courtneidge, 2018). The pathophysiological activity of these protrusions is reflected by the amount of degraded underlying extracellular matrix after the formation of F-actin, cortactin, and SH3 And PX Domains 2A (SH3PXD2A/TKS5) positive puncta and the secretion of matrix metalloproteases (MMPs, Iizuka et al., 2016; Paterson & Courtneidge, 2018). In melanoma, invadopodia formation and activity is regulated by activation of the MAPK signalling pathway through BRAF p.V600E, CDC42, and SH3PXD2A/TKS5, which suggests the convergence of various signalling pathways (Grossmann et al., 2013; Iizuka et al., 2016; H. Lu et al., 2016; Nakahara et al., 2003). Furthermore, the efficacy of checkpoint inhibitors depends on the tumour-infiltrating lymphocytes and it was shown that T cell exclusion is regulated by tumour cell mediated WNT/β-catenin signalling (Spranger et al., 2015). These partly contradictory results most likely originate from context-dependent differences and an insufficient mechanistic knowledge of the cross-regulation of canonical and non-canonical WNT pathways in melanoma.

2.2 Ubiquitin and Ubiquitination

Post-translational modifications (PTMs) of proteins are a powerful, dynamic way to regulate signalling, protein turnover and other fundamental cellular processes. A plethora of PTMs has been identified that ranges molecularly from covalent attachment of small chemical modifications, for example phosphate groups, to sugars or lipids, and to polypeptides and small proteins, among them Ubiquitin (Ub). Ub and Ub-like proteins, such as Small Ub-like Modifier

(SUMO) or Neural Precursor Cell Expressed Developmentally Down-regulated Protein 8 (NEDD8), have been intensively studied in the past, and current research still continues to unravel novel insights into their role in signal transduction, disease, and their reciprocal interaction and regulation, among others (Baek et al., 2020; Barysch et al., 2019; Tatham et al., 2008).

2.2.1 Ub and Ub-binding domains

The discovery of Ub (Goldstein et al., 1975) and its covalent attachment to other proteins (Goldknopf & Busch, 1977; Hunt & Dayhoff, 1977), a process known as ubiquitination, were seminal findings that changed how researchers perceive PTMs. Since then, ubiquitination has been implicated in most cellular functions, among them cell cycle progression, endocytosis, and protein degradation (Dikic et al., 2009; Komander & Rape, 2012).

Ub consists of 76 amino acids and is conserved among eukaryotes, with only 3 amino acid changes between yeast and human (Ciechanover et al., 1984; Özkaynak et al., 1984). Various hydrogen bonds and a hydrophobic core mediate its very stable β-grasp fold (see Figure 7), while the exposed, flexible C-terminus can bind covalently to target proteins or to other Ub molecules (Komander & Rape, 2012; Vijay-Kumar et al., 1987). Ub moieties are recycled after use to replenish the free cellular Ub pool or synthesised de-novo from four mammalian Ub precursor genes (Clague et al., 2019; Grou et al., 2015).

A multitude of Ub-binding domain (UBD) containing proteins interact non-covalently with mono- or poly-Ub modifications and channel downstream effects through the induction of conformational changes (Dikic et al., 2009).

2.2.2 The ubiquitination cascade

Ubiquitination of target proteins is a multi-step process involving three separate enzyme activities: E1, E2, and E3 (Figure 6). In a first endothermic reaction, the Ub activating enzyme (E1) forms a thioester with the C-terminus of Ub (Ciechanover et al., 1981). Then, Ub is transthiolated to a cysteine in the active site of the Ub conjugating enzyme (E2~Ub) and finally to its target substrate with the help of a Ub ligase (E3, Hershko et al., 1983; Metzger et al., 2012). Typically, the ε-amino group of a lysine in the target polypeptide forms a stable isopeptide bond with the carboxy group at Ub's C-terminus after a nucleophilic attack. However, ubiquitination can also occur at other nucleophilic amino acids (threonine, serine, cysteine) or at the N-terminus of proteins (Metzger et al., 2012).

Up to now, the vertebrate genome was found to encode 2 E1s (Jin et al., 2007) that load about 35 E2s with Ub (van Wijk et al., 2009), which interact with over 600 E3s. E3s are

particularly numerous and determine the exquisite substrate specificity of the ubiquitination machinery (W. Li et al., 2008; J. Weber et al., 2019). Three families of E3s have been defined based on their mode of action: RING-type/U-box ligases essentially build a scaffold to enable the transfer of Ub from E2 to the substrate. They are the most numerous type of E3s in vertebrates (W. Li et al., 2008). Homologous to E6AP carboxy-terminus (HECT)-type E3s function by first receiving the Ub from the E2 to their active site and then passing it on to the target protein (Metzger et al., 2012). RING between RING (RBR)-type ligases are a hybrid of the other two (Zheng & Shabek, 2017). Additionally, multiubiquitin chain assembly can be catalysed by so-called E4 enzymes (e.g. UBE4A/UBE4B), which elongate Ub-chains by forming branching points (Koegl et al., 1999; Chao Liu et al., 2017). Some E2, e.g. UBE2K, possess the ability to transfer Ub to client proteins without the involvement of an E3 (Z. Chen & Pickart, 1990; Middleton & Day, 2015). It is worth noting that the initial attachment of Ub to the target substrate (priming) is mechanistically different from the elongation of Ub chains and can involve different enzymes (Deol et al., 2019; A. Weber et al., 2016).

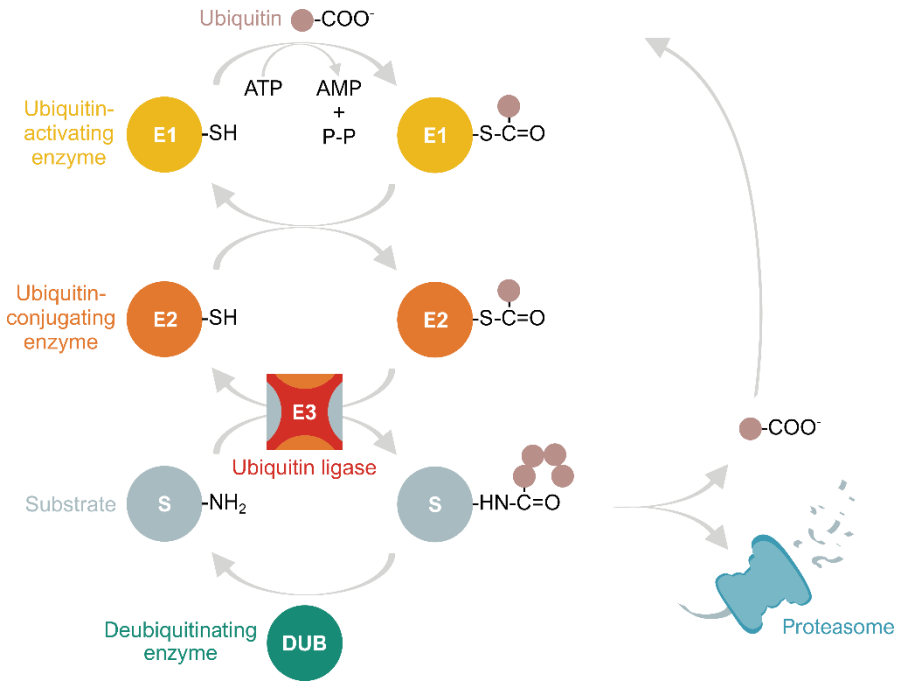

Figure 6. The ubiquitination cascade

Ubiquitin (Ub) is conjugated to target substrates by the coordinated action of enzymes with three main activities: E1, E2 and E3. First, the Ub activating enzyme (E1) uses adenosine triphosphate (ATP) as source of energy to form a thioester with the C-terminus of Ub, which is then transferred to the Ub conjugating enzyme (E2) and to the substrate with the help of the Ub ligase E3. Repeating this process several times can lead to the formation of polyubiquitin chains. This can have various outcomes, one of which is proteasomal degradation of the substrate and recycling of Ub. Deubiquitinating enzymes (DUBs) can remove Ub from substrates or conjoined Ub molecules, thus influencing the substrate's fate. AMP = adenosine monophosphate, P-P = pyrophosphate

Ubiquitination is a reversible PTM and about 100 deubiquitinating enzymes (DUBs) have been described, which can hydrolyse the (iso)peptide bond between Ub and the modified protein or conjoined Ub molecules. Thus, Ub can be recycled and the target protein can be

channelled to different routes (Figure 6). DUB proteases are mainly classified as cysteine proteases or, less common, zinc-dependent metalloproteinases, and some DUBs only cleave selected linkage types and can be used for molecular analysis (Clague et al., 2019).

The target protein's fate is decided by the interplay of ubiquitination, de-ubiquitination, and interaction with Ub-binding proteins and their balance is crucial for cellular homeostasis.

2.2.3 Linkage types and non-lysine ubiquitination

Ub modifies and interacts with various proteins to achieve its diverse repertoire of downstream effects. Monoubiquitination, the modification with a single Ub molecule, is very common and it is estimated to engage about 60 % of all cellular Ub in HEK293 cells, representing a commonly used human cellular model (Clague et al., 2015). It can regulate protein interactions and localisation of target proteins, e.g. of EGFR (Haglund et al., 2003; Huang et al., 2007). Importantly, Ub can be conjugated to other Ub molecules and form poly-Ub chains *via* seven internal lysine (K) residues (K6, K11, K27, K29, K33, K48, and K63) or its N-terminus (Figure 7A). Ub bound in such chains comprise about 11 % of total cellular Ub in HEK293 cells (Clague et al., 2015). These Ub-chains can be homotypic and only contain one linkage type or heterotypic when linkage types are mixed (Swatek & Komander, 2016).

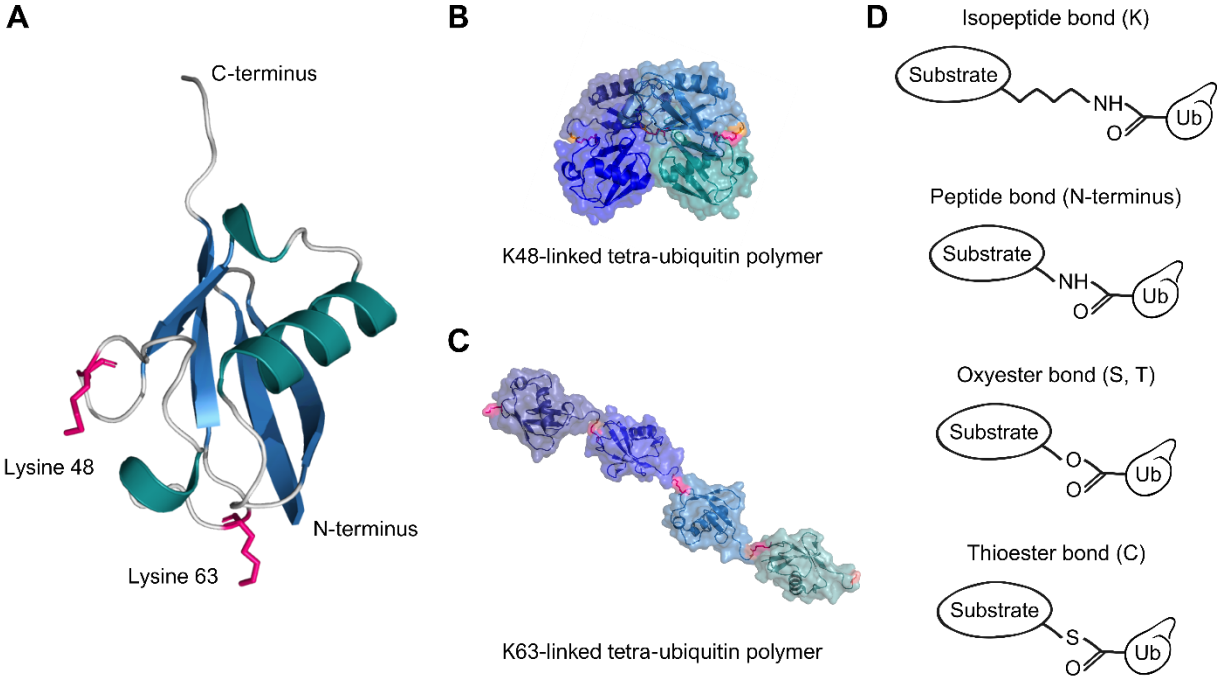

Figure 7. Ubiquitin linkage types and chemical bonds

A. Ribbon representation of ubiquitin (Ub), with lysine (K) residues K48 and K63 highlighted in pink. They are most frequently used to form poly-Ub chains (Protein Data Bank, PDB, identifier 1UBQ).

B, C. Surface and ribbon representations of tetra-Ub polymers with K48- (**B,** PDB identifier 2O6V) or K63 linkage (**C,** PDB identifier 3HM3) show distinct spatial orientation. The C-terminal glycine (pink) and linked K residues (orange) are highlighted.

D. Ub is linked to its substrates *via* distinct chemical bonds, depending on the involved amino acid or protein structure.

Molecule representations based on crystallographic data using PyMOL. N-terminus = amino terminus, C-terminus = carboxy terminus, C = cysteine, S = serine, T = threonine

The linkage type strongly affects the spatial orientation of Ub chains (Figure 7A,B,C) and thus allows or excludes their interaction with UBD containing proteins and mediates downstream effects (Dikic et al., 2009). The two most common Ub-chain types observed in cells are linked *via* K48 or K63 (Clague et al., 2015) and historically, they were described to be either proteolytic (K48) or involved in signal transduction and endocytosis (K63). However, more recent studies showed that multiple linkage types can cause protein degradation, including K63-linked chains, or have various other roles in cell physiology (Swatek & Komander, 2016).

The type of Ub-Ub linkage is mostly determined by the E2 enzyme and how E2, E3, Ub, and substrate are sterically oriented (Deol et al., 2019). Some E2s specifically catalyse a certain linkage type, e.g. UBE2K forms K48-linked poly-Ub chains while UBE2N cooperates with the catalytically inactive UBE2V1 or UBE2V2 to make K63-linked chains (Andersen et al., 2005; Clague et al., 2015). One Ub moiety can even be conjugated to two Ubs, thus leading to branched or forked chains (H. T. Kim et al., 2007). Mass-spectrometry based quantification approaches demonstrated that chains with K48-K63 branched linkages are common in mammalian cells and can influence cellular signalling and protein degradation (Ohtake et al., 2016, 2018).

To increase complexity, ubiquitination can occur at non-lysine residues, e.g. when the E2 enzyme UBE2J2 catalyses the formation of an oxyester bond (Figure 7D) between Ub and the hydroxylated amino acids serine or threonine (Cadwell & Coscoy, 2005; X. Wang et al., 2009; A. Weber et al., 2016). Recently, such non-lysine Ub modifications were reported for the first time in higher eukaryotes (Pao et al., 2018). Furthermore, Ub can carry other PTMs, such as phosphorylation or acetylation (Clague et al., 2019). The above mentioned factors are collectively referred to as the 'Ub Code' (in the style of the 'histone code') and govern distinct cellular consequences for the Ub-labelled substrates (Komander & Rape, 2012).

2.3 Ub-mediated protein degradation

The concept of energy-dependent protein turnover dates back to early studies in the 1940s and 1950s (Schoenheimer, 1942; Simpson, 1953), but did not attract a lot of attention at first. Many years later, the physiological role of protein degradation in cellular homeostasis was demonstrated in experiments about muscle atrophy (Goldberg, 1969a, 1969b), followed by many methodological innovations (Etlinger & Goldberg, 1977). These helped Aaron Ciechanover, Avram Hershko and Irwin Rose to overcome the notion that Ub itself (which they called APF-1, Active Principle of Fraction 1) was an adenosine triphosphate (ATP)-dependent protease. Rather, energy is used to conjugate Ub to target substrates or other Ub-molecules,

followed by protein degradation (Ciechanover et al., 1980, 1978; Hershko et al., 1980). For this discovery, they were awarded the Noble Prize in Chemistry for 2004 (Karigar & Murthy, 2005). Nowadays, two main protein degradation machineries are distinguished that function independently but are interlinked: the Ub-proteasome system and autophagy (Pohl & Dikic, 2019).

2.3.1 The Ub-proteasome system (UPS)

Whereas the autophagic degradation system is mainly in charge of large, cytosolic structures, the UPS is the destination of single, short-lived polypeptides (Dikic, 2017; Pohl & Dikic, 2019). It was estimated that the proteasome degrades up to 30 % of newly translated proteins, which do not fulfil the cellular quality control standards (Kleiger & Mayor, 2014). The proteasome mostly used in mammals is the 26 S proteasome and consists of the 20 S proteasome core subunit and the 19 S regulatory subunit. The regulatory component's main tasks are to recognise and bind substrates with Ub tag and prepare them for proteolysis by ATP-dependent unfolding and cleaving off of the Ub modifications. The minimal Ub signal for proteasomal targeting is currently under debate and the 'Ub threshold' model was proposed to explain the observation that the number of substrate-conjugated Ub molecules seems to be more important than the prevalent linkage type (Swatek & Komander, 2016). After being threaded into the enclosed cavity of the core particle, the substrate is digested into 2 to 24 amino acid long peptides by three catalytically active subunits (Dikic, 2017).

Proteasomal degradation is required for several essential cellular functions: (i) elimination of key regulatory proteins (e.g. β-catenin), and thus regulating signalling, transcription, cell cycle progression, and cell survival, (ii) removal of misfolded or damaged proteins, (iii) recycling of amino acids, (iv) generation of peptides for antigen presentation by major histocompatibility complex (MHC) class I molecules (Dikic, 2017; Rock et al., 1994).

The development of selective proteasome inhibitors, such as MG132 (Rock et al., 1994), greatly advanced our current understanding of the proteasome as a primary proteolytic route and its role for proteome integrity. Another proteasome inhibitor, Bortezomid, is also used in the clinics to treat multiple myeloma, because malignant plasma cells produce high amounts of antibodies without control and therefore have a higher level of ER stress than healthy cells. Inhibiting the proteasome increases this stress and the subsequent stress response leads to cell death (Dikic, 2017; Hungria et al., 2019).

2.3.2 ER-associated degradation (ERAD)

Proteomic studies suggest that one-fourth to one-third of eukaryotic proteins belong to the secretory pathways and are co-translationally translocated into the ER or its membrane

(Ghaemmaghami et al., 2003; Juszkiewicz & Hegde, 2018; Thul et al., 2017). These proteins often undergo elaborate and error prone folding and assembly steps before they reach maturity. Extensive ER quality control mechanisms are important to help them fold in their correct structure or recognise and remove terminally misfolded or unassembled polypeptides. The extraction and destruction of such potentially dangerous proteins is a highly sophisticated process called ERAD and it relies on a network of functionally diverse proteins in different cellular compartments, including the UPS. As shown in Figure 8, the most important steps are: (i) recognition of clients, followed by their (ii) ubiquitination, (iii) dislocation from the ER membrane into the cytosol, (iv) delivery to the proteasome, and (v) proteasomal degradation (Christianson & Ye, 2014; Hirsch et al., 2009).

Importantly, the removal of proteins from the ER can also influence cellular signalling if it affects functionally mature proteins and thus controls their abundance and availability. This mechanism is called regulatory ERAD and presumably functions similar as ERAD of misfolded proteins. The underlying concepts, and some of the involved proteins, are functionally conserved in related degradation mechanisms, for example the recently discovered endosome and Golgi-associated degradation (EGAD, Schmidt et al., 2019). Furthermore, some misfolded proteins elude the ERAD machinery, e.g. by forming large aggregates that cannot pass the ER membrane. These so-called ‘ERAD-resistant proteins’ can be cleared from the ER by autophagy and lysosomal degradation (Fregno & Molinari, 2019). ‘ER-phagy’, the process of autophagic degradation of ER components, was shown to be an important part of the ER stress response and likely plays a role in several diseases, including cancer (Hübner & Dikic, 2020).

Potential substrates that escape from the ER and reach the Golgi can be subjected to ‘Golgi quality control’ mechanisms and face degradation by proteasomes or lysosomes. After the Golgi, only quality control mechanisms at the plasma membrane (leading to lysosomal degradation) can catch misfolded or overabundant client proteins. It should be noted that substrates are constantly shuttled between these compartments and many open questions remain regarding the underlying processes of these distinct but overlapping control mechanisms (Z. Sun & Brodsky, 2019).

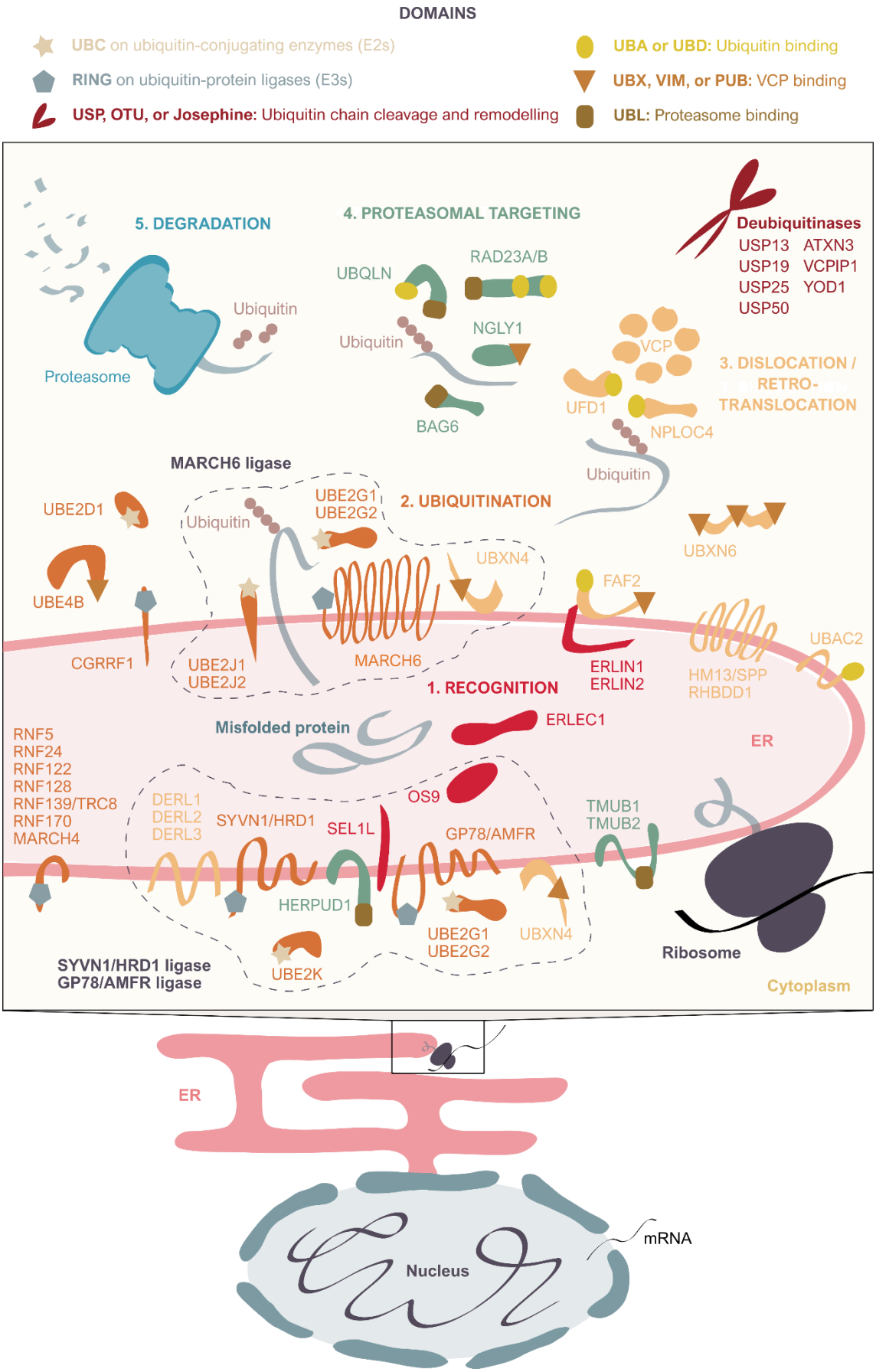

Figure 8. Components of the endoplasmic reticulum (ER) associated degradation (ERAD) pathways
(refer to next page for figure legend)

◄ previous page | Figure 8. Components of the endoplasmic reticulum (ER) associated degradation (ERAD) pathways
Proteins within the secretory routes or transmembrane domain containing proteins are imported into the ER co-translationally. Polypeptides that do not acquire their native fold in a timely manner and thus fail to pass scrutiny by the ER resident protein quality control mechanisms are targeted to ERAD by the proteasome in the cytoplasm. By passing misfolded proteins through an elaborate network of various interaction partners, this process ensures safe and accurate delivery of its substrates. Recurrent protein domains mark the various steps of this process. The five major steps include (1) client recognition, (2) ubiquitination, (3) dislocation/retrotranslocation, (4) targeting to the proteasome, and (5) degradation. According to the substrate, these steps depend on each other and/or presumably occur in parallel (e.g. ubiquitination and dislocation or proteasomal targeting and degradation). However, different substrates can take distinct routes out of the ER and interact only with a subset of the indicated proteins, which is not always well defined. Importantly, mature and properly folded proteins can undergo quantity control by ERAD which regulates cellular signalling, a process called regulatory ERAD. See main text or 6.4.1 for protein name abbreviations and further details.

2.3.2.1 Protein folding and recognition of ERAD clients

In the ER, newly synthesized polypeptides interact with chaperones and proteins associated with oligosaccharides already during translation and translocation. Directly after ER entry, oligosaccharyltransferases (OSTs) attach a 14-part sugar modification to most polypeptides on an asparagine-residue (N) in a short consensus sequence (Hebert & Molinari, 2012). Sequential trimming of the oligosaccharide moieties and concurrent binding of different ER-resident proteins, for example the lectins calnexin (CNX) and calreticulin (CLR), or heat shock protein 70 kDa (HSC70)-like chaperons (such as binding immunoglobin protein, BiP), help the polypeptide to reach its native form and bury exposed hydrophobic patches (Daniels et al., 2003; Hirsch et al., 2009). Proteins with correct folding are shuttled to their final destination by the export machinery.

Glycoproteins that linger in the ER for too long and do not acquire their native fold are processed by ER-resident mannosidases, e.g. members of the ER degradation-enhancing α-mannosidase-like 1 protein (EDEM) family and others. The consecutive removal of mannose molecules from the initial 14-part oligosaccharide exposes binding motifs for amplified in osteosarcoma 9 (OS-9, Yos9 in yeast) and ER lectin 1 (ERLEC1/XTP3-B), which in turn bind to the adaptor protein suppressor of lin-12-like protein 1 (SEL1L) *via* their mannose 6-phosphate receptor homology (MRH) domains (Christianson et al., 2008; Cormier et al., 2009; Hebert & Molinari, 2012). SEL1L is part of a supramolecular protein complex including the membrane-bound ERAD E3 ligase synoviolin (SYVN1/HRD1), which can mediate the poly-ubiquitination of substrates and their dislocation back into the cytoplasm (Hebert & Molinari, 2012). There are further studies suggesting that SEL1L and others might be themselves substrate of ERAD in a process called ERAD tuning (Hebert & Molinari, 2012).

2.3.2.2 ERAD-associated E3 Ub ligase complexes and their E2 partners

In yeast, only two E3 ligase complexes are responsible for the degradation of most client proteins from the ER: degradation of α2 protein (Doa10) and β-hydroxy β-methylglutaryl coenzyme A (HMG-CoA) reductase degradation protein 1 (Hrd1). Additionally, the amino acid sensor-independent (Asi) complex controls protein quality at the nuclear envelope, which is

continuous with the ER membrane. However, no mammalian ortholog has been identified for this yeast complex (Hampton et al., 1996; Mehrtash & Hochstrasser, 2019). The best studied E3 complexes in mammals are the Doa10 ortholog membrane-associated RING-CH protein VI (MARCH6) and the two orthologs of Hrd1, SYVN1/HRD1 and glycoprotein 78 (AMFR/GP78), but so far at least 25 ER membrane-bound E3 ligases were identified in human cells (Fenech et al., 2020). A recent proteomic-based screen uncovered over 450 interaction partners of these E3s, many of them previously unknown. Considering that these interaction networks vary greatly between different E3, it is very likely that their modes of action also differ substantially from the well-studied SYVN1/HRD1 (Fenech et al., 2020). As one result of this study, it was discovered that the WNT cargo protein EVI/WLS is degraded *via* ERAD with the help of CGRRF1, an ER-membrane resident E3 ligase (Glaeser et al., 2018). CGRRF1 was later also implicated in the ubiquitination and degradation of EGFR (Lee et al., 2019) and in the general ER-stress response (Fenech et al., 2020).

The main ERAD associated E2 Ub conjugating enzymes in yeast are the membrane tethered Ubc6 (human UBE2J1 and UBE2J2) and the cytosolic Ubc7 (human UBE2G1 and UBE2G2), which binds the ER-membrane anchored coupling of Ub conjugation to ER degradation 1 (Cue1) and catalyses the formation of K48-linked Ub chains, which are transferred to substrates *en bloc* (Deol et al., 2019; Hirsch et al., 2009; Mehrtash & Hochstrasser, 2019). A recent functional genetic screen in human cells found that UBE2G2 was involved in the degradation of all investigated ERAD substrates (Leto et al., 2019) and it was shown to interact with AMFR/GP78 and MARCH6 (Mehrtash & Hochstrasser, 2019). Ubc6/UBE2J2 seems to be inefficient in making long polyubiquitin chains, but it is indispensable for priming a broad range of substrates with monoubiquitin or K11-linked Ub dimers, due to its ability to ubiquitinate not only lysine, but also hydroxylated amino acids such as serine or threonine. These short modifications can then be elongated by Ubc7/UBE2G2 in cooperation with Doa10 (X. Wang et al., 2009; A. Weber et al., 2016; P. Xu et al., 2009). Notably, other cytosolic E2 enzymes without permanent ER-membrane association are also involved in ERAD of various substrates, such as UBE2D3, which was reported to act together with MARCH6 and UBE2J2 (Stefanovic-Barrett et al., 2018). Ubc1 (human UBE2K) is the most prominent example, which can elongate initial primed Ub with K48-linked chains, even in the absence of a E3 (Middleton & Day, 2015; Rodrigo-Brenni & Morgan, 2007). Ub side chains can be cleaved and modified by several ERAD-associated DUBs, for example Ub-specific protease (USP) 25 or USP50 (Lemus & Goder, 2014).

2.3.2.3 VCP/Cdc48 provides energy for retrotranslocation

The conserved ATPases associated with a variety of cellular activities (AAA ATPase) VCP is involved in various cellular processes including the separation of ubiquitinated substrates from membranes, chromatin, or macromolecular complexes, often followed by their proteasomal degradation (Bodnar & Rapoport, 2017). VCP is a circular homohexamer with a central pore and three distinct domains: the N domain composed of the N-termini of the six monomers, and two AAA ATPase domains (D1 and D2). Various binding partners and cofactors associate with VCP *via* their Ub regulatory X (UBX) or VCP-interacting/binding motifs (VIM/VBM) domains (Meyer & Weihl, 2014). Most prominently, VCP makes a ternary complex with Ub recognition factor in ER-associated degradation protein 1 (UFD1) and nuclear protein localization protein 4 homolog (NPLOC4), which both bind VCP *via* its N domain and help to recruit and bind Ub-chains, e.g. during ERAD (Ye et al., 2001). It is not clear what the minimal Ub signal for recognition by VCP-UFD1-NPLOC4 is, but it was suggested that poly-Ub chains of at least four or five Ub molecules with K48-linkage would be necessary (Bodnar & Rapoport, 2017).

Other UBX domain containing proteins are essential to recruit VCP to the ER membrane, such as FAS-associated factor 2 (FAF2/ETEA/UBXD8) and UBX domain-containing protein 4 (UBXN4/ERASIN/UBXD2). They function in recruiting as much as in mechanical anchoring of VCP at the ER-membrane (Hirsch et al., 2009). These cytosolic proteins use an intramembrane domain as anchor within the ER lipid bilayer, which results in both their N- and C-termini facing the cytoplasm. They are both part of large complexes involved in recruiting VCP and proteasomes to ERAD substrates: UBXN4 and FAF2 interact with Ubiquilin (UBQLN1-4) and FAF2 interacts with SEL1L and ER lipid raft-associated protein 2 (ERLIN2), among others. Additionally, FAF2 can bind to ubiquitinated proteins *via* its Ub-associated (UBA) domain (Christianson et al., 2012; Liang et al., 2006; P. J. Lim et al., 2009; Mueller et al., 2008; Schuberth & Buchberger, 2008). Recent cryo-electron microscopy data contributed to clarifying the mechanism of how substrates are then processed by VCP: energy from ATP hydrolysis is used to unfold a Ub molecule and pull it through the central lumen of VCP, followed by the unfolded substrate (Twomey et al., 2019).

2.3.2.4 Retrotranslocation – shuttling ERAD substrates back to the cytoplasm

Since the ER-lumen does not contain any components of the UPS, all ERAD clients have to be ubiquitinated and degraded in the cytoplasm. Integral membrane substrates of ERAD can be modified with Ub at domains exposed to the cytosol, but luminal substrates need to be transported across the ER membrane before they can face the UPS machinery (Christianson & Ye, 2014). The physical removal of ERAD substrates either from or across the lipid bilayer of the ER membrane poses a significant energy barrier. Recent cryo- experiments in yeast provided

insights into the mechanism for substrates without a transmembrane domain: Yos9 and Hrd1 form a luminal binding site for misfolded glycoproteins and a loop of the polypeptide is then inserted into the membrane by two 'half-channels' made by Hrd1 and its binding partner degradation in the endoplasmic reticulum protein 1 (Der1, a member of the derlin family). Hrd1 and Der1 are linked by U1 SNP1-associating protein 1 (Usa1, HERPUD in mammals), shield the hydrophilic polypeptide from the lipids and distort the membrane to make it thinner and easier to cross (X. Wu et al., 2020). In line with this, it was recently discovered that the rhomboid fold of Der1 itself distorts lipids in its vicinity (Kreutzberger et al., 2019). The loop exposed to the cytoplasm is subsequently ubiquitinated and can serve as 'handle' to facilitate the substrate's extraction from the ER with the help of VCP. However, it remains to be investigated whether this mechanism is universal for all luminal ERAD substrates.

Several mechanisms were proposed for the retrotranslocation of integral ER membrane proteins, a process often referred to as 'dislocation'. In parallel to the mechanism described for luminal substrates, additional possibilities are lateral gated protein channels, again potentially including the Derlin family or the ERAD-associated E3 complexes themselves, such as Hrd1 (B. K. Sato et al., 2009). Single-pass integral membrane proteins with transmembrane domains of low hydrophobicity can engage with the luminal ERAD machinery after complete translocation into the ER, as was shown for the T cell receptor α (TCRα) and others (Feige & Hendershot, 2013), whereas other proteins have to be proteolytically processed before they can engage the ERAD machinery. For example, proteins with charged residues in transmembrane domains and a Ub tag can be cleaved by the intramembranous protease rhomboid-related protein 4 (RHBDL4/RHBDD1), initiating substrate dislocation into the cytoplasm and proteasomal degradation (Fleig et al., 2012; Knopf et al., 2020). Similarly, signal peptide peptidase (SPP) is required for the cleavage and turnover of several tail-anchored proteins within the ER membrane (Boname et al., 2014) and for proteins regulating ER shape (Avci et al., 2019). Although it was demonstrated that VCP is crucial for the solubility of extracted full-length clients with transmembrane domains in the cytoplasm, it remains questionable whether VCP alone would be able to remove proteins from a lipid bilayer (S. Neal et al., 2017). It should be noted that all these mechanisms are not mutually exclusive. In fact, some substrates use one of many parallel routes, probably in a context dependent manner, that allows to clear misfolded or aggregated proteins as well as stoichiometric misfits and regulatory targets. For example, the dislocation of TCRα can be triggered by RHBDL4/RHBDD1-dependent cleavage but its full-length protein could also be found in the cytoplasm (Fleig et al., 2012) and in the ER (Feige & Hendershot, 2013).

2.3.2.5 *Targeting to the proteasome and degradation of ERAD substrates*

ERAD substrates have to be delivered to the 26 S proteasome for degradation after successful retrotranslocation or dislocation. In eukaryotic cells, direct interaction between VCP and the proteasome can only be observed under extreme stress conditions (Isakov & Stanhill, 2011), implicating that shuttling factors are required to mediate substrate 'handoff'. It was proposed that the subsequent binding of different factors might depend on the length of the provided Ub chain on the substrates (Richly et al., 2005). In the yeast cytoplasm, Ufd2 (human UBE4A/B) modifies Ub chains on substrates and thus allows their interaction with Rad23 (human RAD23A/B) or Dsk2 (human UBQLN, Medicherla et al., 2004; Richly et al., 2005). In mammals, UBQLN1 and VCP are recruited to the ER membrane by UBXN4, and UBQLN1 then recruits proteasomes, possibly binding to the substrate's poly-Ub chains and the proteasome simultaneously (P. J. Lim et al., 2009). UBQLN2 was shown to interact with FAF2 (Xia et al., 2014) and several members of the UBQLN family interact with HERPUD, an ER membrane resident protein involved in the HRD1 complex (T.-Y. Kim et al., 2008). The delivery of dislocated ERAD substrates with hydrophobic transmembrane domains to the proteasome is especially difficult as these domains could potentially aggregate in the cytoplasm and harm the cell. BCL2-associated athanogene 6 (BAG6) can bind such proteins in their unfolded state and chaperones them to the proteasome, together with its interaction partners transmembrane domain recognition complex 35 kDa subunit (TRC35/GET4) and Ub-protein ligase 4A (UPL4A, Christianson & Ye, 2014; Q. Wang et al., 2011). Additionally, BAG6 and UBQLN are important chaperones for so called 'orphans', proteins which do not localise to their appropriate compartments after translation, and they help to recognise and deliver them to the proteasome (Juszkiewicz & Hegde, 2018).

Bulky oligosaccharyl chains on a substrate could potentially hinder its degradation within the narrow proteasome pore. Therefore, these modifications are often cleaved off, for example by peptide:N-glycanase (NGLY1), which interacts with VCP and hands the deglycosylated substrates over to RAD23A/B, a direct interaction partner of the proteasome (Hirsch et al., 2009; Katiyar et al., 2004; McNeill et al., 2004). Furthermore, (poly)ubiquitin modifications are cleaved and recycled by various proteasome-associated DUBs before degradation (Clague et al., 2019).

2.3.3 Protein quantity control by regulatory ERAD

Protein degradation by the UPS does not only affect misfolded proteins but it is also an important regulatory step and responds to cellular needs in many cellular signalling cascades. A well-described example is the degradation of β-catenin, which is both a component of cell

adhesion complexes at the cell surface and an important effector of the WNT/β-catenin pathway in the cytoplasm and the nucleus. In the absence of active WNT signalling, β-catenin is continuously synthesised, ubiquitinated and degraded by the proteasome (Aberle et al., 1997). The binding of canonical WNT ligands to receptors at the cellular surface inhibits this degradation and accumulated β-catenin translocates into the nucleus, where it activates downstream transcriptional programmes (see also 2.1.4, and Figure 9). Similar regulatory protein quantity control mechanisms also affect proteins in the ER, which are consequently clients of ERAD. Recently, it was shown that this 'regulatory ERAD' targets the conserved WNT ligand cargo protein EVI/WLS. When no WNT ligands are present, EVI/WLS is modified with Ub with the help of the E2 Ub conjugating enzyme UBE2J2 and the E3 Ub ligase CGRRF1, followed by its extraction from the ER membrane with the help of VCP and subsequent proteasomal degradation (Glaeser et al., 2018).

It is assumed that the regulatory ERAD pathway essentially relies on the same basic machinery as ERAD of misfolded proteins but differs in substrate recognition, which must be exquisitely specific (Hegde & Ploegh, 2010). Several mechanisms have been reported to initiate regulatory ERAD: (i) binding of adaptor proteins, (ii) binding of ligands, and (iii) recognition of specific amino acid sequences or protein folding (Z. Sun & Brodsky, 2019). They are illustrated with two examples in the following.

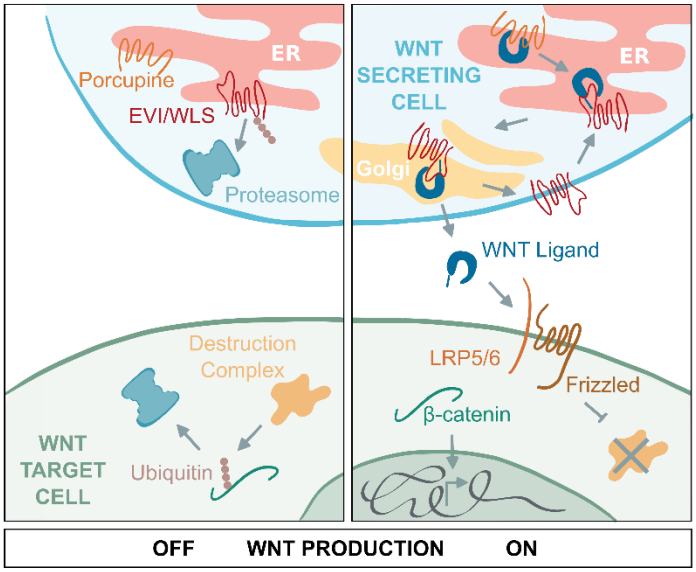

Figure 9. Several components of the WNT signalling pathways are degraded by the ubiquitin-proteasome system (UPS) in the absence of WNT ligand production

WNT ligands produced in the WNT secreting cell interact with the WNT cargo protein EVI/WLS and protect it from being degraded by the UPS. EVI/WLS helps WNT ligands to leave the WNT secreting cell and is itself recycled back to the endoplasmic reticulum (ER). The binding of WNT ligands to receptors on the surface of WNT target cells leads to the inhibition of the destruction complex and the stabilisation of β-catenin, which then translocates into the nucleus, where it leads to the activation of downstream target genes. In the absence of WNTs, β-catenin proteins are constantly phosphorylated by the destruction complex and subsequently subjected to degradation by the UPS. See main text or 6.4.1 for protein name abbreviations and further details.

Probably the most extensively studied substrate of regulatory ERAD is HMG-CoA reductase, an important enzyme in sterol synthesis (Hegde & Ploegh, 2010). In mammals, its ubiquitination by AMFR/GP78 and TRC8, dislocation, and proteasomal degradation are initiated by binding to sterols in the ER membrane and a sterol-induced interaction with insulin-induced gene 1 protein 1 and 2 (INSIG1/2), which in turn recruit E3 ligases (Jo, Lee, et al., 2011; Sever et al., 2003; Song et al., 2005). In addition to INSIG1/2, transmembrane and UBL domain-

containing protein 1 (TMUB1) and ERLIN2 are also important for AMFR/GP78-mediated degradation of HMG-CoA reductase (Jo, Sguigna, et al., 2011). In yeast, the degradation of HMG-CoA reductase depends on Hrd1 and possibly a conformational change which is recognised as degradation signal (Gardner et al., 2001; Garza et al., 2009; Hampton et al., 1996).

Binding of the second messenger IP_3 to its receptor (IP_3R) on the ER membrane releases Ca^{2+} from the ER stores and regulates various cellular functions (Berridge, 2016). IP_3R is an important signalling hub due to its many interaction partners and is rapidly ubiquitinated and degraded by RING finger protein (RNF) 170 after activation by IP_3 (Lu et al., 2011). The adaptor between IP_3R and RNF170 is the ERLIN complex consisting of ERLIN1 and ERLIN2. This complex associates with IP_3R immediately after ligand engagement and links the receptor to various components of the ERAD machinery (Pearce et al., 2007, 2009; Y. Wang et al., 2009).

Only about 20 to 30 endogenous substrates of mammalian regulatory ERAD have been reported so far and it remains unclear in many cases how they are recognised and linked to the ERAD machinery, which interaction partners they have, or even by which E2/E3 proteins they are ubiquitinated (Bhattacharya & Qi, 2019; Printsev et al., 2017). Most of these data was generated *in-vitro* in yeast or mammalian cell lines, but animal studies were included only rarely, although these would help to determine the physiological impact of regulatory ERAD and possible roles in diseases (Bhattacharya & Qi, 2019). For instance, it was recently shown that the knock-out of AXIN interactor, dorsalization-associated protein (AIDA) led to obesity in mice through the stabilisation of enzymes important for fat synthesis (Luo et al., 2018). Moreover, deregulated quantity control of receptor tyrosine-protein kinases (ERBB, e.g. human epidermal growth factor receptor 2, HER2, or EGFR) were implicated in cancer (Carraway, 2010) and the antidiabetic drug metformin induced regulatory ERAD of programmed cell death ligand 1 (PD-L1) via HRD1/SEL1L and thus enhanced the activity of cytotoxic T lymphocytes against breast cancer cells (Cha et al., 2018).

Taken together, these studies argue against a common or canonical route for recognition and degradation of regulatory ERAD substrates. By contrast, it can be assumed that many more substrates and other interaction partners will be discovered in the future. Nevertheless, the understanding of regulatory ERAD and its related proteins has advanced greatly in recent years and the best described endogenous ERAD substrates depend on SYVN1/HRD1 or AMFR/GP78 in mammals (Bhattacharya & Qi, 2019; Printsev et al., 2017; Z. Sun & Brodsky, 2019).

2.3.4 Autophagy and lysosomal degradation

Autophagy is the general term for several cellular pathways that deliver cytosolic cargo to lysosomes for degradation in order to provide nutrients during fasting or degrade and recycle various cellular structures, and thus they are part of the cellular cytoprotective system (Pohl & Dikic, 2019). The best-studied form of autophagy is macroautophagy, a process in which cellular material is engulfed by the autophagosome, a double-membrane structure. This is often initiated by the modification of unc-51-like kinase 1 (ULK1) with K63-linked Ub-chains by tumour necrosis factor (TNF) receptor-associated factor 6 (TRAF6), followed by a tightly regulated enzymatic cascade involving mammalian homologs of the yeast autophagy related genes (ATG) proteins (R.-H. Chen et al., 2019; Dikic & Elazar, 2018). In the end, kinesins use microtubules to transport mature autophagosomes to the lysosomes, with which they fuse using soluble N-ethylmaleimide-sensitive factor attachment protein receptor (SNARE) and homotypic fusion and protein sorting (HOPS) complexes. The cargo is then hydrolysed in the acidic, proteolytic milieu of the resulting autolysosomes (Dikic & Elazar, 2018).

Lysosomes were discovered in the 1950s (de Duve et al., 1955) and for a long time degradation *via* this lytic compartment was considered to be an unselective recycling route. However, bulk degradation of macromolecules happens preferentially as a response to nutrient or growth factor deprivation, while autophagy can also selectively target intra-cellular stressors such as protein aggregates, faulty organelles, or invading bacteria (Pohl & Dikic, 2019). In part, this selective autophagy relies on monoubiquitination or K63-linked Ub chains as molecular ‘eat-me’-signals. Importantly, Ub can initiate and accelerate autophagy but core autophagy proteins can also be targeted to proteasomal degradation if tagged with K48- or K11-linked Ub, thus inhibiting autophagy (R.-H. Chen et al., 2019; Pohl & Dikic, 2019).

2.3.5 Endocytosis and ubiquitination

Internalisation of integral membrane proteins and their interaction partners from the cell surface by endocytosis can lead to their lysosomal degradation or re-distribution within the cell. In this process, ubiquitination has a major role in substrate localisation and fate decision. Typical cargos are transmembrane proteins bound to their extracellular ligands, examples include the well-studied EGFR or the WNT cargo protein EVI/WLS (Cullen & Steinberg, 2018). While both EGFR and EVI/WLS can undergo clathrin-dependent endocytosis, it should be noted that there are also clathrin-independent mechanisms. For EGFR, the dosage of EGF ligand signal decides which of these mechanisms is activated and high EGF leads to clathrin-dependent internalisation (Sigismund et al., 2013) with the help of the adaptor protein growth factor receptor-bound protein 2 (GRB2) and the E3 casitas B-lineage lymphoma proto-oncogene (CBL,

Huang et al., 2007). However, contrary to previous assumptions, the K63-linked and mono-ubiquitination of EGFR is not important for its EGF-induced internalisation (Huang et al., 2007), but functions as sorting signal for its recognition by the multiprotein ESCRT complexes (Cullen & Steinberg, 2018). This modular protein machinery assembles at the surface of early endosomes and sorts proteins with Ub modifications into specialised compartments with degradative fate. These are then internalised and form intraluminal vesicles (ILVs), while the Ub molecules are cleaved off by DUBs. Biogenesis of cargo-enriched ILVs and maturation of the early endosome lead to its transformation into the late endosome which is also known as multivesicular body (MVB). The late endosome's fusion with lysosomes results in the degradation of ILVs and their cargo (Cullen & Steinberg, 2018; Komander & Rape, 2012), whereas its fusion with the plasma membrane leads to the release of ILVs as exosomes (Edgar, 2016).

Sorting signals are also commonly used by the coat complex retromer (and a similar protein complex called retriever), to retrieve and recycle cargos with the help of membrane remodelling and by sorting them in tubule-vesicular transport carriers, following the central dogma of intracellular membrane trafficking (Cullen & Steinberg, 2018). In the absence of motif-dependent recycling, the default route of many endocytosed cargos, such as EVI/WLS, seems to be lysosomal degradation (Cullen & Steinberg, 2018; Franch-Marro et al., 2008; McGough et al., 2018; P.-T. Yang et al., 2008).

It is important to note that ubiquitination of proteins at the plasma membrane can indeed initiate their endocytosis, as shown for G protein coupled receptors (Burton & Grimsey, 2019; Terrell et al., 1998). If and how Ub modifications also help to navigate EVI/WLS through the endocytotic network is currently only rudimentary understood (Zhang et al., 2018).

2.4 Aim of this thesis

The WNT signalling pathways shape tissue development and are associated with various diseases, such as cancer. It was recently shown that EVI/WLS is ubiquitinated by UBE2J2 and CGRRF1 and subjected to ERAD in a WNT ligand dependent manner. However, this Ub signal is presumably too weak to recruit the ERAD machinery. ERAD can affect cellular signalling and cell physiology by degrading mature proteins within the secretory routes, but this type of post-translational regulation is not well studied in mammals. Furthermore, the reciprocal interaction of EVI/WLS with WNT ligands and the availability of EVI/WLS protein are important determinants of the malignancy of various cancers, such as melanoma, but the underlying pathomechanisms are incompletely understood. Therefore, I wanted to gain insights into the regulation of EVI/WLS as an endogenous substrate of regulatory ERAD by analysing its ubiquitination and

interaction with ERAD-associated proteins in cells with or without active WNT ligand secretion. Using melanoma cells as a model system with high WNT ligand production, I further wanted to examine the functional impact of EVI/WLS abundance on cellular invasiveness. Elucidating the correlation of EVI/WLS protein levels and disease progression will also help to develop novel treatment approaches for WNT-related malignancies.

3 Material & Methods

3.1 Material

3.1.1 Antibodies

Table 1. Primary antibodies

Specificity	Host	Clonality (reference)	Reference	Supplier	Dilution (application)
β-ACTIN	ms	mono (AC-15)	ab6276	Abcam	1/10 000 (WB)
β-ACTIN	rb	poly	#4967	Cell Signaling Technology	1/1 000 (WB)
β-CATENIN	ms	mono (14)	610154	BD Biosciences	1/1 000 (WB)
CORTACTIN/p80/85	ms	mono (4F11)	05-180	Merck Millipore	1/1 000 (IF)
ERLIN2/SPFH2	gt	poly	EB06896	VWR	1/1 000 (WB)
EVI/WLS	ms	mono (YJ5)	655902	BioLegend	1/250 - 1/1 000 (WB) 1/100 (IF)
EVI/WLS	rb	poly	PA5-42570	Thermo Fisher Scientific	1/100 (IF)
FAF2/ETEA/UBXD8	gt	poly	GTX14759	GeneTex	1/1 000 (WB)
FLAG-Tag	ms	mono (M2)	F1804	Sigma-Aldrich	1/1 000 (WB)
FLAG-Tag	rb	poly	F7425	Sigma-Aldrich	1/8 000 (WB)
HA-Tag	ms	Mono (6E2)	#2367	Cell Signaling Technology	1/1 000 (WB)
HSC70	ms	mono (B-6)	sc-7298	Santa Cruz Biotechnology	1/2 000 (WB)
K48-linkage Specific Polyubiquitin	rb	mono (D9D5)	#8081	Cell Signaling Technology	1/100 000 (WB)
K63-linkage Specific Polyubiquitin	rb	mono (D7A11)	#5621	Cell Signaling Technology	1/1 000 (WB)
SEL1L	rb	poly	ab78298	Abcam	1/1 000 (WB)
α-TUBULIN	rb	poly	#2144	Cell Signaling Technology	1/3 000 (WB)
UBE2K/E2-25K	ms	mono (701316)	MAB6609	R&D Systems	1/1 000 (WB)

Continued on the next page

Specificity	Host	Clonality (reference)	Reference	Supplier	Dilution (application)
UBE2N	rb	mono (D2A1)	#6999	Cell Signaling Technology	1/1 000 (WB)
Ubiquitin	ms	Mono (P4D1)	#3936	Cell Signaling Technology	1/3 000 (WB) 1/100 000 (WB)
VCP/P97	ms	mono (5)	ab11433	Abcam	1/500 (IF)
VINCULIN	rb	poly	AB6039	Merck Millipore	1/150 000 (WB)
WNT3	rb	poly	GTX128100	GeneTex	1/1 000 (WB)
WNT5A/B	rb	mono (C27E8)	#2530	Cell Signaling Technology	1/1 000 (WB)
WNT11	rb	poly	GTX105971	GeneTex	1/1 000 (WB)

gt: goat; ms: mouse; rb: rabbit; mono: monoclonal; poly: polyclonal; IF: immunofluorescence; WB: Western blot

Table 2. Fluorescence-protein coupled antibodies and labelling substances

Name	Conjugate	Reference	Supplier	Dilution (application)
Gelatin	Fluorescein (FITC)	ECM670	Merck Millipore	NA (gelatin degradation)
Goat anti-Mouse IgG (H+L)	Alexa Fluor® 488	A-11001	Thermo Fisher Scientific	1/500 (IF)
Goat anti-Mouse IgG (H+L)	Alexa Fluor® 633	A-21052	Thermo Fisher Scientific	1/500 (IF)
Goat anti-Rabbit IgG (H+L)	Alexa Fluor® 488	A-11034	Thermo Fisher Scientific	1/500 (IF)
Phalloidin	Tetramethylrhodamine (TRITC)	ECM670	Merck Millipore	1/500 (IF)
Wheat Germ Agglutinin (WGA)	Alexa Fluor® 633	W21404	Thermo Fisher Scientific	1/1 000 (IF)

IgG (H+L): Gamma Immunoglobins heavy and light chains; IF: immunofluorescence; NA: not applicable

Table 3. Horse-radish peroxidase (HRP)-coupled antibodies

Specificity	Host	Clonality	Reference	Supplier	Dilution (application)
β-ACTIN	ms	mono (C4)	SC47778 HRP	Santa Cruz Biotechnology	1/5 000 (WB)
Anti-Goat IgG	rb	poly	6160-05	SouthernBiotech	1/5 000 (WB)
Anti-Mouse IgG (H+L)	gt	poly	AB_10015289	Jackson ImmunoResearch	1/10 000 (WB)
Anti-Rabbit IgG (H+L)	gt	poly	AB_2313567	Jackson ImmunoResearch	1/10 000 (WB)

gt: goa;, ms: mouse; rb: rabbit; mono: monoclonal; poly: polyclonal; WB: Western blot

Table 4. Reagents for protein purifications and controls

Name	Specificity	Conjugate/beads	Reference	Supplier
TUBE Control	Control	Agarose beads	UM400	LifeSensors
TUBE1	Pan-ubiquitin	Magnetic beads	UM401M	LifeSensors
TUBE2	Pan-ubiquitin	Agarose beads	UM402	LifeSensors
K63-TUBE	K63-linked ubiquitin	FLAG-tag	UM604	LifeSensors
M2 AFFINITY GEL	Anti-FLAG	Agarose beads	A2220	Sigma-Aldrich
Monoclonal Anti-HA-Agarose	Anti-HA	Agarose beads	A2095	Sigma-Aldrich
Dynabeads Protein G	Immunoglobulin Fc-region	Magnetic beads	10004D	Thermo Fisher Scientific
BLUE SEPHAROSE 6 Fast Flow	General protein purification from supernatant	Sepharose	17-0948-01	GE Healthcare

3.1.2 Buffers and solutions

Table 5. Buffers and solutions

Name	Purpose	Composition
Blocking solution (IF staining)	Prevention of unspecific antibody binding	1 % goat serum, 3 % FCS, 0.1 % Triton X-100, all volume fraction in PBS
Blocking solution (Western blot)	Prevention of unspecific binding and for antibody dilution	5 % skim milk/TBST (mass fraction)
Blue Sepharose washing buffer	Washing of Blue Sepharose resin	50 mM Tris-HCl, pH 7.5; 150 mM KCl; volume fraction of 1 % Triton X-100 in ddH_2O
Eukaryotic lysis buffer	Cell lysis buffer used for immunoprecipitation and TUBE assays	20 mM Tris-HCl, pH 7.4; 130 mM NaCl; 2 mM EDTA; glycerol at a volume fraction of 10 %; supplemented before use with a volume fraction of 1 % of Triton X-100, 5 mM NEM/ethanol, 2 mM oPA/ethanol, and 1 cOmplete™, mini Protease Inhibitor Cocktail tablet per 10 ml buffer
Fixation solution	Fixation of cells before IF staining	4 % PFA/PBS (mass fraction)
HRP inactivation solution	Inactivation of HRP after Western blot developing	5 % acetic acid/H_2O (volume fraction)
Laemmli buffer (5×)	Reducing sample loading buffer for Western blot	312.5 mM Tris-HCl, pH 6.8; 0.5 M DTT; mass fraction of 10 % SDS, and 0.1 % bromphenol blue; volume fraction of 10 % TCEP, and 50 % glycerol

Continued on the next page

Name	Purpose	Composition
LB medium liquid	Plasmid preparation	1 % Tryptone, 1 % NaCl, 0.5 % yeast extract in ddH_2O (all mass fraction), pH 7.0
LB medium solid (for agar plates)	Plasmid preparation	1 l LB medium liquid, 15 g Agar, antibiotics as needed
MOPS SDS running buffer (20×)	Buffer for SDS-PAGE	1 M MOPS, 1 M Tris-Base, 20 mM EDTA, 69.3 mM SDS in ddH_2O
NuPAGE transfer buffer (20×)	Buffer for Western blot transfer	500 mM Bicine, 500 mM Bis-Tris, 20 mM EDTA (supplement with 10 % volume fraction methanol before use)
PBS (1×)	Various	1.0588236 mM KH_2PO_4, 155.17241 mM NaCl, 2.966418 mM Na_2HPO_4-$7H_2O$ (Thermo Fisher Scientific, 10010056)
Peptide dissolve buffer	Dissolving of 3×FLAG or HA peptide	0.5 M Tris-HCl, pH 7.5, 1 M NaCl in ddH_2O
TBS	Dilution of 3×FLAG or HA peptide	50 mM Tris-HCl, pH 7.4 and 150 mM NaCl in ddH_2O
TBST (10×)	Various	1,37 M NaCl, 200 mM Tris-HCl, pH 7.6, and 1 % Tween-20 (volume fraction)
Urea buffer	General cell lysis	8 M urea, PBS

DTT: Dithiothreitol; EDTA: Ethylenediaminetetraacetic acid; FCS: fetal calf serum; HRP: horse radish peroxidase; IF: immunofluorescence; LB: lysogeny broth; MOPS: 3-(N-morpholino)propanesulfonic acid; NEM: N-ethylmaleimide; oPA: 1,10-phenanthroline; PBS: phosphate buffered saline; PFA: paraformaldehyde; SDS-PAGE: sodium dodecyl sulfate–polyacrylamide gel electrophoresis; TBS: Tris-buffered saline; TBST: TBS with Tween-20; TCEP: Tris-(2-carboxyethyl)-phosphin; TUBE: tandem ubiquitin binding entity

3.1.3 Cell lines and culture media

Table 6. Human cell lines and their culture media

Cell line	Specification	Source	Culture medium
A375	Malignant melanoma	ATCC® CRL-1619™	DMEM, 10 % FBS
A375 sgEVI2_4	EVI/WLS KO	in-house	DMEM, 10 % FBS
HEK293T	Embryonic kidney	ATCC® CRL-11268™	DMEM, 10 % FBS
HEK293T KO2.9	EVI/WLS KO	in-house	DMEM, 10 % FBS
RPMI7951	Malignant melanoma	ATCC® HTB-66™	DMEM, 10 % FBS
WM793	Malignant melanoma	Meenhard Herlyn (Wistar Institute, Philadelphia, USA)	DMEM, 10 % FBS

ATCC®: American Type Culture Collection; KO: knock-out; DMEM: Dulbecco's Modified Eagle's Medium;
FBS: Fetal bovine serum, added as volume fraction

3.1.4 Consumables

Table 7. Consumables

Name	Reference	Supplier
Amersham Hyperfilm ECL	28906836	Cytiva/GE Healthcare
Amersham Protran 0.45 nitrocellulose membranes	10600002	Cytiva/GE Healthcare
Autoklavierband Rolle	27005	neoLab Migge GmbH
Bad Stabil®	16095	neoLab Migge GmbH
Beschriftungsklebeband Rainbow-Pack	817-0027	VWR™
Bolt 4-12 % Bis-Tris plus gels, 10-well	NW04120BOX	Thermo Fisher Scientific
Bolt 4-12 % Bis-Tris plus gels, 12-well	NW04122BOX	Thermo Fisher Scientific
Bolt 4-12 % Bis-Tris plus gels, 15-well	NW04125BOX	Thermo Fisher Scientific
Cell Culture Multiwell Plate, 12 Well, CELLSTAR®	665180	Greiner Bio-One International GmbH
Cell Culture Multiwell Plate, 24 Well, CELLSTAR®	662160	Greiner Bio-One International GmbH
Cell Culture Multiwell Plate, 6 Well, CELLSTAR®	657160	Greiner Bio-One International GmbH
Cell scraper	99002	TPP®
Cover slip, round, 12 mm	9161064	Gerhard Menzel
Disposable scalpel	200140021	Feather®
Falcon® 100 mm TC-treated Cell Culture Dish	353003	Corning, Inc.
Falcon® 14 ml Round-Bottom Tube	352059	Corning, Inc.
Falcon® 25cm² Rectangular Canted Neck Cell Culture Flask with Vented Cap	353108	Corning, Inc.
Falcon® 75cm² Rectangular Canted Neck Cell Culture Flask with Vented Cap	353136	Corning, Inc.
Falcon® 96-well Clear Flat Bottom TC-treated Culture Microplate, with Lid	353072	Corning, Inc.
Falcon® Serological Pipet 1 ml	357521	Corning, Inc.
Falcon® Serological Pipet 10 ml	357551	Corning, Inc.
Falcon® Serological Pipet 2 ml	357507	Corning, Inc.
Falcon® Serological Pipet 25 ml	357525	Corning, Inc.
Falcon® Serological Pipet 5 ml	357543	Corning, Inc.
Falcon® Serological Pipet 50 ml	357550	Corning, Inc.
Filter tip PP, premium surface, 0.1-10 µl	07-612-8300	nerbe plus GmbH & Co. KG
Filter tip PP, premium surface, 0-20 µl	07-622-8300	nerbe plus GmbH & Co. KG
Filter tip PP, premium surface, 0-200 µl	07-662-8300	nerbe plus GmbH & Co. KG
Filter tip PP, premium surface, 100-1000 µl	07-693-8300	nerbe plus GmbH & Co. KG
Finntip™ pipette tips	613-2597	VWR™
Folded Filters	4.303.090	MUNKTELL & FILTRAK GmbH
Gel Saver II Tip 1-200µl (protein gel loading tip)	I1022-0600	STARLAB International GmbH
Grade 3MM Chr Cellulose Chromatography Papers	3030-917	Cytiva/GE Healthcare

Continued on the next page

Name	Reference	Supplier
Hand towel zigzag fold	66424	Essity Hygiene and Health
Incidin™ Foam	30 460 10	ECOLAB Healthcare
Injekt-F Tuberculin (1 ml)	9166017V	BRAUN Melsungen AG
LEITZ 4020, flush fold, Sichthüllen	1079554	Lyreco
Lid for microplate, low profile	656191	Greiner Bio-One International GmbH
LightCycler® 480 Sealing Foil	4729757001	Roche
Medoject 25Gx1"	CH25100	Chirana T. Injecta, a.s.
Microplate, 96 well, clear, F-bottom	655101	Greiner Bio-One International GmbH
Millex-GP Syringe Filter Unit, 0.22 µm	SLGP033RS	Merck Millipore
Müllbeutel Blau 100 L	400.350	DKFZ Lager
Nalgene™ General Long-Term Storage Cryogenic Tubes, 1.2 ml	11740573	Thermo Fisher Scientific
PARAFILM® M	PM996	Merck Millipore
PCR 384-Well TW-MT-Plate, white, for RT-qPCR	712456X	Biozym Scientific GmbH
PCR tubes 12er SoftStrips	711068	Biozym Scientific GmbH
Petri dish, 94 x 16nmm, without vent	632180	Greiner Bio-One International GmbH
profix® Allzweck- und Kosmetiktücher		TEMCA
Safe-Lock microcentrifuge tubes 1.5 ml	0030 120.086	Eppendorf AG
Safe-Lock microcentrifuge tubes 2 ml	0030 120.094	Eppendorf AG
Spezial Vernichtungsbeutel/ disposal bags	646201	Greiner Bio-One International GmbH
SuperFrost Plus™ Adhesion slides	J1800AMNZ	Thermo Fisher Scientific
Syringe, 20 ml, with BD Luer-Lok™ Tip	BDAM302830	VWR™
TipOne® Tip, 10 µl Graduated, Refill (non-sterile)	S1111-3700	STARLAB International GmbH
TipOne® Tips, 1000 µl Blue Graduated, Refill (non-sterile)	S1111-6701	STARLAB International GmbH
TipOne® Tips, 200 µl Yellow, Refill (non-sterile)	S1111-0706	STARLAB International GmbH
TUBE, 15 ML, Centrifuge Tube, CELLSTAR®	188271	Greiner Bio-One International GmbH
TUBE, 50 ML, Centrifuge Tube, CELLSTAR®	227261	Greiner Bio-One International GmbH
Vernichtungsbeutel, 200X300; autoclavable bags	09-302-0020	nerbe plus GmbH & Co. KG
XCEED® Nitrile Gloves, S	XC-INT-S	STARLAB International GmbH
XCEED® Nitrile Gloves, XS	XC-INT-XS	STARLAB International GmbH

3.1.5 Enzymes, reagents, chemicals, and drugs

Table 8. Molecular biology reagents, chemicals, enzymes, and drugs

Name	Reference	Supplier
1,10-Phenanthroline monohydrate (oPA)	P9375-1G	Sigma-Aldrich
3× FLAG peptide	F4799-4MG	Sigma-Aldrich
3-Morpholinopropanesulfonic acid (MOPS)	A1076	AppliChem GmbH
5× siRNA Buffer	B-002000-UB-100	Horizon Discovery
Acetic acid	15642900	Thermo Fisher Scientific
Agar	A0949,0500	AppliChem GmbH
Agarose	A9539	Sigma-Aldrich
Bicine	sc-216087A	Santa Cruz Biotechnology
BIS-Tris	sc-216088A	Santa Cruz Biotechnology
Bond-Breaker TCEP Solution	77720	Thermo Fisher Scientific
Bromophenol Blue sodium salt	B5525-25G	Sigma-Aldrich
BSA Fraction V	1501,05	GERBU Biotechnik GmbH
Carbenicillin; dinatriumsalz	A1491,0010	AppliChem GmbH
cOmplete™, Mini Protease Inhibitor Cocktail	11836153001	Sigma-Aldrich
Cycloheximide solution	C4859-1ML	Sigma-Aldrich
Dimethyl sulfoxide (DMSO)	D8418-50ML	Sigma-Aldrich
DTT BioChemica	A2948,0005	AppliChem GmbH
EDTA, Tetrasodium Tetrahydrate Salt	sc-204735	Santa Cruz Biotechnology
Ethanol absolute	20.821.330	VWR™
Fetal bovine serum (FBS), Lot: CBX9154	F7524-500ml	Merck Millipore/Sigma
Fixation reagent for histology (PFA 4 %)	12004	Morphisto
FuGENE HD Transfection Reagent, 1ml	E2311	Promega Corporation
GelPilot® Loading Dye, 5×	1037650	QIAGEN
GeneRuler 100 bp DNA ladder	SM0243	Thermo Fisher Scientific
Gibco™ DMEM, high glucose	41965062	Thermo Fisher Scientific
Gibco™ PBS, pH 7.4	10010056	Thermo Fisher Scientific
Gibco™ RPMI-1640, without l-glutamine	31870074	Thermo Fisher Scientific
Gibco™ Trypsin-EDTA (0.25 %), Phenolred	25200056	Thermo Fisher Scientific
Glycerol	G5516	Sigma-Aldrich
HA Peptide	HY-P0239	Hölzel Diagnostika
Hydrochloric acid (HCl)	H/1200/PC15	Fisher Chemical
Immobilon Western Chemiluminescent HRP Substrate	WBKLS0100	Merck Millipore
Kanamycinsulfat BioChemica	A1493,0010	AppliChem GmbH
LGK974	Custom	Wuxi AppTec (Tianjin)
Lipofectamine RNAiMAX	13778075	Thermo Fisher Scientific
Methanol	32213	Sigma-Aldrich
MG-132 in solution (1mg)	474791-1MG	Sigma-Aldrich
N-Ethylmaleimide (NEM)	E3876-5G	Sigma-Aldrich
Nitric acid, min 65 %	30709-1L	Sigma-Aldrich
Normal Goat Serum	5425S	Cell Signaling Technology

Continued on the next page

Name	Reference	Supplier
One Shot TOP10 Chemically Competent Escherichia coli	C404006	Thermo Fisher Scientific
PageRuler plus prestained protein ladder, 10 to 250 kDa	26619	Thermo Fisher Scientific
Paraformaldehyde (PFA) BioChemica	A3813,1000	AppliChem GmbH
PHYSIODERM ® CREME	PZN 4632286	Physioderm
Pierce™ Western Blot Signal Enhancer	21050	Thermo Fisher Scientific
Poly D-lysine	A-003-E	Millipore
Ponceau S solution	P7170-1L	Sigma-Aldrich
Potassium chloride (KCl)	P-9541	Sigma-Aldrich
ProLong™ Diamond Antifade Mountant with DAPI	P36962	Thermo Fisher Scientific
Propan-2-ol	33539	Honeywell Research Chemicals
Restore™ Plus Western Blot Stripping-Buffer	46430	Thermo Fisher Scientific
S.O.C. Medium	15544034	Thermo Fisher Scientific
Seraman® sensitive	30 393 80	ECOLAB Healthcare
Shine last & go! gel nail polish	NA	Essence Cosmetics
Skim Milk Powder	70166-500G	Sigma-Aldrich
Sodium chloride (NaCl)	31434-M	Sigma-Aldrich
Sodium dodecyl sulfate (SDS)	75746-250G	Sigma-Aldrich
Sodium hydroxide (NaOH)	UN1824	VWR™
Spitacid™	30 953 70	ECOLAB Healthcare
SuperSignal West Femto Maximum Sensitivity Substrate	34095	Thermo Fisher Scientific
TransIT-LT1 transfection reagent, 10 ml	731-0029	VWR™
Triton™ X-100	T8787-250ml	Sigma-Aldrich
Trizma® base (Tris)	T1503-1KG	Sigma-Aldrich
Tryptone	8952	Carl Roth GmbH + Co. KG
TWEEN® 20	P9416	Sigma-Aldrich
Urea Molecular biology grade	A1049,1000	AppliChem GmbH
Yeast extract	1133	GERBU Biotechnik GmbH

DMEM: Dulbecco's Modified Eagle's Medium; DTT: Dithiothreitol; EDTA: Ethylenediaminetetraacetic acid; PBS: phosphate buffered saline; RPMI: Roswell Park Memorial Institute; TCEP: Tris-(2-carboxyethyl)-phosphin; S.O.C.: Super Optimal broth with Catabolite repression

3.1.6 Kits

Table 9. Commercially available kits and master mixes

Name	Reference	Supplier
Gateway™ LR Clonase II Enzym-Mix	11791020	Thermo Fisher Scientific
LightCycler® 480 Probes Master	4887301001	Roche
NucleoSpin Gel and polymerase chain reaction (PCR) Clean-up Kit	740609	Macherey-Nagel
Pierce™ BCA™ Protein-Assay	23227	Thermo Fisher Scientific
Q5® Site-Directed Mutagenesis Kit	E0554S	New England BioLabs
QCM™ Gelatin Invadopodia Assay (Green)	ECM670	Merck Millipore
QIAGEN Plasmid Maxi Kit	12165	QIAGEN
QIAGEN Plasmid mini Kit	12125	QIAGEN
RevertAid H minus First Strand cDNA Synthesis Kit	K1632	Thermo Fisher Scientific
RNase-Free DNase Set	79254	QIAGEN
RNeasy mini Kit	74106	QIAGEN

3.1.7 Oligonucleotides and antisense oligonucleotides

3.1.7.1 Primers for reverse-transcription quantitative PCR (RT-qPCR)

Table 10. Primer sequences used for RT-qPCR with the Universal ProbeLibrary (Roche)

Target mRNA	Forward primer sequence (5' - 3') Reverse primer sequence (5’ - 3’)	Probe	Probe Reference
ACTB	CCAACCGCGAGAAGATGA CCAGAGGCGTACAGGGATAG	#64	4688635001
AXIN2	GCTGACGGATGATTCCATGT ACTGCCCACACGATAAGGAG	#56	4688538001
CTNNB1	AGCTGACCAGCTCTCTCTTCA CCAATATCAAGTCCAAGATCAGC	#21	4686942001
ERLIN2/SPFH2	GGAAGAAGGCGCTCATTG TGAAATCTTCTCAGTCTCCTTC	#29	4687612001
EVI/WLS	TCATGGTATTTCAGGTGTTTCG GCATGAGGAACTTGAACCTAAAA	#38	4687965001
FAF2/ETEA/UBXD8	GAAGGAGGAGGAGGTGCAA TCCTTTCCTTTTCCTCCTGTAA	#82	4689054001
G6PD	CTGCAGATGCTGTGTCTGGT TGCATTTCAACACCTTGACC	#22	4686969001
GAPDH	AGCCACATCGCTCAGACAC GCCCAATACGACCAAATCC	#60	4688589001
NPLOC4	CGGTTTACATCAATAGAAACAAGACT AACAACAAATCGCCATGCTT	#25	4686993001

Continued on the next page

Target mRNA	Forward primer sequence (5' - 3') Reverse primer sequence (5' - 3')	Probe	Probe Reference
PORCN	GCTACTGCAAGGCTGTCTCC GCTTCAGGTAGGATGGCAAC	#03	4685008001
SDHA	GGACCTGGTTGGTCTTTGGTC CCAGCGTTTGGTTTAATTGG	#80	4689038001
UBE2K	AGGACCTCCAGACACACCAT CGGACCTTAGGGGGATTAAA	#69	4688686001
UBE2N	CGCAGGATCATCAAGGAAA AAATAACGGGCGTTGCTCT	#72	4688953001
UBE2V1	GGGCCTCCAAGATTTCAGTT AAGGCTGTATATTCGGTTTTCATAA	#82	4689054001
UBE2V2	ACAAGGTGGACAGGCATGAT TCTGGGTATTTAGGTCCACATTC	#49	4688104001
UBXN4/ERASIN/ UBXD2	CGCTTCGGTGGTACTGTTG TCCCAACAAGGTCCAAATGT	#04	4685016001
UBXN6	CCTGGACAACATCCACCTG AGGCAGTTAATGCGCTCCT	#63	4688627001
UFD1l/UFD1	CAGCATGAGGAGTCGACAGA CCAGTCTATTGCCAGATCCAG	#67	4688660001
VCP	AGAGGCAGACAAACCCATCA AGTGATCTCGACGGATCTCAG	#35	4687680001
WNT5A	CAGTTCAAGACCGTGCAGAC ACGATCTCCGTGCACTTCTT	#59	4688562001
WNT11	CAGTGAAGTGGGGAGACAGG CCACATCCTGCAGCTCCT	#36	4687949001

3.1.7.2 Small interfering ribonucleic acids (siRNAs)

Table 11. Control siRNA sequences

Name	Supplier	Reference	Sequence (5' - 3')
siGENOME Non-Targeting siRNA Pool #1	Dharmacon™	D-001206-13-20	UAGCGACUAAACACAUCAA UAAGGCUAUGAAGAGAUAC AUGUAUUGGCCUGUAUUAG AUGAACGUGAAUUGCUCAA
siLuciferase/ RLuc Duplex siRNA (targeting the *Renilla reniformis* luciferase gene)	Dharmacon™	P-002070-01-20	AAAAACATGCAGAAAATGCTG

Table 12. siRNA sequences

Target gene	Supplier	Reference	No	Sequence (5' - 3')
EVI/WLS	Ambion™	s36745	1	GGACAUUGCCUUCAAGCUA
		s36747	3	GGAUUUCCAUGACCUUUAU
AMFR/GP78	Dharmacon™	D-006522-01	1	GCAAGGAUCGAUUUGAAUA
		D-006522-02	2	GGAGCUGGCUGUCAACAAU
		D-006522-03	3	GAGGACUGCUCAUGUGAUU
		D-006522-04	4	CGAGCUGGCUGCCGAGUUU
ATXN3	Dharmacon™	D-012013-01	1	GUACAAAUCUUACUUCAGA
		D-012013-02	2	GCUCAGGAAUGUUAGACGA
		D-012013-03	3	GCAGGGCUAUUCAGCUAAG
		D-012013-04	4	ACGAGAAGCCUACUUUGAA
BAG6	Dharmacon™	D-005062-01	1	GGACAAACCUGGAAUUCU
		D-005062-02	2	CAGAAUGGGUCCCUAUUAU
		D-005062-03	3	CAGCAGCUCCGGUCUGAUA
		D-005062-04	4	UGAGCUGGCUGACCACUAU
CGRRF1	Dharmacon™	D-006933-01	1	GAAGAUAGCCUCCUUACAU
		D-006933-02	2	GACCUUAGCUGAUGAGGAU
		D-006933-03	3	UAUGAAUACUCGCCGCUUU
		D-006933-04	4	CUACAUCGCGGUGGUCUUU
CTNNB1	Ambion™	4390824/s438		CUGUUGGAUUGAUUCGAA
DERL1	Dharmacon™	D-010733-02	2	GAACAGAGACAUGAUUGUA
		D-010733-03	3	GAUAUGCAGUUGCUGAUGA
		D-010733-04	4	GGCCAGGGCUUUCGACUUG
		D-010733-18	18	CAAUUAUGUUGCACGUACA
DERL2	Dharmacon™	D-010576-01	1	GAAGAUGUAUUUCCCAAUC
		D-010576-02	2	CAAUAAUGCUCGUCUAUGU
		D-010576-03	3	CAGCAGACUUUGUAUUUAU
		D-010576-04	4	GGAGAUUAAUCACCAACUU
DERL3	Dharmacon™	D-032237-04	4	GGAUUGCGGUGGGCCAUAU
		D-032237-05	5	GGAUUCAGCUUCUUCUUCA
		D-032237-06	6	UCUGGAGGCUCGUCACCAA
		D-032237-07	7	CUUGGGCGCUCAUGGGUU
ERLIN1/SPFH1	Dharmacon™	D-015639-02	2	CGAAUAGAAGUGGUUAAUA
		D-015639-18	18	GAUUAUGACAAGACCUUAA
		D-015639-19	19	AGAGUUAACCUGUGGCAUU
		D-015639-20	20	GGCCCGAGAGAAAGCGAAA
ERLIN2/SPFH2	Dharmacon™	D-017943-02	2	GAACGCAGUGUAUGAUAUA
		D-017943-03	3	GAUAGAAGAGGGACAUAUU
		D-017943-04	4	GAAUGUACCUUGUGGGACU
		D-017943-05	5	CAACAAGAUCCACCACGAA

Continued on the next page

Target gene	Supplier	Reference	No	Sequence (5' - 3')
FAF2/ETEA/UBXD8	Dharmacon™	D-010649-01	1	GGACCUAACUGACGAAUGA
		D-010649-03	3	AGACUUACCUGGUGUCAGA
		D-010649-04	4	CUACAGCUAUGUUGUCUCA
		D-010649-17	17	CCUAAUGAUUCUCGAGUAG
HERPUD1/HERP	Dharmacon™	D-020918-01	1	GACCAGAGGUUAAUUUAUU
		D-020918-02	2	GGGCCACCGUUGUUAUGUA
		D-020918-03	3	CAACAAUAACUUACAGGAA
		D-020918-04	4	CGACAGUACUACAUGCAAU
HM13/SPP	Dharmacon™	D-005896-4	4	AAAUAUUCUCCCAGGAGUA
		D-005896-5	5	CAAGAAUGCUUCAGACAUG
		D-005896-6	6	GCCCUCAGCGAUCCGCAUA
		D-005896-19	19	AUUUCUUCGUGCUGGGAAU
MARCH4	Dharmacon™	D-023172-02	2	CAUCACCACUGUGCUUAUA
		D-023172-03	3	GAGCUGGUCAUGAGAGUCA
		D-023172-05	5	GUACUGCUAUGGAUUGUGU
		D-023172-06	6	GAGGAUCGCUACUCACUGG
MARCH6	Dharmacon™	D-006925-01	1	GAAGACAUAUGUAGAGUGU
		D-006925-02	2	UCAUAGAUCUCGUCGCUUA
		D-006925-03	3	GAAUUGGAAUGCUUUAGAA
		D-006925-04	4	GAGCUUACAUGGGAAAGAA
MITF	Dharmacon™	D-008674-01	1	GAACGAAGAAGAAGAUUUA
		D-008674-02	2	GCAGAUGGAUGAUGUAAUC
		D-008674-03	3	GACCUAACCUGUACAACAA
		D-008674-04	4	AGACGGAGCACACUUGUUA
NGLY/PNG1	Dharmacon™	D-016457-01	1	GAGGAGCUGUUGAAUGUUU
		D-016457-02	2	AGACAAAGCUUAAAUGACC
		D-016457-03	3	GCGAGUGGGCCAAUUGUUU
		D-016457-04	4	GAAAUUGCGAUCUGAUACA
NPLOC4/NPL4	Dharmacon™	D-020796-02	2	AAUAAUGGCUUCUCGGUUU
		D-020796-03	3	GGACACCUAUUUCCUAAGU
		D-020796-04	4	GACAAUAUCAUGUUUGAGA
		D-020796-17	17	AGGAAAAGCAUUGGCGAUU
PORCN	Dharmacon™	D-009613-01	1	GAUCUUCUACCGUCUCAUA
		D-009613-02	2	UCACUUACGUGGAGCAUGU
		D-009613-03	3	GGUGCGAGCCUUAAACUUG
		D-009613-04	4	GGUCAAUGGUGGAAGUUGU
RAD23B	Dharmacon™	D-011759-01	1	GCAGAUAGGUCGAGAGAAU
		D-011759-02	2	GUACAUCGGGUGAUUCUUC
		D-011759-03	3	GAACGAGAGCAAGUAAUUG
		D-011759-04	4	GGGUCAGUCUUACGAGAAU

Continued on the next page

Target gene	Supplier	Reference	No	Sequence (5' - 3')
RHBDD1/RHBDL4	Dharmacon™	D-019378-01	1	CGGCAAUACUACUUUAAUA
		D-019378-02	2	GUACACAGCAGGACUGAGU
		D-019378-03	3	GGGAUAAAUACUGGACUUA
		D-019378-04	4	UGUACUUACUGGAGUGGUA
RNF128	Dharmacon™	D-007061-01	1	GAAUUGAGGUGGAUGUUGA
		D-007061-04	4	CAAAGAGGCAUACAAGUGA
		D-007061-17	17	GGUCAUUGAUCUUCGUUCA
		D-007061-18	18	GAGACUGCUGUUCGAGAAA
RNF139/TRC8	Dharmacon™	D-006942-01	1	GGGAAAAGCUUGACGAUUA
		D-006942-02	2	GAACUGUGCUUAAAAGUAA
		D-006942-04	4	GCACAUGUAUCGAAUUUAC
		D-006942-17	17	AUAAUUAGUGGGUGCGAUU
RNF170	Dharmacon™	D-007078-01	1	GAAACUGGAUGAUGAUUCA
		D-007078-02	2	GGGCAACCCAGAUCUAUUA
		D-007078-03	3	GGCCAAAUAUCAAGGUGAA
		D-007078-04	4	GAGAUUGCAUCAGGAUAUU
RNF5	Dharmacon™	D-006558-01	1	CGGCAAGAGUGUCCAGUAU
		D-006558-02	2	GCUGGGAUCAGCAGAGAGA
		D-006558-03	3	GCAAGAGUGUCCAGUAUGU
		D-006558-18	18	CCGAAGGGCCAAAUCGCGA
SEL1L	Dharmacon™	D-004885-02	2	UAAGAAAGCUGCUGACAUG
		D-004885-03	3	GAAUUAAGCUCGGAGACUA
		D-004885-04	4	GGAGAGGAGUUCAAGUUAA
		D-004885-05	5	GAGAGGAGUUCAAGUUAAU
SH3PXD2A/TKS5	Dharmacon™	D-006657-02	2	CGCGGAAGCUCAAGUAUGA
		D-006657-03	3	CCAGCCACCUCGUACAUGA
		D-006657-05	5	GAAGGCUGGUGGUAUAUCA
		D-006657-06	6	CAUCAUACAUCGAUAAGCG
SYFN/HRD1	Dharmacon™	D-007090-01	1	CAACAAGGCUGUGUACAUG
		D-007090-02	2	UGUCUGGCCUUCACCGUUU
		D-007090-03	3	GGAGAUGCCUGAGGAUGGA
		D-007090-04	4	CCAAGAGACUGCCCUGCAA
TMUB2	Dharmacon™	D-014307-01	1	GCAAAUACUUCCCUGGACA
		D-014307-03	3	UGGGAUGUAUGGACGAUAA
		D-014307-04	4	GGUACUUCCGAAUCAAUUA
		D-014307-18	18	UCUCUGAACAUUACCGACA
UBAC2	Dharmacon™	D-107914-01	1	GAACCCAUCUUCUCUUCUU
		D-107914-02	2	GGAAUGAUCAAUUGGAAUC
		D-107914-03	3	GCACAAGGGAGGCGACAGA
		D-107914-04	4	UGAGAUGUUUCAAGUGG

Continued on the next page

Target gene	Supplier	Reference	No	Sequence (5' - 3')
UBE2G1	Dharmacon™	D-010154-01	1	GCGAAAGAAUGGAGGGAAG
		D-010154-02	2	GCACCCAAAUGUUGAUAAA
		D-010154-04	4	GUGGAAACCAUCAUGAUUA
		D-010154-05	5	CGAUGGGAAGUCCUUAUUA
UBE2G2	Dharmacon™	D-009095-01	1	UCUAUAAGAUUGCCAAGCA
		D-009095-02	2	GAUGGGAGAGUCUGCAUUU
		D-009095-03	3	CCACUUGAUUACCCGUUAA
		D-009095-05	5	GAGCUAACGUGGAUGCGUC
UBE2J1	Dharmacon™	D-007266-01	1	GAAAGAAGCGGCAGAAUUG
		D-007266-03	3	GAAUAUAUCUGGCAAACGA
		D-007266-19	19	GGAAGUAUAUGUAAGGUUA
		D-007266-20	20	GGCUAAUGGUCGAUUUGAA
UBE2J2	Dharmacon™	D-008614-01	1	GAAGGUGGCUAUUAUCAUG
		D-008614-02	2	GCACAAGACGAACUCAGUA
		D-008614-04	4	GUAUAGAGACGUCGGACUU
		D-008614-18	18	CCCAGUAUCUAUAUGAUCA
UBE2K	Dharmacon™	D-009431-17	17	GGGUAUUUGUCUUGAGAAU
		D-009431-18	18	GAAUCAAGCGGGAGUUCA
		D-009431-19	19	UGUUGAGGCUGCUUAAUAA
		D-009431-20	20	GGGCUAUUUGUUUGGAUAU
UBE2N	Dharmacon™	D-003920-01	1	GCACAGUUCUGCUAUCGAU
		D-003920-02	2	GAGCAUGGACUAGGCUAUA
		D-003920-04	4	CAGAUGAUCCAUUAGCAAA
		D-003920-05	5	GCGGAGCAGUGGAAGACCA
UBE2U	Dharmacon™	D-008998-01	1	GAAGUGGAAUACAAACUAU
		D-008998-02	2	GAAUACUGGUUAAAGAUGA
		D-008998-03	3	GUGAAGAUAUGAUGGAAUG
		D-008998-04	4	CAACCUCAUUUAGUGAUUA
UBE2V1	Dharmacon™	D-010064-02	2	GGACAGUGUUACAGCAAUU
		D-010064-21	21	GUGGAUGCAUACCGAAAUA
		D-010064-22	22	GCCGAAGCAUAGAUUGUAA
		D-010064-23	23	UGAGAUUGGCCUUCGGUGA
UBE2V2	Dharmacon™	D-008823-01	1	GCUAAGACGUCUAAUGAUG
		D-008823-02	2	GGACAGGCAUGAUUAUUGG
		D-008823-03	3	GAGUUAAAGUUCCUCGUAA
		D-008823-04	4	GCAUACCAGUGUUAGCAAA
UBE4A	Dharmacon™	D-007200-01	1	CCUCUUCGCUCGCUUAUUA
		D-007200-02	2	GGAAUAUGAUUAUGGCUUU
		D-007200-03	3	GAGUAUCUCCUGCUUAUUA
		D-007200-04	4	GAUAAUAGCGUGUCAGAGA

Continued on the next page

Target gene	Supplier	Reference	No	Sequence (5' - 3')
UBXN4/ERASIN/ UBXD2	Dharmacon™	D-014184-03	3	CUACACAGAUGGCUGCAAG
		D-014184-04	4	GCGGAGACAUUUGGACCUU
		D-014184-17	17	GAAAGUAGCUGGCGAGGUU
		D-014184-18	18	UAGAGUGGACAUACGGAAA
UBXN6/UBXD1	Dharmacon™	D-008785-01	1	CCAAGUACCUGGACAACAU
		D-008785-02	2	GAAACCAGGUGAGAAAGGA
		D-008785-03	3	UCAUGAAGAUCUACACGUU
		D-008785-04	4	ACGAGAACCUGGCCUUGAA
UFD1L/UFD1	Dharmacon™	D-017918-02	2	AAUCAAGCCUGGAGAUAUU
		D-017918-03	3	GACCAAACCCGACAAGGCA
		D-017918-04	4	GAGCGUCAACCUUCAAGUG
		D-017918-17	17	GAGGCAGAUUCGUCGCUUU
USP13	Dharmacon™	D-006064-01	1	GAAGAUGGGUGAUUUACAA
		D-006064-02	2	GCACUGGAUUGGAUCUUUA
		D-006064-03	3	GCACGAAACUGAAGCCAAU
		D-006064-04	4	UGAUUGAGAUGGAGAAUAA
USP19	Dharmacon™	D-006068-03	3	GAUGAGGAAUGACUCUUUC
		D-006068-04	4	GAGGACACCACUAGUAAGA
		D-006068-05	5	UGGCGGAGGUAAUUAAGAA
		D-006068-06	6	UCAAGAAUGACUCGUAUGA
USP25	Dharmacon™	D-006074-02	2	GCAGAUGGAUGAAGUACAA
		D-006074-03	3	UGAAAGGUGUCACAACAUA
		D-006074-04	4	GAGCUGAGGUAUCUAUUUG
		D-006074-05	5	CAAUUAAGUUGGAAUAUGC
USP50	Dharmacon™	D-031837-2	2	UAUGAUACCCUUCCAGUUA
		D-031837-3	3	GAGAACGGAUAUUCAUUAC
		D-031837-4	4	GGUUUGACAUUCAGGGUAC
		D-031837-17	17	CAACACAUGCUGCGUGAAU
VCP	Dharmacon™	D-008727-05	5	GUAAUCUCUUCGAGGUAUA
		D-008727-06	6	AAACAGAUCCUAGCCCUUA
		D-008727-07	7	GAGAGCAACCUUCGUAAAG
		D-008727-08	8	GCACAGGUGGCAGUGUAUA
VCPIP1	Dharmacon™	D-019137-01	1	GAGAAGCUCUGGUGAUUAU
		D-019137-02	2	GACAGAAGUUUGCAAGAUA
		D-019137-03	3	GGGACAGACUUUAGUAAUA
		D-019137-04	4	CAGAAGGACUGGAGUGAUA
WNT5A	Ambion™	s14871	1	UAUCAAUUCCGACAUCGAA
		s14872	2	AGAUGUCAGAAGUAUAUAU
		s14873	3	GGUGGUCGCUAGGUAUGAA

Continued on the next page

Target gene	Supplier	Reference	No	Sequence (5' - 3')
WNT11	Dharmacon™	D-009474-02	2	CAGGAUCCCAAGCCAAUAA
		D-009474-03	3	CGACAGCUGCGACCUUAUG
		D-009474-04	4	GUCGAGCGGUGCCACUGUA
		D-009474-05	5	GGACUCGGAACUCGUCUAU
YOD1	Dharmacon™	D-027369-01	1	CGAUUGAGAUUGAGUAUUA
		D-027369-02	2	GAAUGAGGGUUGAAGCCUA
		D-027369-03	3	GAUCCAGACUUCUAUAGUG
		D-027369-04	4	GCAAUAGAGAUAUCGAUUU

Table 13. siRNA sequences from Dharmacon Genomewide 96 well plates MTP

Target gene	Supplier	Reference	Sequence (5' - 3')
ERLEC1	Dharmacon™	M-010658-00	GAAAGAAACTGGTCAGAAA
			CAAATGAGATTCCCACTAA
			GCAAACATGTACATCAATA
			CATGACAACTGCACATAAA
OS9	Dharmacon™	M-010811-00	GGACATATGAATTCTGTTA
			GGAAACACCTGCTTACCAA
			GGACGAATTTGACTTCTGA
			AAGGAGATCTTCTTCAATA
RAD23A	Dharmacon™	M-005231-00	GAACTTTGATGACGAGTGA
			GAAGATAGAAGCTGAGAAG
			GAACATGCGGCAGGTGATT
			GGAGAAAGAAGCTATAGAG
RNF122	Dharmacon™	M-007068-00	GAACATTGGGATTCTATTG
			TAAAGGTGATGCCAAGAAG
			GGAACCAGGCACAGAGTGA
			CCGCAAGTGTCTGGTGAAA
RNF24	Dharmacon™	M-006943-00	GAATCTGCCTCTCAACATA
			GCTCGGATTTCCCACATTA
			GGGCAGAGAACATTGTATA
			GAATTTACATGAGCTCTGT
TMUB1	Dharmacon™	M-018578-00	ACACAGAGGTCAAGCTGCA
			CGACACCATTGGCTCCTTG
			CCTCAATGATTCAGAGCAG
			GGGAACAGCAGGTGCGACT
TMUB2	Dharmacon™	M-014307-00	GCAAATACTTCCCTGGACA
			TAGCTTGGCTCTCTACCTA
			TGGGATGTATGGACGATAA
			GGTACTTCCGAATCAATTA

Continued on the next page

Target gene	Supplier	Reference	Sequence (5' - 3')
UBAC2	Dharmacon™	M-017914-00	GAACCCATCTTCTCTTCTT GGAATGATCAATTGGAATC GCACAAGGGAGGCGACAGA TGAGAGTGCTTTCAAGTGG
UBE2D1	Dharmacon™	M-009387-01	CAACAGACATGCAAGAGAA GAAAGAATTGAGTGATCTA TACCAGATATTGCACAAAT GCACAAATCTATAAATCAG
UBQLN2	Dharmacon™	M-013566-00	GAGATGATGATCCAAATAA TGAAGCACCTGGCCTGATT TGCAAGAGATGATGAGAAA GCTCAACAACCCAGACATA
UFD2/UBE4B	Dharmacon™	M-007202-01	GCAGACAGATGATAGATTG GACGAGAGCTTCCTGAGAA GGAATTGTTTGAAGAAGTT CAAGAACGCACGCGCAGAA

3.1.8 Plasmids

Table 14. Plasmids

Name	Description	Reference
pRK5-HA-Ubiquitin wt	Mammalian expression of HA-tagged ubiquitin	Addgene #17608 (K. L. Lim et al., 2005)
pRK5-HA-Ubiquitin K11	Mammalian expression of HA-tagged ubiquitin with only K11, other K mutated to R	Addgene #22901 (Livingston et al., 2009)
pRK5-HA-Ubiquitin K48	Mammalian expression of HA-tagged ubiquitin with only K48, other K mutated to R	Addgene #17605 (K. L. Lim et al., 2005)
pRK5-HA-Ubiquitin K63	Mammalian expression of HA-tagged ubiquitin with only K63, other K mutated to R	Addgene #17606 (K. L. Lim et al., 2005)
pcDNA Wnt3	Mammalian expression of WNT3	Addgene #35909 (Najdi et al., 2012)
pcDNA-Wnt5A	Mammalian expression of WNT5A	Addgene #35911 (Najdi et al., 2012)
pcDNA-Wnt11	Mammalian expression of WNT11	Addgene #35922 (Najdi et al., 2012)
pcDNA-V5-hWls (EVI/WLS-V5)	Mammalian expression of V5-tagged EVI/WLS (N-terminal V5-tag at AA166 of EVI/WLS)	Belenkaya et al., 2008
K410/419R Wls (EVI/WLS K410/419R-V5)	Mammalian expression of V5-tagged EVI/WLS, K410 and K419 mutated to R	In-house (Kathrin Glaeser), unpublished

Continued on the next page

Name	Description	Reference
pCMV6-Myc-DDK-tagged PORCN	FLAG-tagged Porcupine	Origene (#RC223764)
ERLIN1-FLAG	Mammalian expression of FLAG-tagged ERLIN1 (C-terminal); Gateway cloning with pENTR #187225731 (open, backbone pENTR221; 1081 bp) and pDEST-FLAG C-terminal, CMV promotor	this study
ERLIN2-FLAG	Mammalian expression of FLAG-tagged ERLIN2 (C-terminal); Gateway cloning with pENTR #127630018 (open, backbone pENTR201; 1059bp) and pDEST-FLAG C-terminal, CMV promotor	this study
FAF2-FLAG	Mammalian expression of FLAG-tagged FAF2 (C-terminal); Gateway cloning with pENTR #191683255 (open, backbone pENTR221; 1294 bp) and pDEST-FLAG C-terminal, CMV promotor	this study
UBXN4-FLAG	Mammalian expression of FLAG-tagged UBXN4 (C-terminal); Gateway cloning with pENTR #178534864 (open, backbone pENTR221; 1567 bp) and pDEST-FLAG C-terminal, CMV promotor	this study
UBE2K FLAG N-terminal STOP	Mammalian expression of FLAG-tagged UBE2K (N-terminal) STOP codon re-introduced by site-directed mutagenesis; Gateway cloning with pENTR #123919860 (open, backbone pENTR221; 643 bp) and pDEST-FLAG N-terminal, CMV promotor	this study

Bp: base pairs; wt: wild type

3.1.9 Software

Table 15. Online and offline software

Software	Version	Source/Reference
Fiji/ImageJ-win64	1.51n	Wayne Rasband, National Institutes of Health (Schindelin et al., 2012)
GeneCards – the human gene database	v5.0.0 Build 318	Weizmann Institute of Science (2020), (Stelzer et al., 2016)
GlycoProtDB	2016-12-05	National Institute of Advanced Industrial Science and Technology (AIST)
IncuCyte™ Basic Software & Scratch Wound Cell Migration Software Module	2013B Rev1	Essen BioScience Inc.
Inkscape	0.92.2	Inkscape-project (2020)
LightCycler® 480 Software	1.5.1.62 SP3	Roche
Microsoft® Excel	Office 2019	Microsoft Corporation
Microsoft® PowerPoint	Office 2019	Microsoft Corporation
Microsoft® Word	Office 2019	Microsoft Corporation
MikroWin 2010 (Mithras LB 940 reader)	5.23	Labsis Laborsysteme GmbH
NanoDrop 1000	3.8.1	Thermo Scientific
NEBaseChanger	1.3.0	New England BioLabs (2020)
PhosphoSitePlus®	v.6.5.9.3	Cell Signaling Technology (2020), Hornbeck et al., 2015
Primer3web tool	4.1.0	Kõressaar et al., 2018; Koressaar & Remm, 2007; Untergasser et al., 2012
PyMOL	2.3	Schrödinger
R	3.6.1	R Core Team (2019)
RStudio	1.2.1335	RStudio Team (2020)
Sequencing Primer Design Tool	/	Eurofins Genomics (2020)
SerialCloner	2.6.1	Serial Basics Softwares
TCGA	/	TCGA Research Network, National Institutes of Health (2019)
UniProt	/	UniProt Consortium (2020)
Universal ProbeLibrary Assay Design Center	/	Roche (2019)
ZEN (blue edition)	2.3	Carl Zeiss Microscopy GmbH
Zotero	5.0.80	Corporation for Digital Scholarship (2020)

3.1.10 Technical equipment

Table 16. Technical equipment

Name	Reference	Supplier
AccuBlock™ Digital dry bath	51602070	Labnet
Agarose gel documentation station	E-Box VX2	PeqLab Biotechnologie GmbH
Carrousel Pipette Stand	F161401	Gilson
Centrifuge	5804	Eppendorf AG
Centrifuge	5804 R	Eppendorf AG
Centrifuge	5415 D	Eppendorf AG
Centrifuge	5810 R	Eppendorf AG
Centrifuge	5424	Eppendorf AG
Centrifuge	5424 R	Eppendorf AG
COMPACT 2 X-Ray Film Processor	1190-1	PROTEC GmbH & Co. KG
Cryo-Safe™ Cooler (Mr. Frosty)	F18844-0000	Bel-Art Products
CryoStorage Systems (liquid nitrogen)	562004JJ4	Taylor Wharton 10K
DynaMag™-2	12321D	Thermo Fisher Scientific
Electrophoresis cell SUB-CELL® GT	710 BR 04827	Bio-Rad
Finnpipette® 50-300 µl	4510	Thermo Scientific
Finnpipette® 5-50 µl	4510	Thermo Scientific
Fluorescence microscope 'Cell observer'	Axio Observer Z1	Zeiss
Freezer -20 °C	G5216	Liebherr
Freezer -20 °C	TGS 5200	Liebherr
Freezer -20 °C	Comfort 77 552 404.86	Liebherr
Fridge 4 °C	Lkexv 3910	Liebherr
Fridge 4 °C	KT-1740	Liebherr
Fridge 4 °C	FKEX 5000	Liebherr
GenPure water purifier	50131323	Thermo Fisher Scientific
HERAfreeze basic	HFU320 BV	Thermo Fisher Scientific
Hypercassette™	RPN11642	Amersham Biosciences
Ice machine	FM-150KE-50	Hoshizaki
Incubator (37 °C)	BD 53	Binder
Incubator (60 °C)	ED 53	Binder
Incubator, with CO_2 sensor	CB210 & CB220	Binder
Incubator, with CO_2 sensor	NU-4750E	IBS Integra Biosciences
IncuCyte® WoundMaker (96-pin woundmaking tool)	4493	Essen BioScience Inc.
IncuCyte® Zoom	40239	Essen BioScience Inc.
Label Manager®	280	DYMO
Laminar flow hood/biosafety cabinet	HERA safe KS18	Kendro
Laminar flow hood/biosafety cabinet	MaxiSafe 2030i	Thermo Fisher Scientific
LightCycler® 480	1220, 5447	Roche
Magnetic hotplate stirrer	MR 3001	Heidolph
Magnetic hotplate stirrer	MR Hei-Standard	Heidolph
Megafuge 1.0R	40618926	Heraeus

Continued on the next page

Name	Reference	Supplier
Microscope Axiovert 25 CFL	3810669840	Zeiss
Microscope EVOS FL	G2616-155G-0348	Thermo Fisher Scientific
Microwave	NA	BOSCH
Mini Blot Module	B1000	Thermo Fisher Scientific
Mini Gel Tank	A25977	Thermo Fisher Scientific
Mithras microplate reader	LB 940	Berthold Technologies
NanoDrop ND-1000 spectrophotometer	C957	PeqLab Biotechnologie GmbH
Neubauer Hemocytometer	718605	Brand GmbH
Peltier Thermal Cycler	PTC-200	MJ Research
PEQPower 300	81119172	PeqLab Biotechnologie GmbH
pH-meter-basic	PB-11	Sartorius
Pinzette Dumont 5 INOX	K342.1	Carl Roth GmbH
Pipetboy	accu-jet® *pro*	BRAND
PIPETMAN L Multichannel P12x200L, 20-200 µL	FA10012	Gilson
PIPETMAN Neo P1000N, 100-1000 µl	F144566	Gilson
PIPETMAN Neo P10G, 1-10 µl	F144055M	Gilson
PIPETMAN Neo P200G, 20-200 µl	F144565	Gilson
PIPETMAN Neo P20G, 2-20 µl	F144056M	Gilson
PIPETMAN Neo P2N, 0.2-2 µl	F144561	Gilson
PowerPac™ 200	JB 892 LC	Bio-Rad
PowerPac™ Basic	1645050	Bio-Rad
PowerPac™ Universal	04 BR 05104	Bio-Rad
Precision balance	BJ 2100D	Precisa
Precision balance	CP124S	Sartorius
PROMIX A40 Automatic Mixer	1180-1-0000	PROTEC GmbH & Co. KG
Research pro 5-100 µl	P6985	Eppendorf AG
Shaker/mixer	Polymax 1040	Heidolph
Shaker/mixer	Duomax 1030	Heidolph
Shaking incubator	AJ 112	Infors AG
Soda Lime Glass Balls; 4mm	Z265934-1EA	Sigma-Aldrich
Spectrafuge Mini	C1301	Labnet
Sprout™	HSD43769	Biozym
Thermocycler Tadvanced	3812230	analytik jena
Thermomixer - Mixer HC	S8012-0000	STARLAB International GmbH
Thermomixer comfort	5355	Eppendorf AG
Tube rotator (1.5 ml or 2 ml)	444-0500	VWR™
Tube rotator (15 ml or 50 ml)	RM 10 W	CAT
Tube rotator (15 ml or 50 ml)	RM 10	CAT
Vacusafe comfort	80877	IBS Integra Biosciences
Vortex Genie® 2	G-560E	Scientific Industries
Waterbath	TW12	Julabo

3.2 Methods

3.2.1 Cell biological methods

3.2.1.1 *Cell lines, culture media, and cell handling*

The human melanoma cell lines A375 (American Type Culture Collection, ATCC, CRL-1619) and RPMI7951 (ATCC HTB-66), as well as the human embryonic kidney cells HEK293T (ATCC CRL-11268) were purchased from ATCC. The human melanoma cell line WM793 was a generous gift by Meenhard Herlyn (The Wistar Institute Melanoma Research Center, Philadelphia, USA). HEK293T KO2.9 and A375 sgEVI2_4 *EVI/WLS* knock-out cell lines were generated in-house using Clustered Regularly Interspaced Short Palindromic Repeats (CRISPR)/Cas9 and single cell clonal expansion by Oksana Voloshanenko or Iris Augustin, respectively. Cells were regularly authenticated and confirmed to be mycoplasma negative. Cell counting was performed with a hemocytometer.

All cells were cultured as monolayers in Dulbecco´s modified Eagle´s medium (DMEM) with 4.5 g/l (high) glucose and L-glutamine supplemented with 10 % fetal bovine serum (FBS, volume fraction) without antibiotics at 37 °C and 5 % CO_2 in a humidified atmosphere. When they reached 80 % to 90 % confluence, cells were washed once with phosphate buffered saline (PBS) and then passaged after trypsinisation with 0.25 % trypsin/ethylenediaminetetraacetic acid (EDTA) for 2 min to 5 min. Typically, cells were re-seeded at 1/10 or 1/20 of initial confluence. No cells with a higher passage number than 25 were used for experiments (for HEK293T cells not higher than 20). It should be noted that RPMI7951 cells with higher passage numbers regularly have multiple nuclei and divide considerably slower than cells with lower passage numbers.

To cryopreserve cells, a minimum of 1×10^6 cells in 1 ml FBS with 10 % dimethyl sulfoxide (DMSO, volume fraction) was frozen at -80 °C in cryotubes with the help of Mr. Frosty Freezing Containers. For long term storage, cells were kept in the liquid nitrogen tank. Defrosting was done by heating the cryotubes to 37 °C for 2 min, followed by resuspension of cells in culture medium. The DMSO was removed by centrifugation at 200 × g for 5 min and one wash with PBS before cells were taken into culture.

3.2.1.2 *Plasmid transfection*

Plasmid transfection for overexpression of genes was either done using TransIT-LT1 Transfection Reagent for HEK293T and A375 cells or FuGENE HD Transfection Reagent for RPMI7951 cells. Cell numbers for seeding and reagent volumes are indicated in Table 17. Cells were seeded 24 h prior to plasmid transfection. The next day, the culture medium was replaced after

one wash with PBS. All reagents were brought to room temperature before use. Plasmid DNA was diluted in serum-free RPMI-1640 medium before adding the transfection reagent and the tube was gently mixed by flipping. TransIT-LT1 reactions were incubated for 15 min at room temperature before being added dropwise to the cells. FuGENE HD reactions were added directly dropwise to the cells. Cells were harvested 48 h after plasmid transfection for immunoprecipitation and/or Western blot assays and fixed after 24 h for immunofluorescence analysis.

Table 17. Volumes for plasmid transfection

	RPMI7951 (FuGENE HD)		A375 (TransIT-LT1)		HEK293T (TransIT-LT1)	
	24-well	**6-well**	**6-well**	**10 cm dish**	**6-well**	**10 cm dish**
Cell number	3×10^4	1.5×10^5	7×10^4	5×10^5	2×10^5	3.5×10^6
Culture medium (ml)	0.5	2	2	10	2	10
Plasmid DNA (µg)	0.375	1.5	1	1.5	0.25 - 1	1.5
Transfection reagent (µl)	1.5	6	6	12	3 - 5	12
RPMI-1640 medium (µl)	25	100	250	500	250	500

3.2.1.3 siRNA transfection

Lipofectamine RNAiMAX Transfection Reagent was used to transfect melanoma cells with siRNA 24 h after seeding, whereas HEK293T cells were transfected in parallel to being seeded (reverse transfection). Cell numbers for seeding and reagent volumes are indicated in Table 18. siRNAs purchased from Ambion (Thermo Fisher Scientific) were diluted to a working concentration of 5 µM with ddH_2O and siRNAs from Dharmacon (Horizon Discovery) were diluted to 20 µM using 1× siRNA Buffer from Dharmacon. All further experimental steps were done with the same volumes for both siRNA suppliers. siRNAs were kept on ice as much as possible, all other reagents were brought to room temperature before use.

For the transfection of melanoma cells, reagent mix A and B were prepared as indicated in Table 18, incubated at room temperature for 2 min and then combined. In the meantime, the cells were washed once with PBS and the culture medium was changed. After incubating the mix for 5 min at room temperature, it was added dropwise to the cells. The culture medium was changed again 24 h before harvest or further processing of the cells, with a total siRNA incubation time of 72 h to 96 h.

For the transfection of HEK293T cells, siRNA working solutions were diluted 1/40 with ddH_2O, resulting in concentrations of 500 nM for Dharmacon and 125 nM for Ambion, and 100 µl of this solution was distributed dropwise to the bottom of wells or dishes. Lipofectamine RNAiMAX was diluted with half of the volume of serum-free RPMI-1640 medium indicated in Table 18 and incubated at room temperature for 10 min, before being further diluted with the

remainder. This mix was then added to the siRNAs in the wells and further incubated for 30 min at room temperature. In the meantime, cells were prepared and seeded in culture medium on top of the siRNA/RNAiMAX mix. Gentle shaking ensured equal distribution of siRNA and cells. Cells were typically harvested 72 h after siRNA transfection.

Table 18. Volumes for siRNA transfections

	Melanoma cells		HEK293T		
	6-well	**10 cm dish**	**12-well**	**6-well**	**10 cm dish**
Cell number	7×10^4 (A375) 1×10^5 (WM793) $1{,}5 \times 10^5$ (RPMI7951)	5×10^5 (A375)	6×10^4	3×10^5	$3{,}5 \times 10^6$
Culture medium (ml)	2	10	0.3	1.4	8
siRNA (µl)	3 (Mix A)	20 (Mix A)	20	100	400
RNAiMAX (µl)	6 (Mix B)	40 (Mix B)	0.8	4	8
RPMI-1640 medium (µl)	125 (Mix A) + 125 (Mix B)	625 (Mix A) + 625 (Mix B)	50 + 50	250 + 250	1 000 + 1 000

3.2.1.4 Inhibitor treatments

LGK974 is an inhibitor of PORCN and was used at 10 µM for 96 h with daily medium changes and PBS washes (stock solution: 50 mM in DMSO). MG132 is an inhibitor of the proteasome and was used at 1 µM for 24 h (stock solution: 10 mM in DMSO). Cycloheximide is an inhibitor of translocation at the ribosomes and thus an inhibitor of protein synthesis (stock solution: 100 mg/ml in DMSO). It was used at 20 µM for the indicated time frames. For all inhibitors, equivalent volumes of DMSO were used as control.

3.2.1.5 Gelatin degradation assay

The gelatin degradation assay was used to assess the invasive potential of melanoma cells *in-vitro*. To this end, gelatin coated cover glasses (diameter 12 mm) were prepared using the QCM Gelatin Invadopodia Assay (Green) following the manufacturer's instructions in 24-well plates, but with only half the suggested volumes (except for washing, disinfection, and blocking steps). Before coating, cover glasses were incubated in 20 % nitric acid for 30 min and then washed in ddH_2O for 2 h with multiple changes of ddH_2O. After drying in a chemical hood, they were autoclaved and stored until needed.

It proofed to be very helpful to mark the uncoated side of the glass slides with a '7' using an ethanol-resistant marker before starting the coating – this way, it was easy to tell whether the slide is upside down or not (looks like '7' means uncoated side up; looks like '4' means coated side up). Additionally, it was of upmost importance to avoid contaminating the cells with ethanol by transferring the glass slides to new wells after both the disinfection step with 70 %

ethanol and after the subsequent washing step before the addition of culture medium. Coated slides could be stored in culture medium overnight in the cell culture incubator or up to one week in PBS at 4 °C. Care was taken to keep the coated cover glasses protected from light as much as possible.

As described above, melanoma cells were pre-treated with LGK974 for 96 h or siRNAs or plasmids for 72 h in 6-well plates. The culture medium was changed 24 h before seeding on gelatin slides. For seeding on the gelatin, the culture medium was removed (and collected for further analyses, if necessary), cells were washed once with PBS and dissociated using 0.5 ml of 0.25 % trypsin/EDTA for as short as possible (note that prolonged incubation with trypsin can negatively influence the cells' gelatin degradation potential). After stopping the trypsinisation with 4.5 ml of culture medium, the cells were counted and seeded on gelatin coated cover glasses in 24-well plates (ca. 30 000 cells in 0.5 ml culture medium). To prevent the cover glasses from floating, they were gently pushed down using a pipette tip. Plates were then incubated at 37 °C and 5 % CO_2 in a humidified atmosphere for 24 h and then fixed using 4 % paraformaledehyde (PFA, pre-warmed to 37 °C) for 10 min at room temperature followed by three 5 min washes with PBS. Fixed cells could be stored in PBS at 4 °C before the immunofluorescence staining (see 3.2.4.1).

3.2.2 Molecular biological methods

3.2.2.1 Molecular cloning and sequencing

3.2.2.1.1 Gateway cloning to generate FLAG-tagged constructs

Plasmids encoding FLAG-tagged constructs of ERLIN1, ERLIN2, FAF2, UBE2K, or UBXN4 with a Cytomegalovirus (CMV) promoter were generated using the Gateway Technology according to the manufacturer's instructions. Therefore, respective 'entry clones' (Kanamycin resistance, 10 µg/ml) carrying full open reading frames (ORF) for each gene were integrated in the destination vectors (pDEST, Ampicillin resistance, 100 µg/ml) 'pDEST-FLAG C-terminal' and 'pDEST-FLAG N-terminal' (UBE2K ORF only). Entry clones and pDEST were provided by the Genomics and Proteomics Core Facility (GPCF) at the German Cancer Research Center (DKFZ). In brief, 1 µl to 7 µl of entry clones (50 ng to 150 ng) and 1 µl of pDEST (150 ng/µl) were mixed and filled to 8 µl with ddH_2O. Then, 2 µl of LR Clonase II Enzyme Mix were added to each reaction and samples were incubated at 25 °C for 1 h. To stop the reaction, 1 µl of Proteinase K solution was added to each sample followed by 10 min incubation at 37 °C. 1 µl of each LR reaction was used to transform One Shot TOP10 Chemically Competent *Escherichia coli* (*E. coli*).

3.2.2.1.2 *Site-directed mutagenesis*

The Q5 Site-Directed Mutagenesis Kit was used according to the manufacturer's instructions to introduce a STOP codon (TAG) at the 3' end of the *UBE2K* ORF in the UBE2K-N-FLAG plasmid. Primers were generated using the NEBaseChanger (5'-3', forward: TGATTGGACCCAGCTTTCTTG, reverse: GTTACTCAGAAGCAATTCTG). In brief, PCR was performed with the settings shown in Table 19 using 12.5 µl Q5 Hot Start High-Fidelity 2× Master Mix, 1.25 µl of both forward and reverse primers (10 µM), 1 µl plasmid (1 ng/µl to 25 ng/µl), and 9 µl ddH_2O. Afterwards, 1 µl of the PCR product together with 3 µl ddH_2O were treated with 5 µl 2× KLD reaction buffer and 1 µl of 10× KLD enzyme mix for 5 min at room temperature. 5 µl of each reaction were used to transform One Shot TOP10 Chemically Competent *E. coli*.

Table 19. Thermocycler conditions used for site-directed mutagenesis.

Temp (°C)	Time (s)		Step
98	30		Denaturation and activation
98	10	} 25 cycles	Denaturation
60	30		Annealing
72	210		extension
72	120		Final extension
4	∞		pause

3.2.2.1.3 *Plasmid DNA amplification and sequencing*

Plasmid DNA was amplified after Gateway cloning (see 3.2.2.1.1), site-directed mutagenesis (see 3.2.2.1.2), or retro-transformation using 30 µl - 50 µl of One Shot TOP10 Chemically Competent *E. coli*. For the transformation, bacteria were defrosted on ice and carefully mixed with plasmid DNA. After 30 min further incubation on ice, a heat-shock was performed by incubation cells at 42 °C for 30 s. Then, 250 µl of pre-warmed (37 °C) Super Optimal broth with Catabolite repression (S.O.C.) medium were added to cells and samples incubated for 1 h at 37 °C with shaking (300 rpm). This pre-culture was plated in full or in parts on selective LB agar plates using glass beads and incubated at 37 °C overnight. The next day, single bacteria colonies were picked to start small liquid cultures in selective LB medium (5 ml - 7 ml, 'Mini-Prep'). After 8 h incubation at 37 °C, these could also be used as starting cultures for large liquid cultures (ca. 250 ml, 'Maxi-Prep').

Plasmid preparations from overnight liquid bacteria culture were performed using the QIAGEN Plasmid Mini and Maxi Kits according to the manufacturer's instructions (Version: March 2016). Plasmid DNA was eluted in ddH_2O and concentration and purity were measured using a NanoDrop ND-1 000 spectrophotometer. DNA was stored at -20 °C.

DNA sequencing was outsourced to Eurofins Genomics using SupremeRun Tube Sanger Sequencing (previously GATC). Primers for sequencing were either provided directly by Eurofins Genomics or generated *in silico* using SerialCloner, the Primer3web tool or the Sequencing Primer Design Tool. Obtained sequences were analysed using SerialCloner.

3.2.2.2 Isolation of total RNA and synthesis of complementary DNA (cDNA)

RNA was isolated from cells using the QIAGEN RNeasy Mini Kit with on-column DNase digestion with the QIAGEN RNase-Free DNase Set to reduce contamination of DNA, both according to the manufacturer's instructions (quick start protocol version: March 2016, including optional centrifugation step at full speed). The DNase digest was especially important for the analysis of genes for which no intron-spanning primers for RT-qPCR could be designed. Before RNA isolation, culture medium was removed and cells were washed twice with PBS. After complete removal of PBS with a pump, cells were lysed directly in the wells with 350 µl RLT buffer, scraped off using a cell scraper and transferred to a 1.5 ml tube. Samples could be stored at this stage at -20 °C or processed further. In the end, RNA was eluted in 30 µl RNase-free ddH_2O and concentration and purity were measured using a NanoDrop ND-1 000 spectrophotometer. RNA was stored at -20 °C and kept on ice as much as possible.

cDNA synthesis was performed in 1.5 ml tubes using the RevertAid H minus First Strand cDNA Synthesis Kit with 1 µg to 5 µg of total RNA input and oligo $(dT)_{18}$ primers. For easier handling, a master mix was prepared with all reagents except for RNA and the respective amount of RNase-free ddH_2O. A non-reverse transcribed control without enzyme was included to check for specificity. The samples with a total volume of 20 µl were incubated at 42 °C for 60 min and then at 75 °C for 5 min to terminate the reaction. Afterwards, the samples were diluted with ddH_2O to a cDNA concentration of 5 ng/ µl to 10 ng/µl. cDNA was stored at -20 °C.

3.2.2.3 RT-qPCR

mRNA expression was quantified using RT-qPCR performed in 384-well plates on a Roche LightCycler 480 Instrument II with dual hybridisation probes from The Universal ProbeLibrary and primers were designed using The Universal Probe Library Assay Design Center. Primers and respective probes are listed in Table 10. All reactions were performed in technical triplicates. Per reaction, 6 µl of primer-enzyme mix (5.5 µl LightCycler 480 Probes Master, 2× concentrated, 0.17 µl dual hybridisation probe, 0.11 µl of both forward and reverse primer, 20 µM, and 0.17 µl ddH_2O) was added to 5 µl of diluted cDNA (see 3.2.2.2). The PCR was run with the settings depicted in Table 20. Threshold or quantification cycles (C_q) were calculated using the LightCycler 480 software.

Table 20. Thermocycler conditions for RT-qPCR

Temp (°C)	Time (s)		Step
95	600		Denaturation
95	10	45 cycles	Denaturation
55	20		Annealing
72	1		extension
40	10		Cooling

RT-qPCRs were performed in accordance with the Minimum Information for Publication of Quantitative Real-Time PCR Experiments (MIQE) guidelines (Bustin et al., 2009), using at least two reference genes per experiment (*GAPDH*, *SDHA*, *G6PD*, or *ACTB*). PCR amplification efficiencies were determined for each primer pair and cell line from a calibration curve resulting from performing a RT-qPCR with the following cDNA concentrations: 10 ng/µl, 2 ng/µl, 0.4 ng/µl, 0.08 ng/µl, 0.0016 ng/µl. The $\log_{10}$ values of these concentrations were plotted on the x-axis and the resulting C_q values on the y-axis. Then, a linear regression curve was fitted, and its slope was used to calculate the efficiency E with the equation: $E = 10^{(-1/slope)}$.

Calculations of relative mRNA expression levels were performed using the Pfaffl method (Pfaffl, 2001), which includes PCR amplification efficiencies, using the following formula:

$$\text{Relative mRNA expression} = (E_{\text{target gene}})^{\Delta Cq,\ \text{target gene (calibrator – sample)}} / (E_{\text{ref. gene}})^{\Delta Cq,\ \text{ref. gene (calibrator – sample)}}$$

Expression levels were calculated relative to *GAPDH* as reference gene and siControl, siLuciferase, or DMSO treatment were used as calibrators. Data analysis was done using Microsoft Excel and R.

3.2.3 Protein biochemical methods

3.2.3.1 Cell lysis and determination of protein concentration

In order to analyse cellular protein content and protein-protein interactions, total protein lysates were isolated from cells using eukaryotic lysis buffer (20 mM Tris-HCl, pH 7.4; 130 mM NaCl; 2 mM EDTA; glycerol at a volume fraction of 10 %; used for immunoprecipitation and TUBE assays) or 8 M urea/PBS (all other assays).

Eukaryotic lysis buffer was supplemented before use with 1 % Triton X-100 (volume fraction), 5 mM N-ethylmaleimide/ethanol (NEM), 2 mM 1,10-phenanthroline/ethanol (oPA), and 1 cOmplete, mini Protease Inhibitor Cocktail tablet per 10 ml buffer. Buffer with inhibitors could be stored for one week at 4 °C. Triton X-100 was used to break up cell membranes, cOmplete contains several protease inhibitors, NEM is an inhibitor of cysteine peptidases, and oPA inhibits metalloproteases. NEM and oPA are important to include when analysing

ubiquitination of proteins, since this type of modification can be cleaved off rapidly by DUBs. Lysis buffer, PBS and reaction tubes were pre-cooled to 4 °C. The cells' medium was removed and cells washed twice with ice cold PBS – after the last wash, cell culture dishes were put in an upright position and remaining PBS was removed as completely as possible with a cell culture pump. Then, 200 µl to 750 µl of ice-cold eukaryotic lysis buffer were added to each dish and the cells collected using a cell scraper. Lysates were transferred to pre-cooled reaction tubes and further homogenised by pipetting up and down 3 to 5 times.

Cells in 6-well format were lysed in ca. 100 µl to 200 µl 8 M urea/PBS buffer (without supplements) after two washes with PBS, then scraped off and transferred to reaction tubes.

After harvesting, cell lysates from both methods were incubated in a tube rotator at 4 °C for at least 20 min and, subsequently, clarified by centrifugation in a pre-cooled table-top centrifuge (4 °C) at maximum speed for 20 min. Pellets containing cell debris were discarded. At this point, protein lysates could be frozen and stored at -20 °C.

To determine protein concentrations for downstream applications, the Pierce bicinchonic acid (BCA) Protein Assay Kit was used according to the manufacturer's instructions. 4 µl of samples were measured in duplicates together with bovine serum albumin (BSA) standards for the standard curve (included in each plate: 2 000 µg/ml, 1 000 µg/ml, 500 µg/ml, 250 µg/ml, 125 µg/ml, and 0 µg/ml) in transparent flat bottom 96-well plates. After a 30 min incubation at 37 °C, a Mithras LB 940 Multimode Microplate Reader was used to measure the absorbance at 562 nm. Protein concentrations of each sample were then calculated according the standard curve using Microsoft Excel.

For protein lysates prepared with 8 M urea/PBS, the respective volumes for 40 µg to 60 µg protein were transferred to a new reaction tube, filled up to 80 µl with ddH_2O and then incubated together with 20 µl 5× Laemmli buffer (312.5 mM Tris-HCl, pH 6.8; 0.5 M Dithiothreitol, DTT; mass fraction of 10 % sodium dodecyl sulphate, SDS, and 0.1 % bromphenol blue; volume fractions of 10 % Tris-(2-carboxyethyl)-phosphin, TCEP, and 50 % glycerol) at 95 °C for 5 min. Samples were immediately cooled down on ice and either used for SDS polyacrylamide gel electrophoresis (SDS-PAGE, 40 µl per sample) or frozen at -20 °C.

3.2.3.2 Isolation of secreted WNTs from supernatant

Secreted WNTs were enriched from cell culture supernatants using the affinity chromatography resin Blue Sepharose 6 Fast Flow and analysed by Western blotting (Glaeser et al., 2016). All steps were carried out at room temperature unless indicated otherwise. Medium was collected from 6-well plates except for endogenous WNT11 studies that were performed in 10 cm dishes with 10 ml of culture medium.

Cell culture medium was changed 24 h before harvesting to accurately compare different treatment conditions at a specific time point. Note that differences in seeding density or viability also influence WNT secretion levels. The next day, 2 ml culture medium from one well of a 6-well plate was transferred to a 2 ml reaction tube and centrifuged at room temperature for 10 min at 8 000 × g. 1,8 ml of the supernatant were then transferred to a new 2 ml tube and the pellet discarded. Samples could be stored at this point at -20 °C. Next, Triton X-100 was added to a final volume fraction of 1 %. Per sample, 30 µl of Blue Sepharose 6 Fast Flow resin was washed twice in washing buffer (50 mM Tris-HCl, pH 7.5; 150 mM KCl; volume fraction of 1 % Triton X-100 in ddH_2O) by centrifugation and decanting of supernatant (3 min, 2 800 × g). Then, resin was distributed equally to all samples and incubated over night at 4 °C in a tube rotator. The following day, resin was washed 2 to 3 times as above, until the wash buffer was clear. After the last wash, ca 100 µl wash buffer were left in the tube together with the resin and 100 µl of 2× Laemmli buffer (see 3.2.3.1) were added. The samples were boiled at 95 °C for 5 min, then cooled on ice and either used for SDS-PAGE (40 µl loading per gel) or frozen at -20 °C.

3.2.3.3 Tandem Ub Binding Entity (TUBE) Assays

TUBEs are stretches of tandem Ub binding domains that bind poly-ubiquitinated proteins and protect them from being degraded but also facilitate their enrichment and their analyses (Hjerpe et al., 2009).

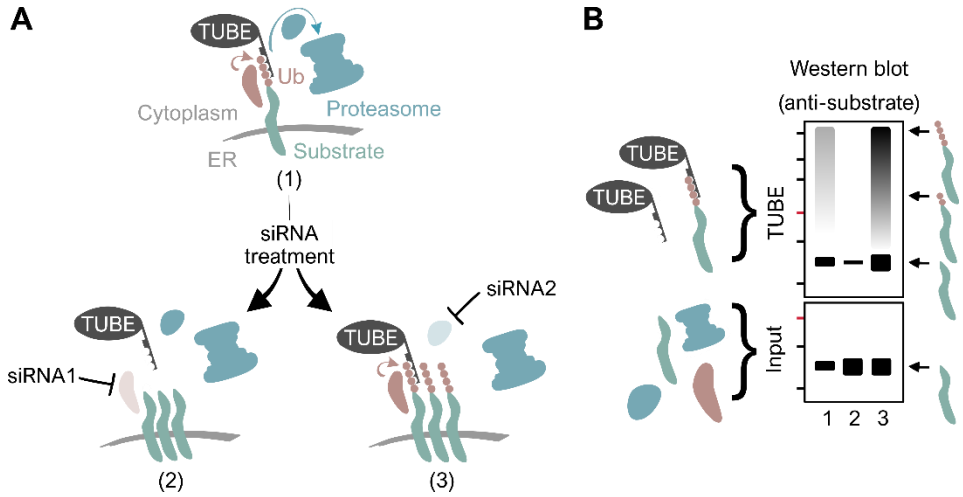

Figure 10. Tandem Ubiquitin Binding Entities (TUBEs) are used to examine the ubiquitination of substrate proteins

A, B. RNAi mediated knock-down of proteins involved in the recognition, ubiquitination, dislocation, targeting to, or degradation by, the proteasome can lead to the accumulation of their substrates with or without ubiquitin modifications, depending on whether the cascade is interrupted before or after substrate ubiquitination. TUBEs are used to stabilise and enrich poly-ubiquitinated proteins from cell lysates. These poly-ubiquitinated substrates will appear as high-molecular bands on a Western blot, because each ubiquitin adds to the protein's molecular mass. Depending on the treatment, protein samples before ('Input') and after ('TUBE') pull-down show characteristic patterns on the Western blot stained for the substrate. ER = endoplasmic reticulum, Ub = poly-ubiquitin

Pull-downs with TUBEs can be used to analyse the ubiquitination of substrates, due to the characteristic 'ladder' patterns poly-ubiquitinated substrates show on Western blots as every ubiquitin adds about 8.5 kDa to the substrate's molecular mass. These patterns can also appear as high molecular 'smear' if the substrate is differentially modified and therefore not all molecules run at the same heights. The observed pattern might change depending on sample treatment (Figure 10).

Four different kinds of TUBEs were used: TUBE1 magnetic and TUBE2 agarose beads bind to both K48- and K63-linked Ub chains, whereas FLAG K48 and K63 TUBEs specifically bind K48- or K63-linked poly-Ub, respectively. All steps were carried out at 4 °C unless stated otherwise.

TUBE1 (magnetic) or TUBE2 (agarose) pull-downs were performed from one 10-cm dish per condition. After cell harvest in 200 µl eukaryotic lysis buffer and protein quantification (see 3.2.3.1), all pull-down samples were adjusted to contain the same amount of protein in 1 ml lysis buffer (between 0.5 mg and 1 mg in total). Per pull-down sample, 15 µl TUBE1 magnetic or control beads or 30 µl TUBE2 agarose or Control Agarose Beads were washed twice with 1 ml Tris-buffered saline with Tween-20 (TBST; 10× TBST contained 1,37 M NaCl, 200 mM Tris-HCl, pH 7.6, and 1 % Tween-20, volume fraction) by centrifugation (3 000 × g, 3 min) at room temperature and added to the diluted protein lysates. After overnight rotation at 4 °C in a tube rotator, samples were washed 4x with 800 µl TBST or eukaryotic lysis buffer without Triton X-100 (pre-cooled to 4 °C, including NEM and oPA) after collecting the beads with centrifugation (4 °C, 3 000 × g, 5 min) or a magnetic rack and 5 min rotation at 4 °C in a tube rotator after each buffer change. After the last wash, buffer was removed completely, beads taken up in 100 µl 1× Laemmli buffer and boiled at 95 °C for 5 min.

FLA K48 or K63 TUBE pull-downs were performed from one 10-cm dish per condition. After cell harvest in 200 µl eukaryotic lysis buffer plus 250 nM FLAG TUBEs and protein quantification (see 3.2.3.1), the same amount of protein for each sample was transferred to a new 2 ml reaction tube (between 0.5 mg and 1 mg in total) and diluted by adding 1.8 ml of eukaryotic lysis buffer without Triton X-100 (but with all other inhibitors), then, the concentration of FLAG TUBEs was restored to 250 nM. Samples were incubated at 4 °C in a tube rotator for 1 h to 2 h to allow for binding of TUBEs to poly-Ub chains. Afterwards, 15 µl of ANTI-FLAG M2 Affinity Gel or 15 µl Control Agarose Beads (negative control) per sample were washed twice in lysis buffer, added to the respective samples and incubated over night at 4 °C in a tube rotator. The next day, samples were transferred to 1.5 ml reaction tubes for easier handling and washed 4× with 800 µl eukaryotic lysis buffer without Triton X-100 (pre-cooled to 4 °C, including NEM and

oPA) by centrifugation (4 °C, 3 000 × g, 5 min) and 5 min rotation at 4 °C in a tube rotator after each buffer change. After the last wash, remaining buffer was removed completely, and beads taken up in 100 µl 3× FLAG Peptide elution solution (see 3.2.3.4) for elution of poly-ubiquitinated proteins from M2 Affinity Gel. The incubation for 30 min at 4 °C in a tube rotator was followed by centrifugation as above and transfer of 100 µl of the supernatant to a new reaction tube. Samples were mixed with 25 µl 5× Laemmli buffer and boiled for 5 min at 95 °C, then cooled on ice.

40 µg of protein from the original clarified lysates were taken as 'input controls' and diluted to 200 µl with ddH_2O to reflect protein content before pull-down experiment. After addition of 50 µl of 5× Laemmli buffer to the 'Input' samples, they were boiled for 5 min at 95 °C and then cooled on ice. 40 µl of 'input' and 'pull-down' were loaded to do SDS-PAGE or samples were frozen at -20 °C.

3.2.3.4 Immunoprecipitation (IP)

To investigate protein interactions within the ERAD pathway, FLAG-tagged proteins were overexpressed in HEK393T wild type and *EVI/WLS* KO cells in 10-cm dishes (see 3.2.1.2 and 3.2.2.1.1). Similarly, pRK5-HA-Ubiquitin constructs were overexpressed in A375 cells to determine the ubiquitination status of EVI/WLS. 48 h after transfection, cells were harvested in 600 µl eukaryotic lysis buffer and protein content was quantified using a BCA assay (see 3.2.3.1). Tubes with equal amount of proteins were prepared (0.5 mg to 3.5 mg). Per sample, 40 µl ANTI-FLAG M2 Affinity Gel, Monoclonal Anti-HA-Agarose or Control Agarose Beads (negative control) were washed twice in 750 µl lysis buffer (centrifuge for 30 s at 5 000 × g), then blocked for 1 h with 2.5 % BSA/TBST (mass fraction) at 4 °C in a tube rotator and washed again twice as previously. The resin was then equally distributed to the respective samples and incubated over night at 4 °C in a tube rotator. The next day, resin was washed five to seven times as previously, and proteins were eluted using 3× FLAG Peptide or HA Peptide. To do so, 3× FLAG Peptide or HA Peptide was dissolved in peptide dissolve buffer (0.5 M Tris-HCl, pH 7.5 and 1 M NaCl in ddH_2O) to obtain a concentration of 0.25 µg/µl and was then further diluted with ddH_2O to a stock solution of 5 µg/µl. The final elution solution of 150 ng/µl was obtained by further diluting 3 µl of the stock solution in 100 µl Tris-buffered saline (TBS, 50 mM Tris-HCl, pH 7.4 and 150 mM NaCl in ddH_2O). After complete removal of wash buffer after the last washing step, 100 µl of elution solution were added to each sample and incubated for 30 min at 4 °C in a tube rotator. Then, samples were centrifuged as previously and 100 µl of the supernatant transferred to a new tube. Samples were mixed with 25 µl 5× Laemmli buffer and boiled for 5 min at 95 °C, then cooled on ice.

100 µg (FLAG) or 40 µg (HA) of protein from the original clarified lysates were taken as 'input controls' and diluted to 240 µl with ddH_2O to reflect protein content before pull-down experiment. After addition of 60 µl 5× Laemmli buffer to 'input' samples, they were boiled for 5 min at 95 °C and then cooled on ice. 40 µl of 'input' and 40 µl of 'pull-down' samples were loaded to do SDS-PAGE or samples were frozen at -20 °C.

3.2.3.5 SDS-PAGE and Western blotting

All steps were carried out at room temperature unless stated otherwise. Samples containing denatured proteins in 1× Laemmli buffer (see 3.2.3.1, 3.2.3.2, 3.2.3.3, and 3.2.3.4) were boiled for 5 min at 95 °C before being loaded on Bolt 4-12% Bis-Tris Plus Gels (10, 12, or 15 wells) in 1× running buffer with 3-(N-morpholino)propanesulfonic acid (MOPS; 20× running buffer: 1 M MOPS, 1 M Tris-Base, 20 mM EDTA, 69.3 mM SDS in ddH_2O). The SDS-PAGE separated proteins and the PageRuler Prestained Protein Ladder by size and was run for 15 min at 80 V and then for 45 min at 180 V or until the blue loading dye left the gel. Then, proteins were transferred to nitrocellulose membranes by wet blotting in 1× NuPage transfer buffer (20× transfer buffer: 500 mM Bicine, 500 mM Bis-Tris, 20 mM EDTA) with 10 % methanol for 75 min at 20 V. Successful and bubble-free transfer was confirmed by Ponceau Red staining. After complete de-staining of the membranes in TBST, they were blocked in 5 % skim milk/TBST (mass fraction) for 30 min at room temperature and then incubated with primary antibody over night at 4 °C or for 1 h at room temperature (see Table 1, typically 3 ml total volume in 50 ml Falcon tube) on a Roller Falcon Tube Mixer. Afterwards, membranes were washed three times for 7 min in TBST on a shaker and incubated with horseradish peroxidase (HRP)-coupled secondary antibody for 1h at room temperature (see Table 3) and then again washed as before. All antibodies were diluted in 5 % skim milk/TBST (mass fraction). Then, membranes were incubated with enhanced chemiluminescence (ECL) substrates and the HRP induced light signals were captured using Amersham Hyperfilm ECL and made visible using the COMPACT 2 X-Ray Film Processor. Immobilon Western HRP Substrate was used for standard application and SuperSignal West Femto Maximum Sensitivity Substrate was used if stronger signal amplification was necessary.

Western blot quantification using Fiji (Fiji is just ImageJ) was performed to analyse the cycloheximide chase assay. To this end, signal intensities were measured in equally sized regions of interest of EVI/WLS staining, HSC70 staining, and areas without signal (background). The background signal was deduced from the EVI/WLS or HSC70 values and their ratio was calculated to account for potential differences in loading. In a last step, each ratio was then normalised to timepoint 0 h.

3.2.4 Microscopy

3.2.4.1 Immunofluorescence staining, imaging, and image analysis

Immunofluorescence staining was performed to examine the intracellular localisation of EVI/WLS and to analyse gelatin degradation assays (see 3.2.1.5). All steps were carried out at room temperature, unless stated otherwise. Gelatin experiments were protected from light as much as possible, all others were protected from light after addition of fluorescent dyes.

All cells were fixed directly after removal of culture medium (without PBS wash) using 4 % PFA/PBS (preheated to 37 °C, volume fraction) for 10 min at room temperature, followed by three washes with PBS for 5 min. Afterwards, cells could be stored in PBS at 4 °C.

To facilitate the entry of staining agents into the cells, plasma membranes were permeabilised using 0.2 % Triton X-100/PBS (volume fraction) for 10 min. Then, blocking solution (1 % goat serum, 3 % FCS, 0.1 % Triton X-100, all volume fraction in PBS) was added for at least 30 min to reduce unspecific binding of antibodies. Afterwards, primary antibodies diluted in 200 µl PBS (for 24 well plate well) were added for 1 h at room temperature or overnight at 4 °C (for dilutions refer to Table 1), followed by three 5 min washes with PBS, 0.05 % Tween-20/PBS (volume fraction), and again PBS on a shaker at high speed. Secondary antibodies and other fluorescent stains were diluted according to Table 2 and added for 1 h, followed by three washes as above. Ultimately, cover glasses were inverted and mounted on microscope slides using ProLong Diamond Antifade Mountant with 4′,6-diamidino-2-phenylindole (DAPI). Once the mounting medium had hardened, cover glasses were additionally fixed with nail polish. Stained specimens were stored at -20 °C.

Images were acquired in the .czi format using a Zeiss motorized inverted Axio Observer.Z1 microscope (‘Cell Observer’) with the ZEISS ZEN (blue edition) software provided by the DKFZ Light Microscopy Facility (excitation sources: mercury arc burner HXP 120 and LED module Colibri; detector: gray scale CCD camera AxioCam; filter sets: 49(DAPI), 38 HE (eGFP), 43 HE (Cy3), 50 (Cy5); objectives: 20× / 0.8 Pln Apo DICII and 63× / 1.4 Oil Pln Apo DICIII).

For gelatin degradation assays, images of 8 to 10 different fields of view (20× objective) with at least 100 cells per replicate of each experiment were taken and analysed. All image analysis was done using Fiji and is described in more detail in 4.7. In brief, cells were counted based on their phalloidin (F-actin) and DAPI signal using the ‘Cell Counter Plugin’ and the area of gelatin degradation was assessed after setting a threshold to capture real degradation events and to exclude any background. This was usually done by automatically adjusting ‘brightness/contrast’ so that the ‘maximum displayed pixel value’ equalled the largest detected

value according to each image's histogram of value intensity distributions, but without adjusting the respective minimum value. Then, the images were converted to the RGB colour system and the 'Colour Threshold' was adjusted to capture brightness values ranging from 0 to 70 using the default thresholding method and no 'dark background' selection. The total area of the selection was measured by selecting 'Analyze Particles' with 'size' settings ranging from 0 to infinity and 'circularity' from 0 to 1. The obtained values were copied to a Microsoft Excel file to calculate the ratio of total thresholded area to cell number and to normalise them to the respective control condition. The normalised values were $\log_{10}$ transformed so that the controls equalled 0, a negative fold change in treatment conditions indicated decreased degradation compared to the control, and a positive fold change indicated increased degradation. The non-parametric one-sample Wilcoxon signed rank test was used in R (mu = 0, alternative = "two-sided") to assess statistical significance.

3.2.4.2 *Migration and proliferation live cell imaging assays*

Time-lapse live cell imaging to assess migration and proliferation capacities of melanoma cells were performed using an IncuCyte ZOOM system together with the IncuCyte Basic Software and the IncuCyte Scratch Wound Cell Migration Software Module. In detail, melanoma cells (Proliferation: 3 000 cells, Migration: 50 000 cells) were seeded in 300 µl of culture medium in transparent, flat bottom 96-well plates with 4 to 5 technical replicates and imaged every 2 h using a 10× objective. For proliferation analysis, confluence of cells was quantified from 4 images per well. For migration analysis, a confluent monolayer of cells was scratched one day after seeding using the 96-well WoundMaker according to the manufacturer's instructions and wound closure was monitored in 2 fields of view per well.

4 Results

4.1 RNAi screen identified novel candidates involved in the ERAD of EVI/WLS

Various proteins are involved in the recognition and retrotranslocation or dislocation of ERAD substrates, but additional regulators of EVI/WLS remain elusive. To address this in a systematic manner, I performed a siRNA and Western blot-based screen in HEK293T cells to investigate candidates chosen from literature. Figures 11B, 11C, S1, and Supplementary Table 1 show the read-out and the summarised results: in total, 52 ERAD- or Ub-associated candidates were tested, including those previously investigated by Glaeser et al., 2018.

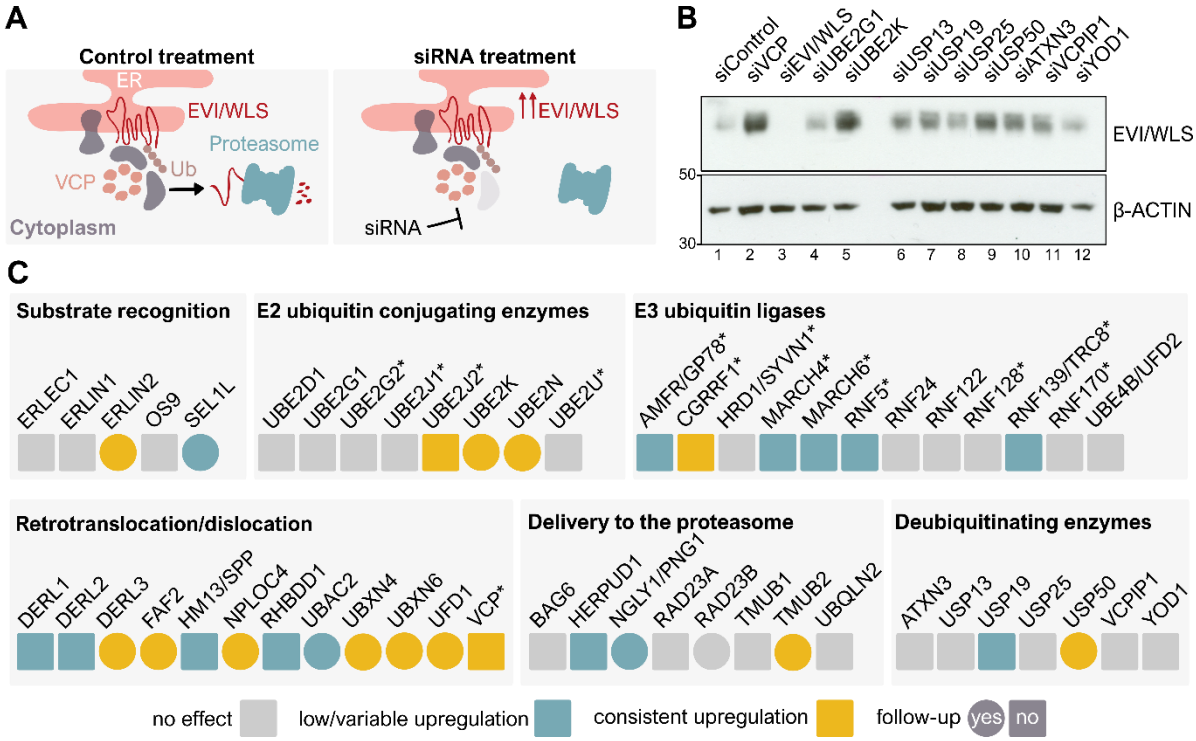

Figure 11. siRNA-based mini-screen identifies novel candidates involved in the degradation of EVI/WLS

A. Schematic illustration of the principle underlying RNAi screening. EVI/WLS protein accumulates if the siRNA targets a mRNA encoding a protein important for EVI/WLS degradation. ER = endoplasmic reticulum, Ub = poly-ubiquitin chain

B. EVI/WLS protein levels were analysed after siRNA mediated knock-down of target genes. Increased EVI/WLS protein levels compared to siControl treatment indicated the candidate's possible involvement in EVI/WLS's ERAD process. HEK293T wild type cells were treated with the indicated siRNAs for 72 h. Then, total cell lysates were analysed by SDS-PAGE and Western blotting for the specified proteins. β-ACTIN served as loading control. Non-targeting siRNA (siControl) was used as negative control and siEVI/WLS was used as on-target control for knock-down efficiency. siVCP was used as positive control as it had been shown previously to increase EVI/WLS protein levels (Glaeser et al., 2018). Western blots are representative of three independent experiments. kDa = kilodalton

C. Results of the siRNA-based screen represented as heat-map. Candidates without effect are marked in grey, candidates with low/variable effects in blue and candidates with strong and consistent upregulation of EVI/WLS in yellow. Asterisks indicate genes that were previously tested by Glaeser et al., 2018. A detailed table including gene accession numbers and phenotypes in HEK293T and A375 cells can be found in Supplementary Table S1, the Western blots underlying this analysis are shown in Figure S1.

Of the 52 candidates, 20 were either E2 Ub conjugating enzymes or E3 Ub ligases and 7 were DUBs. Furthermore, I included 5 proteins important for substrate recognition within the ER and 8 proteins involved in delivery of the substrate to the proteasome in the cytoplasm. The last group of candidates consisted of 12 proteins associated with substrate retrotranslocation or dislocation by either forming a channel, cleaving the substrate, or by recruiting or interacting with VCP.

Each candidate was targeted with a pool of four siRNAs, and I searched for genes whose knock-down resulted in increased EVI/WLS protein levels after transfection, thus indicating impaired degradation (Figure 11A). siEVI/WLS served as a control for assay specificity and siVCP was used as a positive control as it had been previously shown that the knock-down of VCP increased endogenous EVI/WLS protein levels without an effect on *EVI/WLS* mRNA expression (Glaeser et al., 2018). As expected, silencing of protein expression by siEVI/WLS and siVCP was efficient and VCP downregulation induced upregulation of EVI/WLS protein levels (Figures 11B,S1). 15 candidates (DERL3, ERLIN2, FAF2, NGLY1, NPLOC4, RAD23B, SEL1L, TMUB2, UBAC2, UBE2K, UBE2N, UBXN4, UBXN6, UFD1, and USP50) showed predominantly consistent upregulation of EVI/WLS protein levels across three independent replicates and were chosen for further validation experiments (Figures 11C,S1).

In these validation experiments, I tested the effects of the respective four single siRNAs that constitute the siRNA pool on EVI/WLS protein level and, in selected cases, on mRNA level. RT-qPCR was used to analyse on-target knock-down efficiencies and to exclude regulation of *EVI/WLS* gene expression, thus ensuring real post-translational effects. To the greatest extent, the tested siRNAs induced mRNA knock-downs between 5 % and 25 % of initial activity with minimal effects on *EVI/WLS* mRNA expression (Figures 12,16,18,S3). Especially silencing of EVI/WLS or VCP was very efficient on mRNA and protein level (Figures S1,S2,S3). However, the results of some Western blots were not reproducible and varied between biological replicates and single siRNAs, maybe due to non-target effects of the siRNAs (Figures S2,S3). These 10 genes (*DERL3*, *NGLY1*, *NPLOC4*, *RAD23B*, *SEL1L*, *TMUB2*, *UBAC2*, *UBXN6*, *UFD1*, and *USP50*) and their protein product were not chosen for further in-depth analysis, but they might be interesting candidates for future investigations in different cellular systems or with other methods, e.g. CRISPR/Cas9 induced knock-out. Nevertheless, five genes (*FAF2*, *ERLIN2*, and *UBXN4*, as well as the E2 Ub conjugating enzymes *UBE2K* and *UBE2N*) were selected for further experiments because they showed both reproducible on-target gene silencing without regulation of *EVI/WLS* and consistent up-regulation of EVI/WLS protein levels by all four siRNAs and the pool (Figure 12,16,18). The siRNAs targeting *UBXN4* were less efficient in on-target

silencing and the siRNAs #4 and #17 additionally reduced the expression of *VCP*. However, this effect on VCP was not visible on the respective Western blots and no antibody was available to test the effect of these siRNAs on UBXN4 protein expression (Figure 12H,I).

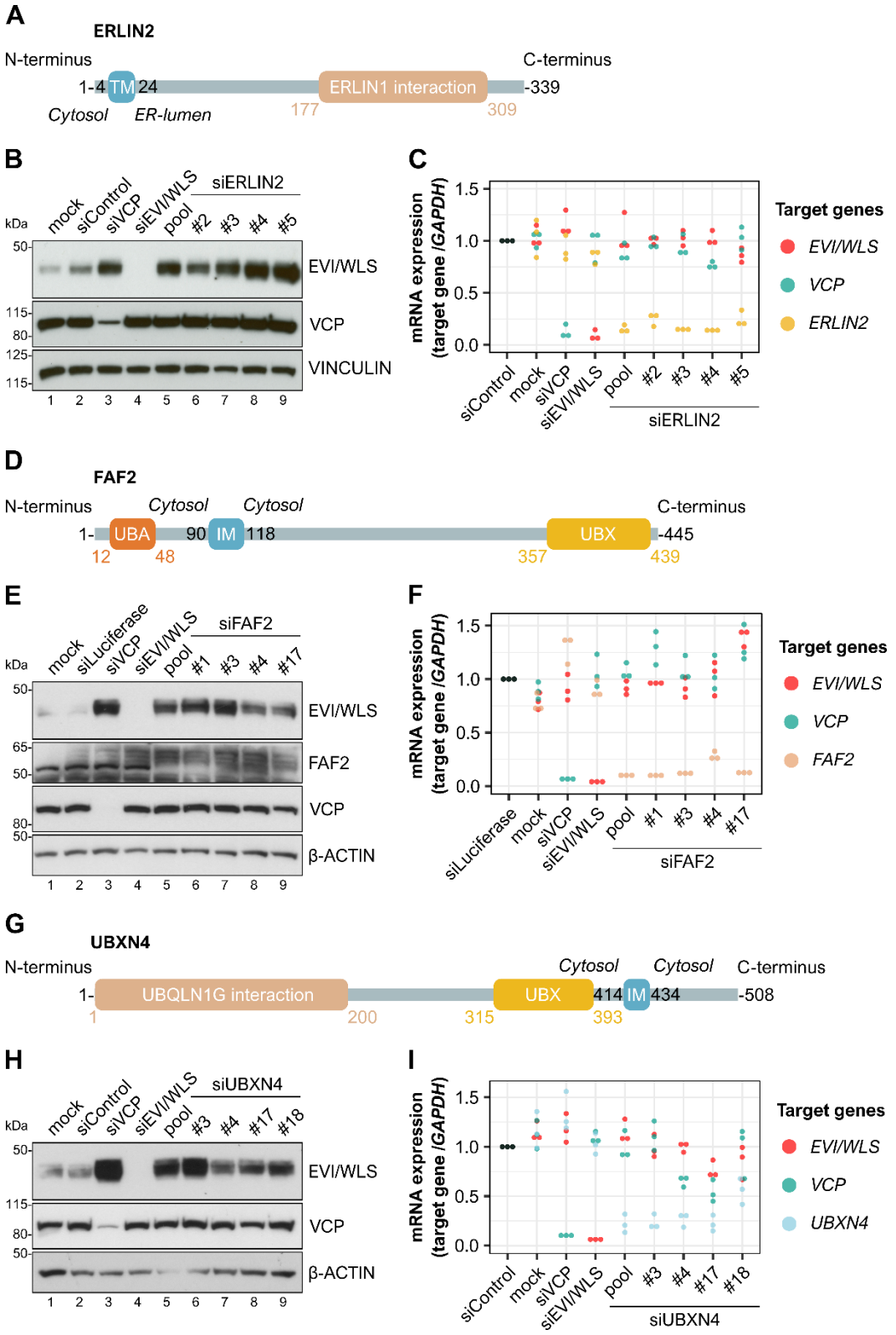

Figure 12. ERLIN2, FAF2, and UBXN4 regulate endogenous EVI/WLS on protein level (see next page for figure legend)

◄ previous page | Figure 12. ERLIN2, FAF2, and UBXN4 regulate endogenous EVI/WLS on protein level

A, D, G. Schematic representations of the proteins ERLIN2, FAF2, and UBXN4 according to UniProt IDs: O94905 (entry version 165), Q96CS3 (entry version 163) and Wang & Lee, 2012, and Q92575 (entry version 162) respectively. Numbers indicate amino acid positions. TM = transmembrane domain, IM = intramembrane domain, UBA = ubiquitin associated domain important for binding to ubiquitin, UBX = ubiquitin regulatory X domain important for binding to VCP, ER = endoplasmic reticulum

B, C, E, F, H, I. Knock-down of ERLIN2, FAF2, or UBXN4 increased EVI/WLS protein levels but had no effect on *EVI/WLS* mRNA expression. HEK293T wild type cells were treated with the indicated siRNAs for 72 h. siRNAs targeting *ERLIN2, FAF2,* or *UBXN4* were used as either single siRNAs or an equimolecular mix of all four respective siRNAs (pool). Samples treated with transfection reagent only (mock), non-targeting siRNA (siControl), or siLuciferase were used as negative control, siVCP as positive control. **B, E, H**, total cell lysates were analysed by SDS-PAGE and Western blotting for the specified proteins. VINCULIN or β-ACTIN served as loading control. Western blots are representative of three independent experiments. kDa = kilodalton. **C, F, I**, total cellular RNA was transcribed to cDNA and used for mRNA expression analyses by RT-qPCR. Target gene expression was normalised to siControl treatment and *GAPDH* served as reference gene. Individual data points from three or four independent experiments are shown.

The experiments shown in **B, C, H,** and **I** were performed by Julie Haenlin, the experiments shown in **E & F** were performed by Annika Lambert.

4.2 ERLIN2, FAF2, and UBXN4 regulate EVI/WLS

The results from the RNAi-based screen indicated the involvement of ERLIN2, FAF2, UBXN4, UBE2K, and UBE2N in the regulation of EVI/WLS protein levels. However, this could be due to indirect effects and does not necessarily imply that the candidates are involved in the ERAD of EVI/WLS. Therefore, I wanted to characterise their role in EVI/WLS degradation further by analysing interaction between EVI/WLS and the selected candidates, but the available antibodies did not allow co-immunoprecipitation experiments of endogenous proteins. Hence, overexpression constructs of ERLIN2, FAF2, UBXN4, and UBE2K with a FLAG-tag were generated using Gateway cloning to check their interaction with endogenous EVI/WLS and VCP. PORCN-FLAG was used as a positive control since it is a known interaction partner of both EVI/WLS and VCP (Glaeser et al., 2018). FAF2 and UBXN4 were described previously to interact with VCP *via* their UBX domain (Figure 12D,G, Schuberth & Buchberger, 2008).

4.2.1 EVI/WLS and VCP interact with ERLIN2-FLAG, FAF2-FLAG, and UBXN4-FLAG

ERLIN2-FLAG, FAF2-FLAG, UBXN4-FLAG, and PORCN-FLAG were overexpressed in HEK293T cells in the absence of WNT ligands. Under these conditions, EVI/WLS is constantly ubiquitinated and degraded by the proteasome (Glaeser et al., 2018) and interactions between EVI/WLS and possible mediators of this degradation should be detectable. Indeed, co-immunoprecipitation experiments demonstrated that endogenous EVI/WLS interacted with ERLIN2-FLAG, FAF2-FLAG, UBXN4-FLAG, and PORCN-FLAG (Figure 13A,C,D). All four proteins also interacted with endogenous VCP. HEK293T EVI/WLS knock-out cells were used to confirm the specificity of the EVI/WLS antibody and showed that the interaction of VCP with FAF2-FLAG, UBXN4-FLAG, and PORCN-FLAG was EVI/WLS independent. However, the binding between ERLIN2-FLAG and VCP was reduced in the absence of EVI/WLS, suggesting that a substrate

is necessary to bridge the two proteins (Figure 13A). The expression of the plasmids was quite different, although the same amount of DNA had been transfected. This indicates that the over-expressed proteins themselves were also regulated extensively. In summary, these results strongly suggest that ERLIN2, FAF2, and UBXN4 are novel interaction partners of EVI/WLS.

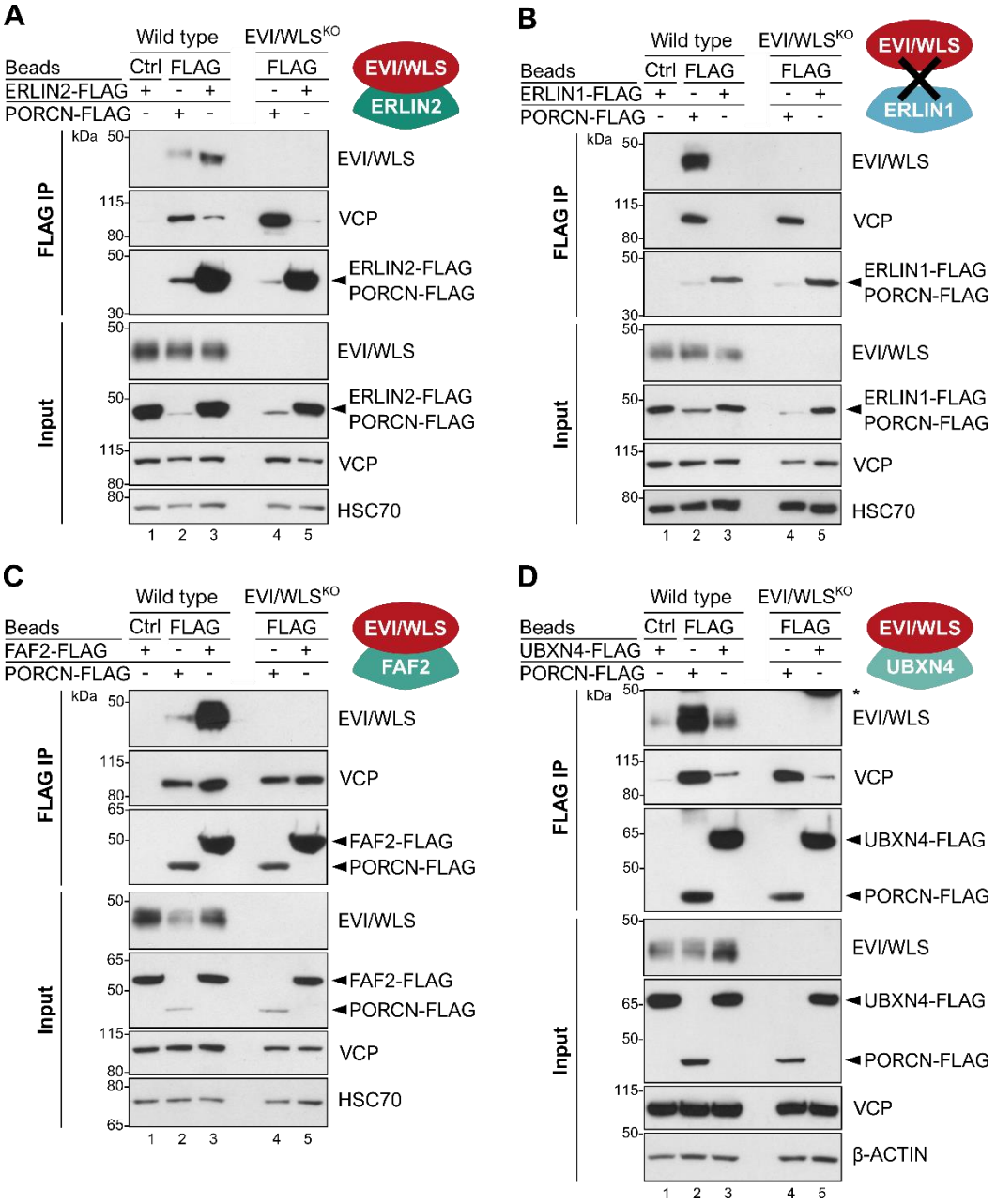

Figure 13. ERLIN2-FLAG, FAF2-FLAG, and UBXN4-FLAG interact with endogenous EVI/WLS

Immunoprecipitation (IP) experiments confirmed interaction between endogenous EVI/WLS and ERLIN2-FLAG (**A**), FAF2-FLAG (**C**), and UBXN4-FLAG (**D**) but not ERLIN1-FLAG (**B**). HEK293T wild type and EVI/WLS knock-out (EVI/WLS^{KO}) cells were transfected with ERLIN1-FLAG, ERLIN2-FLAG, FAF2-FLAG, UBXN4-FLAG, or PORCN-FLAG overexpression plasmids. After 48 h, total cell lysates were harvested for input control or used for FLAG IP to precipitate FLAG-tagged proteins and their interaction partners. Proteins were eluted using competition with 3× FLAG Peptide. Eluates and input control were analysed by SDS-PAGE and Western blotting for the specified proteins. FLAG non-binding Control Agarose Beads showed level of unspecific binding during FLAG IP and EVI/WLS^{KO} cells confirmed specificity and independent effects of EVI/WLS. HSC70 or β-actin served as loading control. Asterisks indicate background bands. Western blots are representative of three independent experiments. The experiments shown here were performed by Annika Lambert. kDa = kilodalton

It had previously been described that the function of ERLIN2 can depend on the formation of a complex with ERLIN1. Surprisingly, ERLIN1 was not identified as a candidate in the screen, in contrast to ERLIN2 (Figures 11C, S1). I included ERLIN1 in the pull-down experiments as a control and did not detect interaction with either EVI/WLS or VCP (Figure 13B). However, I detected its interaction with endogenous ERLIN2, confirming that the overexpression construct worked (Figures 14). This suggests an ERLIN1-independent role of ERLIN2 in the degradation of EVI/WLS.

In addition to their interaction with EVI/WLS and VCP, I also investigated interactions between the novel candidates on endogenous level in the presence or absence of EVI/WLS. Such interactions would suggest the existence of pre-formed complexes which might be important for the ERAD of other proteins as well. Indeed, endogenous ERLIN2 and FAF2 were immunoprecipitated with PORCN-FLAG independent of EVI/WLS (Figure 14). I also validated known interactions within the ERAD machinery, such as between FAF2 and ERLIN2 (Figure 14, Christianson et al., 2012). However, no interaction was found between FAF2 and UBXN4, despite both being interaction partners of VCP (Figure 14A). This suggests that the interaction of FAF2, ERLIN2, and PORCN might have a more general role in ERAD beyond EVI/WLS or that ERLIN2 and FAF2 are involved in the degradation of PORCN.

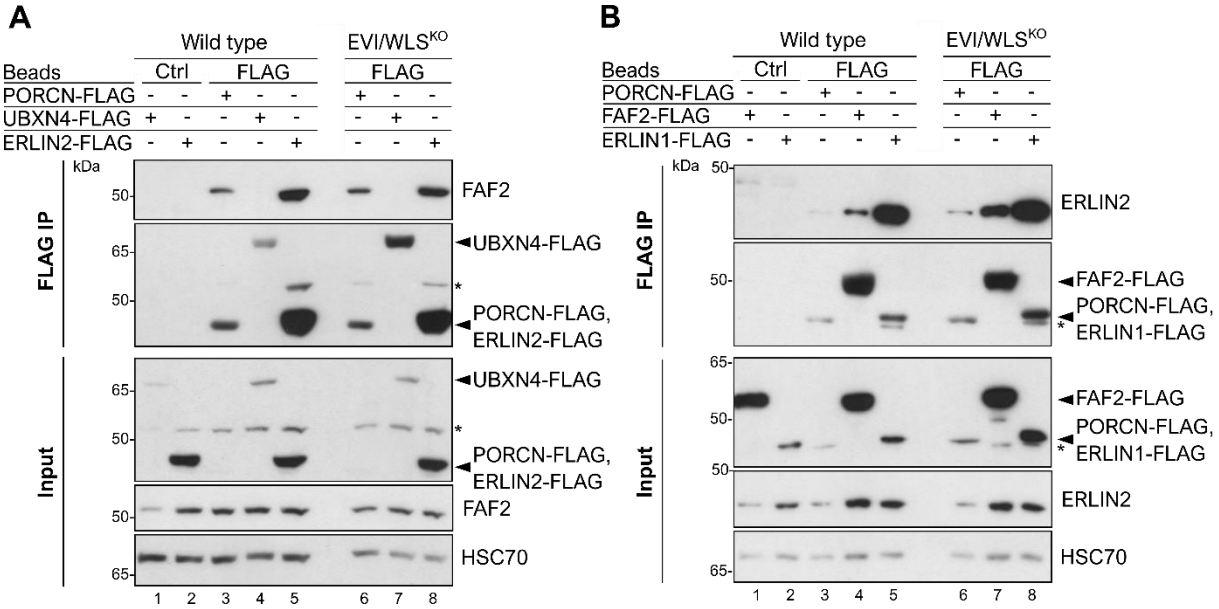

Figure 14. Interactions between novel candidates in the presence and absence of EVI/WLS

IP experiments confirmed endogenous FAF2 and ERLIN2 interacted with PORCN-FLAG and each other. Furthermore, endogenous ERLIN2 interacted with ERLIN1-FLAG. HEK293T wild type and EVI/WLS knock-out (EVI/WLS^{KO}) cells were transfected with UBXN4-FLAG, ERLIN1-FLAG, ERLIN2-FLAG, FAF2-FLAG, or PORCN-FLAG overexpression plasmids. After 48 h, total cell lysates were harvested for input control or used for FLAG IP to precipitate FLAG-tagged proteins and their interaction partners. Proteins were eluted using competition with 3× FLAG Peptide. Eluates and input control were analysed by SDS-PAGE and Western blotting for the specified proteins. FLAG non-binding Control Agarose Beads showed level of unspecific binding during FLAG IP and EVI/WLS^{KO} cells confirmed EVI/WLS independent effects. HSC70 served as loading control. Asterisks mark signal from previous stainings. Representative of three independent experiments. The experiments shown here were performed by Annika Lambert. kDa = kilodalton

4.2.2 FAF2 knock-down impedes EVI/WLS turn-over

My previous results showed interaction between endogenous EVI/WLS and ERLIN2-FLAG, FAF2-FLAG, and UBXN4-FLAG. However, it remained unclear if these candidates are involved in the turn-over of EVI/WLS. Protein homeostasis is the result of balanced translation and degradation. If translation is perturbed, cellular protein levels will decrease according to their intrinsic half-life, unless their degradation is inhibited as well. Analysing the development of EVI/WLS protein levels over time after target gene knock-down can therefore help to clarify the target gene's role in EVI/WLS degradation. Hence, I hypothesised that the knock-down of FAF2 should result in a slower turn-over of EVI/WLS compared to the control if FAF2 is important for its homeostasis.

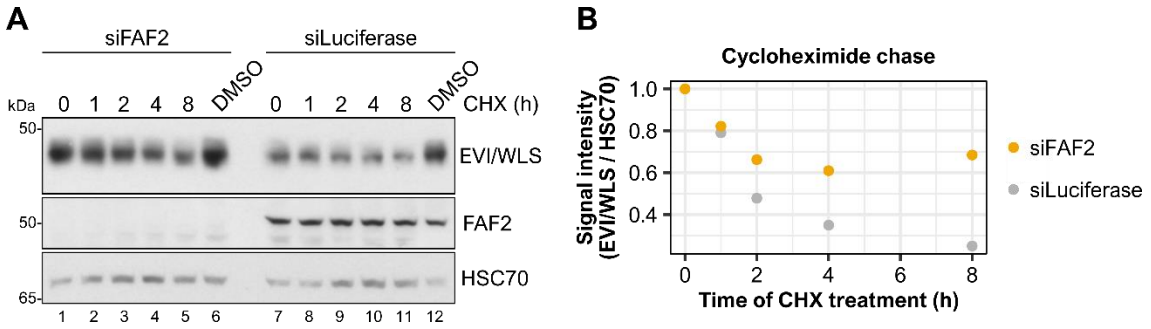

Figure 15. EVI/WLS turnover is decreased after FAF2 knock-down

Cycloheximide (CHX) decay assays demonstrated decreased EVI/WLS turnover dynamics after knock-down of FAF2. HEK293T wild type cells were transfected with pooled siRNAs against FAF2 or Luciferase as control and were challenged with CHX for the indicated times 72 h later. 8 h of DMSO treatment were used as solvent control. **A**, total cell lysates were analysed by SDS-PAGE and Western blotting for the specified proteins. HSC70 served as loading control. **B**, quantification of EVI/WLS signal relative to HSC70 loading control and normalised to timepoint 0 h of CHX treatment of the blot shown in **A**. The experiments shown here were performed by Annika Lambert. Western blots represent an example of three independent experiments. kDa = kilodalton

Cycloheximide (CHX) as a general inhibitor of translation was used to study the effects of siFAF2 on the dynamics of EVI/WLS protein level (Figure 15). Staining for FAF2 confirmed that the knock-down of FAF2 by siRNA was very efficient and EVI/WLS was more abundant in the siFAF2 condition compared to siLuciferase, as expected from previous experiments (see Figure 12). To nevertheless be able to compare the two conditions, the detected bands had to be normalised to the loading control and to timepoint 0 h. In the siLuciferase control, EVI/WLS protein levels declined over time after CHX treatment. In the depicted example, they fell below 50 % of the starting value after 8 h of CHX treatment. Similarly, EVI/WLS protein levels also declined after siFAF2 and CHX treatment. However, the overall decrease was less than in the control condition, indicating that EVI/WLS was more stable after knock-down of FAF2 and strongly suggesting that FAF2 indeed played a role in EVI/WLS turn-over (Figure 15). However, degradation was not completely inhibited, indicating that EVI/WLS is most likely subjected to several parallel degradation mechanism, not all of which are FAF2-dependent. Unexpectedly,

8 h of DMSO treatment also increased EVI/WLS protein levels compared to 0 h of treatment. While the underlying effects should be investigated in more detail in the future, it shows that the regulation of EVI/WLS is multi-layered and complex.

4.3 EVI/WLS is modified with Ub by multiple E2 enzymes

Apart from ERLIN2, FAF2, and UBXN4, two cytosolic E2 Ub conjugating enzymes were identified as potential regulators of EVI/WLS in the RNAi-mediated screen: UBE2K and UBE2N (Figures 11,S1). Both were validated in subsequent analyses by upregulating EVI/WLS protein levels proportional to single siRNA efficiency but without affecting *EVI/WLS* transcription (Figures 16B,C, 18A,B). This raised the possibility that EVI/WLS might be regulated and ubiquitinated by multiple E2 enzymes, beside the previously described UBE2J2 (Glaeser et al., 2018). It should be noted that the single siRNAs targeting *UBE2K* had quite different efficiencies, in so far as #17 and #19 decreased *UBE2K* transcription only to about 60 % of the siControl value, while #18, #20, and the siRNA pool reached up to 30 % of the control. The effect on EVI/WLS protein was correspondingly: #18, #20, and the siRNA pool increased its protein level dramatically, while transfection of #18 and #20 resulted in EVI/WLS protein levels similar to the control treatment (Figure 16B,C). Likewise, siRNAs #2 and #4 targeting *UBE2N* where less efficient than the siRNA pool, #1, and #5 in downregulating UBE2N and had no effect on EVI/WLS protein levels (Figure 18A).

While UBE2N has predominantly proteasome-independent functions through K63-linked ubiquitination, UBE2K is an important mediator of protein degradation and was previously implicated in ERAD (Mehrtash & Hochstrasser, 2019; Swatek & Komander, 2016). To investigate whether it is directly involved in the degradation of EVI/WLS, I first examined if UBE2K interacted with EVI/WLS in HEK293T cells after overexpression of FLAG-UBE2K constructs, as described above (see 4.2). Overexpression of a UBE2K construct with a FLAG-tag close to its UBA domain at the C-terminus did not show interaction with EVI/WLS (data not shown), maybe because the tag interfered with the domain's function and thus prevented interaction with its substrates. However, also N-terminally tagged constructs with a re-introduced STOP codon, which was absent from the *UBE2K* Gateway ORF clone, showed no interaction (Figure 16D). While this could indicate that the effect on EVI/WLS protein stabilisation is indirect, e.g. *via* the ubiquitination of other proteins involved in its degradation, it is also possible that the interaction was not detected because of its transient nature and the stringent pull-down conditions.

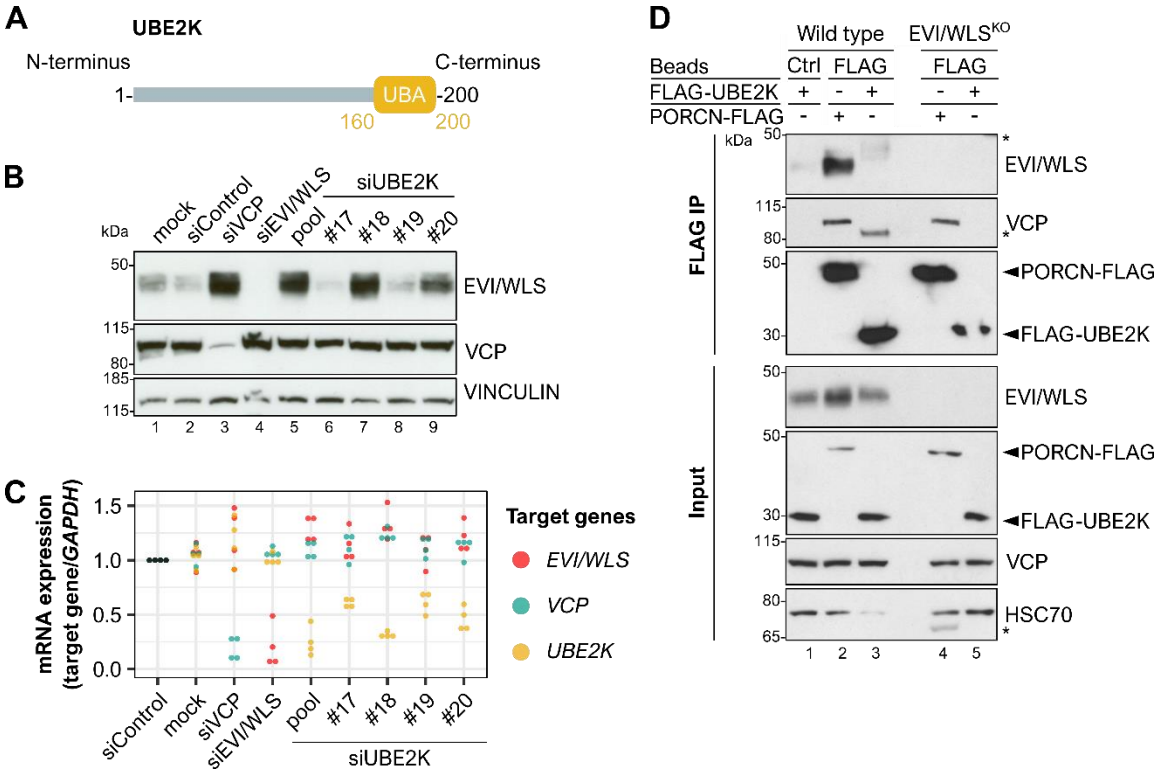

Figure 16. UBE2K regulates EVI/WLS on protein level

A. Schematic representation of the UBE2K protein according to UniProt ID: P61086, entry version 178. Numbers indicate amino acid (AA) positions. UBA = UBA domain important for binding to ubiquitin

B, C. Knock-down of UBE2K increased EVI/WLS protein levels but had no effect on *EVI/WLS* mRNA expression. HEK293T wild type cells were treated with the indicated siRNAs for 72 h. siRNAs targeting *UBE2K* were used as either single siRNAs or an equimolecular mix of all four respective siRNAs (pool). Samples treated with transfection reagent only (mock) or non-targeting siRNA (siControl) were used as negative control, siVCP as positive control. **A**, total cell lysates were analysed by SDS-PAGE and Western blotting for the specified proteins. VINCULIN served as loading control. **B**, total cellular RNA was transcribed to cDNA and used for mRNA expression analyses by RT-qPCR. Target gene expression was normalised to siControl treatment and *GAPDH* served as reference gene. Individual data points from four independent experiments are shown. Western blots are representative of three independent experiments.

D. No interaction between EVI/WLS and FLAG-UBE2K was observed by immunoprecipitation (IP). HEK293T wild type and EVI/WLS knock-out (EVI/WLS^{KO}) cells were transfected with UBE2K FLAG (N-terminal) or PORCN-FLAG overexpression plasmids. After 48 h, total cell lysates were sampled for input control or used for FLAG IP to precipitate FLAG-tagged proteins and their interaction partners. Proteins were eluted using competition with 3× FLAG Peptide and eluates or input control were analysed by SDS-PAGE and Western blotting for the specified proteins. FLAG non-binding Control Agarose Beads showed level of unspecific binding during FLAG IP and EVI/WLS^{KO} cells confirmed specificity and independent effects of EVI/WLS. HSC70 served as loading control. Asterisks indicate background bands. The experiment shown in **D** is a representative of two independent experiments.

The experiments shown here were performed by Annika Lambert. kDa = kilodalton

4.3.1 EVI/WLS is ubiquitinated at several positions

Beside the involvement of additional E2 Ub conjugating enzymes, it was also unclear at which positions EVI/WLS is ubiquitinated. According to publicly available mass spectrometry data (PhosphoSitePlus, Hornbeck et al., 2015) and the presumed structural orientation of EVI/WLS in the ER membrane, the two lysines K410/419 in the third cytosolic loop close to the AEGL endocytosis motif are the most likely primary ubiquitination sites of EVI/WLS (see Figure 2). However, some E2 enzymes, such as UBE2J2, can ubiquitinate non-lysine residues, for

example serines or threonines (X. Wang et al., 2009). To address the question if EVI/WLS is initially ubiquitinated at K410/419, I used V5 tagged EVI/WLS constructs that encoded the wild type protein or a mutant in which the lysines at the positions 410/419 were replaced by arginine (K410/419R), thus inhibiting their modification. Expression of these constructs in EVI/WLS knock-out HEK293T cells in combination with the siRNA mediated knock-down of *VCP*, *CGRRF1*, *UBE2J2,* or *UBE2K* allowed me to determine the relevance of these sites for the degradation of EVI/WLS (Figure 17A). The removal of K410/419 should inhibit the proteasomal degradation of EVI/WLS if these positions were primarily important for its ubiquitination.

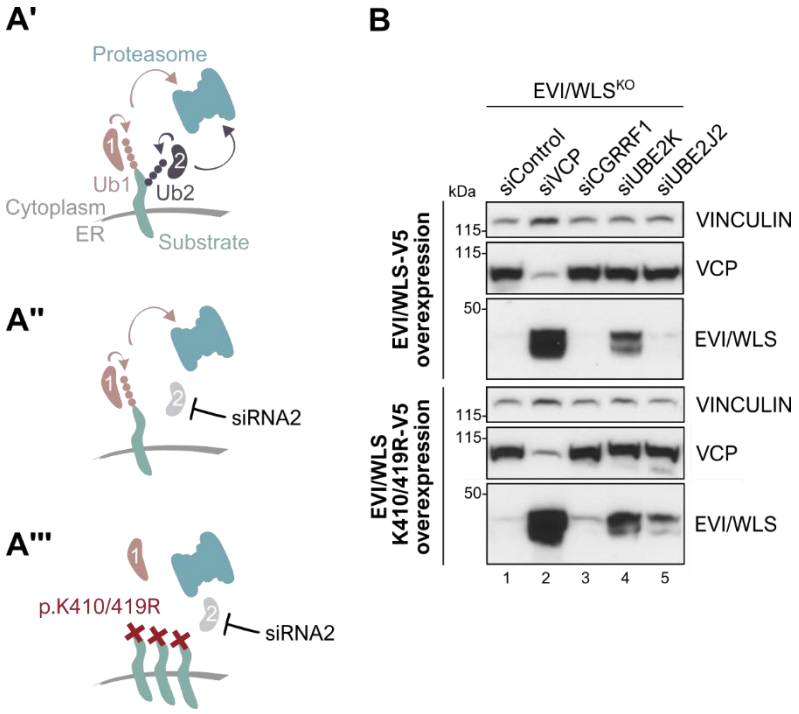

Figure 17. EVI/WLS is ubiquitinated by more than one E2 enzyme

A. Substrates can be targeted for proteasomal degradation after being ubiquitinated by multiple enzymes and at multiple positions. Mutations of single amino acids can abolish ubiquitination at a specific site (e.g. replacing a lysine with an arginine). Combinations of siRNA treatment with such mutated proteins can help to identify site- and enzyme-specific modifications by Western blot.

B. Knock-down of UBE2J2 led to the accumulation of EVI/WLS-V5 K410/419R but not wild type EVI/WLS-V5. HEK293T EVI/WLS knock-out (EVI/WLS^{KO}) cells were treated with the indicated siRNAs. 24 h after siRNA transfection, cells were additionally transfected with 250 ng (per 6-well) of EVI/WLS-V5 plasmids as indicated. Again 48 h later, total cell lysates were analysed by SDS-PAGE and Western blotting for the specified proteins. Non-targeting siRNA (siControl) was used as negative control, siVCP as positive control. VINCULIN served as loading control. Western blots are representative of four independent experiments.

kDa = kilodalton

The effect of siVCP on EVI/WLS protein level was the strongest of the observed phenotypes. Nevertheless, siVCP, siCGRRF1, and siUBE2K had similar effects on EVI/WLS protein levels of both wild type and mutant constructs, while siUBE2J2 specifically stabilised mutant K410/419R EVI/WLS (Figure 17B). The conclusion from this complicated experiment is that the lysines at the positions 410 and 419 are used to target EVI/WLS for degradation but are not the only sites of ubiquitination. It is conceivable that UBE2J2 ubiquitinates serines and

threonines next to K410/419 and that at least one other E2 enzyme is involved in ubiquitinating lysines, potentially UBE2K (Figure 17A). The K410/419R construct is less efficiently degraded in the absence of UBE2J2, as neither serines or threonines, nor the arginines at the lysine-positions can be ubiquitinated.

4.3.2 K63-linked Ub chains regulate WNT secretion

Beside UBE2K, UBE2N (Ubc13) was also identified in the RNAi screen as a putative novel Ub conjugating enzyme important for EVI/WLS regulation. The K63-linkage preference of this enzyme made it an exciting candidate, as K63-linked Ub chains are important for protein localisation and endosomal trafficking (Akutsu et al., 2016; Erpapazoglou et al., 2014; Swatek & Komander, 2016), processes which are also essential for the function of EVI/WLS. UBE2N ubiquitinates different sets of substrates after forming heterodimers with its catalytically inactive interaction partners UBE2V1 or UBE2V2 (Figure 18F), it is therefore also interesting to investigate which of these proteins is important for EVI/WLS (Andersen et al., 2005; McKenna et al., 2001). I hypothesised that if UBE2N was involved in the recycling of EVI/WLS, as well as in the availability of EVI/WLS protein, its knock-down would influence EVI/WLS functionality and thus WNT ligand secretion. Hence, I wanted to examine the role of UBE2N and its partners on WNT secretion, after initial experiments had confirmed the post-translational regulation of EVI/WLS by UBE2N using single siRNAs (18A,B, see paragraph 4.3).

Therefore, I overexpressed WNT3 in HEK293T cells in combination with the transfection of siRNAs against *UBE2N*, *UBE2V1*, or *UBE2V2* (Figure 18C). siEVI/WLS served as target specific control and siVCP was used as a positive control, as its knock-down had increased EVI/WLS protein abundance and WNT5A and WNT3A secretion in previous experiments (Glaeser et al., 2018). As expected, siEVI/WLS abolished WNT3 secretion completely. Importantly, knock-down of *UBE2N* and its interaction partners not only increased EVI/WLS protein levels, but also the secretion of WNT ligands, implying a possible modulatory effect on Wnt signalling in general. However, in my experimental settings, the knock-down of VCP increased both intracellular EVI/WLS and WNT3 protein levels, indicating that WNT3 is also affected by VCP-dependent degradation, but did not increase WNT3 secretion. It should also be noted that siVCP and siUBE2N affect cell viability, which could cause Ub-independent effects as well.

WNT3 seems to be expressed a little less in the siControl condition, although the same amount of DNA was transfected in all samples. This makes the interpretation of the blot more difficult and should be addressed in follow-up experiments. The effects of *UBE2V1* knock-down were variable between replicates, and its involvement in the ubiquitination of EVI/WLS cannot be conclusively confirmed or rejected at this point. However, this variability was not due to

insufficient siRNA efficiency, which was comparably good for all three gene targets. Furthermore, gene expression analyses confirmed that *EVI/WLS* and *VCP* were not regulated by siRNAs targeting either *UBE2N*, *UBE2V1*, or *UBE2V2* (Figure 18B,D,E).

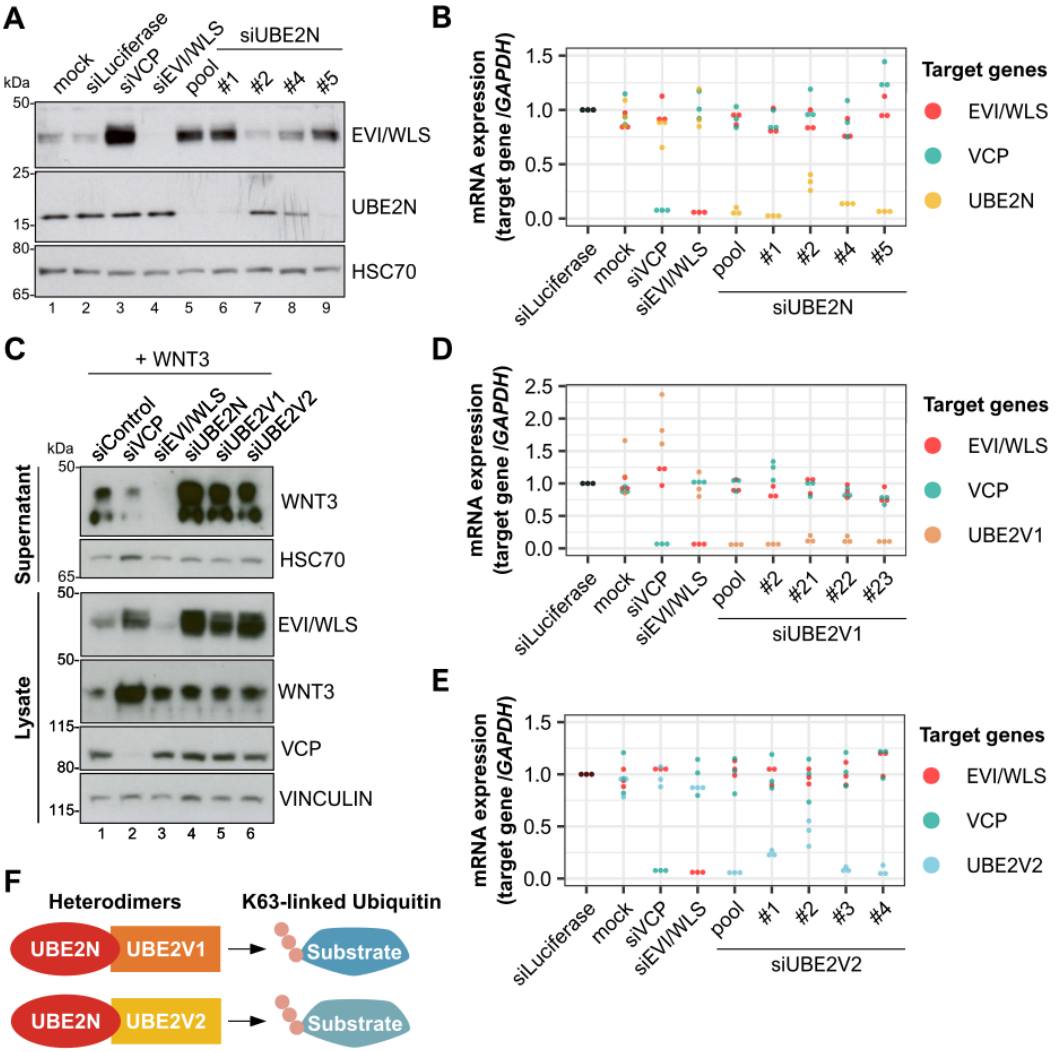

Figure 18. UBE2N and UBE2V1/UBE2V2 regulate EVI/WLS protein levels and WNT secretion

A. Knock-down of UBE2N increased EVI/WLS protein levels. HEK293T wild type cells were treated with the indicated siRNAs for 72 h. siRNAs targeting *UBE2N* were used as either single siRNAs or an equimolecular mix of all four respective siRNAs (pool). Samples treated with transfection reagent only (mock) or siLuciferase were used as negative control, siVCP as positive control. Total cell lysates were analysed by SDS-PAGE and Western blotting for the specified proteins. HSC70 served as loading control.

B, D, E. mRNA expression analyses showed specific gene silencing without cross-regulating other investigated mRNAs. HEK293T wild type cells were treated with the indicated siRNAs for 72 h. Each gene's mRNA was targeted by either single siRNAs or an equimolecular mix of all four respective siRNAs (pool) to analyse their effect on mRNA expression. Samples treated with transfection reagent only (mock) or siLuciferase were used as negative control, siVCP as positive control. Total cellular RNA was transcribed to cDNA and used for mRNA expression analyses by RT-qPCR. Target gene expression was normalised to siLuciferase treatment and *GAPDH* served as reference gene. Individual data points from three independent experiments are shown.

C. Knock-down of UBE2N, UBE2V1, and UBE2V2 increased EVI/WLS protein levels and WNT3 secretion compared to control treatment. HEK293T wild type cells were treated with the indicated siRNAs. 24 h after siRNA transfection, cells were additionally transfected with a pcDNA WNT3 plasmid. Again 48 h later, secreted proteins were precipitated from the supernatant using Blue Sepharose. Eluates and total cell lysates were analysed by SDS-PAGE and Western blotting for the specified proteins. siRNAs without specific target (siControl) and siVCP were used as controls, VINCULIN or HSC70 served as loading control.

F. Schematic representation of the formation of active complexes by UBE2N and UBE2V1 or UBE2V2 to modify target substrates with K63-linked ubiquitin.
Western blots are representative of three independent experiments. kDa = kilodalton

4.4 EVI/WLS is ubiquitinated and degraded in cells with endogenous WNT ligands

Up to this point, my results were generated in HEK293T cells. This cell line is a commonly used cellular model to analyse WNT signalling due to their low endogenous WNT secretion. The striking observation that ubiquitination of EVI/WLS might have an influence on WNT ligand secretion, and thus might regulate WNT signalling itself, opened the question of whether EVI/WLS is also regulated by ubiquitination and ERAD in cells with high endogenous levels of WNT signalling. To investigate this further, I chose melanoma cell lines as a model system as many of them express high amounts of WNT proteins, most notably WNT5A (P.-T. Yang et al., 2012).

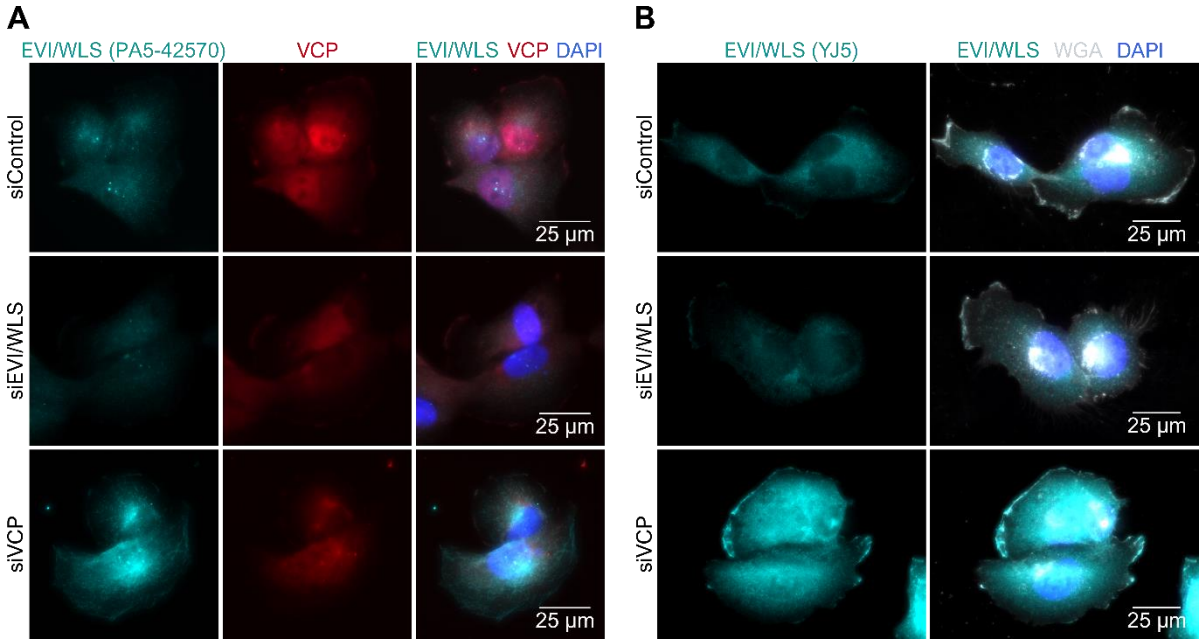

Figure 19. Knock-down of VCP increases endogenous EVI/WLS protein levels in melanoma cells

Immunofluorescence (IF) staining showed elevated endogenous EVI/WLS levels after siVCP treatment. RPMI7951 melanoma cells were transfected with the indicated siRNAs and fixed 72 h later with 4 % paraformaldehyde/PBS. Non-targeting siRNA (siControl) was used as negative control. Cells were stained for EVI/WLS with antibodies from two different providers (cyan) and for VCP (red). Wheat germ agglutinin (WGA) Alexa Fluor 633 Conjugate was used to image cellular membranes (grey). Cover glasses were mounted using ProLong Diamond Antifade Mountant with DAPI, to visualise DNA (blue). Images were acquired using a Zeiss motorised inverted Observer.Z1 microscope with the ZEISS ZEN (blue edition) software and processed with Fiji (Fiji is just ImageJ). Image quality was optimised by adjusting brightness and contrast. Preliminary.

As an initial experiment, I wanted to test whether EVI/WLS was also regulated by VCP in melanoma cells. Therefore, I stained endogenous EVI/WLS with two different antibodies after transfection of siVCP, siEVI/WLS, or siControl in RPMI7951 melanoma cells, which have large, flat cell bodies and are easy to visualise. Cytoplasmic EVI/WLS signal increased after transfection of siVCP and decreased after transfection of siEVI/WLS, indicating that the endogenous staining was specific, and that EVI/WLS is regulated by VCP, and thus potentially by ERAD, in cells with endogenous WNT ligand production. However, some EVI/WLS signal remained after

transfection of siEVI/WLS, either due to insufficient siRNA-mediated knock-down or background signal of the antibodies (Figure 19).

Although RPMI7951 cells are suitable for imaging, they are difficult to transfect with plasmid DNA. Hence, I selected the commonly used melanoma cell line A375 for the next experiments since it is easy to transfect and proliferates fast. Glaeser et al. showed that the overexpression of various WNT ligands led to the stabilisation of EVI/WLS protein in HEK293T cells (Glaeser et al., 2018). Following up on this, I wanted to investigate whether the effect can be reversed in A375 cells by preventing WNT ligands from being lipid-modified by treatment with LGK974, an inhibitor of the acyl-transferase PORCN. The absence of the lipid-modification prevents EVI/WLS-WNT interaction and I hypothesised that this seeming 'absence of WNT ligands' would induce the degradation of EVI/WLS (Figure 20A).

LGK974 treatment did not change intracellular WNT5A ligand abundance but abolished the secretion of WNT5A, as expected (Figure 20B). Indeed, EVI/WLS protein levels were reduced in cell lysates treated with LGK974 compared to DMSO. At the same time, mRNA expression of *EVI/WLS* or *PORCN* was not decreased but rather slightly elevated upon LGK974 treatment compared to the control, suggesting true post-translational regulation of EVI/WLS protein levels. These findings also indicated that the detected WNT ligands that remained in the cell lysates after LGK974 treatment were not functional. *AXIN2* expression as a read-out for canonical/β-catenin dependent WNT signalling was decreased after LGK974 treatment, indicating overall reduced WNT target gene transcription (Figure 20B,C).

This post-translational regulation of EVI/WLS in A375 cells suggests that EVI/WLS is ubiquitinated and degraded by the proteasome in these cells upon LGK974-induced inhibition of WNT ligand lipidation. To directly test this hypothesis, I used TUBEs to enrich A375 protein lysates for ubiquitinated proteins. By doing so, I expected to see the accumulation of ubiquitinated EVI/WLS after LGK974 treatment and inhibition of the proteasome by MG132. Surprisingly, however, proteasome inhibition induced high-molecular EVI/WLS bands after both LGK974 and control DMSO treatment, indicating ubiquitinated EVI/WLS in the absence and presence of endogenous lipid-modified WNTs (Figure 20D). In general, the K48-Ub signal increased in samples treated with MG132 compared to DMSO, indicating the overall accumulation of ubiquitinated proteins and the ubiquitination of β-catenin was detected in all except for the control beads sample, suggesting continuous turn-over of this protein (Figure 20D).

In conclusion, these results show that EVI/WLS protein levels depend on the availability of mature WNT ligands in cells with high endogenous WNT signalling, but a part of the EVI/WLS protein pool is ubiquitinated and targeted for degradation even in the presence of WNT ligands.

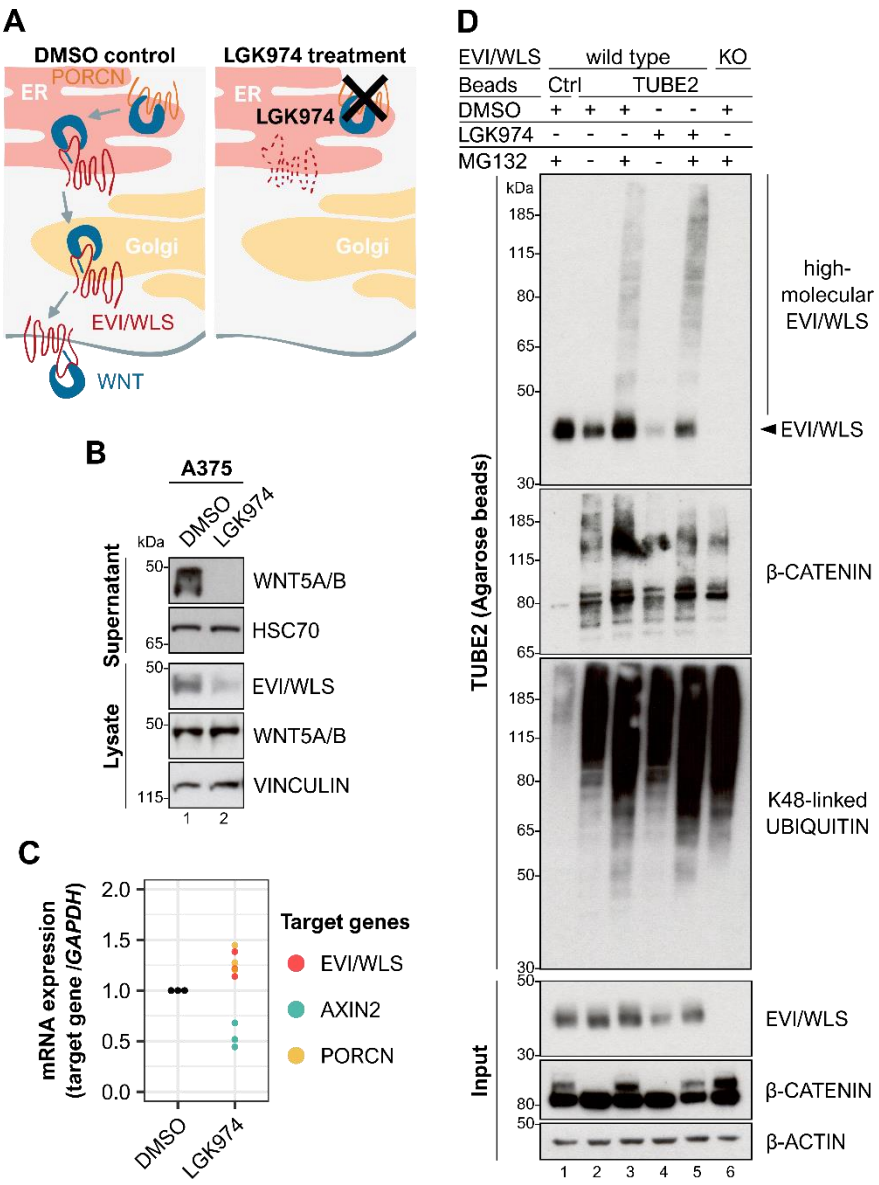

Figure 20. EVI/WLS is ubiquitinated in cells with and without endogenous WNT ligands

A. Schematic illustration of LGK974's mode of action. LGK974 prevents WNT ligands from being lipid-modified in the endoplasmic reticulum (ER) by inhibiting the acyl-transferase PORCN. Un-lipidated WNTs cannot associate with EVI/WLS and are not secreted from the WNT producing cell.

B, C. LGK974 treatment reduced intracellular EVI/WLS levels and abolished the secretion of WNT5A/B ligands, without reducing EVI/WLS gene expression. A375 melanoma cells were treated with LGK974 (10 µM) or equivalent volumes of DMSO as solvent control for 96 h with daily medium changes. **B**, secreted proteins were precipitated from the supernatant 24 h after the last medium change using Blue Sepharose and eluates and total cell lysates were analysed by SDS-PAGE and Western blotting for the specified proteins. VINCULIN or HSC70 served as loading control. **C**, total cellular RNA was transcribed to cDNA and used for mRNA expression analyses by RT-qPCR. Target gene expression was normalised to DMSO treatment and *GAPDH* served as reference gene. Individual data points from three independent experiments are shown.

D. Inhibition of the proteasome led to the accumulation of ubiquitinated EVI/WLS after both LGK974 and control treatment. A375 melanoma wild type and EVI/WLS knock-out (EVI/WLS^{KO}) cells were treated with LGK974 (10 µM) or equivalent volumes of DMSO as solvent control for 96 h with daily medium changes. 24 h before harvest, samples were treated with the proteasome inhibitor MG132 (1 µM) as indicated. Then, total cell lysates were harvested for input control or used for TUBE2 (agarose) pull-down to precipitate poly-ubiquitinated proteins. Eluates or input controls were analysed by SDS-PAGE and Western blotting for the specified proteins. Ubiquitin non-binding Control (Ctrl) Agarose Beads showed level of unspecific binding and EVI/WLS^{KO} cells confirmed specificity for EVI/WLS. β-ACTIN served as loading control. TUBE = tandem ubiquitin binding entity

Western blots are representative of three independent experiments. Note that the WNT5 antibody used in these studies recognises both WNT5A and WNT5B. kDa = kilodalton

I then asked which proteins influence the degradation of EVI/WLS in A375 cells. Hence, I combined LGK974 and transfection of siRNA to analyse which knock-downs of ERAD-associated genes would interfere with the degradation of EVI/WLS. Of the tested genes, only the knock-down of *UBE2J2*, *CGRRF1*, and *VCP* consistently elevated EVI/WLS protein levels, in line with the previously obtained results in HEK293T cells (Figure S4, Glaeser et al., 2018). These results suggest that the underlying mechanisms of EVI/WLS turn-over are conserved between different human cell types.

4.5 EVI/WLS is modified with K11-, K48-, and K63-linked Ub

I decided to study the ubiquitination of EVI/WLS further in A375 cells, as the concurrent presence of a stabilised and a degraded pool of EVI/WLS allowed me to detect both accumulation and depletion of high-molecular EVI/WLS signals. It should also be considered that different Ub modifications might be present at different cycling/recycling stages of EVI/WLS and thus might not be observed in HEK293T cells due to their low endogenous WNT ligand secretion.

As the E2 Ub conjugating enzymes which had been associated with EVI/WLS, namely UBE2J2, UBE2K, and UBE2N, each have a preferential Ub-linkage specificity, I hypothesised that different Ub-linkage types would also be present on EVI/WLS. The TUBE assay presented in Figure 20D showed several high-molecular EVI/WLS bands, indicating poly-Ub chains or several mono Ubs attached to EVI/WLS, but as the TUBEs used here were non-selective, they did not allow to distinguish between different Ub linkage types. Hence, I expressed different mutant Ub constructs with HA-tags to test the presence of Ub linkages *via* K11, K48, or K63 (Clague et al., 2015; Tsuchiya et al., 2018; P. Xu et al., 2009) on endogenous EVI/WLS. Each of these Ub constructs allowed only one linkage type to form, because all other lysines were mutated to arginine. Thus, immunoprecipitation of the HA-tag captured all proteins modified with the respective Ub.

I detected high-molecular EVI/WLS bands in pulldowns from samples with wild type, K11, K48, or K63 ubiquitin-HA overexpression after inhibition of the proteasome, indicating the presence of multiple linkage types on EVI/WLS (Figure 21A). Staining for the HA-tag in the input samples reflected how well the Ub-HA constructs modified substrate proteins. Not surprisingly, the amount of detected wild type Ub-HA was much higher than any of the mutant forms, presumably because it can be used at any position (Figure 21A). That is probably also why it appears as if the Ub-HA constructs were expressed at varying levels, although the same amount of DNA had been transfected. It should be noted that the endogenous, unmodified Ub is still present in these samples and the detected Ub signal is probably a mixture of tagged and

un-tagged Ub. This is difficult to prevent, as the knock-out of Ub is lethal and it would require the combinatorial knock-down of Ub and overexpression of the Ub-HA constructs to perform these experiments without endogenous Ub. Nevertheless, using the present conditions, it is unclear how much endogenous and how much mutant Ub is used for substrate modification. While the overexpressed form is probably more abundant, endogenous Ub might be more stable.

The two E2 Ub conjugating enzymes UBE2K and UBE2N were identified in my screen as post-translational regulators of EVI/WLS and have a specificity for K48- and K63-linkage, respectively (Z. Chen & Pickart, 1990; Middleton & Day, 2015). I therefore assumed that UBE2K and UBE2N mediate the K48- and K63 Ub-linkage I detected on EVI/WLS (Figure 21A). Pan-Ub TUBEs did not show differences in ubiquitination after transfection of siUBE2K (data not shown). Possibly, the effect of siUBE2K was small and might have been masked by other poly- or mono-Ub modifications that are present at the same time on EVI/WLS. However, linkage-type specific TUBEs can be used to specifically enrich proteins modified with either K48- or K63-linked Ub and thus might offer greater sensitivity. Hence, I used linkage-type specific TUBEs with a FLAG-tag to detect differences in high-molecular EVI/WLS bands after transfecting siUBE2K or siUBE2N. Indeed, FLAG K48 TUBEs showed a reduction of high-molecular EVI/WLS bands after transfection of siUBE2K compared to siLuciferase control (Figure 21B). Likewise, siUBE2N markedly reduced the signal of endogenous high-molecular EVI/WLS bands after K63-specific FLAG-TUBE pull-down, as did the knock-down of UBE2V2 (Figure 21C). This data strongly indicates the modification of EVI/WLS with K48-linked Ub by UBE2K and with K63-linked Ub by UBE2N together with UBE2V2 in human cells.

► next page **| Figure 21. EVI/WLS is modified with K11-, K48-, and K68-linked ubiquitin in A375 melanoma cells**

A. Endogenous EVI/WLS is modified with ubiquitin linked *via* K11, K48, and K63. A375 wild type (wt) and EVI/WLS knock-out (EVI/WLS^{KO}) cells were transfected with pRK5-HA-Ubiquitin wt, K11, K48, or K63 overexpression plasmids or left untreated (ut). The K11, K48, and K63 ubiquitin constructs can only be elongated with further ubiquitins at the specified position, all others have been mutated to arginines. 24 h before harvest, samples were treated with the proteasome inhibitor MG132 (1 µM) or equivalent voume of DMSO as solvent control. After 72 h, total cell lysates were harvested for input control or used for HA immunoprecipitation to analyse proteins modified with HA-tagged ubiquitin. Proteins were eluted using competition with HA Peptide. Eluates and input control were analysed by SDS-PAGE and Western blotting for the specified proteins. HA non-binding Control (Ctrl) Agarose Beads showed level of unspecific binding during HA IP and EVI/WLS^{KO} cells confirmed specificity and independent effects of EVI/WLS. Tubulin served as loading control.

B, C. FLAG K48 specific TUBE pull-down confirmed that EVI/WLS is modified with K48-linked ubiquitin chains by UBE2K and FLAG K63 specific TUBE pull-down confirmed that EVI/WLS is modified with K63-linked ubiquitin chains by UBE2N. A375 melanoma wild type and EVI/WLS knock-out (EVI/WLS^{KO}) cells were treated with the indicated siRNAs for 72 h. 24 h before harvest, samples were treated with the proteasome inhibitor MG132 (1 µM) or equivalent volume of DMSO as solvent control. Total cell lysates were harvested for input control or used for FLAG TUBE pull-down to specifically precipitate proteins modified with K48- (**B**) or K63-linked (**C**) poly-ubiquitin. Proteins were eluted using competition with 3× FLAG Peptide and eluates or input controls were analysed by SDS-PAGE and Western blotting for the specified proteins. Ubiquitin non-binding Control (Ctrl) Agarose Beads showed level of unspecific binding and EVI/WLS^{KO} cells confirmed specificity for EVI/WLS. β-ACTIN served as loading control.

Asterisks indicate background/unspecific signals. Western blots are representative of three independent experiments. kDa = kilodalton, TUBE = tandem ubiquitin binding entity

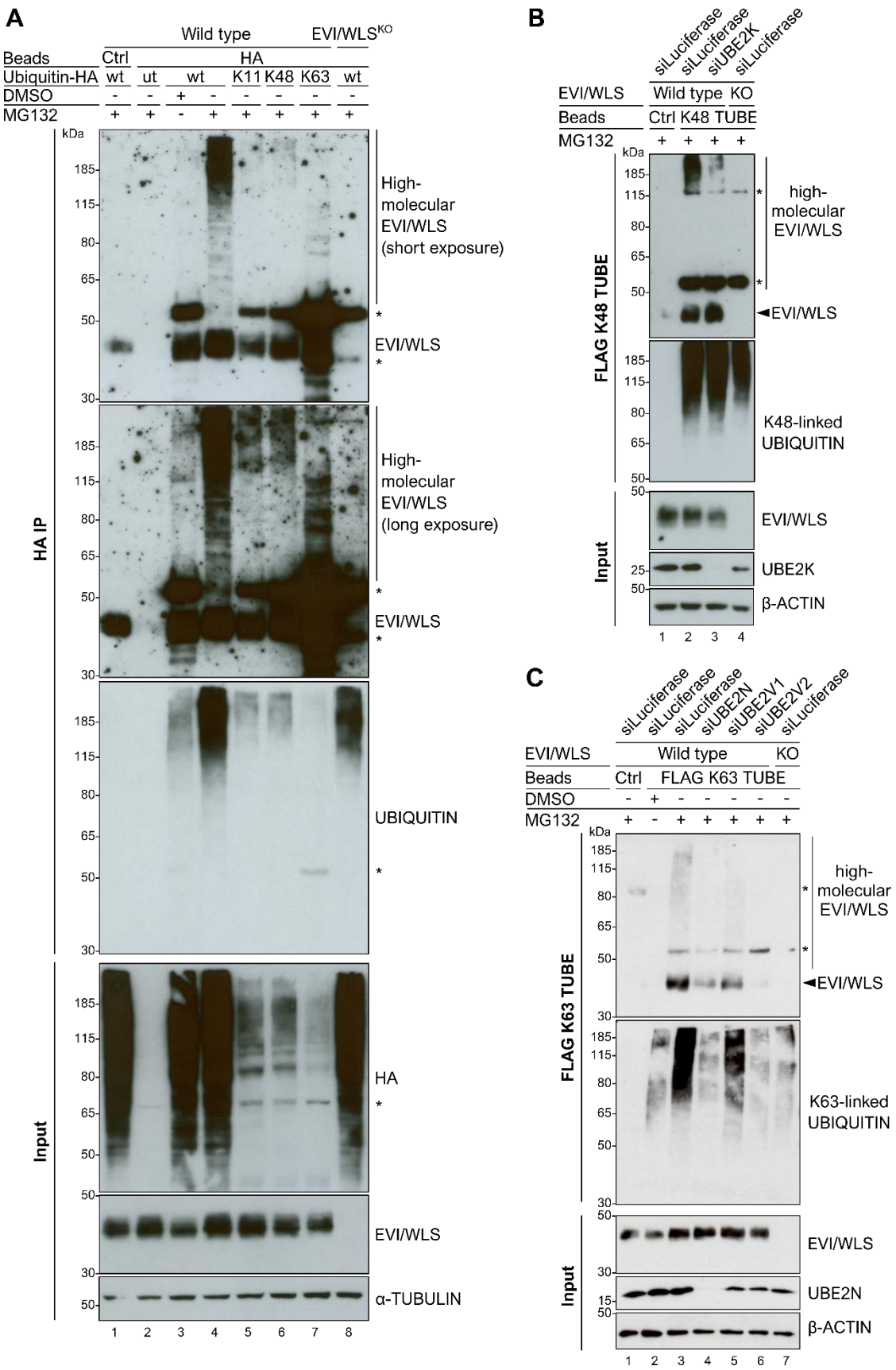

Figure 21. EVI/WLS is modified with K11-, K48-, and K68-linked ubiquitin in A375 melanoma cells
(see previous page for figure legend)

In general, it should be noted that EVI/WLS protein staining was often visible in the control bead samples after immunoprecipitation (Figures 20D,22A,B,23A). This is probably due to insufficient washing and unspecific binding of proteins to the beads. Nevertheless, interpretation of the data was still possible because of the absence of high-molecular EVI/WLS bands, even after inhibition of the proteasome, and intensity differences to the samples of interest. Along the same line, signals detected just above 50 kDa corresponded most likely to the gamma immunoglobin heavy chains (Figure 21). It is surprising that these bands were detected after sample elution using competition with either HA- or FLAG peptide. They probably indicate that a few antibodies dissociated from their beads over time and are visible after the long exposure times necessary to detect endogenous EVI/WLS.

4.6 ERLIN2 links EVI/WLS to the ubiquitination machinery

The obtained results show that EVI/WLS can be both stabilised and degraded in cells with endogenous WNT signalling. Its degradation depends on Ub signals which are mediated by UBE2K and UBE2N, in addition to the previously reported UBE2J2 and CGRRF1 (Glaeser et al, 2018). Furthermore, ERLIN2, FAF2, and UBXN4 are important for the regulation of EVI/WLS protein levels. However, it remains elusive how the latter three proteins influence the ubiquitination of EVI/WLS. This is important to examine, because it can indicate whether ERLIN2, FAF2, and UBXN4 interact with EVI/WLS before or after it is ubiquitinated. As ERLIN2 had been implicated in linking the regulatory ERAD substrates IP_3R and HMG-CoA reductase to the ubiquitination machinery (Jo, Sguigna, et al., 2011; Pearce et al., 2007), I hypothesised that the knock-down of ERLIN2 would reduce the ubiquitination of EVI/WLS. Conversely, FAF2 and UBXN4 are VCP-interacting proteins, and FAF2 additionally contains an Ub-interacting domain (Schuberth & Buchberger, 2008). Hence, a function in the ERAD of EVI/WLS after it has been ubiquitinated, but before it is removed from the ER-membrane by VCP, is conceivable and ubiquitinated EVI/WLS was expected to accumulate after the knock-down of FAF2 and UBXN4.

Pan-ubiquitin specific TUBE1 magnetic beads were used to investigate the ubiquitination status of EVI/WLS in combination with RNAi mediated knock-down of ERLIN2, FAF2 or UBXN4. Indeed, I observed a strong reduction of high-molecular EVI/WLS bands after transfection of siERLIN2 and the high-molecular EVI/WLS signal increased following knock-down of FAF2 and UBXN4 (Figure 22A). This confirmed the hypothesis that ERLIN2 functions as a linker and connects EVI/WLS to the ubiquitination machinery and that FAF2 and UBXN4 interact with EVI/WLS after it is ubiquitinated, but before it is delivered to the proteasome. siVCP was used as a positive control and it increased the signal of high-molecular EVI/WLS bands

pronouncedly, indicating that the knock-down of VCP prevented the degradation of ubiquitinated EVI/WLS (Figure 22A). Indeed, this signal was much stronger than the one after knock-down of FAF2 or UBXN4, suggesting that EVI/WLS is subject to several recruitment mechanisms which all culminate in dislocation by VCP. Further analysis, e.g. by combinatorial knock-down of ERLIN2 and VCP, should reveal more about the sequence of events.

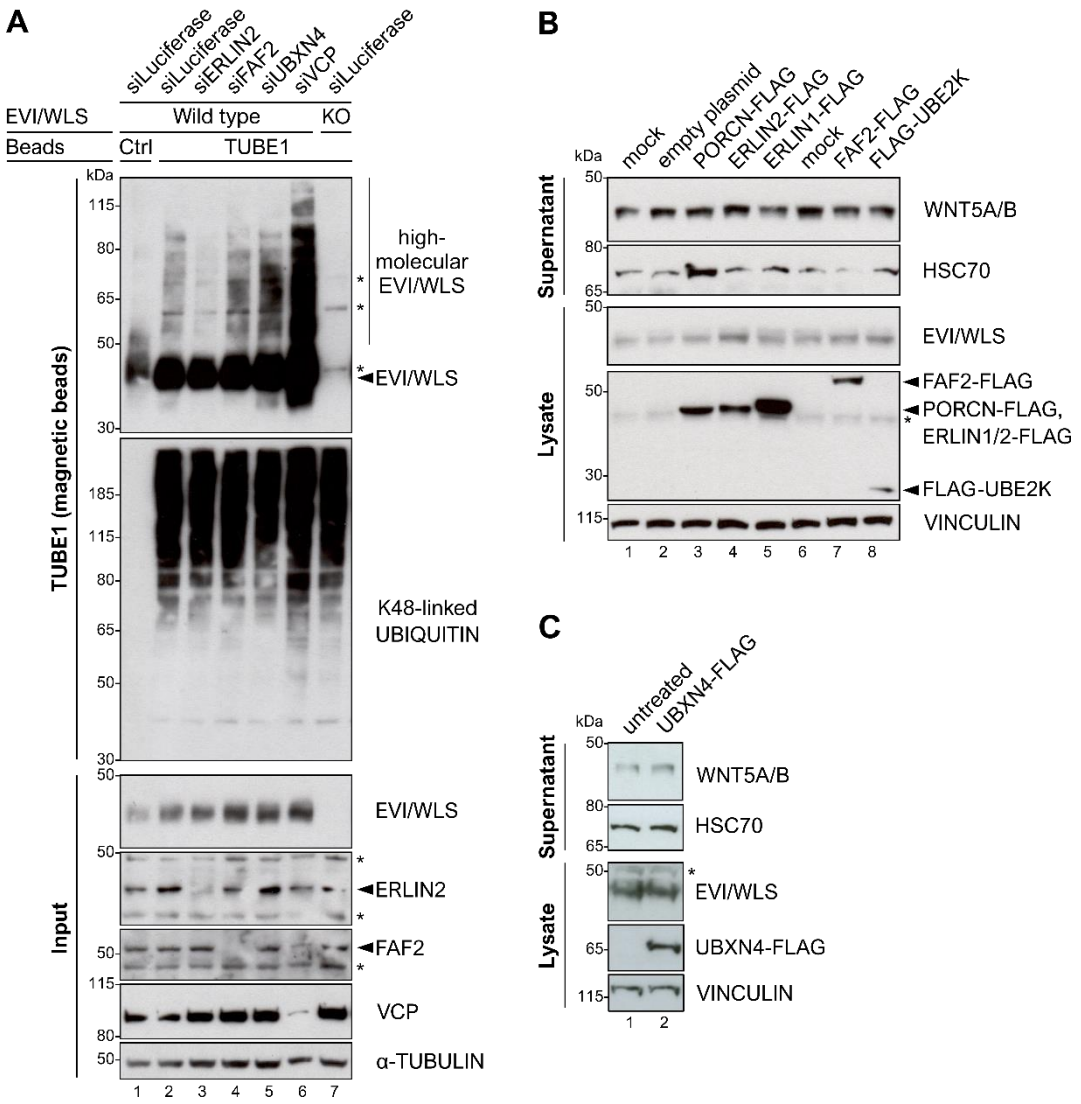

Figure 22. EVI/WLS is linked to the ubiquitination machinery *via* ERLIN2

A. Knock-down of ERLIN2 reduced the ubiquitination of EVI/WLS, while knock-down of FAF2 and UBXN4 increased it. A375 wild type and EVI/WLS knock-out (KO) cells were treated with the indicated siRNAs for 72 h. Then, total cell lysates were harvested for input control or used for TUBE1 (magnetic beads) pull-down to precipitate poly-ubiquitinated proteins. Eluates or input controls were analysed by SDS-PAGE and Western blotting for the specified proteins. Ubiquitin non-binding control (Ctrl) magnetic beads showed level of unspecific binding and EVI/WLS^{KO} cells confirmed specificity for EVI/WLS. α-TUBULIN served as loading control.

B, C. Overexpression of FLAG-tagged UBXN4, ERLIN1, ERLIN2, FAF2, or UBE2K did not change endogenous EVI/WLS protein levels or WNT5A/B secretion. FLAG-tagged constructs were overproduced in wild-type A375 melanoma cells for 48 h. Then, secreted proteins were precipitated from the supernatant using Blue Sepharose. Eluates and total cell lysates were analysed by SDS-PAGE and Western blotting for the specified proteins. VINCULIN or HSC70 served as loading control.

Asterisks indicate background/unspecific signals. Western blots are representative of three independent experiments. Note that the WNT5 antibody used in these studies recognises both WNT5A and WNT5B. kDa = kilodalton, TUBE = tandem ubiquitin binding entity

After having analysed the effect of ERLIN2, FAF2, and UBXN4 knock-down in A375 cells, I next asked whether their overexpression would influence EVI/WLS protein levels as well. It was conceivable that an increase of ERLIN2, FAF2, or UBXN4 abundance would accelerate the degradation of EVI/WLS. However, expression of the FLAG-tagged constructs (see also 4.2) in these cells did neither have an effect on intracellular EVI/WLS protein levels nor on the secretion of WNT5A/B (Figure 22B,C). It was again apparent that these constructs are not equally well expressed, or their protein products are differentially regulated, as was observed previously in HEK293T cells. Nevertheless, this suggested that while the proteins are present, their abundance is not rate limiting for the degradation of EVI/WLS.

4.7 *In-vitro* gelatin degradation assay assesses the invasive capacity of melanoma cells

My results show that EVI/WLS protein levels are regulated on various molecular levels. Next, I wanted to investigate how EVI/WLS abundance functionally affects cellular behaviour. I chose melanoma cells as a cellular model as it has been described previously that WNT signalling plays an important role in determining the switch between a more proliferate and a more invasive phenotype and metastasis in this system (Webster et al., 2015). However, the role of WNT secretion and EVI/WLS in melanoma is still not very well characterised.

Invasion and metastasis are exceedingly complex phenotypes and as such are difficult to recreate and analyse *in-vitro*, despite the possible advantage of having a less time-consuming, less costly, and more flexible assay than *in-vivo* experiments (Kramer et al., 2013). Nevertheless, it is possible to investigate individual steps of these complex organismal processes and recapitulate them *in-vitro*. One example is the analysis of the degradation of gelatin in cell culture as a proxy for the remodelling of extracellular matrix. *In-vivo*, this would help tumour cells to infiltrate and migrate through their surrounding connective tissue (Iizuka et al., 2016; H. Lu et al., 2016; Paterson & Courtneidge, 2018). Therefore, I established the so called ‘gelatin degradation assay’ (also called ‘invadopodia assay’) in our laboratory and developed an analysis pipeline to allow the comparison between different conditions (Figure 23A). In brief, a specified number of cells is seeded on top of a thin layer of fluorescently labelled gelatin. After the cells attach, they start to form small, actin-based protrusions which secrete proteases and degrade both gelatin and fluorophores. This results in black patterns which can be visualised using fluorescence microscopy. These structures are referred to as invadopodia in cancer cells (Paterson & Courtneidge, 2018). According to cell line and treatment, these patterns can be

different in size and shape, ranging from small clusters of dots (e.g. WM793 melanoma cells, Figure 23C) to large patches (e.g. RPMI7951, Figures 24,25,26).

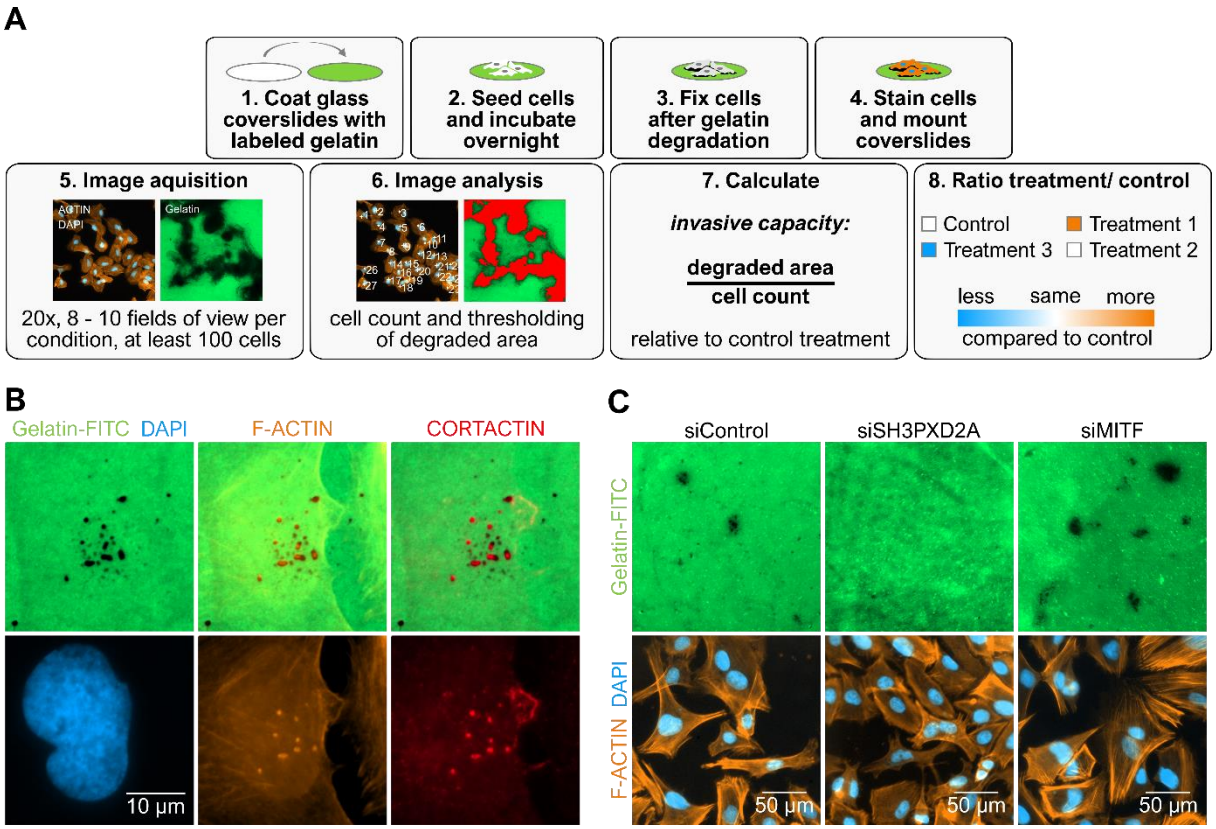

Figure 23. The gelatin degradation assay is a versatile tool to analyse the invasive capacity of cells *in-vitro*

A. Schematic illustration of the gelatin degradation assay and subsequent analysis pipeline.

B. F-ACTIN and CORTACTIN colocalise with gelatin degradation foci. RPMI7951 melanoma cells were seeded on fluorescein-gelatin (green) coated cover glasses and fixed 24 h later with 4 % paraformaldehyde/PBS. Immunofluorescence staining was used to visualise CORTACTIN (red) and ACTIN-filaments were stained using Phalloidin-TRITC (orange).

C. Knock-down of SH3PXD2A or MITF influence the invasive capacity of melanoma cells. WM793 cells were treated with the indicated siRNAs for 72 h before being seeded on fluorescein-gelatin (green) coated cover glasses. Non-targeting siRNA (siControl) was used as negative control. 24 h after seeding, cells were fixed with 4 % paraformaldehyde/PBS and stained for ACTIN-filaments using Phalloidin-TRITC (orange).

Cover glasses were mounted using ProLong Diamond Antifade Mountant with DAPI, in order to visualise DNA (blue). Images were acquired using a Zeiss motorised inverted Observer.Z1 microscope with the ZEISS ZEN (blue edition) software and processed using Fiji (Fiji is just ImageJ). Image quality was optimised by adjusting brightness and contrast.

Consequently, the most unbiased way of quantification is by measuring the size of the area of degradation after thresholding. To compare the invasive capacities between different treatments and replicates, I counted at least 100 cells per condition in each replicate. Then, I normalised the obtained values from thresholding to the number of cells in the respective images and calculated the ratio to the control condition. Thus, the invasive capacity was always 1 in the control conditions, or 0 after log transformation. After log transforming the invasive capacity values of the treatment conditions, negative fold change indicated decreased degradation of the cells compared to the control and a positive fold change indicated increased

degradation (Figure 23A). RPMI7951 and WM793 melanoma cells are adequate tools for this assay considering that they degrade gelatin even in an unperturbed state and deflection of their invasive capacity can be measured in both directions. Since the normalised values are not normally distributed, the non-parametric one-sample Wilcoxon signed rank test was used to assess statistical significance of treatments.

Invadopodia are characterised by the co-localisation of actin and cortactin with areas of proteolytic activity (Paterson & Courtneidge, 2018) as shown in Figure 23B, thus confirming the presence of invadopodia formed by RPMI7951 melanoma cells in this assay. As a proof of concept, I also wanted to examine whether the area degraded by invadopodia would change upon perturbation of the cells with RNAi. As expected, knock-down of an essential scaffolding protein in invadopodia, SH3PXD2A/TKS5, abolished gelatin degradation by WM793 cells, while the knock-down of MITF, the transcription factor regulating melanocyte differentiation, resulted in more abundant degradation foci. This is in agreement with previous publications, which prescribed MITF with an important role in the proliferative phenotype and its knock-down accordingly shifts the cells towards a more invasive phenotype (Webster et al., 2015, Figure 23C).

4.7.1 PORCN inhibition decreased the invasive capacity of melanoma cells

WNT5A mediates melanoma cell invasiveness (Weeraratna et al., 2002). However, the knock-down of EVI/WLS, and thus the abrogation of WNT5A secretion, led to more metastasis formation in a melanoma xenograft mouse model (P.-T. Yang et al., 2012). This apparent contradiction might have important consequences for melanoma pathophysiology but has not been investigated in detail.

To address this conundrum, I first examined the role of WNT ligand acylation and secretion with the help of the PORCN inhibitor LGK974. I hypothesised that if the secretion of mature WNT ligands is important for melanoma cell invasiveness, this treatment should decrease the invasive capacity of RPMI7951 melanoma cells compared to the DMSO vehicle control. As expected, LGK974 treatment reduced gelatin degradation significantly compared to control treatment (Figure 24A,B), decreased intracellular EVI/WLS protein levels, and blocked the secretion of WNT5A/B (Figures 24C, see also Figure 20 for A375 cells). Surprisingly, however, WNT11 was still secreted after LGK974 treatment, albeit in lower amounts compared to DMSO (Figure 24C).

The gelatin degradation assay does not allow to assess migration, as the readout is done from a static image of degraded gelatin after a specified period of time. Since it is important to analyse invasion and migration together, I used a scratch/wound healing assay to

examine the migration of treated cells over time and measured cell proliferation in parallel to exclude that an apparent quicker migration is due to underlying proliferation effects. LGK974 treatment had no significant effect on either proliferation or migration compared to control, but it showed a small trend towards faster migration and slower proliferation (Figure 24D,E).

In conclusion, these results suggest that PORCN activity and the secretion of lipidated WNT5A are important for the gelatin degradation capacity of melanoma cells.

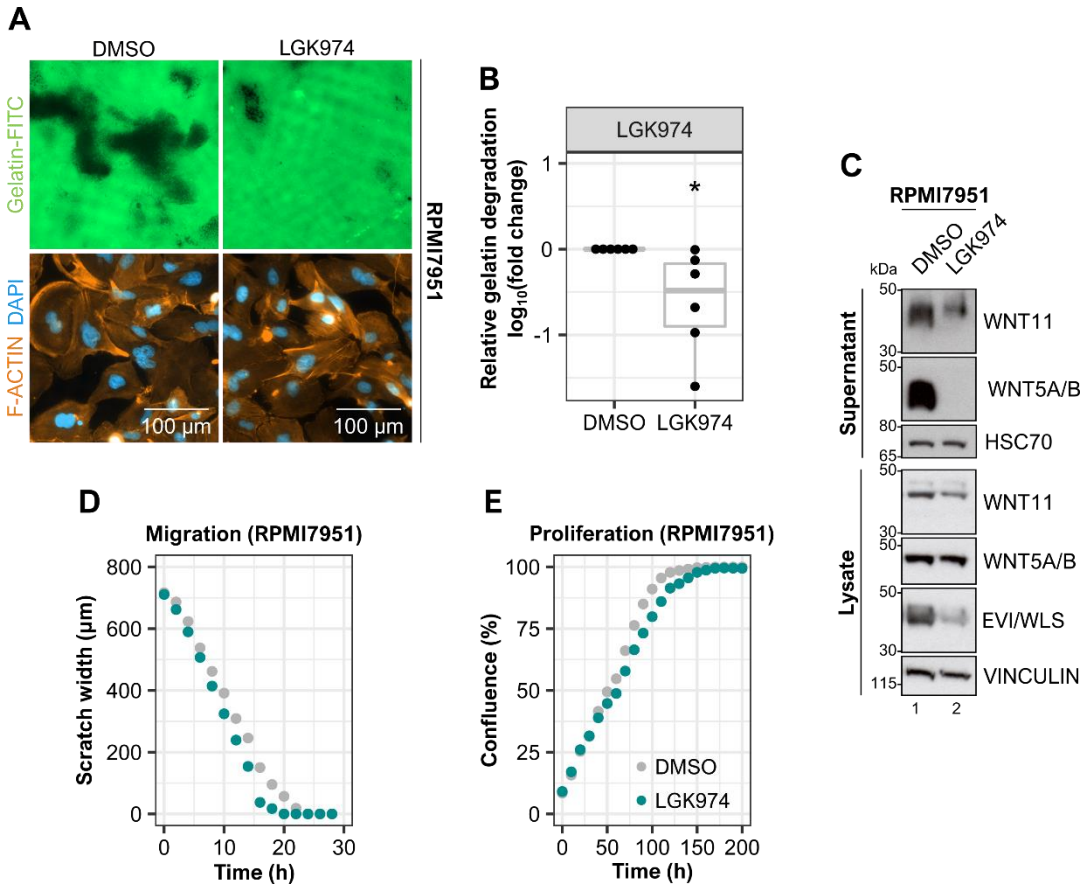

Figure 24. Inhibition of PORCN reduces invasive capacity of melanoma cells

RPMI7951 melanoma cells were treated with LGK974 (10 µM) or equivalent volumes of DMSO as solvent control for 96 h with daily medium changes.

A, B. Treatment with LGK974 reduced gelatin degradation by melanoma cells. After pre-treatment with LGK974 or DMSO, cells were seeded on fluorescein-gelatin (green) coated cover glasses. 24 h after seeding, cells were fixed with 4 % paraformaldehyde/PBS and stained for ACTIN-filaments using Phalloidin-TRITC (orange). Cover glasses were mounted using ProLong Diamond Antifade Mountant with DAPI, in order to visualise DNA (blue). **A,** Images were acquired using a Zeiss motorised inverted Observer.Z1 microscope with the ZEISS ZEN (blue edition) software and processed using Fiji (Fiji is just ImageJ). Image quality was optimised by adjusting brightness and contrast. **B**, quantification of gelatin degradation relative to DMSO and normalised to cell number in six independent experiments with > 100 cells per condition. One-Sample Wilcoxon Signed Rank test, * $p < 0.05$

C. LGK974 treatment reduced intracellular EVI/WLS levels and inhibited the secretion of WNT5A/B ligands, but not the secretion of WNT11. After pre-treatment with LGK974 or DMSO, secreted proteins were precipitated from the supernatant using Blue Sepharose 24 h after the last medium change. Eluates and total cell lysates were analysed by SDS-PAGE and Western blotting for the specified proteins. VINCULIN or HSC70 served as loading controls. Western blots are representative of three independent experiments. kDa = kilodalton

D, E. Migration and Proliferation were similar between LGK974 and DMSO treated melanoma cells. After pre-treatment with LGK974 or DMSO, migration and proliferation were analysed by time-lapse live-cell imaging with the IncuCyte ZOOM system together with the IncuCyte Basic Software and the IncuCyte Scratch Wound Cell Migration Software Module. Plots are representative of three independent experiments.

4.7.2 WNT11 regulates the invasive capacity of melanoma cells

LGK974 treatment revealed a possible PORCN-independent secretion of WNT11, but this compound treatment did not allow to deduce a possible mechanism of how this might be related to melanoma cell invasiveness. Hence, I used RNAi mediated knock-down of components of the WNT transduction cascades to investigate how they specifically affect gelatin degradation. Based on the literature, I expected that siWNT5A would reduce the cells' invasive capacity (Weeraratna et al., 2002), while siEVI/WLS would increase it (P.-T. Yang et al., 2012). The role of WNT11 had not been investigated in detail in melanoma, but as WNT11 and WNT5A are both non-canonical WNT ligands, I assumed WNT11 would have a similar function as WNT5A. I also included siCTNNB1 in these experiments because the role of β-catenin in melanoma is controversial and I wanted to investigate its contribution to gelatin degradation (Webster & Weeraratna, 2013).

Similar phenotypes were observed for the two melanoma cell lines RPMI7951 and WM793 upon transfection of siRNAs (Figure 25A,B;C). The knock-down of mRNA and protein levels by the siRNAs was good in both cell lines and predominantly reduced mRNA expression of all genes below 12 % of the control value (Figure S5). The knock-down of *WNT5A* reduced gelatin degradation significantly, as expected. Surprisingly, the cells' invasive capacity increased dramatically after both the knock-down of *EVI/WLS* or *WNT11*, indicating an important role of the non-canonical WNT11 for melanoma cells which differs from the well characterised WNT5A. At the same time, the results for siEVI/WLS are in line with the previously described increased invasiveness of melanoma cells after EVI/WLS knock-down (P.-T. Yang et al., 2012). The invasive capacity of siCTNNB1 transfected cells resembled the control, suggesting no major influence of β-catenin on the invasive capacity of the tested melanoma cells in this assay.

Migration was investigated in parallel to invasion, revealing that WM793 cells transfected with siCTNNB1 migrated quicker and those transfected with siEVI/WLS migrated slower than all other conditions. Strikingly, both the knock-down of *EVI/WLS* and *WNT11* had a strong negative impact on proliferation in these cells, suggesting that the signalling programmes that made the cells more invasive also slowed down proliferation (Figure 25D,E).

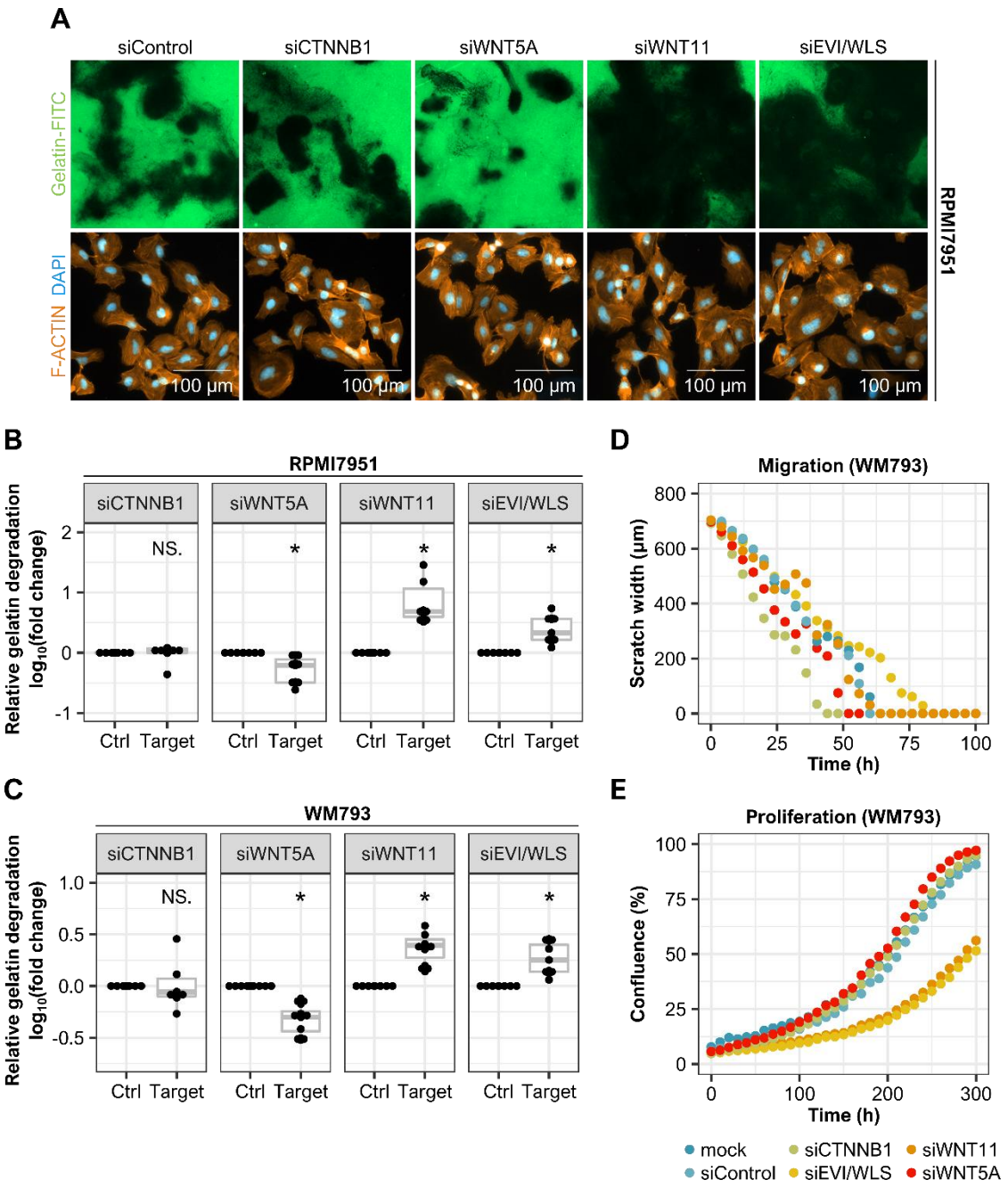

Figure 25. Knock-down of EVI/WLS or WNT11 enhances invasive capacity of melanoma cells

RPMI7951 or WM793 melanoma cells were treated with the indicated siRNAs for 72 h. Samples treated with transfection reagent only (mock) or non-targeting siRNA (siControl) were used as control.

A, B, C. Silencing of EVI/WLS or WNT11 enhanced gelatin degradation by melanoma cells. After pre-treatment with siRNAs, RPMI7951 or WM793 cells were seeded on fluorescein-gelatin (green) coated cover glasses. 24 h after seeding, cells were fixed with 4 % paraformaldehyde/PBS and stained for ACTIN-filaments using Phalloidin-TRITC (orange). Cover glasses were mounted using ProLong Diamond Antifade Mountant with DAPI, in order to visualise DNA (blue). **A,** Images were acquired using a Zeiss motorised inverted Observer.Z1 microscope with the ZEISS ZEN (blue edition) software and processed using Fiji (Fiji is just ImageJ). Image quality was optimised by adjusting brightness and contrast. **B & C**, quantification of gelatin degradation of respective siRNA (Target) relative to siControl (Ctrl) and normalised to cell number in at least six independent experiments with > 100 cells per condition. One-Sample Wilcoxon Signed Rank test, * $p < 0.05$, NS. = not significant

D, E. Proliferation was reduced by knock-down of EVI/WLS or WNT11 in WM793 melanoma cells. After pre-treatment with siRNAs, migration or proliferation were analysed by time-lapse live-cell imaging with the IncuCyte ZOOM system together with the IncuCyte Basic Software and the IncuCyte Scratch Wound Cell Migration Software Module. Plots are representative of three independent experiments.

The role of WNT11 has not yet been investigated in depth in the context of melanoma. After I observed the striking upregulation of invasive capacity upon its knock-down, I next asked if this effect could be reversed by overexpression of WNT11. In parallel, I overexpressed WNT3 and WNT5A, expecting to see a decrease and an increase in gelatin degradation, respectively. Indeed, the overexpression of WNT11 diminished gelatin degradation significantly, in some replicates even nearly completely, thus strengthening the link between WNT11 and melanoma invasiveness. Unexpectedly, overexpression of both WNT3 and WNT5A did not change the invasive capacity of RPMI7951 cells compared to the control. This indicates that the signalling induced by WNT5A is already at its maximum capacity and cannot be increased by further WNT5A secretion. Furthermore, these melanoma cells seem to be committed towards an invasive phenotype beyond the control by canonical WNT ligands, such as WNT3 (Figure 26).

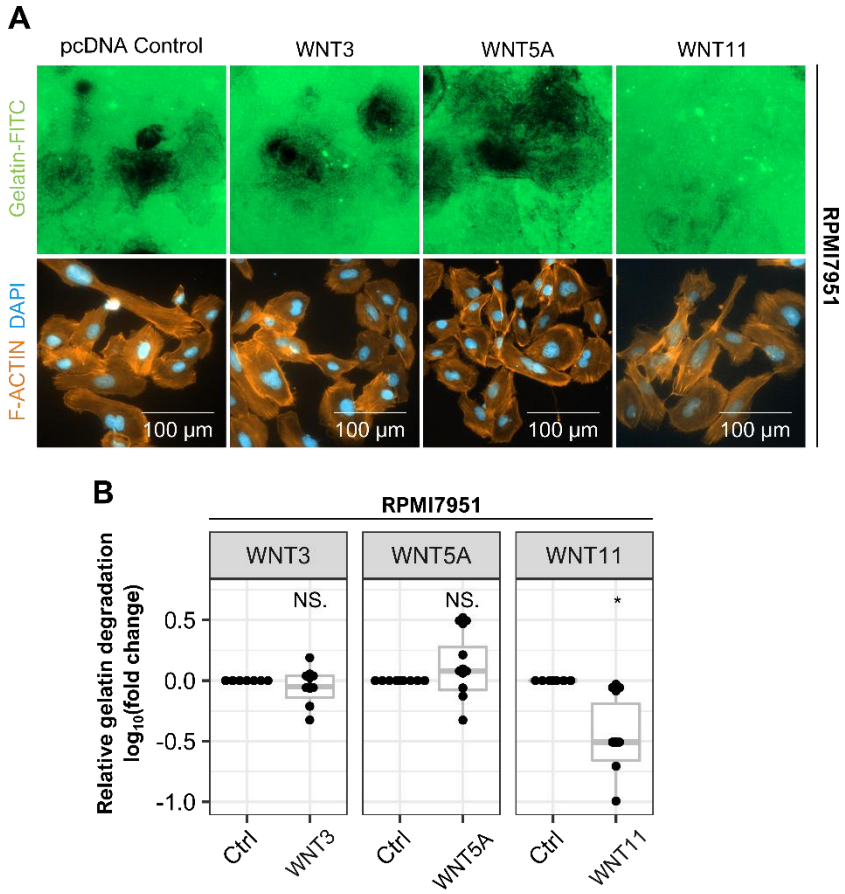

Figure 26. Overexpression of WNT11 reduces invasive capacity of melanoma cells

Overexpression of WNT11 reduced gelatin degradation by melanoma cells. RPMI7951 melanoma cells were transfected with the indicated overexpression constructs and seeded on fluorescein-gelatin (green) coated cover glasses 48 h later. Successful overexpression was confirmed in the remaining cells and their supernatant by Western blotting performed by Oksana Voloshanenko (data not shown). 24 h after seeding, cells were fixed with 4 % paraformaldehyde/PBS and stained for ACTIN-filaments using Phalloidin-TRITC (orange). Cover glasses were mounted using ProLong Diamond Antifade Mountant with DAPI, in order to visualise DNA (blue). **A,** Images were acquired using a Zeiss motorised inverted Observer.Z1 microscope with the ZEISS ZEN (blue edition) software and processed using Fiji (Fiji is just ImageJ). Image quality was optimised by adjusting brightness and contrast. **B**, quantification of gelatin degradation by indicated overexpression constructs relative to an empty pcDNA control plasmid (Ctrl) and normalised to cell number in at least six independent experiments with > 100 cells per condition. One-Sample Wilcoxon Signed Rank test, * $p < 0.05$, NS. = not significant

In summary, I demonstrated that EVI/WLS and WNT11 have an impact on melanoma cell invasiveness *in-vitro*. Moreover, the abundance of EVI/WLS protein in melanoma and HEK293T cells is regulated by ubiquitination in the presence and absence of lipid-modified WNT ligands. Different Ub linkage types mediated by multiple E2 Ub conjugating enzymes implicate a possible role for EVI/WLS trafficking and its WNT cargo function. Un-needed or misfolded EVI/WLS is removed from the ER by ERAD and then degraded by the proteasome. My results show that ERLIN2 links EVI/WLS to the ERAD machinery before it is ubiquitinated and that FAF2 and UBXN4 interact with EVI/WLS and VCP, presumably to ultimately remove it from the ER membrane.

5 Discussion

Cellular signalling frequently regulates and is regulated by protein stability. A prominent example is the canonical WNT signalling pathway: its major effector, β-catenin, is constantly translated and degraded in the absence of pathway activators (T. Zhan et al., 2017). The two most important cellular protein degradation machineries are autophagy and the Ub-proteasome system (Pohl & Dikic, 2019), which can be triggered by post-translational substrate modification with Ub. Substrates within the secretory routes or ER-(membrane)-resident proteins are degraded by ERAD and the proteasome if they fail quality control checkpoints (Christianson & Ye, 2014; Z. Sun & Brodsky, 2019). However, ERAD can also influence cellular signalling by controlling the quantity of proteins through selective degradation of functional proteins. The underlying mechanisms are incompletely understood and only few endogenous substrates of regulatory ERAD have been identified in mammals (Bhattacharya & Qi, 2019; Printsev et al., 2017). One of these substrates is the conserved transmembrane protein EVI/WLS (Glaeser et al., 2018). EVI/WLS is essential for the secretion of WNT ligands and thus has important functions throughout embryogenesis, as well as for tissue homeostasis and diseases, such as cancer (Zhan et al., 2017). This dependency requires a tight regulation of the availability of EVI/WLS itself and it was shown previously that EVI/WLS is ubiquitinated by UBE2J2 and CGRRF1 before it is removed from the ER with the help of VCP and proteasomal degradation (Glaeser et al., 2018). Glaeser et al. showed that EVI/WLS is apparently not ubiquitinated by SYVN1/HRD1 (Glaeser et al., 2018). This makes analysing the degradation of EVI/WLS especially interesting, as SYVN1/HRD1 was reported to be involved with most other known substrates of regulatory ERAD (Bhattacharya & Qi, 2019; Printsev et al., 2017). Nevertheless, many open questions regarding the ubiquitination of EVI/WLS and its link to the proteasome remained. The stability and availability of EVI/WLS influences WNT ligand secretion, but so far it was unknown whether ubiquitination might mediate the retrograde transport of EVI/WLS by different Ub linkage-types. Beside the regulation of EVI/WLS abundance, it is also crucial to define phenotypic or functional consequences of EVI/WLS stability. In melanoma, WNT5A overexpression and EVI/WLS deficiency, and thus reduced WNT5A secretion, are associated with invasiveness and metastasis formation (Webster et al., 2015; P.-T. Yang et al., 2012). The underlying mechanisms are not well understood, and only consistent methodologies and assays can help to resolve this apparent conundrum.

To gain insight into the regulation of EVI/WLS protein abundance in physiology and pathophysiology, I analysed its 'Ub code', novel ERAD-associated interaction partners, and how its relation to melanoma cell invasiveness. The presented results demonstrate that EVI/WLS is modified with K11-, K48-, and K63-linked Ub by different E2 enzymes and at multiple positions, which impacts on its degradation and function. I show that ERLIN2 is an important link between EVI/WLS and the Ub machinery and FAF2 and UBXN4 interact with both EVI/WLS and VCP, possibly to help with the dislocation of EVI/WLS from the ER. EVI/WLS is ubiquitinated and degraded in cells irrespective of the availability of lipid-modified WNT ligands, indicating a tight and conserved regulation across cell types. Furthermore, my data suggests for the first time the secretion of non-lipid-modified WNT11 from melanoma cells and supports a possible role of WNT11 in melanoma progression.

5.1 The EVI/WLS 'destruction complex' contains ERLIN2, FAF2, and UBXN4

To further elucidate the mechanism by which EVI/WLS is recognised by the ERAD machinery and linked to VCP, I performed a screen based on EVI/WLS protein stability after query gene knock-down (Figure 11,S1,S2,S3). This led to the identification of three candidates which increased EVI/WLS protein levels upon knock-down and interacted with endogenous EVI/WLS protein: ERLIN2, FAF2, and UBXN4 (Figures 12,13,15).

FAF2 and UBXN4 contain VCP interaction domains and are anchored at the ER membrane by an 'intramembrane' domain, which leaves both their N- and C-termini facing the cytoplasm (Liang et al., 2006; Meyer & Weihl, 2014; Mueller et al., 2008; Schuberth & Buchberger, 2008). This allows them to hold a firm grip on VCP and to support it during the generation of mechanical force by ATP dependent protein extraction from the ER (Hirsch et al., 2009). FAF2 was found to be involved in the recently discovered endosome and Golgi-associated degradation (EGAD, Schmidt et al., 2019). Accordingly, future studies should consider the possibility that EVI/WLS can be targeted to the proteasome coming from different organelles than the ER.

However, it cannot be excluded that additional proteins regulate EVI/WLS degradation which were not discovered here because of potentially insufficient RNAi mediated knock-down, cell type dependency, or variability between biological replicates. Although it is assumed that most ERAD related proteins have been identified in yeast and mammals (Christianson & Ye, 2014), it is impossible to discover novel ERAD associated proteins with a hypothesis driven

approach as described here. An unbiased genome-wide screen could potentially identify further candidates and add more details to the emerging picture.

While the ERAD substrate IP_3R seems to require a complex of ERLIN2 with ERLIN1 to initiate its degradation (Pearce et al., 2007, 2009; Y. Wang et al., 2009), there are also reports of ERLIN2 acting independently of ERLIN1, for example during the recognition of HMG-CoA reductase (Jo, Sguigna, et al., 2011). Whereas ERLIN2 was identified as a candidate to regulate EVI/WLS protein stability, ERLIN1 failed to do so. Furthermore, ERLIN1 did not interact with EVI/WLS, although immunoprecipitation experiments confirmed the previously described interaction between ERLIN1 and ERLIN2 (Figures 11,14B,S1). These data indicate that EVI/WLS is ubiquitinated and degraded independently of ERLIN1. It is currently unknown if the involvement of ERLIN1 or ERLIN2 depends on properties of the substrate, e.g. general hydrophobicity or topology, or additional binding partners that are potentially only present at specific ER subdomains. Further studies are required to elucidate this mechanism and the specificity of ERLIN2 *versus* ERLIN1 on EVI/WLS stability.

Glaeser et al. demonstrated that increased EVI/WLS abundance resulting from the knock-down of VCP led to augmented WNT ligand secretion (Glaeser et al., 2018). Hence, it will be important in the future to investigate in more detail how these novel components of the EVI/WLS 'destruction complex' influence cellular WNT secretion and thus WNT signalling in general in different cellular models.

5.1.1 ERLIN2 links EVI/WLS to the Ub machinery

The presented data indicate an interaction between EVI/WLS and ERLIN2 prior to its ubiquitination (Figure 21A), suggesting that ERLIN2 is linking EVI/WLS to the ERAD machinery, similar to what has been described for HMG-CoA reductase and IP_3R (Jo, Lee, et al., 2011; Pearce et al., 2007, 2009; Y. Wang et al., 2009). Accordingly, EVI/WLS is the third substrate of regulatory ERAD that depends on ERLIN2 for its ubiquitination. Further studies are required to decipher the underlying processes of client recognition and to identify additional interaction partners.

Immunoprecipitation experiments confirmed the interaction of FAF2 and ERLIN2, which was reported previously in an extensive screening approach for mapping ERAD component interactions (Figure 14, Christianson et al., 2012). Their additional interaction with VCP and PORCN indicates either the formation of a large complex at the ER membrane prior to the degradation of EVI/WLS or a sequential interaction between these proteins (Figures 13,14). A proposed model of this process is depicted in Figure 27.

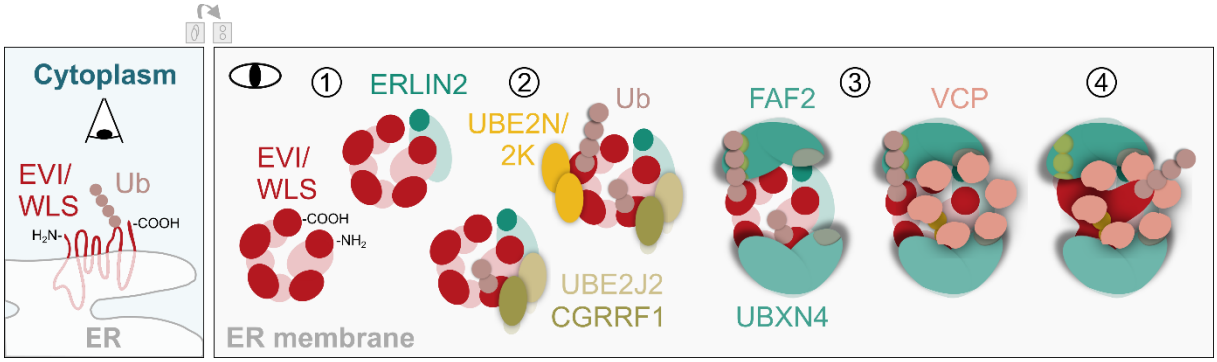

Figure 27. Proposed sequence of events leading to the extraction of EVI/WLS from the ER membrane

Side- (left) and top-view (right) of EVI/WLS inserted in the ER membrane. Unubiquitinated EVI/WLS binds ERLIN2 (1), followed by its poly-ubiquitination by UBE2J2, UBE2K, UBE2N, and CGRRF1 (2). FAF2 and UBXN4 bind to EVI/WLS and recruit VCP to the ER membrane (3). Ubiquitinated EVI/WLS is extracted from the ER membrane by threading it through the lumen of VCP (4).

However, it is necessary to perform time-resolved experiments to conclusively determine the order of events at the ER membrane. These kinds of experiments are hindered by the constant degradation of EVI/WLS, which obscures a clear-cut starting point as all stages of protein translation and degradation are detected at the same time. In the future, these limitations might be overcome by using LGK974 to induce increased EVI/WLS degradation in cells with high WNT ligand expression in combination with quantification of Western blot experiments to detect subtle changes over time.

Furthermore, it will be interesting to analyse how well the described mechanisms are conserved in other animals and whether there are parallel mechanisms that are more relevant in some organisms than in others. In general, many components of the ERAD machinery are conserved from yeast to mammals (Hirsch et al., 2009), and WNT signalling is conserved among metazoans (Holstein, 2012), suggesting that the proteins involved in the regulatory ERAD of EVI/WLS might also be conserved.

5.1.2 Is EVI/WLS cleaved and extracted through a channel protein?

The presented data offers interesting insights into the degradation mechanism of an endogenous substrate of mammalian regulatory ERAD. Still, many open questions remain and especially the existence of a potential ER membrane channel protein for its dislocation remains elusive. Although no such protein could be identified in the screen, this does not exclude that one might exist. However, if there was no such channel protein, the alternative could be that EVI/WLS would be removed from the ER-membrane by application of brute force generated by VCP through the hydrolysis of ATP. Biochemical studies using yeast extracts demonstrated the full-length dislocation of the ER-membrane resident isozyme of HMG-CoA after ubiquitination by Hrd1 and with the help of Cdc48/VCP as energy source. In the same study, the authors

showed that Cdc48/VCP and the proteasome, but not Hrd1 as a channel, were required for the dislocation of an artificial self-ubiquitinating substrate (SUS) with 8-transmembrane domains (Garza et al., 2009). However, it was later discovered that SUS and many other integral membrane ERAD substrates depend on the derlin Dfm1 for their dislocation in yeast (S. Neal et al., 2018). In general, derlins belong to the rhomboid family, a group of intramembrane proteases, which have lost their catalytic activity. Based on recent studies concerning the rhomboid fold and its impact on protein diffusion in cellular membranes, it is tempting to speculate that their main contribution to ERAD is distorting the lipid bilayer when acting together with channel proteins such as Hrd1 (Kreutzberger et al., 2019; Wu et al., 2020). There is no direct ortholog of Dfm1 in mammals and its closest relative is the catalytically active rhomboid protease RHBDL4/RHBDD1 (S. Neal et al., 2018). Cleavage by RHBDL4/RHBDD1 is an important step in the regulatory ERAD of subunits of the OST complex, underlining the general significance of proteolytic processing for ERAD (Knopf et al., 2020). However, recent mass-spectrometry analysis of the commonly used cell line HEK293T identified RHBDL4/RHBDD1 as interaction partner of ERLIN2 and FAF2, but not of EVI/WLS (Knopf et al., 2020). This is in line with the results of my RNAi screen on EVI/WLS abundance, which did not identify RHBDL4/RHBDD1 as a potential regulator of EVI/WLS stability (Figure 11). Together, these data suggest strongly that cleavage by RHBDL4/RHBDD1 is not important for the regulatory ERAD of EVI/WLS. Nevertheless, it is compelling to speculate that the eight-pass transmembrane protein EVI/WLS is cleaved within the ER membrane and that the cleaved fragments are then extracted separately. Data generated in our lab suggests that EVI/WLS can be proteolytically processed (Kathrin Gläser, PhD thesis), but if this occurs in the context of ERAD, or might even be a necessity, remains to be elucidated. In addition, no protease has been identified yet that would mediate the cleavage of EVI/WLS.

Overall, it might be possible that not one, but several mechanisms exist in parallel, as demonstrated for the prototypic substrate of ERAD, cystic fibrosis transmembrane conductance regulator (CFTR): single transmembrane domain constructs can be extracted completely by VCP, but part of the CFTR proteins were still degraded in a reconstituted cell-free system even after the removal of VCP, suggesting VCP-independent ERAD mechanisms (Carlson et al., 2006). However, a hitherto undiscovered channel protein and/or potential cleaving enzymes seem an elegant and potentially less energy-intensive approach than dislocation of EVI/WLS from the ER-membrane just by force generated by VCP. More studies and screening of additional candidates is required to clarify the underlying mechanisms.

5.1.3 Lipid homeostasis is regulated by ERAD components

The ER is associated with lipid homeostasis, for instance because lipid droplets originate from the ER membrane (Olzmann & Carvalho, 2019). Many ERAD-associated proteins have also been implicated in lipid droplet biogenesis or turn over, notably ERLIN2, FAF2, UBXN4, and VCP (Bersuker et al., 2018; Olzmann et al., 2013; G. Wang, Zhang, et al., 2012). It was even proposed that ERAD might preferentially happen at sites of lipid droplet formation and that their lipid composition might facilitate the removal of substrate proteins. However, this notion could not be confirmed (Christianson & Ye, 2014). Lipid droplets are organelles consisting of a hydrophobic core encircled by a phospholipid monolayer (Olzmann & Carvalho, 2019). Hence, the localisation of the eight-pass transmembrane protein EVI/WLS to mature lipid droplets is rather unlikely from an energy-related perspective. Nevertheless, it is tempting to speculate that EVI/WLS is connected to lipid homeostasis or specialised lipid structures, because of its interaction with acylated WNT ligands after the transfer of palmitoleic acid by PORCN (Takada et al., 2006). It has been demonstrated previously that EVI/WLS, PORCN, and WNTs localise to detergent-resistant microdomains with specialised lipid composition in the ER membrane, so called lipid rafts (Galli et al., 2016; Zhai et al., 2004). Moreover, studies in *Drosophila* described the dependence of long-range WNT signalling on the lipid raft protein reggie-1/flotillin-2 (Katanaev et al., 2008). Importantly, ERLIN2 is also a major component of lipid rafts (Browman et al., 2006) and it will be important to test if ERLIN2 acts as a molecular switch regulating either the degradation of EVI/WLS by ERAD or coordinating the events that lead to WNT ligand secretion. ERLIN2 might be involved in both by facilitating crosstalk between proteins and organelles that harbour EVI/WLS in the presence or absence of WNT ligands, possibly in a PORCN-dependent manner (Glaeser et al., 2018).

FAF2 has an important regulatory function for the synthesis of long, unsaturated fatty acids by assisting in the VCP- and proteasome dependent degradation of INSIG1. In the absence of INSIG1, sterol regulatory element-binding protein is activated by proteolysis and mediates the transcription of proteins necessary for fatty acid synthesis. In turn, long-chain unsaturated fatty acids induce the polymerisation of FAF2, thus inhibiting the degradation of INSIG1 and of fatty acid synthesis (H. Kim et al., 2013; J. N. Lee et al., 2010, 2006, 2008). It would be interesting to test whether this polymerisation of FAF2 can be mediated by palmitoleic acid (C16:1), as well as by oleate (C18:1) and arachidonate (C20:4), which were tested in the study by Lee et al., 2010. If yes, this would be exciting to study in the context of EVI/WLS regulation, as EVI/WLS might be protected from ERAD by the lipid modification of the WNT ligands. Palmitoleic acid could have a dual function: (i) it could inhibit FAF2 by causing its polymerisation

and (ii) its presence on WNT ligands allows their secretion. Of course, several questions have to be addressed in the future regarding the localisation of the involved proteins and the delivery of lipids to PORCN, WNT, and FAF2. It should also be noted that WNTs reside in the ER lumen while FAF2 is attached to the ER membrane from the cytosolic side.

5.1.4 ERLIN2 and FAF2 are involved in cancer

Whereas mutations in components of the WNT signalling cascades can be the main drivers of malignancies such as colorectal cancer, WNT signalling has rather a modulatory role in other tumour entities, for example melanoma (Zhan et al., 2017). FAF2 and ERLIN2 have been implicated in uveal melanoma or breast cancer, respectively, cancer types which are also associated with deregulated WNT signalling (W. Li et al., 2020; Y. Li et al., 2018; G. Wang, Liu, et al., 2012; Zhan et al., 2017; Zuidervaart et al., 2007). Only few mechanistic studies analysed the functional role of these proteins in tumorigenesis, and they were attributed to a broad range of cellular functions, for instance lipid homeostasis, ERAD, or cell cycle regulation (G. Wang, Liu, et al., 2012; G. Wang, Zhang, et al., 2012; Xuebao Zhang et al., 2015). It will be interesting to test if the underlying mechanisms are connected to the posttranslational regulation of WNT secretion and if tumours could be targeted *via* ERAD.

In general, ubiquitination, proteasomal degradation, and related processes have been implicated in various steps of tumorigenesis of multiple cancer entities, due to their important role in many signalling pathways. The described mechanisms are manifold, ranging from regulating the tumour metabolism to cancer stem cell maintenance, as Ub and related processes control protein abundance or act as molecular switches (Deng et al., 2020). In the future, it will be important to exploit the specificity of the UPS with regard to the regulation of cellular signalling to develop novel therapeutic approaches for cancer and other diseases, e.g. by improving targeted protein degradation through PROteolysis-TArgeting Chimeras (PROTACs, X. Li & Song, 2020; X. Sun et al., 2019).

5.2 UBE2J2, UBE2K, and UBE2N ubiquitinate EVI/WLS

The E2 Ub conjugating enzyme UBE2J2 and the E3 Ub ligase CGRRF1 have been shown previously to modify EVI/WLS with Ub, but their knock-down does not completely abolish EVI/WLS ubiquitination (Glaeser et al., 2018). This indicates either residual enzyme activity due to incomplete siRNA-mediated knock-down or that additional E2 and/or E3 proteins ubiquitinate EVI/WLS. Here, I show that EVI/WLS is modified by UBE2K with K48-linked Ub (Figures 16,21B) and by UBE2N with K63-linked Ub (Figures 18,21C). The yeast homolog of UBE2J2 (Ubc6)

was reported to prime substrates with short K11-linked Ub modifications, which are then elongated with K48-linked Ub by different E2s to ensure efficient recruitment of the degradation machinery (Mehrtash & Hochstrasser, 2019; Tsuchiya et al., 2018; A. Weber et al., 2016; P. Xu et al., 2009). Considering that K11-linked ubiquitination was also found on human EVI/WLS (Figure 21A), it is tempting to speculate that UBE2K would elongate these initial modifications by UBE2J2 in mammalian cells and allow successful interaction with downstream factors, potentially even without an associated E3 protein (Middleton & Day, 2015; Rodrigo-Brenni & Morgan, 2007; X. Wang et al., 2009). However, it should be noted that IP experiments did not confirm an interaction between UBE2K and EVI/WLS (Figure 16D). This might be due to a transient interaction between these proteins and/or the stringent cell lysis using Triton X-100, which strongly affects the detection of interactions within the ERAD network (Christianson et al., 2012). It should be tested whether interaction between EVI/WLS and UBE2K can be observed by using milder detergents for cell lysis, such as digitonin.

Surprisingly, UBE2G2 was not involved in the ubiquitination of EVI/WLS (Figures 11,S1), although it was previously connected to the degradation of most other ERAD substrates (Leto et al., 2019; Mehrtash & Hochstrasser, 2019). However, only few studies analysed regulatory ERAD substrates in great detail and it is conceivable that their ubiquitination mechanism differs substantially from the one of misfolded substrates (Printsev et al., 2017).

5.2.1 The E3 Ub ligase CGRRF1 ubiquitinates EVI/WLS

Extensive proteomic analyses of ER-membrane associated E3s described CGRRF1, MARCH4, and RNF128 as possible candidates to ubiquitinate EVI/WLS (Fenech et al., 2020), but follow-up experiments only confirmed CGRRF1 (Glaeser et al., 2018). Nevertheless, it is of course possible that cytosolic E3s are also involved in the process and screening approaches will be necessary to cover the several hundred potential candidates in a systematic way, potentially based on known E2/E3 interactions (van Wijk et al., 2009). Beside the effect of cytosolic E3s on EVI/WLS protein abundance, their effect on WNT ligand secretion should also be assessed in parallel as a potential read-out to determine their involvement in EVI/WLS function. It might be worth to investigate MARCH4 and MARCH6 in more detail, possibly in a different cellular system, because they affected EVI/WLS in A375 cells to a small degree and MARCH6 is a known partner of UBE2J2 (Mehrtash & Hochstrasser, 2019).

Although SYVN1/HRD1 is highly important for the degradation of many other ERAD substrates (Bhattacharya & Qi, 2019), it is apparently not involved in the degradation of EVI/WLS. Its knock-down did not regulate EVI/WLS protein levels and there was also no

interaction found in IP experiments (Glaeser et al., 2018). Yeast Hrd1 is involved in several complexes that mediate the ERAD of ER-luminal or transmembrane proteins (Mehrtash & Hochstrasser, 2019). The respective orthologs of components of these SYVN1/HRD1-related complexes in the human system (e.g. SEL1L, HERPUD1, or OS9) did also not give strong phenotypes in my screen on EVI/WLS protein levels, similar to SYVN1/HRD1 (Figures 11,S1,S2). Of course, potential candidates could be missed due to insufficient knock-down. Hence their role in EVI/WLS stability could be evaluated again after introducing knock-outs of the respective gene for example using CRISPR/Cas9 mediated genome engineering. In addition, it might be possible that one E3 ligase alone is not sufficient to induce EVI/WLS degradation and that instead several E3 ligases might be required to work in concert. It would be possible to perform combinatorial knock-down or knock-out experiments to circumvent compensatory mechanisms.

Additionally, my data did not reveal a specific E3 Ub ligase which cooperates with UBE2N to modify EVI/WLS. These results together with published high-throughput studies suggest that the E3 ligase is presumably not an ER-membrane associated protein (Figures 11,S1, Fenech et al., 2020b; Glaeser et al., 2018). It should be considered that earlier *in-vitro* and structural studies showed that UBE2N~ubiquitin together with UBE2V2 can adopt an active conformation even in the absence of an E3 ligase, suggesting E3-independent Ub chain elongation (McKenna et al., 2001; Pruneda et al., 2011). However, recent sophisticated real-time fluorescence resonance energy transfer analysis did not observe Ub transfer events in the absence of an E3 (Branigan et al., 2020).

5.2.2 K63-linked Ub and its possible role in EVI/WLS trafficking

After associating with WNT ligands in the ER, EVI/WLS shuttles them to the cell surface (Bänziger et al., 2006; Bartscherer et al., 2006; Goodman et al., 2006; Routledge & Scholpp, 2019; J. Yu et al., 2014). Then, EVI/WLS is endocytosed with the help of clathrin and recycled back to Golgi and ER in a retromer dependent process (Belenkaya et al., 2008; Port et al., 2008). If trafficking of EVI/WLS is interrupted, it is transported to the lysosomes for degradation (Franch-Marro et al., 2008; Gross et al., 2012; P.-T. Yang et al., 2008). Recently, a study in *C. elegans* found that the knock-out of the K63-specific E2 Ub conjugating enzyme UBC13 also disrupted MIG-14/EVI/WLS trafficking and diverted it to lysosomes but they did not investigate the ubiquitination status of MIG-14/EVI/WLS (J. Zhang et al., 2018). Here, I demonstrate that human EVI/WLS is conjugated with K63-linked Ub chains by UBE2N, the human ortholog of UBC13 (Figures 18,21). In humans, the two heterodimers UBE2N-UBE2V1 and UBE2N-

UBE2V2 have been described to mediate K63-specific ubiquitin linkage. In addition to UBE2N, its enzymatically inactive interaction partner UBE2V2 was also required for K63-linked ubiquitination of EVI/WLS (Figure 21). By contrast, the knock-down of UBE2V1 resulted in more variable phenotypes between replicates and requires more in-depth analysis.

It is exciting to note that the presented data also implies a possible effect of K63-linkage on WNT ligand secretion (Figure 18C), in agreement with recent results in worms, where the knock-down of UBC13/UBE2N led to defects in Wnt-dependent processes (J. Zhang et al., 2018). Glaeser et al. also reported increased WNT ligand secretion after the knock-down of VCP and the resulting increase of EVI/WLS protein (Glaeser et al., 2018). I did not observe the same effect (Figure 18C), most likely due to pleiotropic effects of VCP and the strong effect on viability of its knock-down, which is more apparent if the assay is run for longer. Therefore, it is possible to observe different effects dependent on the timing of the experiment. In the future, it will be important to analyse if increased WNT ligand secretion after depletion of UBE2N or UBE2V2 actually results in increased signal transduction in WNT-receiving cells e.g. by TCF-WNT reporter assays, a notion that was recently challenged in a *Drosophila* study (Hatori & Kornberg, 2020).

Zhang et al. concluded that ubiquitination by UBC13/UBE2N was important for segregating the retromer and ESCRT-associated microdomains on a common endosome after MIG-14/EVI/WLS endocytosis to guarantee efficient trafficking in *C. elegans* (J. Zhang et al., 2018). Indeed, it had previously been observed that substrate ubiquitination was important for sorting to the SNX3-retromer complex or the ESCRT machinery in yeast (Strochlic et al., 2008) and it is in general well established that ESCRT-dependent sorting relies on K63-ubiquitination of the cargo (Frankel & Audhya, 2018; Mosesso et al., 2019). However, in the reported cases K63-linked ubiquitination resulted in lysosomal degradation of the substrates (Cullen & Steinberg, 2018; Pohl & Dikic, 2019), whereas EVI/WLS seems to be preferentially routed to lysosomes in the absence of K63-linkage. Accordingly, intriguing questions arise: why do EVI/WLS protein levels increase and not decline after the knock-down of UBE2N if EVI/WLS is delivered to the lysosomes? Why does EVI/WLS with K63-linked Ub modification accumulate after the inhibition of the proteasome (Figure 21C)? This clearly indicates that EVI/WLS modified with K63-linked Ub is degraded by the proteasome and not (only) by lysosomes. It was shown previously that EVI/WLS protein levels increase after the inhibition of lysosomes with compounds such as bafilomycin A (Glaeser et al., 2018) and it might be interesting to investigate the impact of UBE2N on the lysosomal degradation of EVI/WLS.

Components of the ESCRT machinery are required for sorting EVI/WLS and WNT ligands to MVBs prior to their release on exosomes (Gross et al., 2012), but intracellular retrograde transport of EVI/WLS depends on the retromer complexes. Whether ubiquitination also plays a role in the function of retromer is not yet well understood. Stangl et al. reported recently that the DUB OTULIN regulated retromer-dependent recycling to the cell membrane, albeit in an ubiquitin-independent mechanism (Stangl et al., 2019). Additionally, Hao et al. found that K63-linked ubiquitination of the WASH complex regulated F-actin and thus transport by retromer (Y.-H. Hao et al., 2013). Whether any of these mechanisms are involved in the regulation of EVI/WLS remains to be analysed.

Besides retrograde trafficking, K63-linked ubiquitination could also mediate the internalisation of EVI/WLS from the plasma membrane, which is a well described mechanism for the endocytosis of various other proteins (Piper et al., 2014). In this case, removing the K63-linked ubiquitination should result in the accumulation of EVI/WLS at the plasma membrane in the presence of WNT ligands. EVI/WLS surface levels could be tested by surface staining without membrane permeabilisation either directly by fluorescence activated cell sorting or after the biotinylation of cell surface proteins and subsequent analysis of EVI/WLS protein levels in the surface or intracellular fraction with Western blotting. Using a more advanced approach, it might be possible to compare the ubiquitination profiles of EVI/WLS mutant variants that localise either to the plasma membrane (e.g. the Y/AEGL-construct, Gasnereau et al., 2011) or to the ER (e.g. after introducing a strong ER-retention motif). Cell fractions could be analysed by mass-spectrometry to investigate if the ubiquitination of EVI/WLS is a dynamic process that changes according to its intracellular localisation. Importantly, it should be ensured that the introduced mutations do not affect possible ubiquitination sites. To gain more insights into the possible roles of ubiquitination on EVI/WLS trafficking, it will be important to perform immunofluorescence stainings to investigate the co-localisation of endogenous EVI/WLS with markers of the plasma membrane, MVBs, or other organelles after the knock-down of UBE2N. These studies should either be performed with tagged proteins or with antibodies that allow the staining of endogenous EVI/WLS to avoid confounding effects by protein overexpression.

The involvement of K63-linked Ub in the endocytosis and/or retrograde transport of EVI/WLS would imply that it was most relevant in cells with active WNT secretion – otherwise EVI/WLS would not localise to the plasma membrane. However, the knock-down of UBE2N led to increased EVI/WLS protein levels in HEK293T cells without WNT ligands (Figure 18C). In conclusion, many open questions about how UBE2N and K63-linked Ub influence EVI/WLS physiology remain, which need to be addressed using additional experiments and with the help

of different cellular models. It is likely that the observed phenotypes are results of multiple parallel mechanisms and/or indirect effects of the knock-down of UBE2N that are exceedingly difficult to disentangle.

Multiple Ub linkage types present on EVI/WLS provide the opportunity to investigate additional layers of its regulation. For example, it has been described that UBE2K together with UBE2N builds branched Ub chains with unique downstream signalling properties, such as regulating NF-κB signalling (Ohtake et al., 2016), and it would be exciting to find such branched chains on EVI/WLS as well. It is conceivable that EVI/WLS would be first modified with K63-linked Ub and only additionally with K48-linked Ub if the protein is destined to be degraded by the proteasome (Ohtake et al., 2018). This could be shown indirectly if the knock-down of UBE2N resulted in less K48-linked Ub on EVI/WLS, implying that the lack of K63-linked Ub chains also led to a reduced availability of sites for K48-linkage. The direct observation of branched chains is only possible with mass-spectrometry approaches. However, Ub is usually cleaved at R54 between the positions K48 and K63 during routine sample preparation for mass-spectrometry with trypsin, making it impossible to observe the two branch-points on the same peptide (Ohtake et al., 2016). Therefore, either non-trypsin digestion or Ub mutants without this cut site are necessary in combination with EVI/WLS protein preparations to directly observe these modifications using mass-spectrometry.

5.2.3 Defining the ubiquitination sites of EVI/WLS

To understand the regulation and the impact of K48- and K63-linked Ub chains on EVI/WLS, it is important to determine the ubiquitination sites of EVI/WLS. Publicly available proteomic mass-spectrometry data reported several ubiquitination sites in human EVI/WLS, many of them within the first luminal loop (Figure 2). At least two records within these datasets found ubiquitination at the positions K61, K208, K217, K410, and K419 (PhosphoSitePlus, Hornbeck et al., 2015, accessed Oct 2020). Another recently published dataset found an additional ubiquitination at K12 (Steger et al., 2020).

However, it is unclear whether this data reflects the whole protein sequence. Some ubiquitination sites might not have been identified yet due to their transient nature or because EVI/WLS is a multi-pass transmembrane protein and difficult to extract from the membrane. It is therefore conceivable that some parts of EVI/WLS are more likely to be recovered using mass-spectrometry than others. It is striking that half of the described ubiquitination sites (K61, K208, and K217) are at positions that face the ER lumen, but not the cytoplasm or the ubiquitination machinery, according to the structural model of EVI/WLS (Figure 2). Since there is no

molecular structure of EVI/WLS available yet, its exact topology and even its number of transmembrane domains is still debated (Bartscherer et al., 2006; Jin, Morse, et al., 2010; Korkut et al., 2009). Therefore, it should be considered that the described positions might indeed face the cytosol and not the ER lumen. However, several lines of evidence contradict this notion: (i) two publications performed immunofluorescence staining of V5-tagged EVI/WLS with antibodies targeting the first loop without membrane permeabilisation and found the signal to localise either to the plasma membrane (e.g. outside of the cell) or within the Golgi apparatus (e.g. luminal) after internalisation (Belenkaya et al., 2008; Franch-Marro et al., 2008). (ii) Immunogold staining of electron microscope images using antibodies targeting the loop region also confirmed extracellular or luminal localisation (Korkut et al., 2009). (iii) Immunoprecipitation experiments with shortened EVI/WLS constructs demonstrated the localisation of the WNT-binding domain within this loop. WNTs are secreted proteins and imported into the ER co-translationally (Fu et al., 2009). (iv) N-glycosylation of *C. elegans* MIG-14/EVI/WLS was found at the amino acid positions N158 and N212. These positions are within the loop and their modification infers ER localisation. Glycosylation was also predicted for the positions N9 and N345, but their proximity to the ER membrane make an actual modification unlikely due to sterical hinderance (GlycoProtDB ID: GPDB0000868, accessed Oct 2020). In conclusion, it is more likely that the luminal positions of EVI/WLS are modified after the respective parts of the protein have been extracted from the ER and that the primary ubiquitination sites indeed face the cytoplasm.

MHC class I heavy chains are also endogenous ERAD substrates that were found to be ubiquitinated at ER-facing residues, but not at cytosolic domains. The authors proposed that a part of the protein was dislocated before ubiquitination with the help of OS-9, SEL1L and SYVN1/HRD1 in a mechanism similar to the retrotranslocation of proteins located entirely within the ER lumen. The former luminal domains would then be trapped in the cytosol by ubiquitination and the extraction could be completed by VCP (Burr et al., 2013). While this is a compelling mechanism that is also supported by recent structural data on the function of yeast Hrd1 (X. Wu et al., 2020), there is currently no evidence that supports this hypothesis for EVI/WLS as well, especially considering that its dislocation is apparently SYVN1/HRD1 independent.

The predicted primary ubiquitination sites were therefore K410/419. However, expression of the EVI/WLS-V5 K410/419R mutant variant in HEK293T EVI/WLS knock-out cells did not result in a strong upregulation of EVI/WLS protein levels compared to expression of the wild type construct (Figure 17), indicating that it is still degraded very efficiently. The strong increase of EVI/WLS-V5 K410/419R protein levels after knock-down of VCP additionally

suggests that the degradation is mediated *via* ubiquitination and ERAD, and not by other cellular degradation pathways (e.g. the lysosomes). This can be due to alternative lysine residues that are available for ubiquitination, or it can be a result of ubiquitination of the hydroxylated amino acids serine or threonine by UBE2J2 (Cadwell & Coscoy, 2005; X. Wang et al., 2009; A. Weber et al., 2016). These oxyester-linked modifications cannot be found with standard mass-spectrometry approaches because they are pH sensitive and cleaved during routine sample preparations; it is therefore not surprising that they do not appear in most proteomic data sets (McClellan et al., 2019; A. Weber et al., 2016). Efforts to directly observe non-lysine ubiquitination on EVI/WLS by comparing high-molecular bands before or after acidic hydrolysis of samples were unfortunately unsuccessful (data not shown), maybe the effects were concealed by the additional presence of pH-insensitive lysine-ubiquitinations.

Nevertheless, non-lysine ubiquitination could also help to explain why protein levels of EVI/WLS-V5 K410/419R were higher than wild type EVI/WLS-V5 after the knock-down of UBE2J2 (Figure 17). This observation indicates that the positions K410/419 are indeed important for ubiquitination. However, they can possibly be functionally replaced by serines or threonines in their vicinity in the presence of UBE2J2. In the absence of UBE2J2, the K410/419R mutant is not ubiquitinated and degraded efficiently anymore and accumulates. It should be noted that the effects of silencing either UBE2K or UBE2J2 do not reflect the strong increase of EVI/WLS abundance upon knock-down of VCP, indicating that several additional E2 and/or E3 proteins, maybe even in combination, are required for the ubiquitination of EVI/WLS. Presumably, this then culminates in the extraction of EVI/WLS from the ER membrane with the help of VCP. Combinatorial knock-down of multiple E2 enzymes will help to elucidate the underlying mechanisms and to find potential additionally involved proteins. As next steps, it will also be interesting to investigate the presence of non-lysine ubiquitination on EVI/WLS by suitable unbiased mass-spectrometry approaches. These require efficient immunoprecipitation of either endogenous EVI/WLS or overexpressed EVI/WLS-V5 and customised sample preparation protocols for mass-spectrometry. It might also be interesting to include EVI/WLS constructs with multiple mutated ubiquitination sites and depletion of E2 or E3 proteins in the analysis pipeline. Mutating all possible ubiquitination sites, meaning not only lysines but also serines, threonines, and cysteines, would probably result in a malfunctional or unexpressed protein and is therefore unlikely to be successful. Nevertheless, it might also be interesting to analyse how the lack of ubiquitination sites influence the WNT secretion capacity of EVI/WLS to determine their functional relevance.

5.3 EVI/WLS is ubiquitinated and degraded in cells with and without lipidated WNTs

It was previously reported that EVI/WLS is a target of regulatory ERAD and that the interaction of EVI/WLS with WNT ligands prevented its degradation. This was demonstrated by overexpressing WNT ligands in HEK293T cells, a cell line with low endogenous WNT secretion, which lead to the stabilisation of EVI/WLS (Glaeser et al., 2018). Here, I show that this effect can be reversed by inhibiting PORCN and thus the lipidation of endogenous WNT ligands in A375 melanoma cells which naturally produce a lot of endogenous WNT5A (Figure 20). LGK974 treatment decreased EVI/WLS protein levels, but not mRNA expression, compared to DMSO control treatment, as EVI/WLS is no longer protected from its degradative fate by the interaction with WNT ligands (Figure 20B,C). The reduced expression of *AXIN2* after LGK974 treatment is an indication for decreased canonical/β-catenin dependent WNT-signalling, which can be regulated by WNT5A in melanoma cells (Figure 20C, Webster & Weeraratna, 2013). Inhibiting the proteasome in addition to LGK974 treatment resulted in an increase of high-molecular EVI/WLS bands compared to LGK974 treatment without inhibition of the proteasome, indicating the presence of ubiquitinated proteins that are no longer degraded. Surprisingly, proteasome inhibition even led to the accumulation of ubiquitinated EVI/WLS in DMSO control cells (where lipid-modified WNT ligands are present and actively secreted), indicating a surplus production of EVI/WLS and constant turn-over in cells with active WNT signalling (Figure 20D). Nevertheless, it should be emphasised that it is difficult to distinguish quantity- from quality-control ERAD mechanisms in this experiment and it is possible that the ubiquitinated EVI/WLS present in the DMSO control after inhibition of the proteasome is indeed misfolded.

Of the analysed ERAD-associated proteins which could mediate such a ubiquitination and degradation in A375 cells, VCP, UBE2J2, and CGRRF1 showed the strongest phenotypes, as they did in HEK293T cells (Figure S4, Glaeser et al., 2018). This indicates that the post-translational regulation of EVI/WLS is conserved between different tissues and developmental stages.

It appears to be a waste of cellular resources to constantly translate and degrade EVI/WLS, even in the absence of WNT ligands. Therefore, the question remains why cells would have developed such a mechanism. One possible explanation lies in the dynamics of cellular signalling: if all proteins necessary for WNT secretion, reception and intracellular signal transduction are present at all times, cells have the ability to react very fast and dynamic to changes in WNT ligand expression and signalling without the synthesis of additional proteins. Moreover, cells may require a constantly available pool of some proteins for alternative cellular functions,

such as β-catenin, which is also involved in adhesive junctions (Peifer et al., 1992). It is conceivable that EVI/WLS also has hitherto undiscovered, WNT-independent functions, as Petko et al. described a primate specific splice variant of EVI/WLS that was unable to sustain efficient WNT ligand secretion (Petko et al., 2019). However, more research in this area will be necessary in the future to clarify the underlying mechanisms.

5.4 EVI/WLS protein levels govern melanoma invasiveness

Malignant melanoma is a skin cancer derived from melanocytes with a very poor prognosis if metastasised (Schadendorf et al., 2018). Genetic mutations that drive melanoma development and progression are mainly associated with the MAPK signalling pathway (Schadendorf et al., 2018). Additionally, melanomas also produce a variety of WNT ligands and functional correlations have been established between various WNT pathway components and malignancy (Gajos-Michniewicz & Czyz, 2020). Reduced EVI/WLS protein abundance was detected in human melanoma samples compared to healthy skin and nevi and was also associated with metastasis formation in a xenograft mouse model (P.-T. Yang et al., 2012). Conversely, WNT5A expression is increased in metastatic melanoma compared to non-metastatic lesions and WNT5A is an important regulator of melanoma cell invasion (Forno et al., 2008; Weeraratna et al., 2002). This controversy is understudied, and it remains unclear how EVI/WLS protein levels are functionally correlated to melanoma invasion, not least due to the lack of reliable cellular models for invasiveness that allow the study of multiple conditions in parallel.

5.4.1 The gelatin degradation assay as an indicator for melanoma cell invasiveness

One possibility to study cellular invasiveness *in-vitro* is the gelatin degradation assay, which can be used to detect and quantify the proteolytic activity of membrane protrusions in cancer cells, so-called invadopodia (Figure 23, Paterson & Courtneidge, 2018). Invadopodia are actin-based structures that mediate pericellular degradation of the extra-cellular matrix through MMPs, such as MMP9 or MMP14 (Jacob & Prekeris, 2015). Importantly, invadopodia and their associated proteins, for example SH3PXD2A/TKS5 or CDC42, have been implicated in melanoma cell invasion or were found to be overexpressed in melanoma (Iizuka et al., 2016; H. Lu et al., 2016; Stengel & Zheng, 2011; Jianwei Sun et al., 2014). *MMP14* expression was upregulated in BRAF p.V600E or NRAS p.Q61R mutant melanoma cell lines compared to cell lines without these mutations (Bloethner et al., 2005) and dysregulated MAPK signalling increased *MMP9* expression (Napoli et al., 2020). Mechanistically, BRAF p.V600E signalling was implicated in the secretion of MMPs and the regulation of actin dynamics through the

phosphorylation of cortactin and components of the exocyst vesicle secretion complex by ERK (Clark & Weaver, 2008; H. Lu et al., 2016).

The role of WNT signalling in melanoma and invadopodia formation is not well understood, albeit several studies positively correlated components of the non-canonical WNT/Ca^{2+} signalling pathway, e.g. PKC, CDC42, or Ca^{2+} release from the ER, to melanoma cell invasion (Nakahara et al., 2003; Jianwei Sun et al., 2014; Weeraratna et al., 2002). Furthermore, stabilisation of β-catenin promoted invadopodia formation in melanoma cells (Grossmann et al., 2013) and WNT5A and ROR2 signalling was associated with increased invadopodia activity in other cancer entities, such as osteosarcoma (Enomoto et al., 2009).

5.4.2 WNT11 is secreted independent of PORCN activity and involved in invasion

After setting up the gelatin degradation assay, I established an analysis pipeline to quantify the invasive capacity of melanoma cells (Figure 23). To test how inhibition of WNT secretion could influence melanoma cell behaviour, I treated RPMI7951 melanoma cells with the PORCN inhibitor LGK974 (Figure 24). Western blot analyses confirmed that WNT5A was no longer secreted after LGK974 treatment and, accordingly, gelatin degradation by these cells was reduced, while migration and proliferation was not significantly affected (Figure 24,28). The protein levels of EVI/WLS were reduced compared to the DMSO treated control, presumably due to the lack of interaction with acylated WNT ligands, as discussed earlier for the cell line A375 (see 5.3). As a note on the side: this reduction of EVI/WLS protein levels is difficult to recapitulate using siRNAs against WNTs, as melanoma cells express several different WNT ligands and it would therefore presumably be necessary to perform combinatorial knock-downs of WNTs to see an effect on EVI/WLS abundance.

Surprisingly, WNT11 was still detected in the supernatant of LGK974 treated cells, albeit in lower amounts than in DMSO control cells (Figure 24C). This suggests that WNT11 can be secreted independent of PORCN activity. This exciting novel insight is currently under investigation in various model systems in our lab (Oksana Voloshanenko, personal communication). It seems as if a part of the WNT11 pool can be secreted independent of PORCN and EVI/WLS and is differentially modified, which would also explain the difference in size visible in Figure 24C. The two differentially secreted fractions of WNT11 seem to induce distinct downstream signalling in their target cells, as EVI/WLS-dependent WNT11 induces non-canonical effects like WNT5A and EVI/WLS-independent WNT11 apparently loses its non-canonical character. It is important to analyse if and how the two subpopulations influence melanoma cell invasiveness, e.g. with the help of mutant constructs that can only be secreted EVI/WLS

independently or *vice versa*. Once the two subpopulations and their regulation are better characterised, it will also be interesting to analyse melanoma patient samples to see if they have relevant functions *in-vivo*.

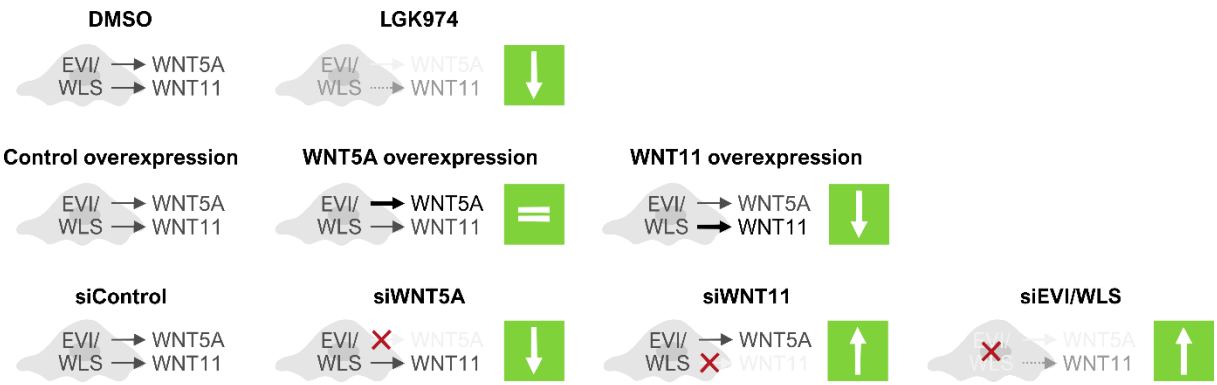

Figure 28. Summary of the observed phenotypes using the gelatin degradation assay

Compilation of different melanoma cell treatments and their effect on EVI/WLS, WNT5A, and WNT11 protein levels, as well as gelatin degradation/invasive capacity (green squares). Upward pointing white arrows indicate increased, downward white arrow decreased degradation compared to the control. Data summarised from Figures 24, 25, and 26.

So far, only limited information on WNT11 and melanoma is available, hence, I examined the effect of WNT11 knock-down and overexpression on gelatin degradation (Figures 25, 26). The observed phenotypes are summarised in Figure 28. Surprisingly, the knock-down of *WNT11* resulted in a significant upregulation of invasive capacity in RPMI7951 and WM793 melanoma cells, whereas its overexpression had the opposite effect in RPMI7951 cells (Figures 25,26,28). This was interesting, considering that it counteracts the effects of WNT5A, the knock-down of which reduced the invasive capacity of RPMI7951 and WM793 cells (Figure 26). WNT5A overexpression had no effect, presumably because RPMI7951 cells already secrete a lot of WNT5A and signal transduction is already at its maximum (Figures 26,28).

The role of WNT11 in melanoma was not yet studied in-depth, until a recent paper described its involvement in tumour initiation and invasion (Rodriguez-Hernandez et al., 2020). They report that WNT11 promotes an amoeboid phenotype in melanoma cells *via* FZD7 and DAAM1. Amoeboid cells are found at the invasive fronts of mouse and human melanomas and in metastasis. Their study revealed that siRNA-mediated knock-down of *WNT11* in A375M2 and WM1361 melanoma cells decreased invasion in a 3D assay. In contrast, I showed that transfection of siWNT11 induced degradation of extracellular matrix. While the applied assays reflect different aspects of the invasive process and different cell lines were used, it is also obvious that their invasion assay is very variable, similar to the gelatin degradation assay. Presumably, their data would profit from more replicates and a stringent statistical analysis. It should also be mentioned that there were differences in siRNA knock-down efficiencies

comparing the two studies. They still observed 40 % to 50 % of remaining *WNT11* mRNA expression, whereas in my experiments efficiency nearly reached 100 % as *WNT11* mRNA levels after knock-down were often below detection limit (Figure S5). Furthermore, it would be important to demonstrate that the observed effects depend on the interaction between WNT11 and FZD7, and not on the presence of other WNTs in these cell lines, for example WNT5A. Overall, further studies are required to investigate the underlying mechanisms and differences, but nevertheless the work by Rodriguez-Hernandez et al. provides an important additional link between non-canonical/β-catenin-independent WNT signalling and melanoma tumourigenesis.

In general, it cannot be dismissed that both WNT5A and WNT11 play a role in melanoma pathogenesis, given their important role in WNT/PCP signalling and the migration of neural crest derived cells, such as melanocytes (De Calisto et al., 2005; Y. Yang & Mlodzik, 2015). In future studies, it will be important to determine if their apparently opposite effects on melanoma cells in the gelatin degradation assay depend on varying levels of secretion, e.g. due to differential PTMs (Yamamoto et al., 2013) and their interaction with EVI/WLS, or their engagement with different receptors and further intracellular downstream signal transduction in the WNT receiving cell.

WNT11 was also identified as a tumour suppressor in hepatocellular carcinoma (Toyama et al., 2010), which would possibly reflect its role in melanoma indicated by my data. WNT11 expression was variable and, in most cases, lower than WNT5A expression in human melanoma patient samples in the TCGA datasets (309/367 patients, TCGA Research Network, accessed Mar 2019). However, WNT11 protein levels and their signalling capacity might be regulated at other levels, for example through post-translational mechanisms or by the availability of receptors at the target cell.

WNT signalling is an important way of communication between tumour cells and their microenvironment. Accordingly, tumour-intrinsic WNT/β-catenin signalling regulates T cell infiltration in melanoma (Spranger et al., 2015). Additionally, WNT5A was shown to promote the release of immunosuppressive exosomes from melanoma cells in a Ca^{2+} and CDC42-depent mechanism (Ekström et al., 2014). Therefore, and especially in the light of the recent study that correlated WNT11 to an invasive cell phenotype (Rodriguez-Hernandez et al., 2020), it will be important to characterise WNT-dependent melanoma cell plasticity in the presence of other cell types that constitute the microenvironment. WNT11 might be derived from cells in the microenvironment and not tumour cells themselves in an *in-vivo* setting. The expression of *WNT11* might also be restricted to certain small subpopulations of tumour cells and would therefore not be detectable in bulk analysis. Single cell sequencing of tumour and

microenvironment might be helpful to determine which cells produce *WNT11* and which cells carry the according receptors. Furthermore, these results should be confirmed with animal models, to prove the *in-vivo* relevance of WNT11 on melanoma cell invasiveness and migration and to evaluate whether the insights gained with the gelatin degradation assay can be transferred to *in-vivo* conditions.

5.4.3 EVI/WLS protein levels regulate melanoma invasiveness

The effects of knock-down and overexpression of WNT5A and WNT11 (Figures 25,26) are coherent within themselves (Figure 28). Unexpectedly, EVI/WLS downregulation increased gelatin degradation by melanoma cells, suggesting that lower secretion of WNT ligands makes melanoma cells more invasive. In contrast, LGK974 treatment showed a similar effect on WNT ligand secretion as the knock-down of EVI/WLS, but decreased gelatin degradation. These apparently contradicting phenotypes could be due to differences in WNT ligand acylation, considering that PORCN is still active in the siEVI/WLS transfected cells, or be due to other WNT ligands that the cells might produce and which I did not analyse in these experiments. It should be noted that a recent study suggested acylation and secretion independent, cell autonomous signalling by WNT3A and WNT4 in several human cancer cell lines (Rao et al., 2019), but further studies are required to evaluate this hypothesis. Nevertheless, it should be considered that there are possible additional layers of WNT secretion-dependent regulation that remain hitherto undiscovered. To gain more insights into the mechanism and to determine how the observed phenotypes are connected, it will be important to perform combinatorial knock-downs or overexpression of EVI/WLS, WNT11, and WNT5A (and possible further candidates). These epistasis experiments can clarify if the observed effects are independent or if they act in parallel.

The enhancement of the cells' invasive capacity after *EVI/WLS* knock-down is, however, in line with a previous study correlating reduced EVI/WLS abundance to increased metastasis formation in a xenograft mouse model (P.-T. Yang et al., 2012). The authors explained this effect with the EVI/WLS and WNT ligand secretion-dependent activation of WNT/β-catenin signalling in melanoma cells, which inhibited melanoma cell proliferation and metastasis. However, the general role of β-catenin and its regulation in melanoma pathogenesis is under considerable debate and studies showed both its degradation and its stabilisation as response to WNT5A signalling (Gajos-Michniewicz & Czyz, 2020; Grossmann et al., 2013). By contrast, I did not detect changes in gelatin degradation capacity or in proliferation after knock-down of *CTNNB1* and cellular migration was slightly enhanced after β-catenin depletion, while it was

decreased after knock-down of EVI/WLS (Figure 25). Therefore, my data does not indicate that EVI/WLS would regulate melanoma invasiveness through β-catenin, as it was suggested by a previous study (P.-T. Yang et al., 2012). There are model and cell line specific differences to be considered, such as the variable expression status of WNT receptors in different melanoma cell lines, and more experiments are needed to clarify the correlations.

5.4.4 EVI/WLS and WNT11 induce phenotype switching in melanoma cells

The knock-down of EVI/WLS or WNT11 induced a profound decrease in proliferation of WM793 cells compared to transfection of all other siRNAs (Figure 25E). Together with the increased gelatin degradation observed upon silencing of EVI/WLS or WNT11 (Figure 25A,B;C), this shows that EVI/WLS and WNT11 protein levels can induce switching between a more proliferative and a more invasive phenotype in these cells. Phenotype switching is an important feature of melanoma cells that has emerged as crucial regulator of tumour progression and metastasis (Rambow et al., 2019). While it resembles processes involved in epithelial-to-mesenchymal transition, it is called differently because melanocytes are not epithelial (Rambow et al., 2019). This change in phenotypic characteristics of melanoma cells due to external cues, e.g. hypoxia, is primarily associated with varying expression levels of *MITF*, a key transcriptional regulator in melanocytes (Hoek et al., 2006; Kawakami & Fisher, 2017; Michael P. O'Connell et al., 2013; Rambow et al., 2019). *MITF* is not only transcriptionally regulated by WNT/β-catenin signalling, but MITF can also interact with β-catenin to induce transcription of target genes (Gajos-Michniewicz & Czyz, 2020). Furthermore, canonical/β-catenin-dependent signalling by WNT3A was shown to stabilise MITF post-translationally *via* the inhibition of its phosphorylation by GSK3 and the WNT/STOP pathway (Ploper et al., 2015). Conversely, expression of *MITF* and its target genes is downregulated by WNT5A and they are, accordingly, less expressed in melanoma cells with an invasive phenotype and high *WNT5A* expression (Dissanayake et al., 2008; Hoek et al., 2008, 2006; Widmer et al., 2012). Albeit my data and previous work by others demonstrate an important contribution, it remains largely unknown how WNT11, EVI/WLS, and WNT secretion are tied to this intricate signalling network.

A recent review of the existing data on phenotypic plasticity in melanoma suggests that the current model should be revised to include many more intermediate stages between the 'proliferative – MITF high' and 'invasive – MITF low' state (Rambow et al., 2019). These intermediate states most likely do not represent cells that are transitioning between stages but have distinct and probably stable phenotypes. It is likely that many of these states exist in parallel and exert different functions *in-vivo*, for example one could envision that one subpopulation is

more proliferative, while another is prone to metastasise, and a third primarily regulates the tumour microenvironment. However, this complexity cannot be reflected by single cell lines, hence, it will be exciting to further disentangle the WNT-dependent effects on phenotypic diversity of melanoma cells. The multi-layered reciprocal regulation of MITF-dependent transcriptional networks and WNT signalling suggests melanocyte lineage-specific, dynamic genetic interactions (Billmann et al., 2018; Rauscher et al., 2019). In the future, it will be important to further disentangle this intricate network by analysing melanoma subpopulations in combination with genetic perturbations of WNT signalling effectors in multiple cellular models, potentially using single-cell sequencing approaches.

5.4.5 MAPK signalling cooperates with WNT signalling

Melanoma tumorigenesis is mainly associated with an overactivation of the MAPK signalling pathway and the most common driver mutations affect BRAF p.V600 and NRAS p.Q61 (Hodis et al., 2012). The BRAF p.V600E mutation was found to promote invadopodia formation and invasion in melanoma cells (H. Lu et al., 2016). Notably, melanoma cells with an invasive, WNT5A-associated phenotype show decreased sensitivity to BRAF inhibitors and a high expression of WNT5A correlated with reduced clinical response in melanoma patients treated with the BRAF inhibitor vemurafenib (Anastas et al., 2014; Michael P. O'Connell et al., 2013). Diverse interactions of the MAPK and WNT/β-catenin signalling pathways in melanoma have been described, which most likely depend on tumour stage and genetic background of the samples (Gajos-Michniewicz & Czyz, 2020; Zhan et al., 2017). In colorectal cancer, MEK1/2 inhibition downstream of BRAF induced canonical WNT signalling and stem cell plasticity (Zhan et al., 2019), underlining the cooperation of both pathways in other tumour entities as well.

This data shows how important it is to consider the interactions between different signalling pathways, especially in a tumour as heterogenous and adaptable as melanoma. Detailed and comprehensive understanding of the underlying characteristics of the cancer genome and posttranslational regulatory mechanisms are required for the development of novel treatment approaches and they can pave the way for combinatorial therapies. Accordingly, it is important to extend the insights gained in this thesis by additional studies, not only focusing on WNT but especially on the interactions of WNT signalling with other pathways. However, since these kind of experiments with potentially hundreds of conditions are difficult to perform *in-vivo*, adapting the gelatin degradation assay to fit a large-scale, plate-based format with an automated analysis pipeline might contribute to perform genetic interaction screens with a functional read-out *in-vitro* (Quintavalle et al., 2011).

5. 5 Conclusions and future perspectives

The regulation of protein abundance is a major effect of signal transduction pathways and important for cellular homeostasis. Various diseases are associated with uncontrolled protein synthesis or degradation, among them many cancers. Several components of the WNT signalling pathways are known to be post-translationally regulated with important consequences for development and tumourigenesis (Zhan et al., 2017).

Here, I investigated how the ER-membrane associated protein EVI/WLS, a crucial mediator of WNT ligand secretion, is ubiquitinated and delivered to the proteasome. Based on my data, I propose a model wherein EVI/WLS interacts with ERLIN2 before it is ubiquitinated by UBE2K and UBE2N, as well as by UBE2J2 and CGRRF1. Then, the ER-membrane anchored proteins FAF2 and UBXN4 bind to ubiquitinated EVI/WLS and recruit the cytosolic ATPase VCP to the ER-membrane. FAF2 and UBXN4 support VCP during the membrane extraction of EVI/WLS before it is targeted to the proteasome for degradation (Figure 29).

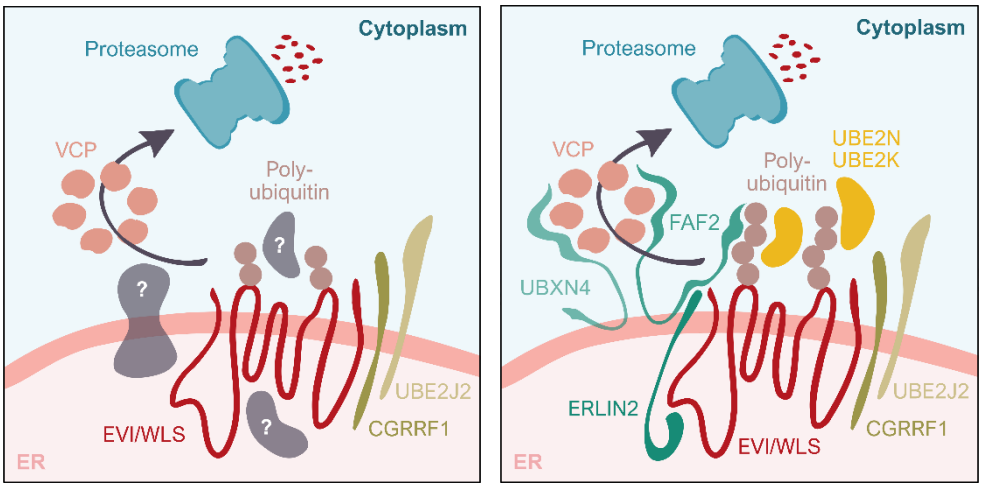

Figure 29. Summary of the ubiquitination and degradation of EVI/WLS

It was known previously that EVI/WLS is ubiquitinated by UBE2J2 and CGRRF1 and extracted from the endoplasmic reticulum (ER) membrane with the help of VCP (left). My thesis provided evidence that ERLIN2 is an important link between EVI/WLS and other ERAD components and potentially helps to recruit the ubiquitination machinery, consisting at least of UBE2K, UBE2N, UBE2J2, and CGRRF1. Poly-ubiquitinated EVI/WLS interacts with FAF2 and UBXN4, which recruit VCP to the ER membrane, resulting in the dislocation and eventually the proteasomal degradation of EVI/WLS.

A better understanding of these processes helps to gain insights into how the degradation of mature, properly folded ER-associated proteins can be achieved in general in human cells. In the future, it will be important to correlate these findings to substrates of regulatory ERAD in other signalling pathways, for example EGFR, which is also ubiquitinated by CGRRF1 (Y.-J. Lee et al., 2019). It is likely that some regulators of EVI/WLS protein stability are still undiscovered and an unbiased, genome-wide screen could not only shed light on the processes involved in EVI/WLS degradation, but potentially also discover novel, hitherto unknown

mediators of ERAD. Furthermore, questions regarding the sites of EVI/WLS ubiquitination, the presence of branched Ub chains, or non-lysine ubiquitination remain open and further studies using mass spectrometry-based approaches will be needed to address them. Using these techniques, it might be possible to discover additional Ub-like proteins that are involved in the post-translational regulation of EVI/WLS. These insights will not only lead to a better understanding of the posttranslational regulation of EVI/WLS abundance, and thus WNT signalling itself, but will be important to develop novel treatment options for WNT-related diseases.

EVI/WLS protein levels are dysregulated in human malignancies, for example in colorectal cancer or cutaneous melanoma (Glaeser et al., 2018; P.-T. Yang et al., 2012), and it is necessary to better understand its relation to tumour progression. Hence, it is important to further examine the role of its 'destruction complex' in cancer and cellular invasiveness. As a first step, the gelatin degradation assay could be used to analyse the effects of knock-down of ERLIN2, FAF2, UBXN4, UBE2K, and UBE2N on the invasive potential of melanoma cells. Later, it will be important to extend insights generated in this thesis and by others to other cancer entities and to non-malignant settings to investigate how well the processes are conserved between tissues and other organisms. It will also be necessary to conclusively clarify to what extend ubiquitination of EVI/WLS regulates WNT ligand secretion in different systems and if this affects canonical or non-canonical WNT ligands differently.

To better understand how EVI/WLS and other WNT signalling components affect melanoma cell invasiveness, I used the gelatin degradation assay as an *in-vitro* tool to visualise cellular proteolytic activity. Thus, I provided evidence in melanoma cells that EVI/WLS and WNT11 are involved in the remodelling of the microenvironment. Since my data indicate opposite effects of the two non-canonical WNT ligands WNT5A and WNT11 in melanoma pathology, epistasis experiment should be performed to elucidate the connection between the observed phenotypes and possibly also to examine how they are linked to MITF expression and phenotype switching. If the effect of WNT11 can be validated in these studies, it will be important to use animal models to further analyse how it influences melanoma malignancy *in-vivo* and the expression of WNT11 should be better characterised in patient samples. Here, it will be important to consider the presence of multiple tumour cell subpopulations, as WNT11 might only be relevant for some of them. In this case, single cell sequencing techniques will help to disentangle WNT11 producing and receiving cells.

In this context, the lipidation independent secretion of WNT11 from melanoma cells that I observed is of upmost importance and it is necessary to further characterise the mechanisms of PORCN and EVI/WLS-independent WNT ligand processing. It will be interesting to elucidate

the mechanism of this alternative secretion route, to investigate how well it is conserved across organisms, and how it influences the function of WNT ligands. These analyses will also further the understanding of how posttranslational regulation influences the WNT signalling pathways. Importantly, many compounds targeting WNT signalling in clinical trials affect the classical WNT secretion route. It should be clarified if this treatment could potentially aggravate melanoma cell invasiveness by promoting the PORCN or EVI/WLS-independent secretion of WNT ligands with potentially carcinogenic potential.

In conclusion, EVI/WLS is a substrate of ERAD in cells with and without endogenous WNT ligand expression and its ubiquitination is potentially important for WNT ligand secretion. EVI/WLS abundance also regulates many human diseases. In the future, it will be important to better characterise the underlying processes and relate them to cancer progression and potential treatment options.

6 References

6.1 Literature

Aberle, H.; Bauer, A.; Stappert, J.; Kispert, A.; & Kemler, R. (1997). **Beta-catenin is a target for the ubiquitin-proteasome pathway.** *The EMBO Journal*, *16*(13), 3797–3804. PMID: 9233789.

Acebron, S. P.; & Niehrs, C. (2016). **β-Catenin-Independent Roles of Wnt/LRP6 Signaling**. *Trends in Cell Biology*, *26*(12), 956–967. PMID: 27568239.

Afzal, A. R.; Rajab, A.; Fenske, C. D.; Oldridge, M.; Elanko, N.; Ternes-Pereira, E.; Tüysüz, B.; Murday, V. A.; Patton, M. A.; Wilkie, A. O.; & Jeffery, S. (2000). **Recessive Robinow syndrome, allelic to dominant brachydactyly type B, is caused by mutation of ROR2**. *Nature Genetics*, *25*(4), 419–422. PMID: 10932186.

Akutsu, M.; Dikic, I.; & Bremm, A. (2016). **Ubiquitin chain diversity at a glance**. *Journal of Cell Science*, *129*(5), 875–880. PMID: 26906419.

Alberts, B.; Johnson, A.; Lewis, J.; Roberts, K.; Raff, M.; & Walter, P. (2008). ***Molecular Biology of the Cell*** (5th ed.). Garland Science.

Alexandre, C.; Baena-Lopez, A.; & Vincent, J.-P. (2014). **Patterning and growth control by membrane-tethered Wingless**. *Nature*, *505*(7482), 180–185.

Alexandrov, L. B.; Nik-Zainal, S.; Wedge, D. C.; Aparicio, S. A. J. R.; Behjati, S.; Biankin, A. V.; Bignell, G. R.; Bolli, N.; Borg, A.; Børresen-Dale, A.-L.; Boyault, S.; Burkhardt, B.; Butler, A. P.; Caldas, C.; Davies, H. R.; Desmedt, C.; Eils, R.; Eyfjörd, J. E.; Foekens, J. A.; … Stratton, M. R. (2013). **Signatures of mutational processes in human cancer**. *Nature*, *500*(7463), 415–421. PMID: 23945592.

Anastas, J. N.; Kulikauskas, R. M.; Tamir, T.; Rizos, H.; Long, G. V.; von Euw, E. M.; Yang, P.-T.; Chen, H.-W.; Haydu, L.; Toroni, R. A.; Lucero, O. M.; Chien, A. J.; & Moon, R. T. (2014). **WNT5A enhances resistance of melanoma cells to targeted BRAF inhibitors**. *The Journal of Clinical Investigation*, *124*(7), 2877–2890. PMID: 24865425.

Andersen, P. L.; Zhou, H.; Pastushok, L.; Moraes, T.; McKenna, S.; Ziola, B.; Ellison, M. J.; Dixit, V. M.; & Xiao, W. (2005). **Distinct regulation of Ubc13 functions by the two ubiquitin-conjugating enzyme variants Mms2 and Uev1A**. *The Journal of Cell Biology*, *170*(5), 745–755. PMID: 16129784.

Augustin, I.; Dewi, D. L.; Hundshammer, J.; Rempel, E.; Brunk, F.; & Boutros, M. (2016). **Immune cell recruitment in teratomas is impaired by increased Wnt secretion**. *Stem Cell Research*, *17*(3), 607–615. PMID: 27838585.

Augustin, I.; Goidts, V.; Bongers, A.; Kerr, G.; Vollert, G.; Radlwimmer, B.; Hartmann, C.; Herold-Mende, C.; Reifenberger, G.; von Deimling, A.; & Boutros, M. (2012). **The Wnt secretion protein Evi/Gpr177 promotes glioma tumourigenesis**. *EMBO Molecular Medicine*, *4*(1), 38–51. PMID: 22147553.

Avci, D.; Malchus, N. S.; Heidasch, R.; Lorenz, H.; Richter, K.; Neßling, M.; & Lemberg, M. K. (2019). **The intramembrane protease SPP impacts morphology of the endoplasmic**

reticulum by triggering degradation of morphogenic proteins. *The Journal of Biological Chemistry*, *294*(8), 2786–2800. PMID: 30578301.

Baek, K.; Krist, D. T.; Prabu, J. R.; Hill, S.; Klügel, M.; Neumaier, L.-M.; von Gronau, S.; Kleiger, G.; & Schulman, B. A. (2020). **NEDD8 nucleates a multivalent cullin-RING-UBE2D ubiquitin ligation assembly**. *Nature*, *578*(7795), 461–466. PMID: 32051583.

Baker, C. V.; Bronner-Fraser, M.; Le Douarin, N. M.; & Teillet, M. A. (1997). **Early- and late-migrating cranial neural crest cell populations have equivalent developmental potential in vivo**. *Development (Cambridge, England)*, *124*(16), 3077–3087. PMID: 9272949.

Bänziger, C.; Soldini, D.; Schütt, C.; Zipperlen, P.; Hausmann, G.; & Basler, K. (2006). **Wntless, a conserved membrane protein dedicated to the secretion of Wnt proteins from signaling cells**. *Cell*, *125*(3), 509–522. PMID: 16678095.

Bartscherer, K.; Pelte, N.; Ingelfinger, D.; & Boutros, M. (2006). **Secretion of Wnt ligands requires Evi, a conserved transmembrane protein**. *Cell*, *125*(3), 523–533. PMID: 16678096.

Barysch, S. V.; Stankovic-Valentin, N.; Karaca, S.; Doppel, J.; Nait Achour, T.; Sticht, C.; Urlaub, H.; & Melchior, F. (2019). **Transient deSUMOylation of IRF2BP proteins controls early transcription in EGFR signaling**. *BioRxiv*, 819730.

Behrens, J.; Jerchow, B.-A.; Würtele, M.; Grimm, J.; Asbrand, C.; Wirtz, R.; Kühl, M.; Wedlich, D.; & Birchmeier, W. (1998). **Functional Interaction of an Axin Homolog, Conductin, with β-Catenin, APC, and GSK3β**. *Science*, *280*(5363), 596–599. PMID: 9554852.

Behrens, J.; von Kries, J. P.; Kühl, M.; Bruhn, L.; Wedlich, D.; Grosschedl, R.; & Birchmeier, W. (1996). **Functional interaction of beta-catenin with the transcription factor LEF-1**. *Nature*, *382*(6592), 638–642. PMID: 8757136.

Belenkaya, T. Y.; Wu, Y.; Tang, X.; Zhou, B.; Cheng, L.; Sharma, Y. V.; Yan, D.; Selva, E. M.; & Lin, X. (2008). **The retromer complex influences Wnt secretion by recycling wntless from endosomes to the trans-Golgi network**. *Developmental Cell*, *14*(1), 120–131. PMID: 18160348.

Berridge, M. J. (2016). **The Inositol Trisphosphate/Calcium Signaling Pathway in Health and Disease**. *Physiological Reviews*, *96*(4), 1261–1296. PMID: 27512009.

Bersuker, K.; Peterson, C. W. H.; To, M.; Sahl, S. J.; Savikhin, V.; Grossman, E. A.; Nomura, D. K.; & Olzmann, J. A. (2018). **A Proximity Labeling Strategy Provides Insights into the Composition and Dynamics of Lipid Droplet Proteomes**. *Developmental Cell*, *44*(1), 97-112.e7.

Bhattacharya, A.; & Qi, L. (2019). **ER-associated degradation in health and disease – from substrate to organism**. *Journal of Cell Science*, *132*(23). PMID: 31792042.

Billmann, M.; Chaudhary, V.; ElMaghraby, M. F.; Fischer, B.; & Boutros, M. (2018). **Widespread Rewiring of Genetic Networks upon Cancer Signaling Pathway Activation**. *Cell Systems*, *6*(1), 52-64.e4. PMID: 29199019.

Bloethner, S.; Chen, B.; Hemminki, K.; Müller-Berghaus, J.; Ugurel, S.; Schadendorf, D.; & Kumar, R. (2005). **Effect of common B-RAF and N-RAS mutations on global gene expression in melanoma cell lines**. *Carcinogenesis*, *26*(7), 1224–1232.

Bodnar, N.; & Rapoport, T. (2017). **Toward an understanding of the Cdc48/p97 ATPase**. *F1000Research*, *6*. PMID: 28815021.

Boname, J. M.; Bloor, S.; Wandel, M. P.; Nathan, J. A.; Antrobus, R.; Dingwell, K. S.; Thurston, T. L.; Smith, D. L.; Smith, J. C.; Randow, F.; & Lehner, P. J. (2014). **Cleavage by signal peptide peptidase is required for the degradation of selected tail-anchored proteins**. *The Journal of Cell Biology*, *205*(6), 847–862. PMID: 24958774.

Boutros, M.; Paricio, N.; Strutt, D. I.; & Mlodzik, M. (1998). **Dishevelled activates JNK and discriminates between JNK pathways in planar polarity and wingless signaling**. *Cell*, *94*(1), 109–118. PMID: 9674432.

Branigan, E.; Carlos Penedo, J.; & Hay, R. T. (2020). **Ubiquitin transfer by a RING E3 ligase occurs from a closed E2~ubiquitin conformation**. *Nature Communications*, *11*(1), 2846.

Briscoe, J.; & Small, S. (2015). **Morphogen rules: Design principles of gradient-mediated embryo patterning**. *Development (Cambridge, England)*, *142*(23), 3996–4009. PMID: 26628090.

Browman, D. T.; Resek, M. E.; Zajchowski, L. D.; & Robbins, S. M. (2006). **Erlin-1 and erlin-2 are novel members of the prohibitin family of proteins that define lipid-raft-like domains of the ER**. *Journal of Cell Science*, *119*(Pt 15), 3149–3160. PMID: 16835267.

Buechling, T.; Chaudhary, V.; Spirohn, K.; Weiss, M.; & Boutros, M. (2011). **P24 proteins are required for secretion of Wnt ligands**. *EMBO Reports*, *12*(12), 1265–1272. PMID: 22094269.

Burr, M. L.; van den Boomen, D. J. H.; Bye, H.; Antrobus, R.; Wiertz, E. J.; & Lehner, P. J. (2013). **MHC class I molecules are preferentially ubiquitinated on endoplasmic reticulum luminal residues during HRD1 ubiquitin E3 ligase-mediated dislocation**. *Proceedings of the National Academy of Sciences of the United States of America*, *110*(35), 14290–14295. PMID: 23929775.

Burton, J. C.; & Grimsey, N. J. (2019). **Ubiquitination as a Key Regulator of Endosomal Signaling by GPCRs**. *Frontiers in Cell and Developmental Biology*, *7*.

Bustin, S. A.; Benes, V.; Garson, J. A.; Hellemans, J.; Huggett, J.; Kubista, M.; Mueller, R.; Nolan, T.; Pfaffl, M. W.; Shipley, G. L.; Vandesompele, J.; & Wittwer, C. T. (2009). **The MIQE guidelines: Minimum information for publication of quantitative real-time PCR experiments**. *Clinical Chemistry*, *55*(4), 611–622. PMID: 19246619.

Cadwell, K.; & Coscoy, L. (2005). **Ubiquitination on nonlysine residues by a viral E3 ubiquitin ligase**. *Science (New York, N.Y.)*, *309*(5731), 127–130. PMID: 15994556.

Carlson, E. J.; Pitonzo, D.; & Skach, W. R. (2006). **P97 functions as an auxiliary factor to facilitate TM domain extraction during CFTR ER-associated degradation**. *The EMBO Journal*, *25*(19), 4557–4566. PMID: 16977321.

Carpenter, A. C.; Rao, S.; Wells, J. M.; Campbell, K.; & Lang, R. A. (2010). **Generation of mice with a conditional null allele for Wntless**. *Genesis*, *48*(9), 554–558.

Carraway, K. L. (2010). **E3 Ubiquitin Ligases in ErbB Receptor Quantity Control**. *Seminars in Cell & Developmental Biology*, *21*(9), 936–943. PMID: 20868762.

Carreira, S.; Goodall, J.; Denat, L.; Rodriguez, M.; Nuciforo, P.; Hoek, K. S.; Testori, A.; Larue, L.; & Goding, C. R. (2006). **Mitf regulation of Dia1 controls melanoma proliferation and invasiveness**. *Genes & Development*, *20*(24), 3426–3439. PMID: 17182868.

Carvalho, J. R.; Fortunato, I. C.; Fonseca, C. G.; Pezzarossa, A.; Barbacena, P.; Dominguez-Cejudo, M. A.; Vasconcelos, F. F.; Santos, N. C.; Carvalho, F. A.; & Franco, C. A. (2019).

Non-canonical Wnt signaling regulates junctional mechanocoupling during angiogenic collective cell migration. *ELife*, *8*, e45853.

Cavallo, R. A.; Cox, R. T.; Moline, M. M.; Roose, J.; Polevoy, G. A.; Clevers, H.; Peifer, M.; & Bejsovec, A. (1998). **Drosophila Tcf and Groucho interact to repress Wingless signalling activity**. *Nature*, *395*(6702), 604–608. PMID: 9783586.

Cha, J.-H.; Yang, W.-H.; Xia, W.; Wei, Y.; Chan, L.-C.; Lim, S.-O.; Li, C.-W.; Kim, T.; Chang, S.-S.; Lee, H.-H.; Hsu, J. L.; Wang, H.-L.; Kuo, C.-W.; Chang, W.-C.; Hadad, S.; Purdie, C. A.; McCoy, A. M.; Cai, S.; Tu, Y.; … Hung, M.-C. (2018). **Metformin promotes antitumor immunity via endoplasmic reticulum-associated degradation of PD-L1**. *Molecular Cell*, *71*(4), 606-620.e7. PMID: 30118680.

Chen, R.-H.; Chen, Y.-H.; & Huang, T.-Y. (2019). **Ubiquitin-mediated regulation of autophagy**. *Journal of Biomedical Science*, *26*(1), 80.

Chen, Z.; & Pickart, C. M. (1990). **A 25-kilodalton ubiquitin carrier protein (E2) catalyzes multi-ubiquitin chain synthesis via lysine 48 of ubiquitin**. *The Journal of Biological Chemistry*, *265*(35), 21835–21842. PMID: 2174887.

Chien, A. J.; Moore, E. C.; Lonsdorf, A. S.; Kulikauskas, R. M.; Rothberg, B. G.; Berger, A. J.; Major, M. B.; Hwang, S. T.; Rimm, D. L.; & Moon, R. T. (2009). **Activated Wnt/ß-catenin signaling in melanoma is associated with decreased proliferation in patient tumors and a murine melanoma model**. *Proceedings of the National Academy of Sciences of the United States of America*, *106*(4), 1193–1198. PMID: 19144919.

Ching, W.; Hang, H. C.; & Nusse, R. (2008). **Lipid-independent secretion of a Drosophila Wnt protein**. *The Journal of Biological Chemistry*, *283*(25), 17092–17098. PMID: 18430724.

Christianson, J. C.; Olzmann, J. A.; Shaler, T. A.; Sowa, M. E.; Bennett, E. J.; Richter, C. M.; Tyler, R. E.; Greenblatt, E. J.; Wade Harper, J.; & Kopito, R. R. (2012). **Defining human ERAD networks through an integrative mapping strategy**. *Nature Cell Biology*, *14*(1), 93–105.

Christianson, J. C.; Shaler, T. A.; Tyler, R. E.; & Kopito, R. R. (2008). **OS-9 and GRP94 deliver mutant alpha1-antitrypsin to the Hrd1-SEL1L ubiquitin ligase complex for ERAD**. *Nature Cell Biology*, *10*(3), 272–282. PMID: 18264092.

Christianson, J. C.; & Ye, Y. (2014). **Cleaning up in the endoplasmic reticulum: Ubiquitin in charge**. *Nature Structural & Molecular Biology*, *21*(4), 325–335. PMID: 24699081.

Ciechanover, A.; Finley, D.; & Varshavsky, A. (1984). **The ubiquitin-mediated proteolytic pathway and mechanisms of energy-dependent intracellular protein degradation**. *Journal of Cellular Biochemistry*, *24*(1), 27–53. PMID: 6327743.

Ciechanover, A.; Heller, H.; Elias, S.; Haas, A. L.; & Hershko, A. (1980). **ATP-dependent conjugation of reticulocyte proteins with the polypeptide required for protein degradation**. *Proceedings of the National Academy of Sciences of the United States of America*, *77*(3), 1365–1368. PMID: 6769112.

Ciechanover, A.; Heller, H.; Katz-Etzion, R.; & Hershko, A. (1981). **Activation of the heat-stable polypeptide of the ATP-dependent proteolytic system**. *Proceedings of the National Academy of Sciences*, *78*(2), 761.

Ciechanover, A.; Hod, Y.; & Hershko, A. (1978). **A heat-stable polypeptide component of an ATP-dependent proteolytic system from reticulocytes.** *Biochemical and Biophysical Research Communications*, *425*(3), 565–570. PMID: 22925675.

Clague, M. J.; Heride, C.; & Urbé, S. (2015). **The demographics of the ubiquitin system**. *Trends in Cell Biology*, *25*(7), 417–426.

Clague, M. J.; Urbé, S.; & Komander, D. (2019). **Breaking the chains: Deubiquitylating enzyme specificity begets function**. *Nature Reviews Molecular Cell Biology*, *20*(6), 338–352.

Clark, E. S.; & Weaver, A. M. (2008). **A new role for cortactin in invadopodia: Regulation of protease secretion**. *European Journal of Cell Biology*, *87*(8), 581–590.

Coombs, G. S.; Yu, J.; Canning, C. A.; Veltri, C. A.; Covey, T. M.; Cheong, J. K.; Utomo, V.; Banerjee, N.; Zhang, Z. H.; Jadulco, R. C.; Concepcion, G. P.; Bugni, T. S.; Harper, M. K.; Mihalek, I.; Jones, C. M.; Ireland, C. M.; & Virshup, D. M. (2010). **WLS-dependent secretion of WNT3A requires Ser209 acylation and vacuolar acidification**. *Journal of Cell Science*, *123*(19), 3357–3367. PMID: 20826466.

Cormier, J. H.; Tamura, T.; Sunryd, J. C.; & Hebert, D. N. (2009). **EDEM1 recognition and delivery of misfolded proteins to the SEL1L-containing ERAD complex**. *Molecular Cell*, *34*(5), 627–633. PMID: 19524542.

Cornett, B.; Snowball, J.; Varisco, B. M.; Lang, R.; Whitsett, J.; & Sinner, D. (2013). **WNTLESS IS REQUIRED FOR PERIPHERAL LUNG DIFFERENTIATION AND PULMONARY VASCULAR DEVELOPMENT**. *Developmental Biology*, *379*(1), 38–52. PMID: 23523683.

Cullen, P. J.; & Steinberg, F. (2018). **To degrade or not to degrade: Mechanisms and significance of endocytic recycling**. *Nature Reviews Molecular Cell Biology*, *19*(11), 679–696.

Damsky, W. E.; Curley, D. P.; Santhanakrishnan, M.; Rosenbaum, L. E.; Platt, J. T.; Gould Rothberg, B. E.; Taketo, M. M.; Dankort, D.; Rimm, D. L.; McMahon, M.; & Bosenberg, M. (2011). **β-catenin signaling controls metastasis in Braf-activated Pten-deficient melanomas**. *Cancer Cell*, *20*(6), 741–754. PMID: 22172720.

Daniels, R.; Kurowski, B.; Johnson, A. E.; & Hebert, D. N. (2003). **N-Linked Glycans Direct the Cotranslational Folding Pathway of Influenza Hemagglutinin**. *Molecular Cell*, *11*(1), 79–90. PMID: 12535523.

Das, S.; Yu, S.; Sakamori, R.; Stypulkowski, E.; & Gao, N. (2012). **Wntless in Wnt secretion: Molecular, cellular and genetic aspects**. *Frontiers in Biology*, *7*(6), 587–593. PMID: 23439944.

Das, S.; Yu, S.; Sakamori, R.; Vedula, P.; Feng, Q.; Flores, J.; Hoffman, A.; Fu, J.; Stypulkowski, E.; Rodriguez, A.; Dobrowolski, R.; Harada, A.; Hsu, W.; Bonder, E. M.; Verzi, M. P.; & Gao, N. (2015). **Rab8a vesicles regulate Wnt ligand delivery and Paneth cell maturation at the intestinal stem cell niche**. *Development (Cambridge, England)*, *142*(12), 2147–2162. PMID: 26015543.

Davidson, G.; Wu, W.; Shen, J.; Bilic, J.; Fenger, U.; Stannek, P.; Glinka, A.; & Niehrs, C. (2005). **Casein kinase 1 γ couples Wnt receptor activation to cytoplasmic signal transduction**. *Nature*, *438*(7069), 867–872.

De Calisto, J.; Araya, C.; Marchant, L.; Riaz, C. F.; & Mayor, R. (2005). **Essential role of non-canonical Wnt signalling in neural crest migration**. *Development (Cambridge, England)*, *132*(11), 2587–2597. PMID: 15857909.

de Duve, C.; Pressman, B. C.; Gianetto, R.; Wattiaux, R.; & Appelmans, F. (1955). **Tissue fractionation studies. 6. Intracellular distribution patterns of enzymes in rat-liver tissue**. *Biochemical Journal*, *60*(4), 604–617. PMID: 13249955.

de Groot, R. E. A.; Rappel, S. B.; Lorenowicz, M. J.; & Korswagen, H. C. (2014). **Protein kinase CK2 is required for Wntless internalization and Wnt secretion**. *Cellular Signalling*, *26*(12), 2601–2605. PMID: 25178265.

Deng, L.; Meng, T.; Chen, L.; Wei, W.; & Wang, P. (2020). **The role of ubiquitination in tumorigenesis and targeted drug discovery**. *Signal Transduction and Targeted Therapy*, *5*(1), 1–28.

Deol, K. K.; Lorenz, S.; & Strieter, E. R. (2019). **Enzymatic Logic of Ubiquitin Chain Assembly**. *Frontiers in Physiology*, *10*.

Dikic, I. (2017). **Proteasomal and Autophagic Degradation Systems**. *Annual Review of Biochemistry*, *86*(1), 193–224. PMID: 28460188.

Dikic, I.; & Elazar, Z. (2018). **Mechanism and medical implications of mammalian autophagy**. *Nature Reviews Molecular Cell Biology*, *19*(6), 349–364.

Dikic, I.; Wakatsuki, S.; & Walters, K. J. (2009). **Ubiquitin-binding domains—From structures to functions**. *Nature Reviews. Molecular Cell Biology*, *10*(10), 659–671. PMID: 19773779.

Dissanayake, S. K.; Olkhanud, P. B.; O'Connell, M. P.; Carter, A.; French, A. D.; Camilli, T. C.; Emeche, C. D.; Hewitt, K. J.; Rosenthal, D. T.; Leotlela, P. D.; Wade, M. S.; Yang, S. W.; Brant, L.; Nickoloff, B. J.; Messina, J. L.; Biragyn, A.; Hoek, K. S.; Taub, D. D.; Longo, D. L.; … Weeraratna, A. T. (2008). **Wnt5A regulates expression of tumor-associated antigens in melanoma via changes in signal transducers and activators of transcription 3 phosphorylation**. *Cancer Research*, *68*(24), 10205–10214. PMID: 19074888.

Edgar, J. R. (2016). **Q&A: What are exosomes, exactly?** *BMC Biology*, *14*. PMID: 27296830.

Ekström, E. J.; Bergenfelz, C.; von Bülow, V.; Serifler, F.; Carlemalm, E.; Jönsson, G.; Andersson, T.; & Leandersson, K. (2014). **WNT5A induces release of exosomes containing pro-angiogenic and immunosuppressive factors from malignant melanoma cells**. *Molecular Cancer*, *13*, 88. PMID: 24766647.

Enomoto, M.; Hayakawa, S.; Itsukushima, S.; Ren, D. Y.; Matsuo, M.; Tamada, K.; Oneyama, C.; Okada, M.; Takumi, T.; Nishita, M.; & Minami, Y. (2009). **Autonomous regulation of osteosarcoma cell invasiveness by Wnt5a/Ror2 signaling**. *Oncogene*, *28*(36), 3197–3208. PMID: 19561643.

Erpapazoglou, Z.; Walker, O.; & Haguenauer-Tsapis, R. (2014). **Versatile Roles of K63-Linked Ubiquitin Chains in Trafficking**. *Cells*, *3*(4), 1027–1088. PMID: 25396681.

Etlinger, J. D.; & Goldberg, A. L. (1977). **A soluble ATP-dependent proteolytic system responsible for the degradation of abnormal proteins in reticulocytes**. *Proceedings of the National Academy of Sciences of the United States of America*, *74*(1), 54–58. PMID: 264694.

Ewen-Campen, B.; Comny, T.; & Perrimon, N. (2020). **Wnt ligands are not required for planar cell polarity in the Drosophila wing or notum**. *BioRxiv*, 2020.06.05.137182.

Farin, H. F.; Jordens, I.; Mosa, M. H.; Basak, O.; Korving, J.; Tauriello, D. V. F.; de Punder, K.; Angers, S.; Peters, P. J.; Maurice, M. M.; & Clevers, H. (2016). **Visualization of a short-**

range Wnt gradient in the intestinal stem-cell niche. *Nature*, *530*(7590), 340–343. PMID: 26863187.

Feige, M. J.; & Hendershot, L. M. (2013). **Quality Control of Integral Membrane Proteins by Assembly-dependent Membrane Integration**. *Molecular Cell*, *51*(3), 297–309. PMID: 23932713.

Fenech, E. J.; Lari, F.; Charles, P. D.; Fischer, R.; Laétitia-Thézénas, M.; Bagola, K.; Paton, A. W.; Paton, J. C.; Gyrd-Hansen, M.; Kessler, B. M.; & Christianson, J. C. (2020). **Interaction mapping of endoplasmic reticulum ubiquitin ligases identifies modulators of innate immune signalling**. *ELife*, *9*, e57306.

Fiedler, M.; Mendoza-Topaz, C.; Rutherford, T. J.; Mieszczanek, J.; & Bienz, M. (2011). **Dishevelled interacts with the DIX domain polymerization interface of Axin to interfere with its function in down-regulating β-catenin**. *Proceedings of the National Academy of Sciences of the United States of America*, *108*(5), 1937–1942. PMID: 21245303.

Fleig, L.; Bergbold, N.; Sahasrabudhe, P.; Geiger, B.; Kaltak, L.; & Lemberg, M. K. (2012). **Ubiquitin-Dependent Intramembrane Rhomboid Protease Promotes ERAD of Membrane Proteins**. *Molecular Cell*, *47*(4), 558–569.

Forno, P. D. D.; Pringle, J. H.; Hutchinson, P.; Osborn, J.; Huang, Q.; Potter, L.; Hancox, R. A.; Fletcher, A.; & Saldanha, G. S. (2008). **WNT5A Expression Increases during Melanoma Progression and Correlates with Outcome**. *Clinical Cancer Research*, *14*(18), 5825–5832. PMID: 18794093.

Franch-Marro, X.; Wendler, F.; Guidato, S.; Griffith, J.; Baena-Lopez, A.; Itasaki, N.; Maurice, M. M.; & Vincent, J.-P. (2008). **Wingless secretion requires endosome-to-Golgi retrieval of Wntless/Evi/Sprinter by the retromer complex**. *Nature Cell Biology*, *10*(2), 170–177. PMID: 18193037.

Frankel, E. B.; & Audhya, A. (2018). **ESCRT-dependent cargo sorting at multivesicular endosomes**. *Seminars in Cell & Developmental Biology*, *74*, 4–10. PMID: 28797838.

Fregno, I.; & Molinari, M. (2019). **Proteasomal and lysosomal clearance of faulty secretory proteins: ER-associated degradation (ERAD) and ER-to-lysosome-associated degradation (ERLAD) pathways**. *Critical Reviews in Biochemistry and Molecular Biology*, *54*(2), 153–163. PMID: 31084437.

Fu, J.; Jiang, M.; Mirando, A. J.; Yu, H.-M. I.; & Hsu, W. (2009). **Reciprocal regulation of Wnt and Gpr177/mouse Wntless is required for embryonic axis formation**. *Proceedings of the National Academy of Sciences of the United States of America*, *106*(44), 18598–18603. PMID: 19841259.

Gajos-Michniewicz, A.; & Czyz, M. (2020). **WNT Signaling in Melanoma**. *International Journal of Molecular Sciences*, *21*(14), 4852.

Galli, L. M.; Szabo, L. A.; Li, L.; Htaik, Y. M.; Onguka, O.; & Burrus, L. W. (2014). **Concentration-dependent effects of WNTLESS on WNT1/3A signaling**. *Developmental Dynamics : An Official Publication of the American Association of Anatomists*, *243*(9), 1095–1105. PMID: 24866848.

Galli, L. M.; Zebarjadi, N.; Li, L.; Lingappa, V. R.; & Burrus, L. W. (2016). **Divergent effects of Porcupine and Wntless on WNT1 trafficking, secretion, and signaling**. *Experimental Cell Research*, *347*(1), 171–183. PMID: 27492485.

Gao, Chan; & Chen, Y.-G. (2010). **Dishevelled: The hub of Wnt signaling**. *Cellular Signalling*, *22*(5), 717–727.

Gao, Chenxi; Xiao, G.; & Hu, J. (2014). **Regulation of Wnt/β-catenin signaling by posttranslational modifications**. *Cell & Bioscience*, *4*(1), 13.

Gardner, R. G.; Shearer, A. G.; & Hampton, R. Y. (2001). **In Vivo Action of the HRD Ubiquitin Ligase Complex: Mechanisms of Endoplasmic Reticulum Quality Control and Sterol Regulation**. *Molecular and Cellular Biology*, *21*(13), 4276–4291. PMID: 11390656.

Garza, R. M.; Sato, B. K.; & Hampton, R. Y. (2009). **In vitro analysis of Hrd1p-mediated retrotranslocation of its multispanning membrane substrate 3-hydroxy-3-methylglutaryl (HMG)-CoA reductase**. *The Journal of Biological Chemistry*, *284*(22), 14710–14722. PMID: 19324879.

Gasnereau, I.; Herr, P.; Chia, P. Z. C.; Basler, K.; & Gleeson, P. A. (2011). **Identification of an Endocytosis Motif in an Intracellular Loop of Wntless Protein, Essential for Its Recycling and the Control of Wnt Protein Signaling**. *The Journal of Biological Chemistry*, *286*(50), 43324–43333. PMID: 22027831.

Ghaemmaghami, S.; Huh, W.-K.; Bower, K.; Howson, R. W.; Belle, A.; Dephoure, N.; O'Shea, E. K.; & Weissman, J. S. (2003). **Global analysis of protein expression in yeast**. *Nature*, *425*(6959), 737–741.

Glaeser, K.; Boutros, M.; & Gross, J. C. (2016). **Biochemical Methods to Analyze Wnt Protein Secretion**. *Methods in Molecular Biology (Clifton, N.J.)*, *1481*, 17–28. PMID: 27590148.

Glaeser, K.; Urban, M.; Fenech, E.; Voloshanenko, O.; Kranz, D.; Lari, F.; Christianson, J. C.; & Boutros, M. (2018). **ERAD-dependent control of the Wnt secretory factor Evi**. *The EMBO Journal*, *37*(4). PMID: 29378775.

Glinka, A.; Wu, W.; Delius, H.; Monaghan, A. P.; Blumenstock, C.; & Niehrs, C. (1998). **Dickkopf-1 is a member of a new family of secreted proteins and functions in head induction**. *Nature*, *391*(6665), 357–362. PMID: 9450748.

Goldberg, A. L. (1969a). **Protein turnover in skeletal muscle. I. Protein catabolism during work-induced hypertrophy and growth induced with growth hormone**. *The Journal of Biological Chemistry*, *244*(12), 3217–3222. PMID: 5792657.

Goldberg, A. L. (1969b). **Protein turnover in skeletal muscle. II. Effects of denervation and cortisone on protein catabolism in skeletal muscle**. *The Journal of Biological Chemistry*, *244*(12), 3223–3229. PMID: 5792658.

Goldknopf, I. L.; & Busch, H. (1977). **Isopeptide linkage between nonhistone and histone 2A polypeptides of chromosomal conjugate-protein A24**. *Proceedings of the National Academy of Sciences of the United States of America*, *74*(3), 864–868. PMID: 265581.

Goldstein, G.; Scheid, M.; Hammerling, U.; Schlesinger, D. H.; Niall, H. D.; & Boyse, E. A. (1975). **Isolation of a polypeptide that has lymphocyte-differentiating properties and is probably represented universally in living cells**. *Proceedings of the National Academy of Sciences of the United States of America*, *72*(1), 11–15. PMID: 1078892.

Goodman, R. M.; Thombre, S.; Firtina, Z.; Gray, D.; Betts, D.; Roebuck, J.; Spana, E. P.; & Selva, E. M. (2006). **Sprinter: A novel transmembrane protein required for Wg secretion and signaling**. *Development*, *133*(24), 4901–4911. PMID: 17108000.

Griesmann, H.; Ripka, S.; Pralle, M.; Ellenrieder, V.; Baumgart, S.; Buchholz, M.; Pilarsky, C.; Aust, D.; Gress, T. M.; & Michl, P. (2013). **WNT5A-NFAT signaling mediates**

resistance to apoptosis in pancreatic cancer. *Neoplasia (New York, N.Y.)*, *15*(1), 11–22. PMID: 23359789.

Gross, J. C.; Chaudhary, V.; Bartscherer, K.; & Boutros, M. (2012). **Active Wnt proteins are secreted on exosomes**. *Nature Cell Biology*, *14*(10), 1036–1045. PMID: 22983114.

Grossmann, A. H.; Yoo, J. H.; Clancy, J.; Sorensen, L. K.; Sedgwick, A.; Tong, Z.; Ostanin, K.; Rogers, A.; Grossmann, K. F.; Tripp, S. R.; Thomas, K. R.; D'Souza-Schorey, C.; Odelberg, S. J.; & Li, D. Y. (2013). **The small GTPase ARF6 stimulates β-catenin transcriptional activity during WNT5A-mediated melanoma invasion and metastasis**. *Science Signaling*, *6*(265), ra14. PMID: 23462101.

Grou, C. P.; Pinto, M. P.; Mendes, A. V.; Domingues, P.; & Azevedo, J. E. (2015). **The de novo synthesis of ubiquitin: Identification of deubiquitinases acting on ubiquitin precursors**. *Scientific Reports*, *5*(1), 1–16.

Haglund, K.; Sigismund, S.; Polo, S.; Szymkiewicz, I.; Di Fiore, P. P.; & Dikic, I. (2003). **Multiple monoubiquitination of RTKs is sufficient for their endocytosis and degradation**. *Nature Cell Biology*, *5*(5), 461–466. PMID: 12717448.

Hampton, R. Y.; Gardner, R. G.; & Rine, J. (1996). **Role of 26S proteasome and HRD genes in the degradation of 3-hydroxy-3-methylglutaryl-CoA reductase, an integral endoplasmic reticulum membrane protein**. *Molecular Biology of the Cell*, *7*(12), 2029–2044. PMID: 8970163.

Hanahan, D.; & Weinberg, R. A. (2011). **Hallmarks of Cancer: The Next Generation**. *Cell*, *144*(5), 646–674. PMID: 21376230.

Hao, H.-X.; Xie, Y.; Zhang, Y.; Charlat, O.; Oster, E.; Avello, M.; Lei, H.; Mickanin, C.; Liu, D.; Ruffner, H.; Mao, X.; Ma, Q.; Zamponi, R.; Bouwmeester, T.; Finan, P. M.; Kirschner, M. W.; Porter, J. A.; Serluca, F. C.; & Cong, F. (2012). **ZNRF3 promotes Wnt receptor turnover in an R-spondin-sensitive manner**. *Nature*, *485*(7397), 195–200. PMID: 22575959.

Hao, Y.-H.; Doyle, J. M.; Ramanathan, S.; Gomez, T. S.; Jia, D.; Xu, M.; Chen, Z. J.; Billadeau, D. D.; Rosen, M. K.; & Potts, P. R. (2013). **Regulation of WASH-Dependent Actin Polymerization and Protein Trafficking by Ubiquitination**. *Cell*, *152*(5), 1051–1064. PMID: 23452853.

Hari, L.; Brault, V.; Kléber, M.; Lee, H.-Y.; Ille, F.; Leimeroth, R.; Paratore, C.; Suter, U.; Kemler, R.; & Sommer, L. (2002). **Lineage-specific requirements of β-catenin in neural crest development**. *The Journal of Cell Biology*, *159*(5), 867–880. PMID: 12473692.

Harterink, M.; Port, F.; Lorenowicz, M. J.; McGough, I. J.; Silhankova, M.; Betist, M. C.; Weering, J. R. T. van; Heesbeen, R. G. H. P. van; Middelkoop, T. C.; Basler, K.; Cullen, P. J.; & Korswagen, H. C. (2011). **A SNX3-dependent retromer pathway mediates retrograde transport of the Wnt sorting receptor Wntless and is required for Wnt secretion**. *Nature Cell Biology*, *13*(8), 914–923.

Hartman, M. L.; & Czyz, M. (2015). **MITF in melanoma: Mechanisms behind its expression and activity**. *Cellular and Molecular Life Sciences: CMLS*, *72*(7), 1249–1260. PMID: 25433395.

Hassel, J. C.; Heinzerling, L.; Aberle, J.; Bähr, O.; Eigentler, T. K.; Grimm, M.-O.; Grünwald, V.; Leipe, J.; Reinmuth, N.; Tietze, J. K.; Trojan, J.; Zimmer, L.; & Gutzmer, R. (2017). **Combined immune checkpoint blockade (anti-PD-1/anti-CTLA-4): Evaluation and management of adverse drug reactions**. *Cancer Treatment Reviews*, *57*, 36–49.

Hatori, R.; & Kornberg, T. B. (2020). **Regulated delivery controls Drosophila Hedgehog, Wingless and Decapentaplegic signaling**. *BioRxiv*, 2020.08.12.247759.

He, T. C.; Sparks, A. B.; Rago, C.; Hermeking, H.; Zawel, L.; da Costa, L. T.; Morin, P. J.; Vogelstein, B.; & Kinzler, K. W. (1998). **Identification of c-MYC as a target of the APC pathway**. *Science (New York, N.Y.)*, *281*(5382), 1509–1512. PMID: 9727977.

Hebert, D. N.; & Molinari, M. (2012). **Flagging and docking: Dual roles for N-glycans in protein quality control and cellular proteostasis**. *Trends in Biochemical Sciences*, *37*(10), 404–410. PMID: 22921611.

Hegde, R. S.; & Ploegh, H. L. (2010). **Quality and Quantity Control at the Endoplasmic Reticulum**. *Current Opinion in Cell Biology*, *22*(4), 437–446. PMID: 20570125.

Herr, P.; & Basler, K. (2012). **Porcupine-mediated lipidation is required for Wnt recognition by Wls**. *Developmental Biology*, *361*(2), 392–402. PMID: 22108505.

Hershko, A.; Ciechanover, A.; Heller, H.; Haas, A. L.; & Rose, I. A. (1980). **Proposed role of ATP in protein breakdown: Conjugation of protein with multiple chains of the polypeptide of ATP-dependent proteolysis**. *Proceedings of the National Academy of Sciences*, *77*(4), 1783–1786. PMID: 6990414.

Hershko, A.; Heller, H.; Elias, S.; & Ciechanover, A. (1983). **Components of ubiquitin-protein ligase system. Resolution, affinity purification, and role in protein breakdown**. *The Journal of Biological Chemistry*, *258*(13), 8206–8214. PMID: 6305978.

Hirsch, C.; Gauss, R.; Horn, S. C.; Neuber, O.; & Sommer, T. (2009). **The ubiquitylation machinery of the endoplasmic reticulum**. *Nature*, *458*(7237), 453–460.

Hjerpe, R.; Aillet, F.; Lopitz-Otsoa, F.; Lang, V.; England, P.; & Rodriguez, M. S. (2009). **Efficient protection and isolation of ubiquitylated proteins using tandem ubiquitin-binding entities**. *EMBO Reports*, *10*(11), 1250–1258. PMID: 19798103.

Hodis, E.; Watson, I. R.; Kryukov, G. V.; Arold, S. T.; Imielinski, M.; Theurillat, J.-P.; Nickerson, E.; Auclair, D.; Li, L.; Place, C.; Dicara, D.; Ramos, A. H.; Lawrence, M. S.; Cibulskis, K.; Sivachenko, A.; Voet, D.; Saksena, G.; Stransky, N.; Onofrio, R. C.; … Chin, L. (2012). **A landscape of driver mutations in melanoma**. *Cell*, *150*(2), 251–263. PMID: 22817889.

Hoek, K. S.; Eichhoff, O. M.; Schlegel, N. C.; Döbbeling, U.; Kobert, N.; Schaerer, L.; Hemmi, S.; & Dummer, R. (2008). **In vivo switching of human melanoma cells between proliferative and invasive states**. *Cancer Research*, *68*(3), 650–656. PMID: 18245463.

Hoek, K. S.; Schlegel, N. C.; Brafford, P.; Sucker, A.; Ugurel, S.; Kumar, R.; Weber, B. L.; Nathanson, K. L.; Phillips, D. J.; Herlyn, M.; Schadendorf, D.; & Dummer, R. (2006). **Metastatic potential of melanomas defined by specific gene expression profiles with no BRAF signature**. *Pigment Cell Research*, *19*(4), 290–302.

Holstein, T. W. (2012). **The Evolution of the Wnt Pathway**. *Cold Spring Harbor Perspectives in Biology*, *4*(7), a007922.

Hornbeck, P. V.; Zhang, B.; Murray, B.; Kornhauser, J. M.; Latham, V.; & Skrzypek, E. (2015). **PhosphoSitePlus, 2014: Mutations, PTMs and recalibrations**. *Nucleic Acids Research*, *43*(Database issue), D512-520. PMID: 25514926.

Huang, F.; Goh, L. K.; & Sorkin, A. (2007). **EGF receptor ubiquitination is not necessary for its internalization**. *Proceedings of the National Academy of Sciences of the United States of America*, *104*(43), 16904–16909. PMID: 17940017.

Hübner, C. A.; & Dikic, I. (2020). **ER-phagy and human diseases**. *Cell Death & Differentiation*, *27*(3), 833–842.

Hungria, V. T. de M.; Crusoé, E. de Q.; Bittencourt, R. I.; Maiolino, A.; Magalhães, R. J. P.; Sobrinho, J. do N.; Pinto, J. V.; Fortes, R. C.; Moreira, E. de S.; & Tanaka, P. Y. (2019). **New proteasome inhibitors in the treatment of multiple myeloma**. *Hematology, Transfusion and Cell Therapy*, *41*(1), 76–83. PMID: 30793108.

Hunt, L. T.; & Dayhoff, M. O. (1977). **Amino-terminal sequence identity of ubiquitin and the nonhistone component of nuclear protein A24**. *Biochemical and Biophysical Research Communications*, *74*(2), 650–655. PMID: 836318.

Iizuka, S.; Abdullah, C.; Buschman, M. D.; Diaz, B.; & Courtneidge, S. A. (2016). **The role of Tks adaptor proteins in invadopodia formation, growth and metastasis of melanoma**. *Oncotarget*, *7*(48), 78473–78486. PMID: 27802184.

Ikeda, S.; Kishida, S.; Yamamoto, H.; Murai, H.; Koyama, S.; & Kikuchi, A. (1998). **Axin, a negative regulator of the Wnt signaling pathway, forms a complex with GSK-3beta and beta-catenin and promotes GSK-3beta-dependent phosphorylation of beta-catenin**. *The EMBO Journal*, *17*(5), 1371–1384. PMID: 9482734.

Ikeya, M.; Lee, S. M.; Johnson, J. E.; McMahon, A. P.; & Takada, S. (1997). **Wnt signalling required for expansion of neural crest and CNS progenitors**. *Nature*, *389*(6654), 966–970. PMID: 9353119.

Isakov, E.; & Stanhill, A. (2011). **Stalled Proteasomes Are Directly Relieved by P97 Recruitment**. *The Journal of Biological Chemistry*, *286*(35), 30274–30283. PMID: 21733848.

Ishitani, T.; Kishida, S.; Hyodo-Miura, J.; Ueno, N.; Yasuda, J.; Waterman, M.; Shibuya, H.; Moon, R. T.; Ninomiya-Tsuji, J.; & Matsumoto, K. (2003). **The TAK1-NLK Mitogen-Activated Protein Kinase Cascade Functions in the Wnt-5a/Ca2+ Pathway To Antagonize Wnt/β-Catenin Signaling**. *Molecular and Cellular Biology*, *23*(1), 131–139. PMID: 12482967.

Jacob, A.; & Prekeris, R. (2015). **The regulation of MMP targeting to invadopodia during cancer metastasis**. *Frontiers in Cell and Developmental Biology*, *3*.

Janda, C. Y.; Waghray, D.; Levin, A. M.; Thomas, C.; & Garcia, K. C. (2012). **Structural basis of Wnt recognition by Frizzled**. *Science (New York, N.Y.)*, *337*(6090), 59–64. PMID: 22653731.

Ji, Y.; Hao, H.; Reynolds, K.; McMahon, M.; & Zhou, C. J. (2019). **Wnt Signaling in Neural Crest Ontogenesis and Oncogenesis**. *Cells*, *8*(10). PMID: 31569501.

Jiang, M.; Ku, W.; Fu, J.; Offermanns, S.; Hsu, W.; & Que, J. (2013). **Gpr177 regulates pulmonary vasculature development**. *Development (Cambridge, England)*, *140*(17), 3589–3594. PMID: 23884445.

Jin, J.; Kittanakom, S.; Wong, V.; Reyes, B. A. S.; Bockstaele, E. J. V.; Stagljar, I.; Berrettini, W.; & Levenson, R. (2010). **Interaction of the mu-opioid receptor with GPR177 (Wntless) inhibits Wnt secretion: Potential implications for opioid dependence**. *BMC Neuroscience*, *11*, 33. PMID: 20214800.

Jin, J.; Morse, M.; Frey, C.; Petko, J.; & Levenson, R. (2010). **Expression of GPR177 (Wntless/Evi/Sprinter), a Highly Conserved Wnt-Transport Protein, in Rat Tissues, Zebrafish Embryos, and Cultured Human Cells**. *Developmental Dynamics : An Official Publication of the American Association of Anatomists*, *239*(9), 2426–2434. PMID: 20652957.

Jo, Y.; Lee, P. C. W.; Sguigna, P. V.; & DeBose-Boyd, R. A. (2011). **Sterol-induced degradation of HMG CoA reductase depends on interplay of two Insigs and two ubiquitin ligases, gp78 and Trc8**. *Proceedings of the National Academy of Sciences of the United States of America*, *108*(51), 20503–20508. PMID: 22143767.

Jo, Y.; Sguigna, P. V.; & DeBose-Boyd, R. A. (2011). **Membrane-associated ubiquitin ligase complex containing gp78 mediates sterol-accelerated degradation of 3-hydroxy-3-methylglutaryl-coenzyme A reductase**. *The Journal of Biological Chemistry*, *286*(17), 15022–15031. PMID: 21343306.

Jung, Y.-S.; & Park, J.-I. (2020). **Wnt signaling in cancer: Therapeutic targeting of Wnt signaling beyond β-catenin and the destruction complex**. *Experimental & Molecular Medicine*, *52*(2), 183–191.

Juszkiewicz, S.; & Hegde, R. S. (2018). **Quality Control of Orphaned Proteins**. *Molecular Cell*, *71*(3), 443–457.

Karigar, C. S.; & Murthy, K. R. S. (2005). **The Nobel Prize in Chemistry 2004**. *Resonance*, *10*(1), 41–49.

Katanaev, V. L.; Solis, G. P.; Hausmann, G.; Buestorf, S.; Katanayeva, N.; Schrock, Y.; Stuermer, C. A.; & Basler, K. (2008). **Reggie-1/flotillin-2 promotes secretion of the long-range signalling forms of Wingless and Hedgehog in Drosophila**. *The EMBO Journal*, *27*(3), 509–521.

Katiyar, S.; Li, G.; & Lennarz, W. J. (2004). **A complex between peptide:N-glycanase and two proteasome-linked proteins suggests a mechanism for the degradation of misfolded glycoproteins**. *Proceedings of the National Academy of Sciences of the United States of America*, *101*(38), 13774–13779. PMID: 15358861.

Kawakami, A.; & Fisher, D. E. (2017). **The master role of microphthalmia-associated transcription factor in melanocyte and melanoma biology**. *Laboratory Investigation*, *97*(6), 649–656.

Kim, H. T.; Kim, K. P.; Lledias, F.; Kisselev, A. F.; Scaglione, K. M.; Skowyra, D.; Gygi, S. P.; & Goldberg, A. L. (2007). **Certain pairs of ubiquitin-conjugating enzymes (E2s) and ubiquitin-protein ligases (E3s) synthesize nondegradable forked ubiquitin chains containing all possible isopeptide linkages**. *The Journal of Biological Chemistry*, *282*(24), 17375–17386. PMID: 17426036.

Kim, H.; Zhang, H.; Meng, D.; Russell, G.; Lee, J. N.; & Ye, J. (2013). **UAS domain of Ubxd8 and FAF1 polymerizes upon interaction with long-chain unsaturated fatty acids**. *Journal of Lipid Research*, *54*(8), 2144–2152. PMID: 23720822.

Kim, T.-Y.; Kim, E.; Yoon, S. K.; & Yoon, J.-B. (2008). **Herp enhances ER-associated protein degradation by recruiting ubiquilins**. *Biochemical and Biophysical Research Communications*, *369*(2), 741–746.

Kitagawa, M.; Hatakeyama, S.; Shirane, M.; Matsumoto, M.; Ishida, N.; Hattori, K.; Nakamichi, I.; Kikuchi, A.; Nakayama, K.; & Nakayama, K. (1999). **An F-box protein, FWD1, mediates ubiquitin-dependent proteolysis of beta-catenin**. *The EMBO Journal*, *18*(9), 2401–2410. PMID: 10228155.

Kleiger, G.; & Mayor, T. (2014). **Perilous journey: A tour of the ubiquitin–proteasome system**. *Trends in Cell Biology*, *24*(6), 352–359. PMID: 24457024.

Knopf, J. D.; Landscheidt, N.; Pegg, C. L.; Schulz, B. L.; Kühnle, N.; Chao, C.-W.; Huck, S.; & Lemberg, M. K. (2020). **Intramembrane protease RHBDL4 cleaves**

oligosaccharyltransferase subunits to target them for ER-associated degradation. *Journal of Cell Science*, *133*(6). PMID: 32005703.

Koegl, M.; Hoppe, T.; Schlenker, S.; Ulrich, H. D.; Mayer, T. U.; & Jentsch, S. (1999). **A novel ubiquitination factor, E4, is involved in multiubiquitin chain assembly**. *Cell*, *96*(5), 635–644. PMID: 10089879.

Komander, D.; & Rape, M. (2012). **The ubiquitin code**. *Annual Review of Biochemistry*, *81*, 203–229. PMID: 22524316.

Koo, B.-K.; Spit, M.; Jordens, I.; Low, T. Y.; Stange, D. E.; van de Wetering, M.; van Es, J. H.; Mohammed, S.; Heck, A. J. R.; Maurice, M. M.; & Clevers, H. (2012). **Tumour suppressor RNF43 is a stem-cell E3 ligase that induces endocytosis of Wnt receptors**. *Nature*, *488*(7413), 665–669. PMID: 22895187.

Kõressaar, T.; Lepamets, M.; Kaplinski, L.; Raime, K.; Andreson, R.; & Remm, M. (2018). **Primer3_masker: Integrating masking of template sequence with primer design software**. *Bioinformatics (Oxford, England)*, *34*(11), 1937–1938. PMID: 29360956.

Koressaar, T.; & Remm, M. (2007). **Enhancements and modifications of primer design program Primer3**. *Bioinformatics (Oxford, England)*, *23*(10), 1289–1291. PMID: 17379693.

Korkut, C.; Ataman, B.; Ramachandran, P.; Ashley, J.; Barria, R.; Gherbesi, N.; & Budnik, V. (2009). **Trans-Synaptic Transfer of Wnt Signals Through Release of Evi/Wntless Vesicles and Trafficking of Postsynaptic Frizzled-2 Receptors**. *Cell*, *139*(2), 393–404. PMID: 19837038.

Kramer, N.; Walzl, A.; Unger, C.; Rosner, M.; Krupitza, G.; Hengstschläger, M.; & Dolznig, H. (2013). **In vitro cell migration and invasion assays**. *Mutation Research*, *752*(1), 10–24. PMID: 22940039.

Kramps, T.; Peter, O.; Brunner, E.; Nellen, D.; Froesch, B.; Chatterjee, S.; Murone, M.; Züllig, S.; & Basler, K. (2002). **Wnt/wingless signaling requires BCL9/legless-mediated recruitment of pygopus to the nuclear beta-catenin-TCF complex**. *Cell*, *109*(1), 47–60. PMID: 11955446.

Kreutzberger, A. J. B.; Ji, M.; Aaron, J.; Mihaljević, L.; & Urban, S. (2019). **Rhomboid distorts lipids to break the viscosity-imposed speed limit of membrane diffusion**. *Science*, *363*(6426). PMID: 30705155.

Lee, J. N.; Kim, H.; Yao, H.; Chen, Y.; Weng, K.; & Ye, J. (2010). **Identification of Ubxd8 protein as a sensor for unsaturated fatty acids and regulator of triglyceride synthesis**. *Proceedings of the National Academy of Sciences*, *107*(50), 21424–21429. PMID: 21115839.

Lee, J. N.; Song, B.; DeBose-Boyd, R. A.; & Ye, J. (2006). **Sterol-regulated degradation of Insig-1 mediated by the membrane-bound ubiquitin ligase gp78**. *The Journal of Biological Chemistry*, *281*(51), 39308–39315. PMID: 17043353.

Lee, J. N.; Zhang, X.; Feramisco, J. D.; Gong, Y.; & Ye, J. (2008). **Unsaturated Fatty Acids Inhibit Proteasomal Degradation of Insig-1 at a Postubiquitination Step**. *The Journal of Biological Chemistry*, *283*(48), 33772–33783. PMID: 18835813.

Lee, Y.-J.; Ho, S.-R.; Graves, J. D.; Xiao, Y.; Huang, S.; & Lin, W.-C. (2019). **CGRRF1, a growth suppressor, regulates EGFR ubiquitination in breast cancer**. *Breast Cancer Research*, *21*(1), 134.

Leibing, T.; Géraud, C.; Augustin, I.; Boutros, M.; Augustin, H. G.; Okun, J. G.; Langhans, C.-D.; Zierow, J.; Wohlfeil, S. A.; Olsavszky, V.; Schledzewski, K.; Goerdt, S.; & Koch, P.-S.

(2018). **Angiocrine Wnt signaling controls liver growth and metabolic maturation in mice**. *Hepatology (Baltimore, Md.)*, *68*(2), 707–722. PMID: 29059455.

Lemus, L.; & Goder, V. (2014). **Regulation of Endoplasmic Reticulum-Associated Protein Degradation (ERAD) by Ubiquitin**. *Cells*, *3*(3), 824–847. PMID: 25100021.

Leto, D. E.; Morgens, D. W.; Zhang, L.; Walczak, C. P.; Elias, J. E.; Bassik, M. C.; & Kopito, R. R. (2019). **Genome-wide CRISPR analysis identifies substrate-specific conjugation modules in ER-associated degradation**. *Molecular Cell*, *73*(2), 377-389.e11. PMID: 30581143.

Li, W.; Bengtson, M. H.; Ulbrich, A.; Matsuda, A.; Reddy, V. A.; Orth, A.; Chanda, S. K.; Batalov, S.; & Joazeiro, C. A. P. (2008). **Genome-Wide and Functional Annotation of Human E3 Ubiquitin Ligases Identifies MULAN, a Mitochondrial E3 that Regulates the Organelle's Dynamics and Signaling**. *PLoS ONE*, *3*(1). PMID: 18213395.

Li, W.; Liu, J.; Zhang, B.; Bie, Q.; Qian, H.; & Xu, W. (2020). **Transcriptome Analysis Reveals Key Genes and Pathways Associated with Metastasis in Breast Cancer**. *OncoTargets and Therapy*, *13*, 323–335. PMID: 32021278.

Li, X.; & Song, Y. (2020). **Proteolysis-targeting chimera (PROTAC) for targeted protein degradation and cancer therapy**. *Journal of Hematology & Oncology*, *13*(1), 50.

Li, Y.; Yang, X.; Yang, J.; Wang, H.; & Wei, W. (2018). **An 11-gene-based prognostic signature for uveal melanoma metastasis based on gene expression and DNA methylation profile**. *Journal of Cellular Biochemistry*. PMID: 30556166.

Liang, J.; Yin, C.; Doong, H.; Fang, S.; Peterhoff, C.; Nixon, R. A.; & Monteiro, M. J. (2006). **Characterization of erasin (UBXD2): A new ER protein that promotes ER-associated protein degradation**. *Journal of Cell Science*, *119*(19), 4011–4024. PMID: 16968747.

Lim, K. L.; Chew, K. C. M.; Tan, J. M. M.; Wang, C.; Chung, K. K. K.; Zhang, Y.; Tanaka, Y.; Smith, W.; Engelender, S.; Ross, C. A.; Dawson, V. L.; & Dawson, T. M. (2005). **Parkin mediates nonclassical, proteasomal-independent ubiquitination of synphilin-1: Implications for Lewy body formation**. *The Journal of Neuroscience: The Official Journal of the Society for Neuroscience*, *25*(8), 2002–2009. PMID: 15728840.

Lim, P. J.; Danner, R.; Liang, J.; Doong, H.; Harman, C.; Srinivasan, D.; Rothenberg, C.; Wang, H.; Ye, Y.; Fang, S.; & Monteiro, M. J. (2009). **Ubiquilin and p97/VCP bind erasin, forming a complex involved in ERAD**. *Journal of Cell Biology*, *187*(2), 201–217.

Liu, Chao; Liu, W.; Ye, Y.; & Li, W. (2017). **Ufd2p synthesizes branched ubiquitin chains to promote the degradation of substrates modified with atypical chains**. *Nature Communications*, *8*, 14274. PMID: 28165462.

Liu, Chunming; Li, Y.; Semenov, M.; Han, C.; Baeg, G. H.; Tan, Y.; Zhang, Z.; Lin, X.; & He, X. (2002). **Control of beta-catenin phosphorylation/degradation by a dual-kinase mechanism**. *Cell*, *108*(6), 837–847. PMID: 11955436.

Liu, J.; Pan, S.; Hsieh, M. H.; Ng, N.; Sun, F.; Wang, T.; Kasibhatla, S.; Schuller, A. G.; Li, A. G.; Cheng, D.; Li, J.; Tompkins, C.; Pferdekamper, A.; Steffy, A.; Cheng, J.; Kowal, C.; Phung, V.; Guo, G.; Wang, Y.; … Harris, J. L. (2013). **Targeting Wnt-driven cancer through the inhibition of Porcupine by LGK974**. *Proceedings of the National Academy of Sciences of the United States of America*, *110*(50), 20224–20229. PMID: 24277854.

Livingston, C. M.; Ifrim, M. F.; Cowan, A. E.; & Weller, S. K. (2009). **Virus-Induced Chaperone-Enriched (VICE) domains function as nuclear protein quality control centers during HSV-1 infection**. *PLoS Pathogens*, *5*(10), e1000619. PMID: 19816571.

Lorenowicz, M. J.; Macurkova, M.; Harterink, M.; Middelkoop, T. C.; de Groot, R.; Betist, M. C.; & Korswagen, H. C. (2014). **Inhibition of late endosomal maturation restores Wnt secretion in Caenorhabditis elegans vps-29 retromer mutants**. *Cellular Signalling*, *26*(1), 19–31. PMID: 24056045.

Lu, H.; Liu, S.; Zhang, G.; Kwong, L. N.; Zhu, Y.; Miller, J. P.; Hu, Y.; Zhong, W.; Zeng, J.; Wu, L.; Krepler, C.; Sproesser, K.; Xiao, M.; Xu, W.; Karakousis, G. C.; Schuchter, L. M.; Field, J.; Zhang, P. J.; Herlyn, M.; … Guo, W. (2016). **Oncogenic BRAF-mediated Melanoma Cell Invasion**. *Cell Reports*, *15*(9), 2012–2024. PMID: 27210749.

Lu, J. P.; Wang, Y.; Sliter, D. A.; Pearce, M. M. P.; & Wojcikiewicz, R. J. H. (2011). **RNF170 protein, an endoplasmic reticulum membrane ubiquitin ligase, mediates inositol 1,4,5-trisphosphate receptor ubiquitination and degradation**. *The Journal of Biological Chemistry*, *286*(27), 24426–24433. PMID: 21610068.

Luo, H.; Jiang, M.; Lian, G.; Liu, Q.; Shi, M.; Li, T. Y.; Song, L.; Ye, J.; He, Y.; Yao, L.; Zhang, C.; Lin, Z.-Z.; Zhang, C.-S.; Zhao, T.-J.; Jia, W.-P.; Li, P.; Lin, S.-Y.; & Lin, S.-C. (2018). **AIDA Selectively Mediates Downregulation of Fat Synthesis Enzymes by ERAD to Retard Intestinal Fat Absorption and Prevent Obesity**. *Cell Metabolism*, *27*(4), 843-853.e6.

Lustig, B.; Jerchow, B.; Sachs, M.; Weiler, S.; Pietsch, T.; Karsten, U.; van de Wetering, M.; Clevers, H.; Schlag, P. M.; Birchmeier, W.; & Behrens, J. (2002). **Negative Feedback Loop of Wnt Signaling through Upregulation of Conductin/Axin2 in Colorectal and Liver Tumors**. *Molecular and Cellular Biology*, *22*(4), 1184–1193. PMID: 11809809.

Mancini, A.; Howard, S. R.; Marelli, F.; Cabrera, C. P.; Barnes, M. R.; Sternberg, M. J.; Leprovots, M.; Hadjidemetriou, I.; Monti, E.; David, A.; Wehkalampi, K.; Oleari, R.; Lettieri, A.; Vezzoli, V.; Vassart, G.; Cariboni, A.; Bonomi, M.; Garcia, M. I.; Guasti, L.; & Dunkel, L. (2020). **LGR4 deficiency results in delayed puberty through impaired Wnt/β-catenin signaling**. *JCI Insight*, *5*(11). PMID: 32493844.

Maruyama, E. O.; Yu, H.-M. I.; Jiang, M.; Fu, J.; & Hsu, W. (2013). **Gpr177 Deficiency Impairs Mammary Development and Prohibits Wnt-Induced Tumorigenesis**. *PLoS ONE*, *8*(2). PMID: 23457599.

Mattes, B.; Dang, Y.; Greicius, G.; Kaufmann, L. T.; Prunsche, B.; Rosenbauer, J.; Stegmaier, J.; Mikut, R.; Özbek, S.; Nienhaus, G. U.; Schug, A.; Virshup, D. M.; & Scholpp, S. (2018). **Wnt/PCP controls spreading of Wnt/β-catenin signals by cytonemes in vertebrates**. *ELife*, *7*, e36953.

McClellan, A. J.; Laugesen, S. H.; & Ellgaard, L. (2019). **Cellular functions and molecular mechanisms of non-lysine ubiquitination**. *Open Biology*, *9*(9), 190147. PMID: 31530095.

McGough, I. J.; de Groot, R. E. A.; Jellett, A. P.; Betist, M. C.; Varandas, K. C.; Danson, C. M.; Heesom, K. J.; Korswagen, H. C.; & Cullen, P. J. (2018). **SNX3-retromer requires an evolutionary conserved MON2:DOPEY2:ATP9A complex to mediate Wntless sorting and Wnt secretion**. *Nature Communications*, *9*(1), 3737.

McKenna, S.; Spyracopoulos, L.; Moraes, T.; Pastushok, L.; Ptak, C.; Xiao, W.; & Ellison, M. J. (2001). **Noncovalent interaction between ubiquitin and the human DNA repair**

protein Mms2 is required for Ubc13-mediated polyubiquitination. *The Journal of Biological Chemistry*, *276*(43), 40120–40126. PMID: 11504715.

McNeill, H.; Knebel, A.; Arthur, J. S. C.; Cuenda, A.; & Cohen, P. (2004). **A novel UBA and UBX domain protein that binds polyubiquitin and VCP and is a substrate for SAPKs**. *The Biochemical Journal*, *384*(Pt 2), 391–400. PMID: 15362974.

Medicherla, B.; Kostova, Z.; Schaefer, A.; & Wolf, D. H. (2004). **A genomic screen identifies Dsk2p and Rad23p as essential components of ER-associated degradation**. *EMBO Reports*, *5*(7), 692–697. PMID: 15167887.

Mehrtash, A. B.; & Hochstrasser, M. (2019). **Ubiquitin-dependent Protein Degradation at the Endoplasmic Reticulum and Nuclear Envelope**. *Seminars in Cell & Developmental Biology*, *93*, 111–124. PMID: 30278225.

Metzger, M. B.; Hristova, V. A.; & Weissman, A. M. (2012). **HECT and RING finger families of E3 ubiquitin ligases at a glance**. *Journal of Cell Science*, *125*(3), 531–537. PMID: 22389392.

Meyer, H.; & Weihl, C. C. (2014). **The VCP/p97 system at a glance: Connecting cellular function to disease pathogenesis**. *Journal of Cell Science*, *127*(18), 3877–3883. PMID: 25146396.

Middleton, A. J.; & Day, C. L. (2015). **The molecular basis of lysine 48 ubiquitin chain synthesis by Ube2K**. *Scientific Reports*, *5*. PMID: 26592444.

Molenaar, M.; Wetering, M. van de; Oosterwegel, M.; Peterson-Maduro, J.; Godsave, S.; Korinek, V.; Roose, J.; Destrée, O.; & Clevers, H. (1996). **XTcf-3 Transcription Factor Mediates β-Catenin-Induced Axis Formation in Xenopus Embryos**. *Cell*, *86*(3), 391–399. PMID: 8756721.

Mosesso, N.; Nagel, M.-K.; & Isono, E. (2019). **Ubiquitin recognition in endocytic trafficking – with or without ESCRT-0**. *Journal of Cell Science*, *132*(16). PMID: 31416855.

Mueller, B.; Klemm, E. J.; Spooner, E.; Claessen, J. H.; & Ploegh, H. L. (2008). **SEL1L nucleates a protein complex required for dislocation of misfolded glycoproteins**. *Proceedings of the National Academy of Sciences of the United States of America*, *105*(34), 12325–12330. PMID: 18711132.

Munemitsu, S.; Albert, I.; Rubinfeld, B.; & Polakis, P. (1996). **Deletion of an amino-terminal sequence beta-catenin in vivo and promotes hyperphosporylation of the adenomatous polyposis coli tumor suppressor protein.** *Molecular and Cellular Biology*, *16*(8), 4088–4094. PMID: 8754807.

Najdi, R.; Proffitt, K.; Sprowl, S.; Kaur, S.; Yu, J.; Covey, T. M.; Virshup, D. M.; & Waterman, M. L. (2012). **A uniform human Wnt expression library reveals a shared secretory pathway and unique signaling activities**. *Differentiation; Research in Biological Diversity*, *84*(2), 203–213. PMID: 22784633.

Nakahara, H.; Otani, T.; Sasaki, T.; Miura, Y.; Takai, Y.; & Kogo, M. (2003). **Involvement of Cdc42 and Rac small G proteins in invadopodia formation of RPMI7951 cells**. *Genes to Cells*, *8*(12), 1019–1027.

Napoli, S.; Scuderi, C.; Gattuso, G.; Di Bella, V.; Candido, S.; Basile, M. S.; Libra, M.; & Falzone, L. (2020). **Functional Roles of Matrix Metalloproteinases and Their Inhibitors in Melanoma**. *Cells*, *9*(5), 1151.

Neal, J. W.; & Clipstone, N. A. (2001). **Glycogen Synthase Kinase-3 Inhibits the DNA Binding Activity of NFATc**. *Journal of Biological Chemistry*, *276*(5), 3666–3673. PMID: 11063740.

Neal, S.; Jaeger, P. A.; Duttke, S.; Benner, C.; Glass, C.; Ideker, T.; & Hampton, R. (2018). **The Dfm1 derlin is required for ERAD retrotranslocation of integral membrane proteins**. *Molecular Cell*, *69*(2), 306-320.e4. PMID: 29351849.

Neal, S.; Mak, R.; Bennett, E. J.; & Hampton, R. (2017). **A Cdc48 'Retrochaperone' Function Is Required for the Solubility of Retrotranslocated, Integral Membrane Endoplasmic Reticulum-associated Degradation (ERAD-M) Substrates**. *The Journal of Biological Chemistry*, *292*(8), 3112–3128. PMID: 28077573.

Niehrs, C. (2012). **The complex world of WNT receptor signalling**. *Nature Reviews. Molecular Cell Biology*, *13*(12), 767–779. PMID: 23151663.

Nusse, R.; & Clevers, H. (2017). **Wnt/β-Catenin Signaling, Disease, and Emerging Therapeutic Modalities**. *Cell*, *169*(6), 985–999. PMID: 28575679.

Nusse, R.; & Varmus, H. E. (1982). **Many tumors induced by the mouse mammary tumor virus contain a provirus integrated in the same region of the host genome**. *Cell*, *31*(1), 99–109. PMID: 6297757.

O'Connell, M. P.; Fiori, J. L.; Xu, M.; Carter, A. D.; Frank, B. P.; Camilli, T. C.; French, A. D.; Dissanayake, S. K.; Indig, F. E.; Bernier, M.; Taub, D. D.; Hewitt, S. M.; & Weeraratna, A. T. (2010). **The orphan tyrosine kinase receptor, ROR2, mediates Wnt5A signaling in metastatic melanoma**. *Oncogene*, *29*(1), 34–44. PMID: 19802008.

O'Connell, M. P.; & Weeraratna, A. T. (2009). **Hear the Wnt Ror: How Melanoma Cells Adjust to Changes in Wnt**. *Pigment Cell & Melanoma Research*, *22*(6), 724–739. PMID: 19708915.

O'Connell, Michael P.; Marchbank, K.; Webster, M. R.; Valiga, A. A.; Kaur, A.; Vultur, A.; Li, L.; Herlyn, M.; Villanueva, J.; Liu, Q.; Yin, X.; Widura, S.; Nelson, J.; Ruiz, N.; Camilli, T. C.; Indig, F. E.; Flaherty, K. T.; Wargo, J. A.; Frederick, D. T.; … Weeraratna, A. T. (2013). **Hypoxia induces phenotypic plasticity and therapy resistance in melanoma via the tyrosine kinase receptors ROR1 and ROR2**. *Cancer Discovery*, *3*(12), 1378–1393. PMID: 24104062.

Ohtake, F.; Saeki, Y.; Ishido, S.; Kanno, J.; & Tanaka, K. (2016). **The K48-K63 Branched Ubiquitin Chain Regulates NF-κB Signaling**. *Molecular Cell*, *64*(2), 251–266. PMID: 27746020.

Ohtake, F.; Tsuchiya, H.; Saeki, Y.; & Tanaka, K. (2018). **K63 ubiquitylation triggers proteasomal degradation by seeding branched ubiquitin chains**. *Proceedings of the National Academy of Sciences of the United States of America*, *115*(7), E1401–E1408. PMID: 29378950.

Olzmann, J. A.; & Carvalho, P. (2019). **Dynamics and functions of lipid droplets**. *Nature Reviews Molecular Cell Biology*, *20*(3), 137–155.

Olzmann, J. A.; Richter, C. M.; & Kopito, R. R. (2013). **Spatial regulation of UBXD8 and p97/VCP controls ATGL-mediated lipid droplet turnover**. *Proceedings of the National Academy of Sciences of the United States of America*, *110*(4), 1345–1350. PMID: 23297223.

Ossipova, O.; & Sokol, S. Y. (2011). **Neural crest specification by noncanonical Wnt signaling and PAR-1**. *Development (Cambridge, England)*, *138*(24), 5441–5450. PMID: 22110058.

Ouspenskaia, T.; Matos, I.; Mertz, A. F.; Fiore, V. F.; & Fuchs, E. (2016). **WNT-SHH Antagonism Specifies and Expands Stem Cells Prior to Niche Formation**. *Cell*, *164*(1–2), 156–169. PMID: 26771489.

Özkaynak, E.; Finley, D.; & Varshavsky, A. (1984). **The yeast ubiquitin gene: Head-to-tail repeats encoding a polyubiquitin precursor protein**. *Nature*, *312*(5995), 663–666.

Pan, C.-L.; Baum, P. D.; Gu, M.; Jorgensen, E. M.; Clark, S. G.; & Garriga, G. (2008). **C. elegans AP-2 and retromer control Wnt signaling by regulating mig-14/Wntless**. *Developmental Cell*, *14*(1), 132–139. PMID: 18160346.

Pao, K.-C.; Wood, N. T.; Knebel, A.; Rafie, K.; Stanley, M.; Mabbitt, P. D.; Sundaramoorthy, R.; Hofmann, K.; van Aalten, D. M. F.; & Virdee, S. (2018). **Activity-based E3 ligase profiling uncovers an E3 ligase with esterification activity**. *Nature*, *556*(7701), 381–385. PMID: 29643511.

Paterson, E. K.; & Courtneidge, S. A. (2018). **Invadosomes are coming: New insights into function and disease relevance**. *The FEBS Journal*, *285*(1), 8–27. PMID: 28548369.

Pearce, M. M. P.; Wang, Y.; Kelley, G. G.; & Wojcikiewicz, R. J. H. (2007). **SPFH2 mediates the endoplasmic reticulum-associated degradation of inositol 1,4,5-trisphosphate receptors and other substrates in mammalian cells**. *The Journal of Biological Chemistry*, *282*(28), 20104–20115. PMID: 17502376.

Pearce, M. M. P.; Wormer, D. B.; Wilkens, S.; & Wojcikiewicz, R. J. H. (2009). **An Endoplasmic Reticulum (ER) Membrane Complex Composed of SPFH1 and SPFH2 Mediates the ER-associated Degradation of Inositol 1,4,5-Trisphosphate Receptors**. *The Journal of Biological Chemistry*, *284*(16), 10433–10445. PMID: 19240031.

Peifer, M.; McCrea, P. D.; Green, K. J.; Wieschaus, E.; & Gumbiner, B. M. (1992). **The vertebrate adhesive junction proteins beta-catenin and plakoglobin and the Drosophila segment polarity gene armadillo form a multigene family with similar properties**. *The Journal of Cell Biology*, *118*(3), 681–691. PMID: 1639851.

Perotti, V.; Baldassari, P.; Molla, A.; Vegetti, C.; Bersani, I.; Maurichi, A.; Santinami, M.; Anichini, A.; & Mortarini, R. (2016). **NFATc2 is an intrinsic regulator of melanoma dedifferentiation**. *Oncogene*, *35*(22), 2862–2872. PMID: 26387540.

Petko, J.; Thileepan, M.; Sargen, M.; Canfield, V.; & Levenson, R. (2019). **Alternative splicing of the Wnt trafficking protein, Wntless and its effects on protein-protein interactions**. *BMC Molecular and Cell Biology*, *20*(1), 22.

Pfaffl, M. W. (2001). **A new mathematical model for relative quantification in real-time RT–PCR**. *Nucleic Acids Research*, *29*(9), e45. PMID: 11328886.

Piper, R. C.; Dikic, I.; & Lukacs, G. L. (2014). **Ubiquitin-Dependent Sorting in Endocytosis**. *Cold Spring Harbor Perspectives in Biology*, *6*(1). PMID: 24384571.

Ploper, D.; Taelman, V. F.; Robert, L.; Perez, B. S.; Titz, B.; Chen, H.-W.; Graeber, T. G.; von Euw, E.; Ribas, A.; & De Robertis, E. M. (2015). **MITF drives endolysosomal biogenesis and potentiates Wnt signaling in melanoma cells**. *Proceedings of the National Academy of Sciences of the United States of America*, *112*(5), E420-429. PMID: 25605940.

Pohl, C.; & Dikic, I. (2019). **Cellular quality control by the ubiquitin-proteasome system and autophagy**. *Science (New York, N.Y.)*, *366*(6467), 818–822. PMID: 31727826.

Port, F.; Hausmann, G.; & Basler, K. (2011). **A genome-wide RNA interference screen uncovers two p24 proteins as regulators of Wingless secretion**. *EMBO Reports*, *12*(11), 1144–1152. PMID: 21886182.

Port, F.; Kuster, M.; Herr, P.; Furger, E.; Bänziger, C.; Hausmann, G.; & Basler, K. (2008). **Wingless secretion promotes and requires retromer-dependent cycling of Wntless**. *Nature Cell Biology*, *10*(2), 178–185. PMID: 18193032.

Printsev, I.; Curiel, D.; & Carraway, K. L. (2017). **Membrane Protein Quantity Control at the Endoplasmic Reticulum**. *The Journal of Membrane Biology*, *250*(4), 379–392. PMID: 27743014.

Pruneda, J. N.; Stoll, K. E.; Bolton, L. J.; Brzovic, P. S.; & Klevit, R. E. (2011). **Ubiquitin in Motion: Structural Studies of the Ubiquitin-Conjugating Enzyme~Ubiquitin Conjugate**. *Biochemistry*, *50*(10), 1624–1633.

Quintana, E.; Shackleton, M.; Foster, H. R.; Fullen, D. R.; Sabel, M. S.; Johnson, T. M.; & Morrison, S. J. (2010). **Phenotypic heterogeneity among tumorigenic melanoma cells from patients that is reversible and not hierarchically organized**. *Cancer Cell*, *18*(5), 510–523. PMID: 21075313.

Quintana, E.; Shackleton, M.; Sabel, M. S.; Fullen, D. R.; Johnson, T. M.; & Morrison, S. J. (2008). **Efficient tumour formation by single human melanoma cells**. *Nature*, *456*(7222), 593–598. PMID: 19052619.

Quintavalle, M.; Elia, L.; Price, J. H.; Heynen-Genel, S.; & Courtneidge, S. A. (2011). **A cell-based, high content screening assay reveals activators and inhibitors of cancer cell invasion**. *Science Signaling*, *4*(183), ra49. PMID: 21791703.

Rambow, F.; Marine, J.-C.; & Goding, C. R. (2019). **Melanoma plasticity and phenotypic diversity: Therapeutic barriers and opportunities**. *Genes & Development*, *33*(19–20), 1295–1318.

Rao, D. M.; Shackleford, M. T.; Bordeaux, E. K.; Sottnik, J. L.; Ferguson, R. L.; Yamamoto, T. M.; Wellberg, E. A.; Bitler, B. G.; & Sikora, M. J. (2019). **Wnt family member 4 (WNT4) and WNT3A activate cell-autonomous Wnt signaling independent of porcupine O-acyltransferase or Wnt secretion**. *The Journal of Biological Chemistry*, *294*(52), 19950–19966. PMID: 31740580.

Rauscher, B.; Henkel, L.; Heigwer, F.; & Boutros, M. (2019). **Lineage specific core-regulatory circuits determine gene essentiality in cancer cells**. *BioRxiv*, 609552.

Restivo, G.; Diener, J.; Cheng, P. F.; Kiowski, G.; Bonalli, M.; Biedermann, T.; Reichmann, E.; Levesque, M. P.; Dummer, R.; & Sommer, L. (2017). **The low affinity neurotrophin receptor CD271 regulates phenotype switching in melanoma**. *Nature Communications*, *8*(1), 1988.

Richly, H.; Rape, M.; Braun, S.; Rumpf, S.; Hoege, C.; & Jentsch, S. (2005). **A series of ubiquitin binding factors connects CDC48/p97 to substrate multiubiquitylation and proteasomal targeting**. *Cell*, *120*(1), 73–84. PMID: 15652483.

Rock, K. L.; Gramm, C.; Rothstein, L.; Clark, K.; Stein, R.; Dick, L.; Hwang, D.; & Goldberg, A. L. (1994). **Inhibitors of the proteasome block the degradation of most cell proteins and the generation of peptides presented on MHC class I molecules**. *Cell*, *78*(5), 761–771. PMID: 8087844.

Rodrigo-Brenni, M. C.; & Morgan, D. O. (2007). **Sequential E2s Drive Polyubiquitin Chain Assembly on APC Targets**. *Cell*, *130*(1), 127–139. PMID: 17632060.

Rodriguez-Hernandez, I.; Maiques, O.; Kohlhammer, L.; Cantelli, G.; Perdrix-Rosell, A.; Monger, J.; Fanshawe, B.; Bridgeman, V. L.; Karagiannis, S. N.; Penin, R. M.; Marcolval, J.; Marti, R. M.; Matias-Guiu, X.; Fruhwirth, G. O.; Orgaz, J. L.; Malanchi, I.; & Sanz-Moreno, V. (2020). **WNT11-FZD7-DAAM1 signalling supports tumour initiating abilities and melanoma amoeboid invasion**. *Nature Communications*, *11*(1), 5315.

Roose, J.; Molenaar, M.; Peterson, J.; Hurenkamp, J.; Brantjes, H.; Moerer, P.; van de Wetering, M.; Destrée, O.; & Clevers, H. (1998). **The Xenopus Wnt effector XTcf-3 interacts with Groucho-related transcriptional repressors**. *Nature*, *395*(6702), 608–612. PMID: 9783587.

Routledge, D.; & Scholpp, S. (2019). **Mechanisms of intercellular Wnt transport**. *Development*, *146*(10). PMID: 31092504.

Sato, B. K.; Schulz, D.; Do, P. H.; & Hampton, R. Y. (2009). **Misfolded membrane proteins are specifically recognized by the transmembrane domain of the Hrd1p ubiquitin ligase**. *Molecular Cell*, *34*(2), 212–222. PMID: 19394298.

Sato, T.; Vries, R. G.; Snippert, H. J.; van de Wetering, M.; Barker, N.; Stange, D. E.; van Es, J. H.; Abo, A.; Kujala, P.; Peters, P. J.; & Clevers, H. (2009). **Single Lgr5 stem cells build crypt-villus structures in vitro without a mesenchymal niche**. *Nature*, *459*(7244), 262–265. PMID: 19329995.

Schadendorf, D.; Fisher, D. E.; Garbe, C.; Gershenwald, J. E.; Grob, J.-J.; Halpern, A.; Herlyn, M.; Marchetti, M. A.; McArthur, G.; Ribas, A.; Roesch, A.; & Hauschild, A. (2015). **Melanoma**. *Nature Reviews Disease Primers*, *1*(1), 1–20.

Schadendorf, D.; van Akkooi, A. C. J.; Berking, C.; Griewank, K. G.; Gutzmer, R.; Hauschild, A.; Stang, A.; Roesch, A.; & Ugurel, S. (2018). **Melanoma**. *Lancet (London, England)*, *392*(10151), 971–984. PMID: 30238891.

Schatoff, E. M.; Leach, B. I.; & Dow, L. E. (2017). **Wnt Signaling and Colorectal Cancer**. *Current Colorectal Cancer Reports*, *13*(2), 101–110. PMID: 28413363.

Schindelin, J.; Arganda-Carreras, I.; Frise, E.; Kaynig, V.; Longair, M.; Pietzsch, T.; Preibisch, S.; Rueden, C.; Saalfeld, S.; Schmid, B.; Tinevez, J.-Y.; White, D. J.; Hartenstein, V.; Eliceiri, K.; Tomancak, P.; & Cardona, A. (2012). **Fiji: An open-source platform for biological-image analysis**. *Nature Methods*, *9*(7), 676–682.

Schlessinger, K.; McManus, E. J.; & Hall, A. (2007). **Cdc42 and noncanonical Wnt signal transduction pathways cooperate to promote cell polarity**. *The Journal of Cell Biology*, *178*(3), 355–361. PMID: 17646398.

Schmidt, O.; Weyer, Y.; Baumann, V.; Widerin, M. A.; Eising, S.; Angelova, M.; Schleiffer, A.; Kremser, L.; Lindner, H.; Peter, M.; Fröhlich, F.; & Teis, D. (2019). **Endosome and Golgi-associated degradation (EGAD) of membrane proteins regulates sphingolipid metabolism**. *The EMBO Journal*, *38*(15), e101433.

Schoenheimer, R. (1942). **The Dynamic State of Body Constituents**. *Cancer Research*, *2*(11), 810.

Schuberth, C.; & Buchberger, A. (2008). **UBX domain proteins: Major regulators of the AAA ATPase Cdc48/p97**. *Cellular and Molecular Life Sciences*, *65*(15), 2360–2371.

Seo, J.; Kee, H. J.; Choi, H. J.; Lee, J. E.; Park, S.-Y.; Lee, S.-H.; Jeong, M.-H.; Guk, G.; Lee, S.; Choi, K.-C.; Choi, Y. Y.; Kim, H.; Noh, S. H.; Yoon, H.-G.; & Cheong, and J.-H. (2018).

Inhibition of Wntless/GPR177 suppresses gastric tumorigenesis. *BMB Reports*, *51*(5), 255–260.

Sever, N.; Song, B.-L.; Yabe, D.; Goldstein, J. L.; Brown, M. S.; & DeBose-Boyd, R. A. (2003). **Insig-dependent Ubiquitination and Degradation of Mammalian 3-Hydroxy-3-methylglutaryl-CoA Reductase Stimulated by Sterols and Geranylgeraniol**. *Journal of Biological Chemistry*, *278*(52), 52479–52490. PMID: 14563840.

Shain, A. H.; Yeh, I.; Kovalyshyn, I.; Sriharan, A.; Talevich, E.; Gagnon, A.; Dummer, R.; North, J.; Pincus, L.; Ruben, B.; Rickaby, W.; D'Arrigo, C.; Robson, A.; & Bastian, B. C. (2015, November 11). ***The Genetic Evolution of Melanoma from Precursor Lesions***; Massachusetts Medical Society.

Sheldahl, L. C.; Slusarski, D. C.; Pandur, P.; Miller, J. R.; Kühl, M.; & Moon, R. T. (2003). **Dishevelled activates Ca2+ flux, PKC, and CamKII in vertebrate embryos**. *The Journal of Cell Biology*, *161*(4), 769–777. PMID: 12771126.

Siegel, R. L.; Miller, K. D.; & Jemal, A. (2020). **Cancer statistics, 2020**. *CA: A Cancer Journal for Clinicians*, *70*(1), 7–30.

Siegfried, E.; Wilder, E. L.; & Perrimon, N. (1994). **Components of wingless signalling in Drosophila**. *Nature*, *367*(6458), 76–80. PMID: 8107779.

Sigismund, S.; Algisi, V.; Nappo, G.; Conte, A.; Pascolutti, R.; Cuomo, A.; Bonaldi, T.; Argenzio, E.; Verhoef, L. G. G. C.; Maspero, E.; Bianchi, F.; Capuani, F.; Ciliberto, A.; Polo, S.; & Di Fiore, P. P. (2013). **Threshold-controlled ubiquitination of the EGFR directs receptor fate**. *The EMBO Journal*, *32*(15), 2140–2157. PMID: 23799367.

Simpson, M. V. (1953). **The release of labeled amino acids from the proteins of rat liver slices**. *The Journal of Biological Chemistry*, *201*(1), 143–154. PMID: 13044783.

Slusarski, D. C.; Corces, V. G.; & Moon, R. T. (1997). **Interaction of Wnt and a Frizzled homologue triggers G-protein-linked phosphatidylinositol signalling**. *Nature*, *390*(6658), 410–413. PMID: 9389482.

Song, B.-L.; Sever, N.; & DeBose-Boyd, R. A. (2005). **Gp78, a Membrane-Anchored Ubiquitin Ligase, Associates with Insig-1 and Couples Sterol-Regulated Ubiquitination to Degradation of HMG CoA Reductase**. *Molecular Cell*, *19*(6), 829–840.

Speer, K. F.; Sommer, A.; Tajer, B.; Mullins, M. C.; Klein, P. S.; & Lemmon, M. A. (2019). **Non-acylated Wnts can promote signaling**. *Cell Reports*, *26*(4), 875-883.e5. PMID: 30673610.

Spranger, S.; Bao, R.; & Gajewski, T. F. (2015). **Melanoma-intrinsic β-catenin signalling prevents anti-tumour immunity**. *Nature*, *523*(7559), 231–235.

Stangl, A.; Elliott, P. R.; Pinto-Fernandez, A.; Bonham, S.; Harrison, L.; Schaub, A.; Kutzner, K.; Keusekotten, K.; Pfluger, P. T.; El Oualid, F.; Kessler, B. M.; Komander, D.; & Krappmann, D. (2019). **Regulation of the endosomal SNX27-retromer by OTULIN**. *Nature Communications*, *10*(1), 4320.

Steger, M.; Ihmor, P.; Backman, M.; Müller, S.; & Daub, H. (2020). **Deep ubiquitination site profiling by single-shot data-independent acquisition mass spectrometry**. *BioRxiv*, 2020.07.23.218651.

Steingrímsson, E.; Copeland, N. G.; & Jenkins, N. A. (2004). **Melanocytes and the microphthalmia transcription factor network**. *Annual Review of Genetics*, *38*, 365–411. PMID: 15568981.

Stelzer, G.; Rosen, N.; Plaschkes, I.; Zimmerman, S.; Twik, M.; Fishilevich, S.; Stein, T. I.; Nudel, R.; Lieder, I.; Mazor, Y.; Kaplan, S.; Dahary, D.; Warshawsky, D.; Guan-Golan, Y.; Kohn, A.; Rappaport, N.; Safran, M.; & Lancet, D. (2016). **The GeneCards Suite: From Gene Data Mining to Disease Genome Sequence Analyses**. *Current Protocols in Bioinformatics*, *54*, 1.30.1-1.30.33. PMID: 27322403.

Stengel, K.; & Zheng, Y. (2011). **Cdc42 in oncogenic transformation, invasion, and tumorigenesis**. *Cellular Signalling*, *23*(9), 1415–1423. PMID: 21515363.

Strochlic, T. I.; Schmiedekamp, B. C.; Lee, J.; Katzmann, D. J.; & Burd, C. G. (2008). **Opposing Activities of the Snx3-Retromer Complex and ESCRT Proteins Mediate Regulated Cargo Sorting at a Common Endosome**. *Molecular Biology of the Cell*, *19*(11), 4694–4706. PMID: 18768754.

Sun, Jianwei; Lu, F.; He, H.; Shen, J.; Messina, J.; Mathew, R.; Wang, D.; Sarnaik, A. A.; Chang, W.-C.; Kim, M.; Cheng, H.; & Yang, S. (2014). **STIM1- and Orai1-mediated Ca2+ oscillation orchestrates invadopodium formation and melanoma invasion**. *The Journal of Cell Biology*, *207*(4), 535–548. PMID: 25404747.

Sun, Jiaxin; Yu, S.; Zhang, X.; Capac, C.; Aligbe, O.; Daudelin, T.; Bonder, E. M.; & Gao, N. (2017). **A Wntless-SEC12 complex on the ER membrane regulates early Wnt secretory vesicle assembly and mature ligand export**. *Journal of Cell Science*, *130*(13), 2159–2171. PMID: 28515233.

Sun, X.; Gao, H.; Yang, Y.; He, M.; Wu, Y.; Song, Y.; Tong, Y.; & Rao, Y. (2019). **PROTACs: Great opportunities for academia and industry**. *Signal Transduction and Targeted Therapy*, *4*(1), 1–33.

Sun, Z.; & Brodsky, J. L. (2019). **Protein quality control in the secretory pathway**. *Journal of Cell Biology*, *218*(10), 3171–3187.

Swatek, K. N.; & Komander, D. (2016). **Ubiquitin modifications**. *Cell Research*, *26*(4), 399–422. PMID: 27012465.

Takada, R.; Satomi, Y.; Kurata, T.; Ueno, N.; Norioka, S.; Kondoh, H.; Takao, T.; & Takada, S. (2006). **Monounsaturated fatty acid modification of Wnt protein: Its role in Wnt secretion**. *Developmental Cell*, *11*(6), 791–801. PMID: 17141155.

Tatham, M. H.; Geoffroy, M.-C.; Shen, L.; Plechanovova, A.; Hattersley, N.; Jaffray, E. G.; Palvimo, J. J.; & Hay, R. T. (2008). **RNF4 is a poly-SUMO-specific E3 ubiquitin ligase required for arsenic-induced PML degradation**. *Nature Cell Biology*, *10*(5), 538–546. PMID: 18408734.

Tauriello, D. V. F.; Jordens, I.; Kirchner, K.; Slootstra, J. W.; Kruitwagen, T.; Bouwman, B. A. M.; Noutsou, M.; Rüdiger, S. G. D.; Schwamborn, K.; Schambony, A.; & Maurice, M. M. (2012). **Wnt/β-catenin signaling requires interaction of the Dishevelled DEP domain and C terminus with a discontinuous motif in Frizzled**. *Proceedings of the National Academy of Sciences of the United States of America*, *109*(14), E812-820. PMID: 22411803.

Terrell, J.; Shih, S.; Dunn, R.; & Hicke, L. (1998). **A Function for Monoubiquitination in the Internalization of a G Protein–Coupled Receptor**. *Molecular Cell*, *1*(2), 193–202. PMID: 9659916.

Thul, P. J.; Åkesson, L.; Wiking, M.; Mahdessian, D.; Geladaki, A.; Blal, H. A.; Alm, T.; Asplund, A.; Björk, L.; Breckels, L. M.; Bäckström, A.; Danielsson, F.; Fagerberg, L.; Fall, J.; Gatto,

L.; Gnann, C.; Hober, S.; Hjelmare, M.; Johansson, F.; … Lundberg, E. (2017). **A subcellular map of the human proteome**. *Science*, *356*(6340). PMID: 28495876.

Toyama, T.; Lee, H. C.; Koga, H.; Wands, J. R.; & Kim, M. (2010). **Noncanonical Wnt11 inhibits hepatocellular carcinoma cell proliferation and migration**. *Molecular Cancer Research: MCR*, *8*(2), 254–265. PMID: 20103596.

Tsuchiya, H.; Burana, D.; Ohtake, F.; Arai, N.; Kaiho, A.; Komada, M.; Tanaka, K.; & Saeki, Y. (2018). **Ub-ProT reveals global length and composition of protein ubiquitylation in cells**. *Nature Communications*, *9*. PMID: 29410401.

Twomey, E. C.; Ji, Z.; Wales, T. E.; Bodnar, N. O.; Ficarro, S. B.; Marto, J. A.; Engen, J. R.; & Rapoport, T. A. (2019). **Substrate processing by the Cdc48 ATPase complex is initiated by ubiquitin unfolding**. *Science*. PMID: 31249135.

Untergasser, A.; Cutcutache, I.; Koressaar, T.; Ye, J.; Faircloth, B. C.; Remm, M.; & Rozen, S. G. (2012). **Primer3—New capabilities and interfaces**. *Nucleic Acids Research*, *40*(15), e115. PMID: 22730293.

van Amerongen, R.; Fuerer, C.; Mizutani, M.; & Nusse, R. (2012). **Wnt5a can both activate and repress Wnt/β-catenin signaling during mouse embryonic development**. *Developmental Biology*, *369*(1), 101–114.

van Bokhoven, H.; Celli, J.; Kayserili, H.; van Beusekom, E.; Balci, S.; Brussel, W.; Skovby, F.; Kerr, B.; Percin, E. F.; Akarsu, N.; & Brunner, H. G. (2000). **Mutation of the gene encoding the ROR2 tyrosine kinase causes autosomal recessive Robinow syndrome**. *Nature Genetics*, *25*(4), 423–426. PMID: 10932187.

van Wijk, S. J. L.; de Vries, S. J.; Kemmeren, P.; Huang, A.; Boelens, R.; Bonvin, A. M. J. J.; & Timmers, H. T. M. (2009). **A comprehensive framework of E2–RING E3 interactions of the human ubiquitin–proteasome system**. *Molecular Systems Biology*, *5*, 295. PMID: 19690564.

Vijay-Kumar, S.; Bugg, C. E.; & Cook, W. J. (1987). **Structure of ubiquitin refined at 1.8 A resolution**. *Journal of Molecular Biology*, *194*(3), 531–544. PMID: 3041007.

Voloshanenko, O.; Erdmann, G.; Dubash, T. D.; Augustin, I.; Metzig, M.; Moffa, G.; Hundsrucker, C.; Kerr, G.; Sandmann, T.; Anchang, B.; Demir, K.; Boehm, C.; Leible, S.; Ball, C. R.; Glimm, H.; Spang, R.; & Boutros, M. (2013). **Wnt secretion is required to maintain high levels of Wnt activity in colon cancer cells**. *Nature Communications*, *4*, 2610. PMID: 24162018.

Voloshanenko, O.; Gmach, P.; Winter, J.; Kranz, D.; & Boutros, M. (2017). **Mapping of Wnt-Frizzled interactions by multiplex CRISPR targeting of receptor gene families**. *FASEB Journal: Official Publication of the Federation of American Societies for Experimental Biology*, *31*(11), 4832–4844. PMID: 28733458.

Voloshanenko, O.; Schwartz, U.; Kranz, D.; Rauscher, B.; Linnebacher, M.; Augustin, I.; & Boutros, M. (2018). **β-catenin-independent regulation of Wnt target genes by RoR2 and ATF2/ATF4 in colon cancer cells**. *Scientific Reports*, *8*. PMID: 29453334.

Wagle, N.; Emery, C.; Berger, M. F.; Davis, M. J.; Sawyer, A.; Pochanard, P.; Kehoe, S. M.; Johannessen, C. M.; Macconaill, L. E.; Hahn, W. C.; Meyerson, M.; & Garraway, L. A. (2011). **Dissecting therapeutic resistance to RAF inhibition in melanoma by tumor genomic profiling**. *Journal of Clinical Oncology: Official Journal of the American Society of Clinical Oncology*, *29*(22), 3085–3096. PMID: 21383288.

Wang, C.-W.; & Lee, S.-C. (2012). **The ubiquitin-like (UBX)-domain-containing protein Ubx2/Ubxd8 regulates lipid droplet homeostasis**. *Journal of Cell Science*, *125*(Pt 12), 2930–2939. PMID: 22454508.

Wang, G.; Liu, G.; Wang, X.; Sethi, S.; Ali-Fehmi, R.; Abrams, J.; Zheng, Z.; Zhang, K.; Ethier, S.; & Yang, Z.-Q. (2012). **ERLIN2 promotes breast cancer cell survival by modulating endoplasmic reticulum stress pathways**. *BMC Cancer*, *12*(1), 225.

Wang, G.; Zhang, X.; Lee, J.-S.; Wang, X.; Yang, Z.-Q.; & Zhang, K. (2012). **Endoplasmic reticulum factor ERLIN2 regulates cytosolic lipid content in cancer cells**. *The Biochemical Journal*, *446*(3), 415–425. PMID: 22690709.

Wang, J. X.; Fukunaga-Kalabis, M.; & Herlyn, M. (2016). **Crosstalk in skin: Melanocytes, keratinocytes, stem cells, and melanoma**. *Journal of Cell Communication and Signaling*, *10*(3), 191–196. PMID: 27553358.

Wang, Q.; Liu, Y.; Soetandyo, N.; Baek, K.; Hegde, R.; & Ye, Y. (2011). **A Ubiquitin Ligase-Associated Chaperone Holdase Maintains Polypeptides in Soluble States for Proteasome Degradation**. *Molecular Cell*, *42*(6), 758–770. PMID: 21636303.

Wang, X.; Herr, R. A.; Rabelink, M.; Hoeben, R. C.; Wiertz, E. J. H. J.; & Hansen, T. H. (2009). **Ube2j2 ubiquitinates hydroxylated amino acids on ER-associated degradation substrates**. *The Journal of Cell Biology*, *187*(5), 655–668. PMID: 19951915.

Wang, Y.; Pearce, M. M. P.; Sliter, D. A.; Olzmann, J. A.; Christianson, J. C.; Kopito, R. R.; Boeckmann, S.; Gagen, C.; Leichner, G. S.; Roitelman, J.; & Wojcikiewicz, R. J. H. (2009). **SPFH1 and SPFH2 Mediate the Ubiquitination and Degradation of Inositol 1,4,5-Trisphosphate Receptors in Muscarinic Receptor-Expressing Hela Cells**. *Biochimica et Biophysica Acta*, *1793*(11), 1710–1718. PMID: 19751772.

Weber, A.; Cohen, I.; Popp, O.; Dittmar, G.; Reiss, Y.; Sommer, T.; Ravid, T.; & Jarosch, E. (2016). **Sequential Poly-ubiquitylation by Specialized Conjugating Enzymes Expands the Versatility of a Quality Control Ubiquitin Ligase**. *Molecular Cell*, *63*(5), 827–839. PMID: 27570077.

Weber, J.; Polo, S.; & Maspero, E. (2019). **HECT E3 Ligases: A Tale With Multiple Facets**. *Frontiers in Physiology*, *10*.

Webster, M. R.; Kugel, C. H.; & Weeraratna, A. T. (2015). **The Wnts of Change: How Wnts Regulate Phenotype Switching in Melanoma**. *Biochimica et Biophysica Acta*, *1856*(2), 244–251. PMID: 26546268.

Webster, M. R.; & Weeraratna, A. T. (2013). **A Wnt-er migration: The confusing role of β-catenin in melanoma metastasis**. *Science Signaling*, *6*(268), pe11. PMID: 23532332.

Weeraratna, A. T.; Jiang, Y.; Hostetter, G.; Rosenblatt, K.; Duray, P.; Bittner, M.; & Trent, J. M. (2002). **Wnt5a signaling directly affects cell motility and invasion of metastatic melanoma**. *Cancer Cell*, *1*(3), 279–288. PMID: 12086864.

Widlund, H. R.; Horstmann, M. A.; Price, E. R.; Cui, J.; Lessnick, S. L.; Wu, M.; He, X.; & Fisher, D. E. (2002). **Beta-catenin-induced melanoma growth requires the downstream target Microphthalmia-associated transcription factor**. *The Journal of Cell Biology*, *158*(6), 1079–1087. PMID: 12235125.

Widmer, D. S.; Cheng, P. F.; Eichhoff, O. M.; Belloni, B. C.; Zipser, M. C.; Schlegel, N. C.; Javelaud, D.; Mauviel, A.; Dummer, R.; & Hoek, K. S. (2012). **Systematic classification of melanoma cells by phenotype-specific gene expression mapping**. *Pigment Cell & Melanoma Research*, *25*(3), 343–353. PMID: 22336146.

Wiese, K. E.; Nusse, R.; & Amerongen, R. van. (2018). **Wnt signalling: Conquering complexity**. *Development*, *145*(12). PMID: 29945986.

Willert, K.; Brown, J. D.; Danenberg, E.; Duncan, A. W.; Weissman, I. L.; Reya, T.; Yates, J. R.; & Nusse, R. (2003). **Wnt proteins are lipid-modified and can act as stem cell growth factors**. *Nature*, *423*(6938), 448–452. PMID: 12717451.

Winston, J. T.; Strack, P.; Beer-Romero, P.; Chu, C. Y.; Elledge, S. J.; & Harper, J. W. (1999). **The SCFβ-TRCP–ubiquitin ligase complex associates specifically with phosphorylated destruction motifs in IκBα and β-catenin and stimulates IκBα ubiquitination in vitro**. *Genes & Development*, *13*(3), 270–283. PMID: 9990852.

Wu, J.; Roman, A.-C.; Carvajal-Gonzalez, J. M.; & Mlodzik, M. (2013). **Wg and Wnt4 provide long-range directional input to planar cell polarity orientation in Drosophila**. *Nature Cell Biology*, *15*(9), 1045–1055. PMID: 23912125.

Wu, X.; Siggel, M.; Ovchinnikov, S.; Mi, W.; Svetlov, V.; Nudler, E.; Liao, M.; Hummer, G.; & Rapoport, T. A. (2020). **Structural basis of ER-associated protein degradation mediated by the Hrd1 ubiquitin ligase complex**. *Science (New York, N.Y.)*, *368*(6489). PMID: 32327568.

Xia, Y.; Yan, L. H.; Huang, B.; Liu, M.; Liu, X.; & Huang, C. (2014). **Pathogenic mutation of UBQLN2 impairs its interaction with UBXD8 and disrupts endoplasmic reticulum-associated protein degradation**. *Journal of Neurochemistry*, *129*(1), 99–106. PMID: 24215460.

Xu, H.; Jiang, W.; Zhu, F.; Zhu, C.; Wei, J.; & Wang, J. (2016). **Expression of Wntless in colorectal carcinomas is associated with invasion, metastasis, and poor survival**. *APMIS: Acta Pathologica, Microbiologica, et Immunologica Scandinavica*, *124*(6), 522–528. PMID: 27102079.

Xu, P.; Duong, D. M.; Seyfried, N. T.; Cheng, D.; Xie, Y.; Robert, J.; Rush, J.; Hochstrasser, M.; Finley, D.; & Peng, J. (2009). **Quantitative Proteomics Reveals the Function of Unconventional Ubiquitin Chains in Proteasomal Degradation**. *Cell*, *137*(1), 133–145. PMID: 19345192.

Yamamoto, H.; Awada, C.; Hanaki, H.; Sakane, H.; Tsujimoto, I.; Takahashi, Y.; Takao, T.; & Kikuchi, A. (2013). **The apical and basolateral secretion of Wnt11 and Wnt3a in polarized epithelial cells is regulated by different mechanisms**. *Journal of Cell Science*, *126*(Pt 13), 2931–2943. PMID: 23613470.

Yang, P.-T.; Anastas, J. N.; Toroni, R. A.; Shinohara, M. M.; Goodson, J. M.; Bosserhoff, A. K.; Chien, A. J.; & Moon, R. T. (2012). **WLS inhibits melanoma cell proliferation through the β-catenin signalling pathway and induces spontaneous metastasis**. *EMBO Molecular Medicine*, *4*(12), 1294–1307. PMID: 23129487.

Yang, P.-T.; Lorenowicz, M. J.; Silhankova, M.; Coudreuse, D. Y. M.; Betist, M. C.; & Korswagen, H. C. (2008). **Wnt signaling requires retromer-dependent recycling of MIG-14/Wntless in Wnt-producing cells**. *Developmental Cell*, *14*(1), 140–147. PMID: 18160347.

Yang, Y.; & Mlodzik, M. (2015). **Wnt-Frizzled/Planar Cell Polarity Signaling: Cellular Orientation by Facing the Wind (Wnt)**. *Annual Review of Cell and Developmental Biology*, *31*, 623–646. PMID: 26566118.

Ye, Y.; Meyer, H. H.; & Rapoport, T. A. (2001). **The AAA ATPase Cdc48/p97 and its partners transport proteins from the ER into the cytosol**. *Nature*, *414*(6864), 652–656. PMID: 11740563.

Yu, J.; Chia, J.; Canning, C. A.; Jones, C. M.; Bard, F. A.; & Virshup, D. M. (2014). **WLS Retrograde Transport to the Endoplasmic Reticulum during Wnt Secretion**. *Developmental Cell*, *29*(3), 277–291.

Yu, J. J. S.; Maugarny-Calès, A.; Pelletier, S.; Alexandre, C.; Bellaiche, Y.; Vincent, J.-P.; & McGough, I. J. (2020). **Frizzled-dependent Planar Cell Polarity without Wnt Ligands**. *BioRxiv*, 2020.05.23.108977.

Zeng, L.; Fagotto, F.; Zhang, T.; Hsu, W.; Vasicek, T. J.; Perry, W. L.; Lee, J. J.; Tilghman, S. M.; Gumbiner, B. M.; & Costantini, F. (1997). **The Mouse Fused Locus Encodes Axin, an Inhibitor of the Wnt Signaling Pathway That Regulates Embryonic Axis Formation**. *Cell*, *90*(1), 181–192.

Zeng, X.; Tamai, K.; Doble, B.; Li, S.; Huang, H.; Habas, R.; Okamura, H.; Woodgett, J.; & He, X. (2005). **A dual-kinase mechanism for Wnt co-receptor phosphorylation and activation**. *Nature*, *438*(7069), 873–877.

Zhai, L.; Chaturvedi, D.; & Cumberledge, S. (2004). **Drosophila wnt-1 undergoes a hydrophobic modification and is targeted to lipid rafts, a process that requires porcupine**. *The Journal of Biological Chemistry*, *279*(32), 33220–33227. PMID: 15166250.

Zhan, T.; Ambrosi, G.; Wandmacher, A. M.; Rauscher, B.; Betge, J.; Rindtorff, N.; Häussler, R. S.; Hinsenkamp, I.; Bamberg, L.; Hessling, B.; Müller-Decker, K.; Erdmann, G.; Burgermeister, E.; Ebert, M. P.; & Boutros, M. (2019). **MEK inhibitors activate Wnt signalling and induce stem cell plasticity in colorectal cancer**. *Nature Communications*, *10*(1), 2197.

Zhan, T.; Rindtorff, N.; & Boutros, M. (2017). **Wnt signaling in cancer**. *Oncogene*, *36*(11), 1461–1473. PMID: 27617575.

Zhang, J.; Liu, J.; Norris, A.; Grant, B. D.; & Wang, X. (2018). **A novel requirement for ubiquitin-conjugating enzyme UBC-13 in retrograde recycling of MIG-14/Wntless and Wnt signaling**. *Molecular Biology of the Cell*, *29*(17), 2098–2112. PMID: 29927348.

Zhang, L.-S.; & Lum, L. (2018). **Chemical Modulation of WNT Signaling in Cancer**. *Progress in Molecular Biology and Translational Science*, *153*, 245–269. PMID: 29389519.

Zhang, P.; Wu, Y.; Belenkaya, T. Y.; & Lin, X. (2011). **SNX3 controls Wingless/Wnt secretion through regulating retromer-dependent recycling of Wntless**. *Cell Research*, *21*(12), 1677–1690. PMID: 22041890.

Zhang, Xianjun; Dong, S.; & Xu, F. (2018). **Structural and Druggability Landscape of Frizzled G Protein-Coupled Receptors**. *Trends in Biochemical Sciences*, *43*(12), 1033–1046.

Zhang, Xuebao; Cai, J.; Zheng, Z.; Polin, L.; Lin, Z.; Dandekar, A.; Li, L.; Sun, F.; Finley, R. L.; Fang, D.; Yang, Z.-Q.; & Zhang, K. (2015). **A novel ER–microtubule-binding protein, ERLIN2, stabilizes Cyclin B1 and regulates cell cycle progression**. *Cell Discovery*, *1*(1), 1–18.

Zhao, S.-B.; Dean, N.; Gao, X.-D.; & Fujita, M. (2020). **MON2 Guides Wntless Transport to the Golgi through Recycling Endosomes**. *Cell Structure and Function*, *45*(1), 77–92. PMID: 32404555.

Zhou, C.; Yang, X.; Sun, Y.; Yu, H.; Zhang, Y.; & Jin, Y. (2016). **Comprehensive profiling reveals mechanisms of SOX2-mediated cell fate specification in human ESCs and NPCs**. *Cell Research*, *26*(2), 171–189.

Zuidervaart, W.; Pavey, S.; van Nieuwpoort, F. A.; Packer, L.; Out, C.; Maat, W.; Jager, M. J.; Gruis, N. A.; & Hayward, N. K. (2007). **Expression of Wnt5a and its downstream effector beta-catenin in uveal melanoma**. *Melanoma Research*, *17*(6), 380–386. PMID: 17992121.

6.2 List of Figures

Figure Title **Page**

Supplementary Figure Title **Page**

6.3 List of Tables

Table Title Page

6.4 Abbreviations & Units

6.4.1 Abbreviations

Table 21. Abbreviations (Abbr.)

Abbr.	Designation
Abbr.	Abbreviations
ADP	Adenosine diphosphate
AIDA	AXIN interactor, dorsalization-associated protein
AMFR/ GP78	Autocrine motility factor receptor
AMP	Adenosine monophosphate
AP-2	Adaptor protein 2
APC	Adenomatous polyposis coli
APF-1	Active principle of fraction 1
ARF	ADP-ribosylation factor
Asi	Amino acid sensor-independent
ATCC	American Type Culture Collection
ATF2	AMP-dependent transcription factor 2
ATG	Autophagy related genes
ATP	Adenosine triphosphate
ATP9A	Probable phospholipid-transporting ATPase IIA
ATXN3	Ataxin 3
AXIN	Axis inhibition protein
BAG6	BCL2-associated athanogene 6
BCA	Bicinchonic acid
BCL9	B-cell lymphoma 9
BiP	Binding ig protein
Bp	Base pairs
BSA	Bovine serum albumin
C. elegans	*Caenorhabditis elegans*
CAM	Calmodulin
CAMKII	Ca^{2+}/CAM-dependent kinase II
CBL	Casitas B-lineage lymphoma proto-oncogene
CDC42	Cell division control protein 42
CDKN2A	Cyclin-dependent kinase-inhibitor 2A
cDNA	Complementary DNA
CELSR	Cadherin EGF LAG seven-pass G-type receptor
CFTR	Cystic fibrosis transmembrane conductance regulator
CGRRF1	Cell growth regulator with RING finger domain 1
CHX	Cycloheximide
CK	Casein kinase
CLR	Calreticulin
CNX	Calnexin
COP	Coat protein complex
C_q	Quantification cycles
CRD	Cysteine-rich domain
CRISPR	Clustered regularly interspaced short palindromic repeats
C-terminus	Carboxy terminus
CTNNB1	β-catenin gene
Ctrl	Control
Cue1	Coupling of Ub conjugation to ER degradation 1
DAAM1	DVL associated activator of morphogenesis 1
DAG	Diacylglycerol
DAPI	4′,6-diamidino-2-phenylindole
DERL	Derlin
DKFZ	German Cancer Research Center
DKK	Dickkopf
DMEM	Dulbecco's modified Eagle's medium
DMSO	Dimethyl sulfoxide

Continued on the next page

Abbr.	Designation
DNA	Deoxyribonucleic acid
Doa10	Degradation of α2 protein
Dr. rer. nat.	Doctor rerum naturalium
DTT	Dithiothreitol
DUB	Deubiquitinating enzyme
DVL	Dishevelled
EDEM	ER degradation-enhancing α-mannosidase-like 1 protein
EDTA	Ethylenediaminetetraacetic acid
e.g.	*Exempli gratia*, for example
EGAD	Endosome and Golgi-associated degradation
EGF	Epidermal growth factor
EGFR	Epidermal growth factor receptor
ER	Endoplasmic reticulum
ERAD	ER-associated degradation
ERGIC2	ER-Golgi intermediate compartment protein 2
ERK	Extracellular signal-regulated kinase
ERLEC1	ER lectin 1
ERLIN	ER lipid raft associated
ESCRT	Endosomal sorting complexes required for transport
EVI	Evenness interrupted
FAF2	Fas associated factor family member 2
FCS	Fetal calf serum
FZD	Frizzled
G protein	Guanine nucleotide-binding protein
GPCF	Genomics and Proteomics Core Facility
GRB2	Growth factor receptor-bound protein 2
GSK3	Glycogen synthase kinase-3
gt	Goat
HECT	Homologous to E6AP carboxy-terminus
HEK	Human embryonic kidney
HER2	Human epidermal growth factor receptor 2
HERPUD	Homocysteine inducible ER protein with Ub like domain
HMG-CoA	β-hydroxy β-methylglutaryl coenzyme A
HOPS	Homotypic fusion and protein sorting
Hrd	HMG-CoA reductase degradation protein
SYVN1	Synoviolin 1
HRP	Horse radish peroxidase
HSC70	Heat shock protein 70 kDa
ID	Identifier
IF	Immunofluorescence
IgG (H+L)	Gamma immunoglobins heavy and light chains
ILV	Intraluminal vesicles
INSIG	Insulin-induced gene 1
IP	Immunoprecipitation
IP_3	Inositol 1,4,5-trisphosphate
IP_3R	IP_3 receptor
JNK	JUN N-terminal kinase
kDa	Kilodalton
KO	Knock-out
LB	Lysogeny broth
LEF	Lymphoid enhancer factor
LGR4/5	Leucine-rich repeat containing G protein-coupled receptor 4/5
LRP5/6	Low-density lipoprotein-receptor-related proteins 5/6
MAPK	Mitogen-activated protein kinase
MARCH	Membrane associated RING-CH-type finger
MHC	Major histocompatibility complex
MIQE	Minimum Information for Publication of RT-qPCR Experiments

Continued on the next page

Abbr.	Designation
MITF	Microphthalmia-associated transcription factor
MLANA	Melan-A
MMP	Matrix metalloproteases
mono	Monoclonal
MOPS	3-(N-morpholino)propane-sulfonic acid
MRH	Mannose 6-phosphate receptor homology
ms	Mouse
MVB	Multivesicular body
NA	Not applicable
NEDD8	Neural precursor cell expressed developmentally down-regulated protein 8
NEM	N-ethylmaleimide
NFAT	Nuclear factor of activated T cells
NGLY	N-Glycanase 1
NLK	Nemo-like kinase
NPLOC4	Nuclear protein localization protein 4 homolog
N-terminus	Amino terminus
oPA	1,10-Phenanthroline
ORF	Open reading frame
OS9	Osteosarcoma 9, ER lectin
OST	Oligosaccharyltransferase
p.	Protein sequence
PBS	Phosphate buffered saline
PCP	Planar cell polarity
PCR	Polymerase chain reaction
PD-1	Programmed cell death protein 1
PDB	Protein data bank
PD-L1	Programmed cell death ligand 1
PFA	Paraformaldehyde
pH	Pondus Hydrogenii
PhD	Doctor of Philosophy
PIP_2	Phosphatidylinositol-4,5-bisphosphate
PK	Prickle-like protein
PKC	Protein kinase C
PLC	Phospholipase C
PMEL	Premelanosome protein
poly	Polyclonal
PORCN	Protein-serine O-palmitoleoyltransferase porcupine
P-P	Pyrophosphate
PROTAC	PROteolysis-TArgeting Chimera
PTEN	Phosphatase-and-tensin homologue
PTK	Protein tyrosine kinase 7
PTM	Post-translational modifications
RAB	RAS-associated binding
RAD23	RAD23 homolog, nucleotide excision repair protein
RAS	Rat sarcoma
rb	Rabbit
RBR	RING between RING
RHBDD	Rhomboid domain containing 1
Rho	RAS homolog family
RING	Really interesting new gene
RNA	Ribonucleic acid
RNF	RING finger protein
ROCK	Rho-associated protein kinase
ROR	Receptor tyrosine kinase like orphan receptor
RPMI	Roswell Park Memorial Institute
RSPO	R-Spondin
RT-qPCR	Reverse-transcription quantitative PCR
RYK	Receptor like tyrosine kinase
S.O.C.	Super optimal broth with catabolite repression
SAR1	Secretion associated RAS related GTPase 1
SDS	Sodium dodecyl sulfate

Continued on the next page

Abbr.	Designation
SDS-PAGE	SDS-polyacrylamide gel electrophoresis
SEL1L	Suppressor of lin-12-like protein 1
sFRP	Soluble frizzled related protein
SH3PXD 2A	SH3 and PX domains 2A
siRNA	Small interfering ribonucleic acid
SNARE	Soluble N-ethylmaleimide-sensitive factor attachment protein receptor
SNX3	Sorting nexin 3
SOST	Sclerostin
SPP	Signal peptide peptidase
SUMO	Small Ub-like modifier
SUS	Self-ubiquitinating substrate
SWIM	Secreted wingless-interacting molecule
TBS	Tris-buffered saline
TBST	TBS with Tween-20
TCEP	Tris-(2-carboxyethyl)-phosphin
TCF	T cell factor
TCGA	The Cancer Genome Atlas
TCRα	T cell receptor α
TERT	Telomerase reverse-transcriptase
TLE	Transducin-like enhancer protein
TMED	Transmembrane p24 trafficking proteins
TMUB1/2	Transmembrane and Ub like domain containing 1/2
TNF	Tumour necrosis factor
TRAF6	TNF receptor-associated factor 6
TRC35	Transmembrane domain recognition complex 35 kDa subunit

Abbr.	Designation
TrCP	transducin repeat-containing protein
TUBE	Tandem Ub binding entity
TYR	Tyrosinase
Ub	Ubiquitin
UBA	Ub-associated
UBAC2	UBA domain containing 2
UBC	Ub-conjugating domain
UBD	Ub-binding domain
UBE2	Ub conjugating enzyme E2
UBE4B	Ubiquitination factor E4B
UBQLN2	Ubiquilin 2
UBX	Ubiquitin regulatory X
UBXN4	UBX domain protein 4
UBXN6/ UBXD1	UBX domain protein 6
UFD1	Ub recognition factor in E-RAD 1
ULK1	Unc-51-like kinase 1
UPL	Ub-protein ligase
UPS	Ub-proteasome system
USA	United States of America
Usa1	U1 SNP1-associating protein 1
USP	Ub-specific protease
UV	Ultraviolet
VANGL	Vang-like protein
VCP	Valosin-containing protein
VCPIP1	VCP interacting protein 1
VIM/VBM	VCP-interacting/binding motifs
WB	Western blot
Wg	Wingless
WGA	Wheat germ agglutinin
WIF	WNT inhibitory protein
WLS	Wntless
WNT/ STOP	WNT-dependent stabilisation of proteins
YOD1	YOD1 deubiquitinase
ZNRF3	Zinc and RING finger 3

6.4.2 Parameter & Units

Table 22. Parameter & Units

Parameter	Unit	Symbol	Comments
Amount of substance	Mole	mol	1 mol = 6.022x 10^{23} particles
Atomic mass	Dalton	Da	No SI unit, 1 Da ~ 1.660 538 92 x 10^{-27} kg
Centrifugation force	Gravity	x g	Here: used to indicate centrifugation speeds
Concentration	Molarity	M	Mol/l or g/l
Enzyme activity	Unit	U	Amount of enzyme converting 1 µl substrate/min
Mass	Gram	g	-
pondus Hydrogenii		pH	$-\log_{10}(H_3O^+)$
Sedimentation coefficient	Svedberg	S	Relates to a particle's size
Temperature	Kelvin	K	1 K = 273 °C; RT = 20 - 25 °C
Time	Second	s, sec	1 day (d) = 24 h; 1 hour (h) = 60 minutes (min); 1 min = 360 s
Voltage	Volt	V	-
Volume	Liter	l	1 l = 1 dm³

Table 23. Amino acids and IUPAC codes

Amino acid	3-letter IUPAC Code	1-letter IUPAC Code
Alanine	Ala	A
Arginine	Arg	R
Asparagine	Asn	N
Aspartic acid	Asp	D
Cysteine	Cys	C
Glutamic acid	Glu	E
Glutamine	Gln	Q
Glycine	Gly	G
Histidine	His	H
Isoleucine	Ile	I
Leucine	Leu	L
Lysine	Lys	K
Methionine	Met	M
Phenylalanine	Phe	F
Proline	Pro	P
Serine	Ser	S
Threonine	Thr	T
Tryptophan	Tyr	W
Tyrosine	Tyr	Y
Valine	Val	V
Nonsense, stop-codon		X

Table 24. Nucleotides

IUPAC symbol	Nucleotide
A	Adenine
C	Cytosine
G	Guanine
T	Thymine

Table 25. Prefixes for units

Prefix - name	Prefix - symbol	10^n
giga	G	10^9
mega	M	10^6
kilo	k	10^3
deci	d	10^{-1}
centi	c	10^{-2}
milli	m	10^{-3}
micro	µ	10^{-6}
nano	n	10^{-9}
pico	p	10^{-12}

7 Appendix

7.1 Supplementary figures

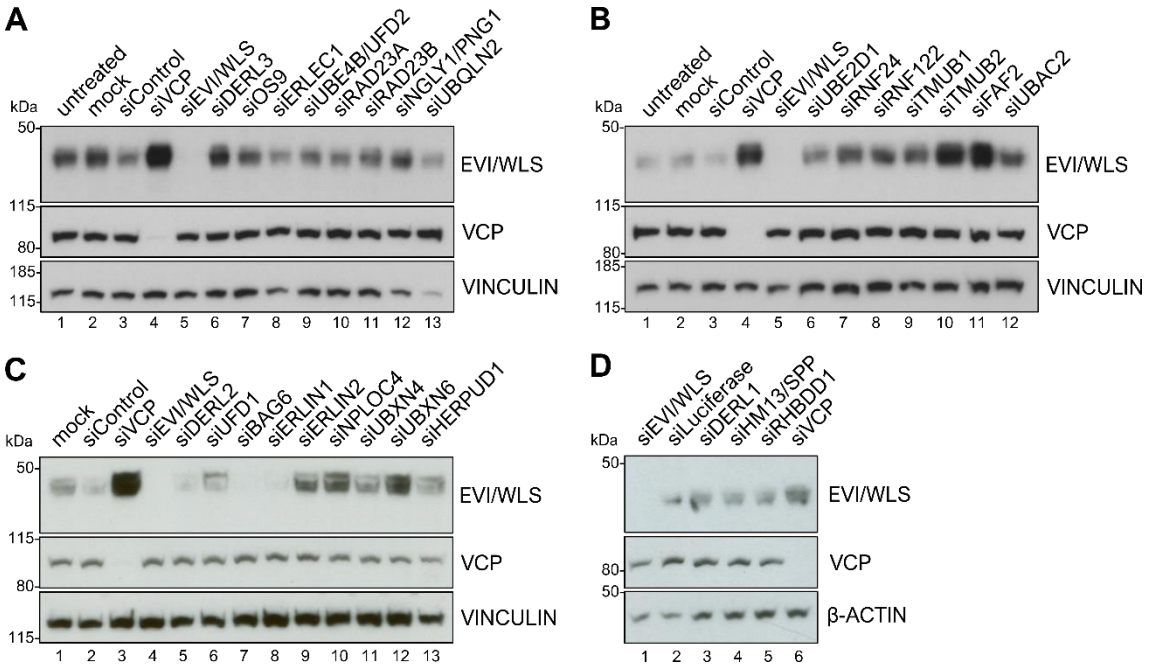

Supplementary Figure S1. Western blots to Figure 1 'siRNA-based mini-screen identifies novel candidates involved in the degradation of EVI/WLS in HEK293T cells'

EVI/WLS protein levels were analysed after siRNA mediated knock-down of target genes. Increased EVI/WLS protein levels compared to siControl/siLuciferase treatment indicated the candidate's possible involvement in EVI/WLS's ERAD process. HEK293T wild type cells were treated with the indicated siRNAs for 72 h. Then, total cell lysates were analysed by SDS-PAGE and Western blotting for the specified proteins. VINCULIN and β-ACTIN served as loading controls. Untreated samples or samples treated with transfection reagent only (mock), non-targeting siRNA (siControl), or siLuciferase were used as negative control. siVCP was used as positive control. The experiments shown in **A & B** were performed by Julie Haenlin, the experiment shown in **C** was performed by Annika Lambert. kDa = kilodalton

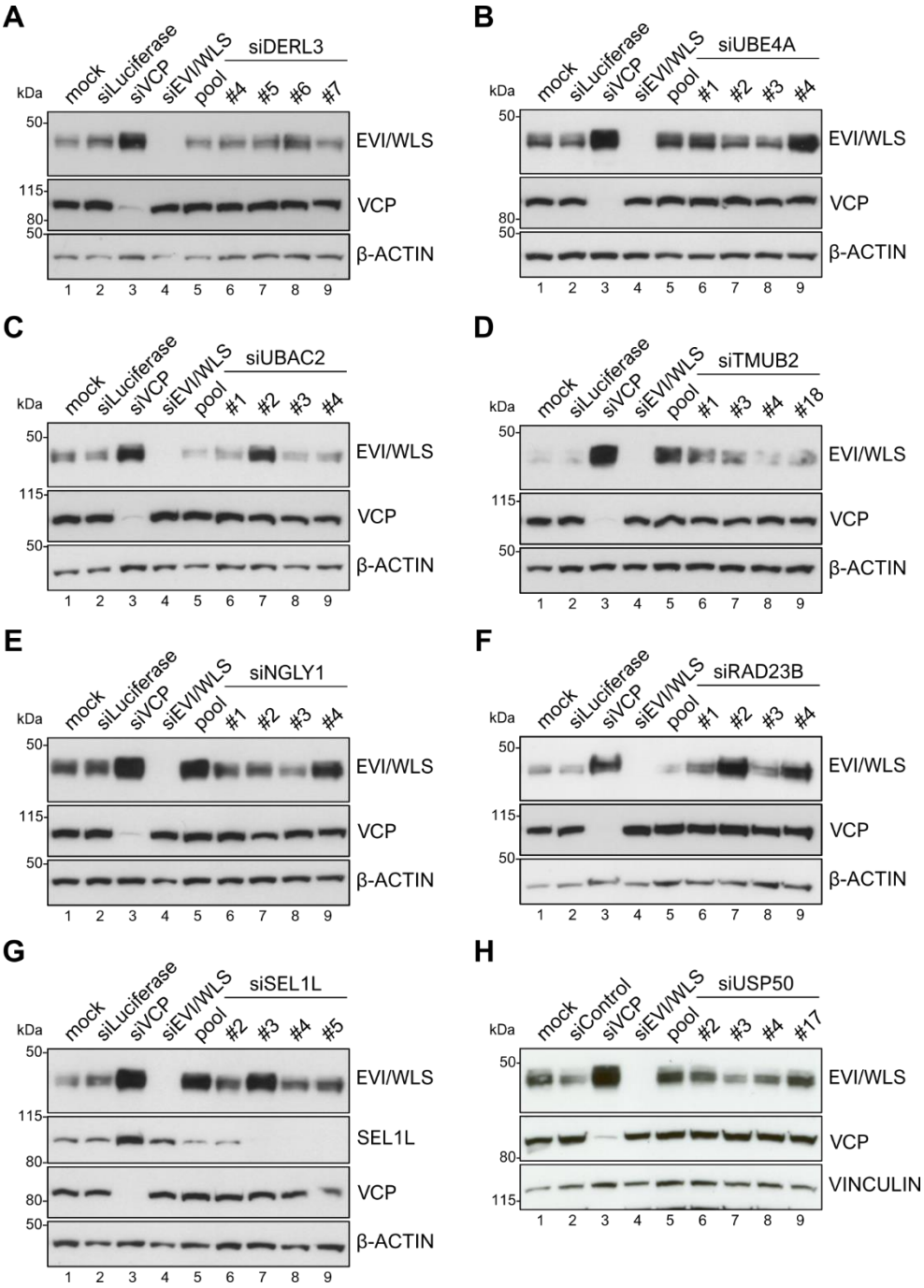

Supplementary Figure S2. The knock-down of DERL3, UBE4A, UBAC2, TMUB2, NGLY1, RAD23B, SEL1L, or USP50 by single siRNAs did not show consistent upregulation of EVI/WLS

EVI/WLS protein levels did not differ from the control or varied between biological replicates and single siRNAs against the candidates investigated in **A - H**. HEK293T wild type cells were treated with the indicated siRNAs for 72 h. Each gene's mRNA was targeted by either single siRNAs or an equimolecular mix of all four respective siRNAs (pool) to analyse their effect on EVI/WLS protein level. Total cell lysates were analysed by SDS-PAGE and Western blotting for the specified proteins. VINCULIN or β-ACTIN served as loading controls. Samples treated with transfection reagent only (mock), non-targeting siRNA (siControl), or siLuciferase were used as negative control, siVCP as positive control. The experiments shown here were performed by Annika Lambert. Western blots represent an example of three independent experiments. kDa = kilodalton

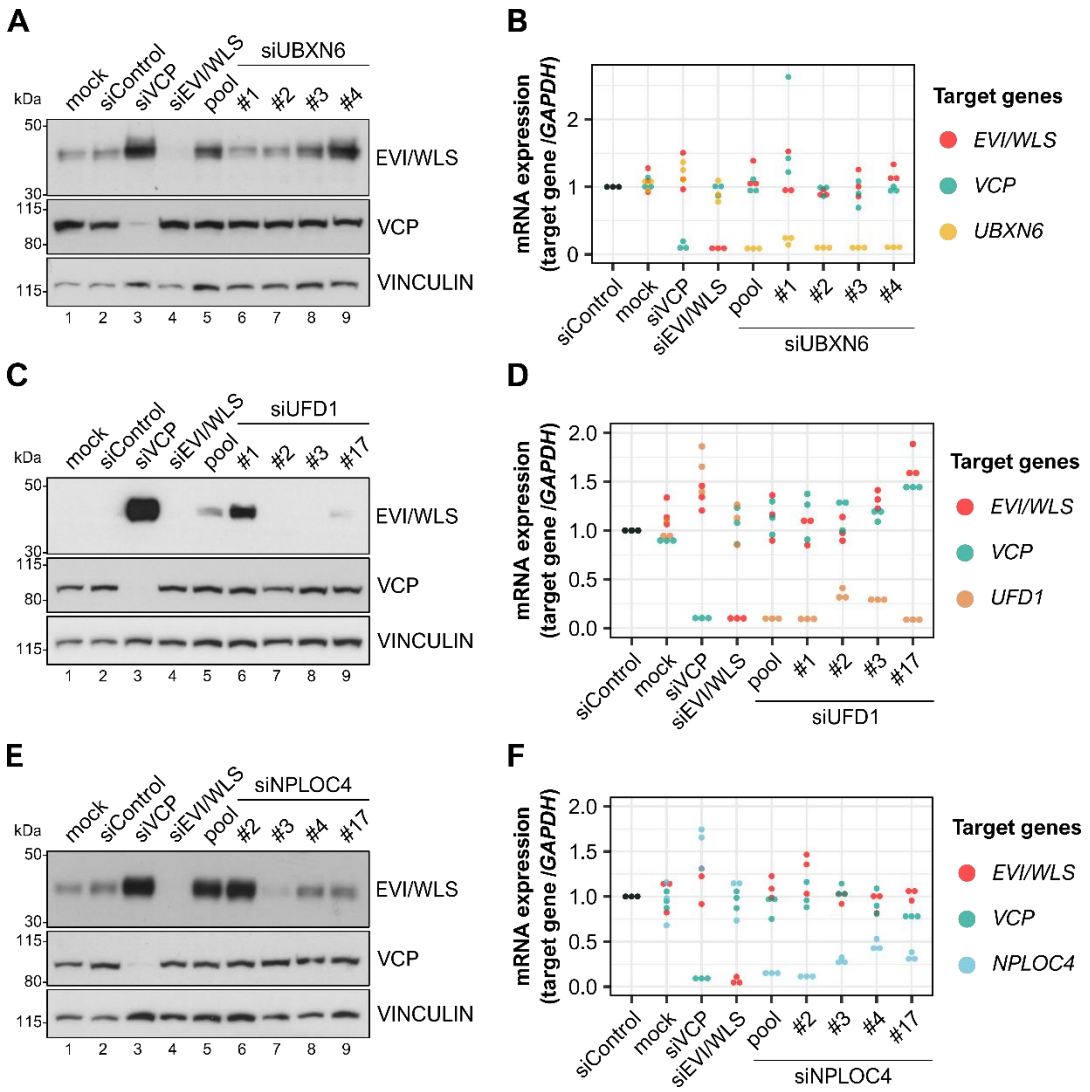

Supplementary Figure S3.The knock-down of UBXN6, UFD1, or NPLOC4 by single siRNAs did not show consistent upregulation of EVI/WLS

EVI/WLS protein levels did not differ from the control or varied between biological replicates and different single siRNAs after treatment with single or pooled siRNAs against the candidates investigated here (**A, C, E**). mRNA expression analyses demonstrated mostly efficient gene silencing by pooled or single siRNAs with little effects on other investigated mRNAs (**B, D, F**).

HEK293T wild type cells were treated with the indicated siRNAs for 72 h. Each gene's mRNA was targeted by either single siRNAs or an equimolecular mix of all four respective siRNAs (pool) to analyse their effect on EVI/WLS protein level or mRNA expression. Samples treated with transfection reagent only (mock) and non-targeting siRNA (siControl) were used as negative control, siVCP as positive control. The experiments shown here were performed by Julie Haenlin.

A, C, E. Total cell lysates were analysed by SDS-PAGE and Western blotting for the specified proteins. VINCULIN served as loading control. Western blots are representative of three independent experiments. kDa = kilodalton

B, D, F. Total cellular RNA was transcribed to cDNA and used for mRNA expression analyses by RT-qPCR. Target gene expression was normalised to siControl treatment and *GAPDH* served as reference gene. Individual data points from three independent experiments are shown.

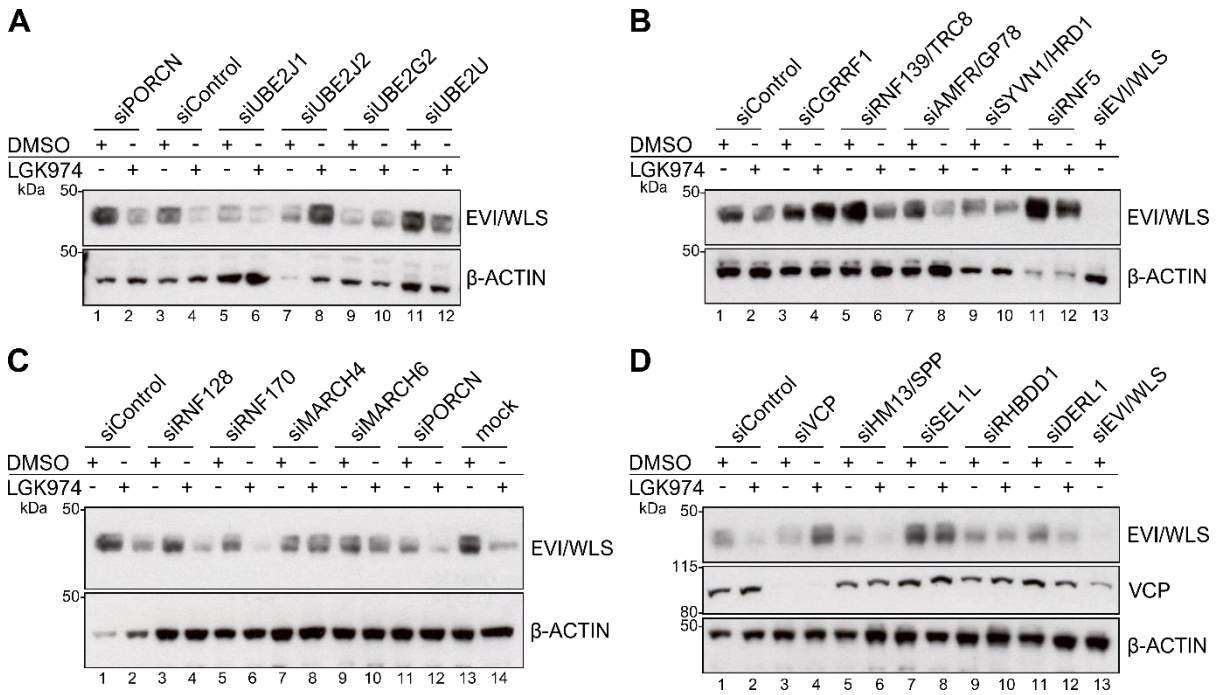

Supplementary Figure S4. EVI/WLS is degraded with the help of VCP, CGRRF1, and UBE2J2 in A375 melanoma cells

Knock-down of VCP, CGRRF1, or UBE2J2 prevented degradation of EVI/WLS after LGK974 treatment. A375 melanoma cells were treated with LGK974 (10 µM) or equivalent volumes of DMSO as solvent control with daily medium changes. 24 h after start of compound treatment, cells were additionally transfected with siRNAs, as indicated. Samples treated with transfection reagent only (mock) and non-targeting siRNA (siControl) were used as negative control, siVCP as positive control. Again 72 h later, total cell lysates were analysed by SDS-PAGE and Western blotting for the specified proteins. β-ACTIN served as loading control. Western blots are representative of three independent experiments. kDa = kilodalton

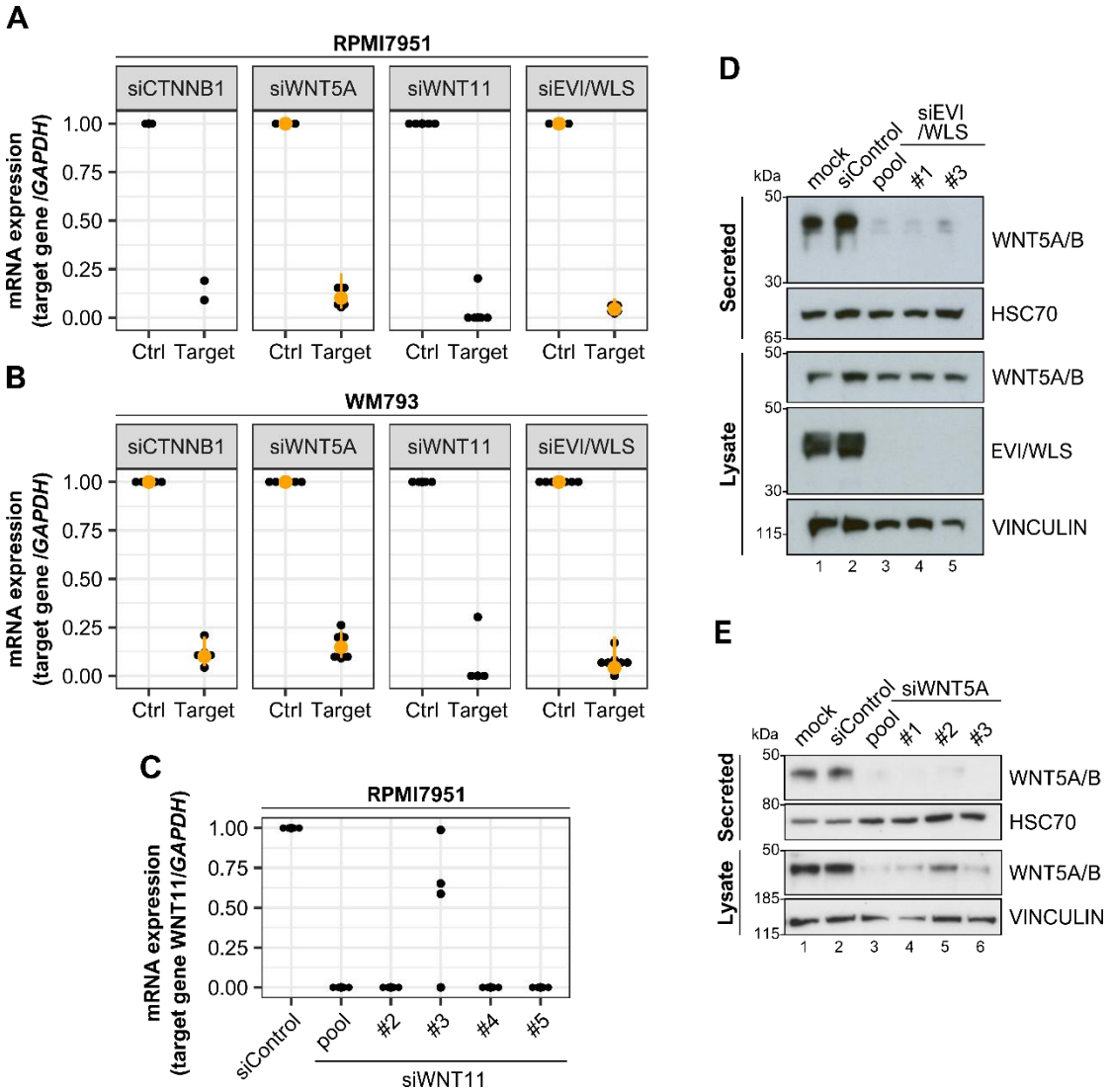

Supplementary Figure S5. siRNA mediated knock-down of targets is efficient in melanoma cells

RPMI7951 or WM793 melanoma cells were treated with the indicated siRNAs for 72 h. Each gene's mRNA was targeted by either single siRNAs or an equimolecular mix of the single siRNAs (pool). Samples treated with transfection reagent only (mock) or non-targeting siRNA (siControl) were used as negative control.

A, B, C. After pre-treatment with siRNAs, total cellular RNA was transcribed to cDNA and used for mRNA expression analyses by RT-qPCR. Target gene expression was normalised to siControl treatment (Ctrl) and *GAPDH* served as reference gene. Individual data points from at least two independent experiments are shown with mean and confidence interval (orange), where applicable. *WNT11* values shown as 0 were below detection limit.

D, E. After pre-treatment of RPMI7951 cells with siRNAs, secreted proteins were precipitated from the supernatant using Blue Sepharose. Eluates and total cell lysates were analysed by SDS-PAGE and Western blotting for the specified proteins. VINCULIN or HSC70 served as loading control. The experiment shown in **E** was performed by Annika Lambert. Western blots are representative of three independent experiments. kDa = kilodalton

7.2 Supplementary table

Supplementary Table 1. Genes investigated for EVI/WLS protein stability and phenotypes in HEK293T and A375 cells

	Gene	NCBI gene ID	UniProt KB	Cell line	Re-sult	Refe-rence
	UBE2D1	7321	P51668	HEK293T	-	this work
	UBE2G1	7326	P62253	HEK293T	-	this work
	UBE2G2	7327	P60604	HEK293T	-	Glaeser
				A375	-/+	this work
E2 Ub conjuga-ting en-zymes	UBE2J1	51465	Q9Y385	HEK293T	-	Glaeser
				A375	-	this work
	UBE2J2	118424	Q8N2K1	HEK293T	++	Glaeser
				A375	++	this work
	UBE2K	3093	P61086	HEK293T	++	this work
	UBE2N/UBC13	7334	P61088	HEK293T	+/++	this work
	UBE2U	148581	Q5VVX9	HEK293T	-	Glaeser
				A375	-	this work
E3 Ub ligases	AMFR/GP78/RNF45	267	Q9UKV5	HEK293T	-/+	Glaeser
				A375	+	this work
	CGRRF1/ RNF197	10668	Q99675	HEK293T	++	Glaeser
				A375	++	this work
	HRD1/SYVN1	84447	Q86TM6	HEK293T	-	Glaeser
				A375	-	this work
	MARCH4/ RNF174	57574	Q9P2E8	HEK293T	-	Glaeser
				A375	+/++	this work
	MARCH6/TEB4/ RNF176	10299	O60337	HEK293T	+	Glaeser
				A375	-/+	this work
	RNF5	6048	Q99942	HEK293T	-/+	Glaeser
				A375	+	this work
	RNF24	11237	Q9Y225	HEK293T	-/+	this work
	RNF122	79845	Q9H9V4	HEK293T	-/+	this work
	RNF128	79589	Q8TEB7	HEK293T	-	Glaeser
				A375	-/+	this work
	RNF139/TRC8	11236	Q8WU17	HEK293T	+	Glaeser
				A375	-	this work
	RNF170	81790	Q96K19	HEK293T	-	Glaeser
				A375	-	this work
	UBE4B/UFD2	10277	O95155	HEK293T	-	this work

Continued on the next page

	Gene	NCBI gene ID	UniProt KB	Cell line	Re-sult	Refe-rence
Sub-strate recogni-tion	ERLEC1	27248	Q96DZ1	HEK293T	-/+	this work
	ERLIN1/SPFH1	10613	O75477	HEK293T	-	this work
	ERLIN2/SPFH2	11160	O94905	HEK293T	+/++	this work
	OS9/ERLEC2	10956	Q13438	HEK293T	-	this work
	SEL1L/HRD3	6400	Q9UBV2	HEK293T	+	this work
				A375	+	this work
Retro-trans-location/ Disloca-tion	DERL1	79139	Q9BUN8	HEK293T	+	this work
				A375	-	this work
	DERL2	51009	Q9GZP9	HEK293T	+	this work
	DERL3	91319	Q96Q80	HEK293T	+/++	this work
	FAF2/ETEA/UBXD8	23197	Q96CS3	HEK293T	+/++	this work
	HM13/SPP	81502	Q8TCT9	HEK293T	+	this work
				A375	-	this work
	NPLOC4/NPL4	55666	Q8TAT6	HEK293T	+/++	this work
	RHBDD1/ RHBDL4	84236	Q8TEB9	HEK293T	+	this work
				A375	-	this work
	UBAC2	337867	Q8NBM4	HEK293T	+	this work
	UBXN4/ERASIN/UBXD2	23190	Q92575	HEK293T	+/++	this work
	UBXN6/ UBXD1	80700	Q9BZV1	HEK293T	+/++	this work
	UFD1/UFD1L	7353	Q92890	HEK293T	+/++	this work
	VCP/P97/CDC48	7415	P55072	HEK293T	++	Glaeser
				A375	++	this work
Delivery to the protea-some	BAG6/BAT3/ SCYTHE	7917	P46379	HEK293T	-	this work
	HERPUD1/HERP	9709	Q15011	HEK293T	+	this work
	NGLY/PNG1	55768	Q96IV0	HEK293T	+	this work
	RAD23A	5886	P54725	HEK293T	-/+	this work
	RAD23B	5887	P54727	HEK293T	-/+	this work
	TMUB1/HOPS	83590	Q9BVT8	HEK293T	-	this work
	TMUB2	79089	Q71RG4	HEK293T	+/++	this work
	UBQLN2/DSK2	29978	Q9UHD9	HEK293T	-	this work
De-ubiquiti-nating enzmes	ATXN3	4287	P54252	HEK293T	-	this work
	USP13	8975	Q92995	HEK293T	-	this work
	USP19	10869	O94966	HEK293T	+	this work
	USP25	29761	Q9UHP3	HEK293T	-	this work
	USP50	373509	Q70EL3	HEK293T	+/++	this work
	VCPIP1	80124	Q96JH7	HEK293T	-	this work
	YOD1/OTUD2	55432	Q5VVQ6	HEK293T	-	this work

Ub: Ubiquitin; - no effect, + low/variable upregulation, ++ consistent upregulation; Glaeser: Glaeser et al., 2018, PMID: 29378775

7.3 Scientific publications, presentations, and supervision

Publications

Dix CL, Matthews HK, Uroz M, McLaren S, Wolf L, Heatley N, Win Z, Almada P, Henriques R, Boutros M, Trepat X, Baum B (2018). **The Role of Mitotic Cell-Substrate Adhesion Re-modeling in Animal Cell Division.** *Developmental Cell*, PMID: 29634933

Wolf L, Lambert A, Haenlin J, Boutros M. **EVI/WLS is ubiquitinated by multiple E2 enzymes and linked to ERAD by ERLIN2**. *In preparation*

Voloshanenko O, Aponte D, Seidl C, Wolf L, Kranz D, Ivanova A, Rindtorff N, Augustin I, Russel R, Niehrs C, Brügger B, Boutros M. **Molecular determinants in Wnts for canonical and non-canonical signaling.** *In preparation*

Rauscher B, Henkel L, Heigwer F, Wolf L, Erdmann G, Boutros M. **A Pan-Cancer Analysis of Tumor Cell Lineage Dependencies.** *In preparation*

Oral presentations

7th Anglo-French-German Workshop on Skin Cancer Biology, 2018, Mannheim, Germany

Identification of genes linked to aberrant Wnt signalling in melanoma, Wolf L

5th Anglo-German Workshop on Skin Cancer Biology, 2016, London, United Kingdom

Identification of genes linked to aberrant Wnt signalling in melanoma, Wolf L

Poster presentations

DKFZ FSP-B Retreat, 2020, Kloster Schöntal, Germany

Gone with the WNT – WNT ligand dependent endoplasmic reticulum associated degradation (ERAD) of EVI/WLS, Wolf L, Lambert A, Haenlin J & Boutros M

EMBO Workshop: The ubiquitin system, 2019, Cavtat, Croatia

Gone with the WNT – WNT ligand dependent endoplasmic reticulum associated degradation (ERAD) of EVI/WLS, Wolf L, Lambert A, Haenlin J & Boutros M

Gordon Research Conference: Wnt signaling, 2019, Mount Snow, USA

Gone with the WNT – WNT ligand dependent endoplasmic reticulum associated degradation (ERAD) of EVI/WLS, Wolf L, Lambert A, Haenlin J & Boutros M

6th Heidelberg Forum For Young Life Scientists, 2019, Heidelberg, Germany

Gone with the Wnt – Wnt ligand dependent stabilization of EVI/WLS, Wolf L, Lambert A, Gläser K & Boutros M

Ubiquitin & Friends, 2019, Vienna, Austria

Gone with the WNT – WNT ligand dependent endoplasmic reticulum associated degradation (ERAD) of EVI/WLS, Wolf L, Lambert A, Gläser K & Boutros M

European Wnt Meeting, 2018, Heidelberg, Germany

Feel the Wnt on your Skin - How Wnt Signalling Shapes Melanoma's Invasive Potential, Wolf L & Boutros M

DKFZ PhD Poster Presentation, 2017, Heidelberg, Germany

Having their Feet on the Ground: Ect2 Independent Cytokinesis in RPE1 Cells Depends on Adhesion and Daughter Cell Respreading, Wolf L, Dix C, Matthews H, Boutros M & Baum B

Hallmarks of Skin Cancer Conference, 2017, Heidelberg, Germany

Having their Feet on the Ground: Ect2 Independent Cytokinesis in RPE1 Cells Depends on Adhesion and Daughter Cell Respreading, Wolf L, Dix C, Matthews H, Boutros M & Baum B

22nd DKFZ PhD Retreat, 2017, Weil der Stadt, Germany

Daughter Cell Respreading and Adhesion Are Required for Ect2 Independent Cytokinesis in RPE1 cells, Wolf L, Dix C, Matthews H, Boutros M & Baum B

5th Heidelberg Forum For Young Life Scientists, 2017, Heidelberg, Germany

Daughter Cell Respreading and Adhesion Are Required for Ect2 Independent Cytokinesis in RPE1 cells, Wolf L, Dix C, Matthews H, Boutros M & Baum B

DKFZ FSP-B Retreat, 2015, Kloster Schöntal, Germany

A high-content screening approach to identify Wnt dependent invasion/metastasis mechanisms in malignant melanoma, Wolf L & Boutros M

4th Anglo-German Workshop on Skin Cancer Biology, 2015, Heidelberg, Germany

A high-content screening approach to identify Wnt dependent invasion/metastasis mechanisms in malignant melanoma, Wolf L & Boutros M

Student supervision

Lambert A (2020), **ERLIN2, UBXN4 and FAF2 are involved in ER- associated protein degradation of the Wnt cargo receptor EVI in human cells.** Master thesis, Faculty of Science, University of Tuebingen

Haenlin J (2019), **Ubiquitin dependent ER associated degradation and localisation of EVI in human cells.** Bachelor thesis, Faculty of Biosciences, Heidelberg University

7.4 Danksagung

Viele haben zum Gelingen dieser Arbeit beigetragen, mich inspiriert, motiviert, unterstützt und durch ihr Mitwirken an den vielen großen und kleinen Projekten meine Zeit als Doktorandin unvergesslich gemacht – ich möchte sie hier nicht ungenannt lassen. Alle, die ich versäumt habe zu erwähnen mögen mir verzeihen und sich trotzdem bedankt fühlen.

Michael Boutros: meine Zeit als Doktorandin in deinem Labor wird für mich immer besonders bleiben. Nur durch deine Unterstützung in den vielen Phasen meiner Projekte war es mir möglich, mich während meines Aufenthalts in London, der HOSC2017 Konferenz, und meinen zahlreichen außerwissenschaftlichen Aktivitäten persönlich und wissenschaftlich weiterzuentwickeln. Ich bin dankbar für die wissenschaftliche Freiheit, die Ressourcen, und die vielen Konferenzen, die ich besuchen durfte. Und für das Ubiquitin-Projekt, auch wenn ich das zunächst nicht gedacht hätte. Durch dein Feedback und deine Ideen inspirierst du uns alle zu immer besserer Arbeit, auch wenn der Weg manchmal mühsam ist.

Michael Boutros, Buzz Baum, Viktor Umansky und Iris Augustin: für eure wissenschaftliche Unterstützung, die Anregungen und Ideen während meiner TAC Treffen und natürlich zusätzlich *Britta Brügger und Irmi Sinning* dafür, Teil meiner Prüfungskommission zu sein.

Thomas Sommer, dem Sommer Lab, Sina Barysch und Ron Kopito: für sehr wertvolle Einsichten in das Ubiquitin-Feld und gute Ideen und Hilfestellungen für mein Projekt.

Dem RTG2099, ganz besonders Sergij Goerdt, Cyrill Géraud, Jochen Utikal, Viktor Umansky und Adrian Hayday: für die initiale Finanzierung meines Projektes, die vielen unvergesslichen und inspirierenden Aufenthalte in London und die gute Zusammenarbeit während meiner Zeit in der MD und PhD Doktorandenvertretung des RTG2099. Auch, wenn wir nicht immer einer Meinung waren, die HOSC2017 bleibt unvergessen! Außerdem den vielen anderen Mitstreitern des RTG2099, besonders Ashik Ahmed Abdul Pari, Katharina Kober und Georg Sedlmeier. Und Olga Strobl-Freidekind, Lisa Jakobi und Martina Nolte-Bohres für die viele organisatorische Unterstützung.

Der DKFZ Graduate School, Lindsay Murrells und ihrem Team: für die gute Zusammenarbeit während meiner Zeit im PhD Council, und davor und danach und immer.

Den vielen großartigen Kollegen von B110: ihr habt lange gewartet und ich hab lange gebraucht, aber durch eure persönliche und wissenschaftliche Unterstützung, den Austausch, die tiefsinnigen Gespräche, die Kinder Schoko-Bons und die vielen witzigen Momente verging die Zeit wie im Flug. Ich teile viele Erinnerungen mit euch, die man auch mit einem Glitzi Schwann nicht wegwischen kann, wir brauchen aber doch noch eine B110 Playlist. An meine

Mitleidenden des Hot-Offices: es wird keine Klimaanlage kommen. Vor allem möchte ich mich bei Dominique Kranz und Oksana Voloshanenko für die viele Hilfe im Labor und bei der Korrektur der Doktorarbeit bedanken. Außerdem für unschätzbare Unterstützung im Labor und in allen Lebenslagen bei: Katharina Kober, Josephine Bageritz, Maja Funk, Luisa Henkel, Fillip Port, Michaela Holzem, Antonia Schubert, Kathrin Gläser, Benedikt Rauscher, Florian Heigwer, Bojana Pavlovic, Christian Scheeder, Alena Ivanova, Jan Winter, Giulia Ambrosi, Tianzuo Zhan, Siu Wang Ng, Diego Aponte, Jan Gleixner, Jun Zhou, Erica Valentini, Siamak Redhai, John Hawkins, Kim Boonekamp, Shiv Bahuguna, Katharina Imkeller, Niklas Rindtorff und unseren vielen Studenten, Angestellten und Laborgästen: Markus Brown, René Riedke, Arek Kendirli, Phillip Gmach, Schayan Yousefian, Elena Tonin, Zeynep Aydin, Michaela Wölk, Nancy Klemm, Alessio Falzone, Leo Bamberg, Michael Endres, Niklas Krauße, Jenny Hundshammer, Manuela Urban, um nur ein paar wenige zu nennen (die Namen sind außerdem in willkürlicher Reihenfolge, es sind zu viele). Ulrike Hardeland, Angelika Manz, Felicitas Olschowsky: für immerwährende Unterstützung mit Organisatorischem, vor allem auch während der HOSC2017 Konferenz und im Zusammenhang mit dem RTG2099. Claudia Blass, Claudia Strein, Barbara Schmidt, Thilo Miersch: für die vielen großen und kleinen Hilfen, die das Leben in B110 so viel einfacher und besser machen. Den Medizinern am Schreibtisch neben mir, Thomas Worst, Niklas Westhoff, Christian Galata: tut mir leid, dass ich immer euren Schreibtisch belagert habe. Die Mauer aus Ordnern, die Niklas gebaut hat, war aber trotzdem nicht ok. Dharanija: für ein unvergessliches Musikerlebnis.

Katharina Kober: unsere gemeinsame Zeit in B110 werde ich nie vergessen. Wir haben viel zusammen durchgestanden und uns immer gut ergänzt, nicht nur deshalb ist die HOSC2017 so außergewöhnlich gut gelungen.

Annika Lambert, Julie Haenlin, Lelia Wagner und Ridzky Yuda: für das Krebszellkuscheltier, die Enton Karte, die Super Mario Kette, den Schlüsselanhänger, die viele Schokolade und andere Süßigkeiten. Aber vor allem für die vielen lehrreichen und witzigen Momente, eure Initiative, Ideen, Fragen und die viele Arbeit für unsere Projekte.

Den Zentralen Einheiten am DKFZ, vor allem der Lichtmikroskopie und der Genom- und Proteomforschung: für wertvolle Unterstützung durch kompetente Beratung und Hilfe wann immer nötig. Mein Dank gilt vor allem Manuela Brom und Damir Krunic, dem ich mal ein Glas Wasser gereicht habe.

Den vielen Leute, die ich am DKFZ kennengelernt habe: was für eine großartige Zeit wir hatten! Vor allem hervorheben möchte ich Sebastian Kruse – mit unseren Party Plänen in Straßburg hat meine Zeit in den PhD Council Teams begonnen. Und die unvergleichliche Mira

Bujupi, die das Beste an unserer Reise durch Indien war. Besonders möchte ich auch den Doktoranden aus der Winter Selection 2015 dafür danken, dass sie mir den Start in Heidelberg so einfach gemacht haben. Und den vielen Freunden, bei denen ich mich viel zu selten melde: Ashik, Sharavan, Jan, Fereydoon, Laura, Meli, Sara, Juliane …

Den PhD Council Mitgliedern 2016/2017 und 2017/2018: Isabelle Everlien, Felix Frauhammer, Britta Ismer, Manasi Ratnaparkhe, Jacqueline Taylor und besonders Maria Bonsack, Florian Köhler, Michael Persicke und Ginny Valinciute. Außerdem den vielen Mitgliedern unserer Teams, ganz besonders natürlich dem unermüdlichen Party Team – ich habe euch viel abverlangt! Meine Zeit in der Doktorandenvertretung des DKFZ war mit die schönste, lustigste, lehrreichste, lohnendste, aber auch anstrengendste Phase als Doktorandin überhaupt. Ich bin dankbar für die vielen Projekte, die wir zusammen gemeistert haben und dass ich nicht bei jedem Treffen von Michaels Freundschaftsliste gestrichen wurde. Zusammen haben wir viel für die Doktoranden erreicht und die besten Partys geschmissen, die das DKFZ je gesehen hat. Bedanken möchte ich mich auch bei den Council Mitgliedern vor und nach uns, deren Zeit zwar bei Weitem nicht so cool war wie unsere, aber mit denen die Zusammenarbeit immer spaßig und produktiv war.

Buzz Baum und sein Labor in London, vor allem Christina Dix und Helen Matthews: für den herzlichen Empfang und die tolle Arbeitsatmosphäre. Mal wieder eine großartige Zeit in London, die mir viele schöne Erinnerungen und neue Eindrücke beschert hat. Buzz, du bist einer der besten und inspirierendsten Gruppenleiter, mit denen ich bisher arbeiten durfte.

Frédéric Chevessier: alles im Labor habe ich von dir gelernt und mein innerer Fred sagt mir, was zu tun ist. Zumindest hat jetzt niemand anderes mehr meinen Kittel an.

Den Leuten, die ich in London wieder getroffen habe, vor allem Gabi Carreno, Sara Pozzi und Mario Gonzalez Meljem: für eine schöne Zeit, an die ich oft und gerne zurückdenke.

Der Ananas: für wertvolle Nährwertangaben und treue Begleitung.

Marius Bruer und Iman Meziane: das L.I.M Team ist das Beste!

Meinen Mitbewohnern: für sinnvolle und weniger sinnvolle Unterhaltungen und vor allem Sarah für gute Gesellschaft während des Lockdowns.

Meinen Freunden aus der Schulzeit und ihren Familien: ich hoffe, wir bleiben in Kontakt.

Den Dragonball Leuten: Pizza essen und bis drei zählen kann man eben nur, wenn auch eine Studentin der Musikwissenschaften dabei ist …

Christopher Dächert: für unzählige schöne Restaurant-, Kino- und Theaterbesuche, gemeinsames Kochen und Trinken. Und ja, ich habe diesen Text von dir kopiert.

Den Adequate tools: eine Ananas: 3,99 €, eine halbe Makrele: 30 Kronen, ein Corona-Pitcher Murphy's: 5,70 €, Freunde mit demselben Humor: unbezahlbar. Vor allem *Andi Wild* für seine dummen (?) Kommentare zu meiner Einleitung, die die letzten Korrekturen viel leichter gemacht haben.

Elfriede und Wolfgang Feyerabend, Hilde und Bill Lingenfelter: für die Erinnerungen.

Erika Lachmann und Ullrich Wolf: hoffentlich bis bald.

Meinen Eltern: für alles.

Am Ende ist alles gut. Und wenn es nicht gut ist, dann ist es auch noch nicht das Ende.

Unbekannt

7.5 Acknowledgements

Many contributed to this work directly or indirectly by motivating, inspiring, and supporting me throughout the many projects during my time as a PhD student/doctoral researcher. They made this journey so extraordinary and unforgettable and I do not want to leave them unmentioned. And my regards to all the people I forgot to list.

Michael Boutros: my time as a PhD student in your lab will always remain special to me. Only your support made it possible to improve myself personally and scientifically during my time in London, the HOSC2017 conference, and my countless extra-curricular activities. I am thankful for the scientific freedom, the resources, and the many conferences I attended. And for suggesting the ubiquitin project, although I wouldn't have though that in the beginning. Your feedback and ideas inspire all of us to do better work, although it might be tedious at times.

Michael Boutros, Buzz Baum, Viktor Umansky and Iris Augustin: for your scientific support, ideas, and suggestions during my TAC meetings, and of course *Britta Brügger and Irmi Sinning* for being part of my Doctoral Defense Examination Commission.

Thomas Sommer, the Sommer Lab, Sina Barysch and Ron Kopito: for very helpful insights into the ubiquitin field and good ideas and suggestions for my project.

The RTG2099, especially Sergij Goerdt, Cyrill Géraud, Jochen Utikal, Viktor Umansky and Adrian Hayday: for the initial financing of my project, the many unforgettable and inspiring visits to London, and the great collaboration during my time as MD and PhD representative of the RTG2099. We did not always agree, but the HOSC2017 was extraordinary. Furthermore, all the people I met through the RTG2099, notably Ashik Ahmed Abdul Pari, Katharina Kober and Georg Sedlmeier. And Olga Strobl-Freidekind, Lisa Jakobi and Martina Nolte-Bohres for organisational help.

The DKFZ Graduate School, Lindsay Murrells and her team: for the great collaboration during my time in the council and before, and after, and always.

The many brilliant colleagues at B110: I took a long time, but time flew thanks to your personal and scientific help, the exchange, the meaningful conversations, the Kinder Schoko-Bons and the many laughs we shared. I owe many fond memories to you that cannot be wiped away, but we still need a B110 playlist. To my fellow inhabitants of the hot office: AC is not going to come. I especially would like to thank Dominique Kranz and Oksana Voloshanenko for their help in the lab and for feedback to this thesis. Moreover for support in the lab and life by Katharina Kober, Josephine Bageritz, Maja Funk, Luisa Henkel, Fillip Port, Michaela Holzem, Antonia Schubert, Kathrin Gläser, Benedikt Rauscher, Florian Heigwer, Bojana Pavlovic,

Christian Scheeder, Alena Ivanova, Jan Winter, Giulia Ambrosi, Tianzuo Zhan, Siu Wang Ng, Diego Aponte, Jan Gleixner, Jun Zhou, Erica Valentini, Siamak Redhai, John Hawkins, Kim Boonekamp, Shiv Bahuguna, Katharina Imkeller, Niklas Rindtorff and our many students, employees, and guests: Markus Brown, René Riedke, Arek Kendirli, Phillip Gmach, Schayan Yousefian, Elena Tonin, Zeynep Aydin, Michaela Wölk, Nancy Klemm, Alessio Falzone, Leo Bamberg, Michael Endres, Niklas Krauße, Jenny Hundshammer, Manuela Urban, just to name few in a random order. Ulrike Hardeland, Angelika Manz, Felicitas Olschowsky: for all the help with organisational matters, even throughout HOSC2017 and connected to the RTG2099. Claudia Blass, Claudia Strein, Barbara Schmidt, Thilo Miersch: for all the many things you do that make B110 life so much better. The MDs at the desk next to mine, Thomas Worst, Niklas Westhoff, Christian Galata: I'm sorry to have occupied so much of your desk space. Still, it was not ok of Niklas to build a wall out of folders. Dharanija: for a very special music experience.

Katharina Kober: I'm never going to forget our time at B110. We went through a lot together and in the end it turned out great, especially HOSC2017.

Annika Lambert, Julie Haenlin, Lelia Wagner and Ridzky Yuda: for the cancer soft toy, the psyduck card, the Super Mario necklace, the keychain and the many sweets. But most of all for the many educational and funny moments, your initiative, ideas, questions, and all the hard work you put into our projects.

The DKFZ Core facilities, especially light microscopy and genomics and proteomics: for invaluable help and proficient consulting whenever necessary. I would like to thank Manuela Brom and Damir Krunic, whom I once handed a glass of water.

The many people I met at DKFZ: what a great time we had! I would like to mention Sebastian Kruse, our talk about parties in Strasbourg initiated my Council career. And the extraordinary Mira Bujupi, who was the best during our travels through India. Further, I would like to thank the people from the PhD Winter Selection 2015 for making my start in Heidelberg so easy and the many friends who I contact too rarely: Ashik, Sharavan, Jan, Fereydoon, Laura, Meli, Sara, Juliane, …

The PhD Council Members 2016/2017 and 2017/2018: Isabelle Everlien, Felix Frauhammer, Britta Ismer, Manasi Ratnaparkhe, Jacqueline Taylor and especially Maria Bonsack, Florian Köhler, Michael Persicke and Ginny Valinciute. Moreover, all the members of our teams, most notably the tireless Party Team – I asked a lot! My time as a PhD Student representative was amongst the best, funniest, most educational, most rewarding, but also most exhausting periods as a PhD student. I'm thankful for all the projects we pursued together and that I wasn't

crossed off Michael's friendship list in every meeting. Together, we accomplished a lot and we had the best parties ever at DFKZ! I would also like to thank the council members before and after us. Although your terms were less cool than ours, the teamwork was always great.

Buzz Baum and his lab in London, especially Christina Dix and Helen Matthews: for the great start and the wholesome work environment. Once more, a great time in London with fond memories and new impressions. Buzz, you are one of the best and most inspiring PIs I ever had the pleasure to work with.

Frédéric Chevessier-Tünnesen: everything I know in the lab I learned from you and my inner Fred always tells me what to do. At least nobody else wears my lab coats anymore.

All the people I met again in London, especially Gabi Carreno, Sara Pozzi and Mario Gonzalez Meljem: for a great time I like to recall.

The pineapple: for valuable nutrition facts and loyal company.

Marius Bruer and Iman Meziane: L.I.M is the best!

My flat mates: for meaningful and less meaningful conversations and especially Sarah for the good company during the Lockdown.

My friends from school and their families: I hope we stay in touch.

The Dragonball people: eating pizza and counting to three is only possible, if there is also a student of musicology present…

Christopher Dächert: for countless nice visits to restaurants, the movies, and the theatre, and for cooking and eating together. And yes, I copied this text from you.

The adequate tools: a pineapple: 3.99 €, half a mackerel: 30 Danish kroner, a Corona-Pitcher Murphy's: 5.70 €, friends with the same sense of humour: priceless. Especially *Andi Wild* for his stupid (?) comments on my introduction, which made the last corrections so much better.

Elfriede and Wolfgang Feyerabend, Hilde and Bill Lingenfelter: for the memories.

Erika Lachmann and Ullrich Wolf: see you soon.

My parents: for everything.

Everything will be all right in the end. If it's not all right, then it's not yet the end.

Unknown

7.6 Erklärung zur wissenschaftlichen Praxis

NATURWISSENSCHAFTLICH-MATHEMATISCHE GESAMTFAKULTÄT

Eidesstattliche Versicherung gemäß § 8 der Promotionsordnung für die Naturwissenschaftlich-Mathematische Gesamtfakultät der Universität Heidelberg

1. Bei der eingereichten Dissertation zu dem Thema:
   Ubiquitin-dependent regulation of the WNT cargo protein EVI/WLS
   handelt es sich um meine eigenständig erbrachte Leistung.

2. Ich habe nur die angegebenen Quellen und Hilfsmittel benutzt und mich keiner unzulässigen Hilfe Dritter bedient. Insbesondere habe ich wörtlich oder sinngemäß aus anderen Werken übernommene Inhalte als solche kenntlich gemacht.

3. Die Arbeit oder Teile davon habe ich bislang nicht an einer Hochschule des In- oder Auslands als Bestandteil einer Prüfungs- oder Qualifikationsleistung vorgelegt.

4. Die Richtigkeit der vorstehenden Erklärungen bestätige ich.

5. Die Bedeutung der eidesstattlichen Versicherung und die strafrechtlichen Folgen einer unrichtigen oder unvollständigen eidesstattlichen Versicherung sind mir bekannt.

Ich versichere an Eides statt, dass ich nach bestem Wissen die reine Wahrheit erklärt und nichts verschwiegen habe.

Heidelberg, den 24. November 2020

……..

Lucie M. Wolf, M.Sc.

7.7 Declaration on scientific standards

COMBINED FACULTY OF NATURAL SCIENCES AND MATHEMATICS

Sworn Affidavit according to § 8 of the doctoral degree regulations of the Combined Faculty of Natural Sciences and Mathematics

1. The thesis I have submitted entitled:
   Ubiquitin-dependent regulation of the WNT cargo protein EVI/WLS
   is my own work.

2. I have only used the sources indicated and have not made unauthorised use of services of a third party. Where the work of others has been quoted or reproduced, the source is always given.

3. I have not yet presented this thesis or parts thereof to a university as part of an examination or degree.

4. I confirm that the declarations made above are correct.

5. I am aware of the importance of a sworn affidavit and the criminal prosecution in case of a false or incomplete affidavit.

I affirm that the above is the absolute truth to the best of my knowledge and that I have not concealed anything.

Heidelberg, 24th November 2020

……..

Lucie M. Wolf, M.Sc.